PAGE NUMBERING AS ORIGINAL

PHYSICOCHEMICAL AND TABLETING PROPERTIES OF CRYSTALLISED AND SPRAY-DRIED PHENYLBUTAZONE CONTAINING POLYMERIC ADDITIVES

Effect of polymeric additives (hydroxypropyl methylcellulose and a polyoxyethylene-polyoxypropylene glycol) on the crystalline structure, physicochemical properties and tableting behaviour of crystallised and spray-dried phenylbutazone powders

A thesis presented for the degree of Ph.D.

at The University of Bradford

by

Mohammed A.S. Al-Meshal

Postgraduate School of Studies in Pharmacy

October 1985

To my loving wife

Sections of the material in this thesis have already been published in the following form:-

Al Meshal, M. & York, P. Effect of crystallisation rate on the polymorphism and dissolution of spray dried phenylbutazone. J.Pharm.Pharmacol., 1983, 35 Suppl., 1P.

Al Meshal, M. & York, P. Studies on phenylbutazone-hydroxypropyl methylcellulose "high energy" compounds. J.Pharm.Pharmacol., 1984, 36 Suppl., 18P.

Al Meshal, M., York, P. & Grant, D. Disruptant effect of surfactant molecules incorporated into phenylbutazone crystals. Presented at British Pharmaceutical Conference, Leeds, 1985.

Acknowledgements

Firstly, my gratitude and grateful thanks to Dr. P. York for his constant support, interest, useful discussions, kindness and guidance at all stages of this work which were fundamental to this thesis and in making it possible and successful.

My thanks are also given to Professor B.W. Barry for the facilities in his department; to Mr. P. Marshall and Mrs. D. Butterworth for their help during the tableting work. To all the technical staff in the Department of Pharmaceutical Technology for specialist assistance particularly with the scanning electron microscope. To Ugine Kuhlmann (Manchester) and Ciba-Geigy (Basle) for providing poloxamers and phenylbutazone degradation products respectively. To all my friends and colleagues for the friendly atmosphere which enabled me to overcome home sickness. To the Saudi Arabian Government for giving me the chance to carry out this project and for providing a generous grant. To the Saudi Educational Attache in the U.K. for their continuous support and help.

My grateful thanks also go to Mrs. J. Maleki for her efficient typing of this thesis.

Finally, to my wife for her conscientious love, encouragement and patience.

Abstract

The physicochemical properties of a drug affect to a large extent its subsequent biological absorption and bioavailability profile. Considerable pharmaceutical interest is therefore directed torwards the improvement of drug dissolution characteristics of drugs with low aqueous solubility.

This thesis has considered the controlled modification of drug dissolution profiles by means of incorporating low concentrations of hydrophilic polymers by different processes into a host drug substance.

In order to examine this approach and its potential use, the physicochemical, solid state, stability and tableting properties of a poorly aqueous soluble drug, phenylbutazone, in alternative polymorphic form and containing low levels of two hydrophilic polymers - hydroxypropyl methylcellulose (H.P.M.C.) and the surfactant poloxamer 188 - prepared by both conventional crystallisation and spray drying are reported.

As an integral part of the work attempts were made to identify the different polymorphic forms of phenylbutazone. The δ-form, the commercially available stable form and the α and β metastable forms (nomenclature after Muller, 1978) were isolated. The α form was found to be unstable on storage. A 2 fold increase in intrinsic dissolution rate was observed for the metastable β-polymorph compared with the stable δ-polymorphic form.

The effect of crystallisation rate on the formation of polymorphs of phenylbutazone was studied using a mini-spray dryer, and slower rates of crystallisation were found to favour polymorph formation.

The hydrophilic polymers, H.P.M.C. and poloxamer 188 were incorporated by conventional crystallisation and spray drying into the drug crystal. Samples were subjected to a series of tests including differential scanning calorimetry, X-ray powder diffraction, scanning electron microscopy, and intrinsic dissolution and solubility. When prepared by conventional crystallisation H.P.M.C. was found to form a "high energy" complex with phenylbutazone which melted 10°C lower than the parent drug. When prepared by spray drying H.P.M.C. inhibited the formation of the metastable β-polymorph of phenylbutazone. A 2 fold increase in intrinsic dissolution rate was observed for crystallised and spray dried samples containing 2% w/w or more added polymer.

Poloxamer 188 did not form a complex with phenylbutazone and unlike H.P.M.C. did not inhibit the formation of the β-polymorph. For both crystallised and spray dried samples a 3 fold increase in dissolution rate was obtained at polymer levels of 1% w/w or above. The increase in dissolution has been attributed to facilitated wetting by lowering of interfacial tension rather than through the formation of micelles.

The stability of selected phenylbutazone:polymer samples was tested at elevated temperatures. The stability was found to be affected both by the method of sample preparation and the type of additive. Large breakdowns occurring by a hydrolytic effect were identified for the crystallised phenylbutazone samples containing poloxamer 188.

The effects on compaction of phenylbutazone in alternative form and presence of polymeric additives were studied by compressing samples of similar particle sizes of phenylbutazone as supplied (δ-form), samples of

spray dried phenylbutazone (β-form) and samples containing different concentrations of H.P.M.C. prepared both by conventional crystallisation and spray drying. Compaction data were analysed according to the Heckel relationship and by force transmission ratio as well as from the tensile strengths of prepared tablets.

The presence of H.P.M.C. up to 5% w/w concentration in phenylbutazone did not change the mean yield pressure for the crystallised or spray dried samples, although a difference in mean value was observed between the crystallised and spray dried materials, 93.22 MPa and 147.02 MPa respectively. Force transmission was found to be improved for samples containing H.P.M.C. prepared by both techniques and in general, the tablet tensile strengths for crystallised samples containing H.P.M.C. were approximately three times greater than for spray dried samples at equivalent tablet porosity. Differences are attributed to variation in solid state and particulate properties between samples.

CONTENTS

List of Tables

List of Figures

CHAPTER 1

CHAPTER 1

1. General Introduction

Gastrointestinal absorption and bioavailability of hydrophobic drugs are often limited by their poor aqueous solubility and low dissolution rate. This can result in undesirable effects since larger amounts of drug may be required to raise the amount of dissolved drug to the levels needed to achieve the desired therapeutic effects. Slow dissolution will also prolong the drug contact time with the gastric mucosa which might result in unwanted side effects such as irritation or risk of developing ulceration. Improving the solubility and dissolution rate generally increases the absorption and total bio-availability.

With a view to improving these parameters, a great deal of research has been carried out using different procedures, all aiming to achieve higher drug dissolution rates. These procedures include reducing the size of drug particles, as the dissolution rate increases with the associated increase in surface area of the drug exposed to the dissolution medium. Examples include the 50% reduction in the therapeutic dose of griseofulvin after micronisation of the drug (Atkinson et al. 1962) and the enhanced absorption of spironolactone following particle size reduction (Levy 1962).

A second way of improving the dissolution rate is to change the crystallographic nature of the substance i.e. using a different polymorphic form such as a metastable polymorph. Metastable forms are at higher energy levels than stable polymorphs and generally exhibit higher dissolution rates. Many workers, including Twashi (1968), Matsuda et al. (1984), Hamlin et al. (1962), have used the phenomenon of polymorphism to increase the dissolution rate of studied materials.

Other attempts to increase dissolution rate include incorporating a hydrophilic polymer into the drug crystal, to form solid dispersions (Sekiguchi & Obi 1961, Tachibana & Nakamora 1965). Different hydrophilic polymers have been introduced into the drug crystal, following different procedures which include a melting technique and solvent evaporation. Some workers have used a combination of techniques (Chiou & Riegelman 1971).

An additional way of achieving an increase in the dissolution rate of sparingly water soluble drugs is to incorporate surfactant molecules into the drug host in an attempt to lower the solid/liquid interfacial tension which will lead to better wetting and as a result, increase the dissolution rate (e.g.Naggar et al. 1980, Chiou et al. 1976).

Further studies are required to elucidate the mechanisms whereby dissolution rate is increased and the associated changes induced in crystallographic character of drug:additive combinations.

The primary objective of this study is to incorporate polymeric additives at low levels into a model hydrophobic drug, phenylbutazone, using two preparation techniques - conventional crystallisation and spray drying - and examine the crystallographic and physicochemical characteristics dependent on polymer inclusion and explore relationships between monitored property changes. In addition the stability of the drug-polymer materials and processing performance, as reflected in tableting, are examined. Both stability and processing performance represent critically important aspects in the formulation and development of dosage forms containing the drug:polymer materials.

It is now appropriate to consider briefly the general properties of crystals.

1.1 Properties of crystals and crystal habit

The habit of a crystal may be defined as the description of the outer appearance of a crystal (Chopra & Dhall 1981). If the environment of a growing crystal affects the crystal shape without changing its internal structure a different habit is obtained (Haleblian 1975), generally resulting from different rates of growth of the various faces of the crystal. Under certain conditions of crystallisation one set of faces may be induced to grow faster than the other, and the growth of another set of faces may be retarded (Mullin 1972). Crystal growth may also be retarded by adjacent crystals. As a result the regular surface of the crystal may be inhibited or an irregular-shaped crystal may occur since the latter crystal should occupy only the space left and it has to adjust its shape according to the available space.

The degree of supersaturation may affect the crystal habit. The higher the supersaturation the tendency of the crystal to change from granular to needle-like shape (Mullin 1972)

The interaction between solute and solvent has a great effect on the final shape of the crystal. For example, resorcinol crystallises from benzene into fine needles, whilst squat prisms are obtained when crystallised from butylacetate (Haleblian 1975).

The presence of impurities in a system can have an important effect on the growth of a crystal. Some impurities may retard crystal growth, others may enhance growth, while others may exert a highly selective effect, acting only on certain crystallographic faces and thus modify crystal habit (Fairbrother & Grant 1978, 1979 , Chow et al. 1984).

Impurities may influence the crystal growth in various ways, including changing the properties of the solution, or the equilibrium saturation concentration or by adsorbing to the crystal faces and exerting a blocking effect. Alternatively, they might interfere with the growth steps and thus disrupt the flow of growth layers across the faces (Mullin 1972).

The internal structure of the crystal and the difference in the arrangement of the molecules is likely to be more important than changes in the crystal habit, and has a greater influence on changing the physicochemical properties of the material. Crystals can be broadly divided into two categories according to the internal structure of the crystal:-

a. Crystalline
b. Non-crystalline (amorphous)

1.1.1 The crystalline state

The true solid crystal comprises a rigid lattice of molecules, atoms or ions, the locations of which are characteristic for the substance. The regularity of the internal structure of this solid body results in the crystal having a characteristic shape (Mullin 1972).

The crystalline state is that thermodynamically favoured for solids. It is characterised by the three-dimensional order of the molecules within its crystal lattice. The molecules are arranged in a pattern that minimises the total energy of the crystal, both kinetic and potential. This usually results in a minimum amount of void space between the molecules. The packing arrangement for a compound will be a function of both its molecular shape and the chemical groups in the molecule involved in the intermolecular bonding e.g. hydrogen bonding, dipole-dipole interaction and change transfer.

1.1.2 The amorphous state

Under certain conditions it is possible to isolate solids in which the molecules do not have sufficient time to organise themselves into three-dimenional patterns or arrays. There is thus no regularity in the structure which influences the X-ray powder diffraction pattern.

A pattern from a crystalline powder consists of many sharp diffraction maxima. In contrast the pattern for a non-crystalline powder may show only a few diffuse diffraction peaks at low angles. Amorphous compounds are thermodynamically unstable since they are the most energetic form so there will be a tendency to entropically drive these solids to a stable crystalline state. The instability of these compounds makes their preparation and isolation difficult (Haleblian & McCrone 1969, Haleblian 1975).

1.1.2.1. Pharmaceutical applications of amorphous material

The thermodynamic instability of amorphous compounds has retarded their general use as they will revert to the stable form especially if the formulation is in aqueous suspension. Special treatment for the formulation is needed to retard reversion.

Mullins & Macek (1960) showed that amorphous novobiocin was ten times more soluble than the crystalline form. These workers also demonstrated that the amorphous material was readily absorbed after oral administration while the crystalline was not bioavailable. Simonelli et al. (1976) showed that sulphathiazole could exist in an amorphous form. Moustafa et al. (1971), when studying sulphamethoxazole and Gouda et al. (1977) with sulphapyrine showed both materials could form amorphous compounds, and these materials gave faster dissolution rate and higher solubility than the crystalline form.

1.1.3 Polymorphism

Polymorphism is the ability of a substance to occur in several different molecular arrangements, which are known as polymorphs. The various polymorphs of an individual substance exhibit different physical properties such as density, optical properties, energy content, X-ray diffraction pattern, infrared spectrum, solubility and dissolution rate (Kuhnert-Bradstatter 1971).

As a result of energy differences the polymorphic forms will transform from the metastable modifications which exist in higher energy levels to the stable form which is in a lower energy level. The transformation of one form into another is accompanied by the absorption or evolution of latent heat. If the transformation is reversible, i.e. one form can convert into the other and vice versa by altering the temperature or pressure, then the polymorphism is said to be enantiotropic. If the transformation proceeds only in one direction from an unstable modification at all temperatures, then this type of polymorphism is called monotropic (Hartshorne & Stuart 1970; Verma & Krishna 1966).

The transformation rate of one polymorph to another depends on the mobility of the molecules in the solid, the type of structural change that takes place and environmental factors. If the transformation involves only a small degree of alteration in the intermolecular bonding, a rapid conversion of metastable form to the stable form occurs. When a substantial difference in the packing arrangement exists between the forms, the transformation can be extremely slow (Verma & Krishna 1966). When the metastable polymorphic form is placed in contact with dissolving solvent it will be rapidly converted to the more stable form as in solution polymorphism does not exist

(Carstensen 1980). The solubility of each form depends on the ability of molecules to leave the crystals to the solvent. The stable form possesses lowest free energy in a definite environment so it has the lowest solubility.

Several techniques are widely used to study polymorphism. Optical microscopy shows the effect of polymorphism on the transmission of light in different directions through the crystal. Since the alternative polymorphic forms have different internal structure they have different refractive indices (Bile 1962). A hot stage attachment fitted to a polarising microscope enables the melting of the polymorph and the change in crystal associated with it to be followed (Koflers 1954). X-ray powder diffraction is a useful tool as the crystalline sections in powders give characteristic X-ray diffraction patterns which consist of peaks at certain positions of varying intensities. Each powder pattern of the crystal lattice is characteristic for a given polymorph due to differences in packing. Several workers have used this method to identify polymorphs (e.g. Bile 1963, Trivedi et al. 1959).

Differential scanning calorimetry has been successfully used to demonstrate polymorphism in materials as the heat loss or gain resulting from physical or chemical changes occurring in samples is recorded as a function of temperature as the substance is heated at uniform rate. Other techniques used include infrared spectroscopy, dissolution rate and solubility (Muller 1978, Ibrahim et al. 1977, Tuladhar et al. 1983, Guillory 1967).

The phenomenon of polymorphism and its effect on physicochemical properties has attracted many workers to investigate different materials. For example, Perrin & Michel (1973a,b), Aguiar et al. (1967), Aguiar & Zolmer (1969), Banerjee et al. (1971) studied the polymorphism of chloramphenicol and its influence on dissolution rate and

absorption. Tawashi (1968), and Summers et al. (1970) reported the existence of aspirin in different polymorphic forms.

Other examples of compounds reported to exist in different polymorphic forms include phenylbutazone (Ibrahim et al. 1977, Muller 1978, Tuladhar et al. 1983 and Matsuda et al. 1984), methylchloromethane (Silver & Rudman 1970), mebrobamate (Clements 1973), barbiturates (Mesley & Clements 1968; Mesley et al. 1968), sulphonamides (Mesley & Houghton 1967) and cortisone acetate (Carless et al. 1966).

1.1.3.1 Pharmaceutical applications of polymorphism

Solubility and dissolution rate:

The metastable polymorphic forms of sparingly soluble drugs can be used instead of the lower solubility stable form. Molecules in the higher energy forms will have more tendency to leave the crystal to go into solution and may enhance absorption and bioavailability. Many workers (e.g. Muller 1978, Matsuda et al. 1984, Tuladhar et al. 1983) used this phenomenon to study the dissolution rate of the different polymorphic forms of the same material in vitro in an attempt to predict in vivo bioavailability. However further work is required to confirm the prediction of in vivo bioavailability.

Summers et al. (1973) found that the tensile strength of tablets formed from metastable polymorphs was weaker than those formed from the stable form. These workers related this observation to the strength of the particle-particle bond with the metastable polymorph forming weaker bonds. Some workers have studied polymorphic transmission during compression (Chan & Doelker 1984).

When metastable polymorphs are dissolved in suitable solvents, clear solutions are eventually obtained. However with time crystals can start appearing or the solubility of the stable form may have been exceeded. The precipitated crystals can also form cakes making it difficult to disperse (Carless et al. 1966). Clearly such changes in the formulation are unacceptable.

1.2 Solid dispersions

A further way of improving the dissolution rate of water insoluble drugs is to incorporate a hydrophilic material such as polymer or surfactant. One way of achieving this, which many workers have successfully used is by the formation of solid dispersions.

The solid dispersion term is applied to those systems in which a drug is homogeneously distributed through a solid matrix. Depending on whether the matrix is water soluble or not, dissolution of the drug can be increased or decreased. When attempting to enhance drug dissolution the matrix should be water soluble.

Two basic procedures have been used to prepare solid dispersions - fusion or solvent evaporation. The fusion technique involves heating both the drug and the carrier to a temperature at which they melt. Then the molten liquor is left to cool in an attempt to entrap the drug molecules between the carrier molecules in a fine particulate form. The method was first used by Sekiguchi & Obi (1961) and since that report, studies of solid dispersions have attracted many workers. These include Simonelli et al. (1969), Bates et al. (1969), Goldberg et al. (1966), and Chiou & Riegelman (1969). Whilst this process has the advantage of being rapid it suffers from the disadvantage of risk of decomposition of the components or evaporation due to high temperatures used.

The solvent method uses a suitable volatile solvent which dissolves both the drug and the carrier. The solvent is then evaporated by means of vacuum or gentle heat. This method was first reported by Tachibana & Nakamura (1965) and the technique has subsequently been widely used (e.g.Myersohn et al. (1966), Malone et al. (1966), Hoelgaard & Møller (1975), Sekikawa et al. (1979), Anastasiadou (1982)). The main advantage of this technique is that it does not involve the risk of decomposition or evaporation of a component by heat due to the lower temperature required for the evaporation of the organic solvent. However incomplete solvent evaporation may result which might reduce the stability of the product. Difficulties can also be experienced in selecting a common solvent.

Some workers (e.g. Chiou & Riegelman 1971) have used a combination of both the fusion and solvent techniques. The dissolution rate of the drug from the resulting products is markedly enhanced when the incorporated matrices were water soluble. Chiou & Riegelman (1971) listed the possible mechanisms involved:-

1. decrease in drug particle size.
2. possibility of solubilising the drug by the carrier.
3. good separation of the drug particles from each other which prevents them aggregating or agglomerating, thereby increasing the exposed surface area of the drug to the solvent.
4. better wettabilityand dispersibility due to the fact that the drug particles are encircled by the soluble carrier which can readily dissolve and enable water to contact and wet the drug particles.

The main application of solid dispersions in pharmacy is in improving solubility and dissolution rate. Numerous workers have researched this field and used different hydrophilic carriers with different types of

hydrophobic drugs.

Various additional explanations for observed increases in dissolution rate have been proposed, including glass solution formation (Chiou & Riegelman 1969), solid solution formation (Goldberg 1965), decrease in particle size (Gibaldi et al. 1968), eutectic mixture (Sekiguchi & Obi 1961) and higher energy compounds (Simonelli et al. 1976).

Direct crystallisation can also be used to add carrier to the drug. This technique involves flocculating a solution of the hydrophobic drug in an organic solvent (mainly alcohol) by the addition of an aqueous solution containing the required amount of carrier. This method is rapid, has no risk of decomposition of the component, but problems associated with removing the water and the solvent from the product can occur. This method has been used by Naggar et al. (1980) and Chiou et al. (1976), and is employed in this study to incorporate hydrophilic polymer and surfactant molecules and will be discussed further in Chapters 4 and 5 of this thesis.

1.3 Spray drying

Spray drying can be defined as the transformation of the feed from a liquid state into dried particles by spraying them into a hot drying medium (Masters 1979). The feed is dispersed as fine droplets into the drying chamber which has a current of hot air or gas where the solvent evaporates rapidly forming dried often spherical particles before they reach the wall of the drying chamber (Lachman, Lieberman, Kanig 1970). The dried powder is carried by the airstream to the collection system and the gaseous solvent is expelled by the exhaust pipe to the air or where it could be recovered depending on the type of spraying process.

The process of spray drying can be illustrated diagrammatically as described by Marshall (1954).

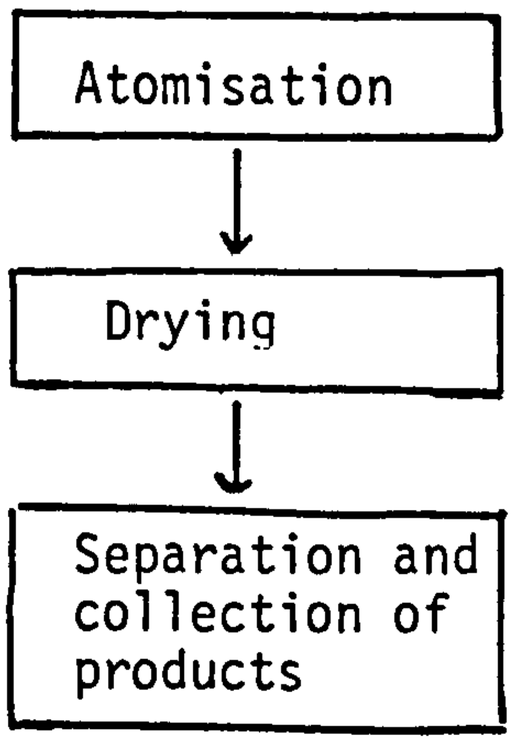

1.3.1 Atomisation

Atomisation is the process of changing the feed tofine droplets. It is the most important part of the spray drying as it disintegrates the feed into fine droplets. The atomiser is usually placed inside the drying chamber to bring the droplet into contact with the hot drying air which could be flowing upwards, downwards or outwards to dry the feed before it reaches the wall of the chamber. The ideal atomiser is that which generates monosized droplets.

Fig. 1.1 The various types of atomisation available for spray driers

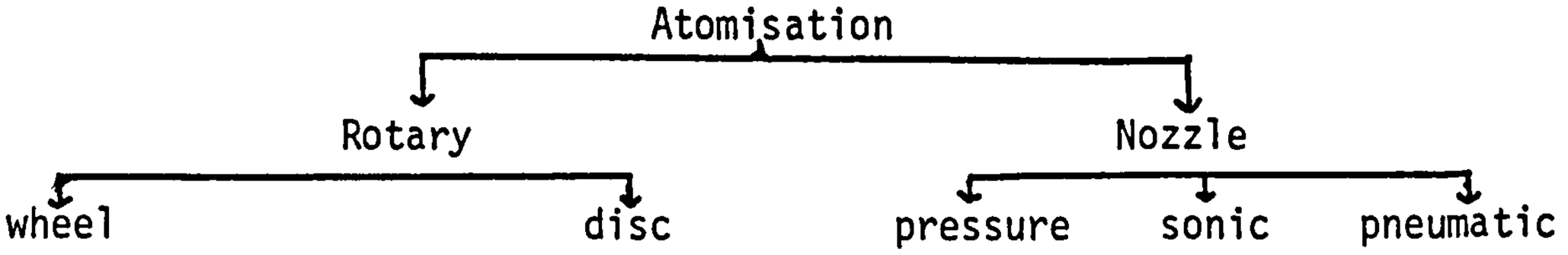

1.3.1.1 Rotary

In this type of atomisation the feed is introduced to the centre of a rotating disc or wheel, which rotates at a high speed. The feed will distribute towards the edge of the disc by means of centrifugal force. When the feed reaches the edge of the disc it has to gain disc speed

before leaving the disc to the chamber. So the degree of atomisation depends upon peripheral speed, feed rate, liquid properties and atomiser design (Masters 1979, Friedman et al. 1952). There are two types of rotary atomiser - disc and wheel (see Fig. 1.1).

There are two types of rotary disc, either smooth surface or with vanes. The smooth surface type has the disadvantage that at high speed the liquid feed might slip and would not form an intact film on the disc and this will affect the homogeneity of the droplet particle size. The problem of slipping in the smooth disc can be overcome by increasing the friction between the feed and the disc. This could be achieved by fitting the disc upside down as an inverted plate or cup and introducing the feed onto the lower surface in the centre (Dombrowski et al. 1968, 1974). By means of centrifugal force the feed will move outwards from the centre and will be pushed downward by the concave edge of the disc which will apply pressure on the liquid preventing slipping (Hinze & Milborn 1950, Frazer 1957, Masters 1979, Beuttener & Steiger 1956).

The other type of discs are fitted with vanes which will control the spread of the feed film over the disc by confining it to the vanes surface, and at the periphery the maximum liquid release velocity possible is attained (Masters 1979, Marshall 1954, Tate 1965).

The principle of the rotating wheel atomiser is similar to that of the rotating disc, except that no feed slippage occurs as the feed travels through radial vanes to the surface (Kurabyasi 1960). At low speeds and feed rates, viscous and surface tension forces predominate in droplet formation. For intermediate speed, the disintegration of the liquid ligaments at the edge of the vanes is by centrifugal forces and to a lesser extent by gravitational forces. At high liquid flow and high wheel speed the disintegration of the liquid occurs at the edge of the

vanes by frictional effect between the liquid and the air with the liquid emerging as a thin film from the vanes.

This procedure, whilst not achieving a homogeneous spray, produces a spray of a small droplet size. Homogeneity of the spray can be improved by increasing the viscosity and the surface tension, but this will tend to increase droplet size (Masters 1979).

1.3.1.2 Nozzle

The function of the nozzle atomiser is the acceleration and disintegration of the bulk liquid flow, terminating with the dispersion of the resulting droplets to form a spray. A single orifice or ejector cannot be considered an atomiser. The liquid is disintegrated if the liquid jets are turbulent enough, but the droplets are not dispersed by the action of the nozzle (Masters 1979). There are three different types of nozzle atomiser - pressure, sonic and pneumatic (see Fig. 1.1).

The principle of the pressure nozzle is the conversion of pressure energy with the liquid bulk into kinetic energy of thin moving liquid sheets. The sheet breaks up under the influence of the physical liquid properties or friction with the medium in which the sheet is discharged. Any change that causes fluctuations in the order of the sheet thickness promotesdisintegration. Centrifugal pressure nozzles are employed where the feeds are of low viscosity and contain no large solid particles in the suspension. With correct nozzle selection both fine and coarse sprays can be obtained. The pressure nozzle atomiser has the advantage of having low cost and ease of replacement. The main disadvantages are the need for high pressure pumps, and the restriction on the type of feed material which can be used without causing wear to the nozzle (Marshal 1954, Masters 1979).

In the pneumatic nozzle atomiser, the liquid feed is broken up into very fine droplets by impacting the liquid bulk with a high velocity gas (Bradley 1973a,b). The principle of breaking up the fluid can be considered to occur in two phases. The first phase involves tearing the liquid into large droplets or filaments. The second phase involves breaking these large filaments into smaller and smaller droplets. This process is influenced to a large extent by the viscosity, density and surface tension of the liquid and the gaseous flow. The spray produced by this procedure is characterised by high homogeneity. This type of atomiser is usually used to spray viscous liquids and to produce fine droplets. (Frazer et al. 1963, Masters 1979).

Sonic nozzle atomisers break up the liquid through sonic excitation. The need for such atomisers became necessary with the increasing number of liquids that cannot be atomised successfully by the ordinary atomisers. Such liquids include the non-Newtonian, highly viscous systems and have long chain molecular structure and need excessive pressure for effective atomisation in centrifugal pressure nozzles to increase drying rates (Katta & Gauvin 1975, Masters 1979).

1.3.2 Drying

Drying is the process of removing the solvents (usually water) from the feed to leave the solid component of the feed in fine powder form. Drying takes place in two stages, the first stage occurring when the droplet leaves the atomiser. It will then be faced by the hot air in the chamber and so evaporation of the solvent will take place immediately from the surface of the droplet. At this stage there is enough solvent in the droplet to maintain a solvent film at the surface of the droplet by diffusion of liquid from the interior of the droplet. When the critical point is reached there is insufficient liquid in the droplet to

replace at an equivalent rate the evaporating liquid and a solid shell will form around the droplet. The second stage of drying starts after shell formation. The evaporation rate now depends on the rate of diffusion of the liquid through the shell, and the thickness of the shell will increase with time (Masters 1979).

Increasing the concentration of the solid in the feed will decrease the vapour pressure of the liquid and hence reduce drying rate. Also drying rate will be increased when drying in a medium other than air if this medium has higher diffusivity and thermal conductivity. This can be seen when drying using light gases, such as hydrogen (Masters 1979).

Charlesworth & Marshall (1960) illustrated the shape, composition and changes occurring during drying of spray dried particles. These authors divided the spray dried particles into two groups - those spray dried in drying air temperature above or below the boiling point of the liquid droplet (Fig. 1.2).

From the diagram shown in Fig. 1.2 one can conclude that the properties of the solid part in the spray's feed play a major role in the final shape of the spray dried particles. For porous rigid materials fine intact spherical particles are generally produced while decreasing porosity increases the chance of imperfection. For the non-porous plastic material different shapes are produced with different possible imperfections, but generally non-spherical with almost non-reproducible shape and size. Also the boiling point of droplet contributes when determining the final shape of the formed particle (see Fig. 1.2).

1.3.3 Collection

Collection involves separating the dried powder from the solvent and collecting the product from the drier. The separation either takes place in one or two stages. In two stage separation, product is collected at

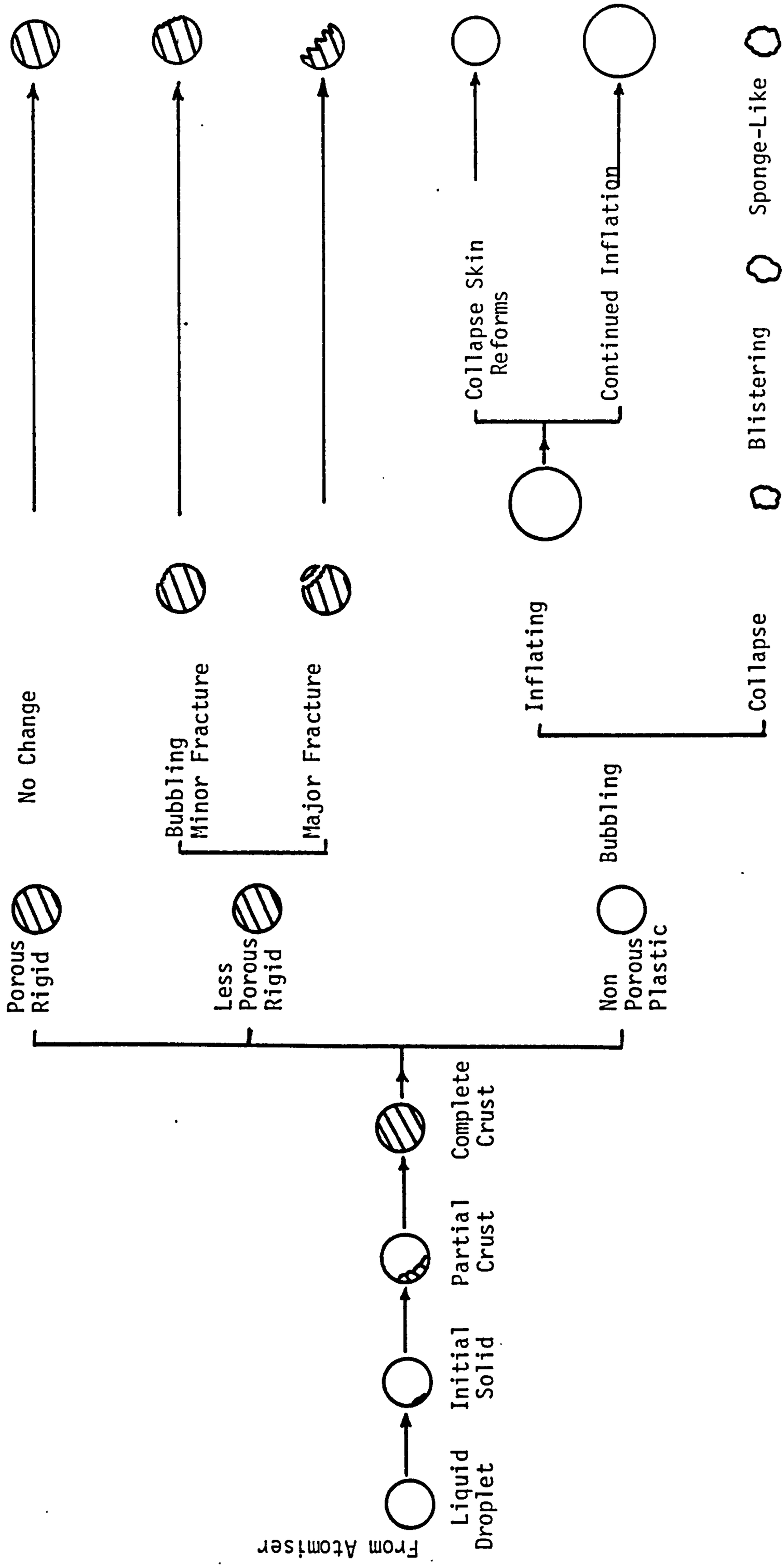

Fig. 1.2a Characteristics of droplet undergoing drying (based on Charlesworth & Marshall 1960)

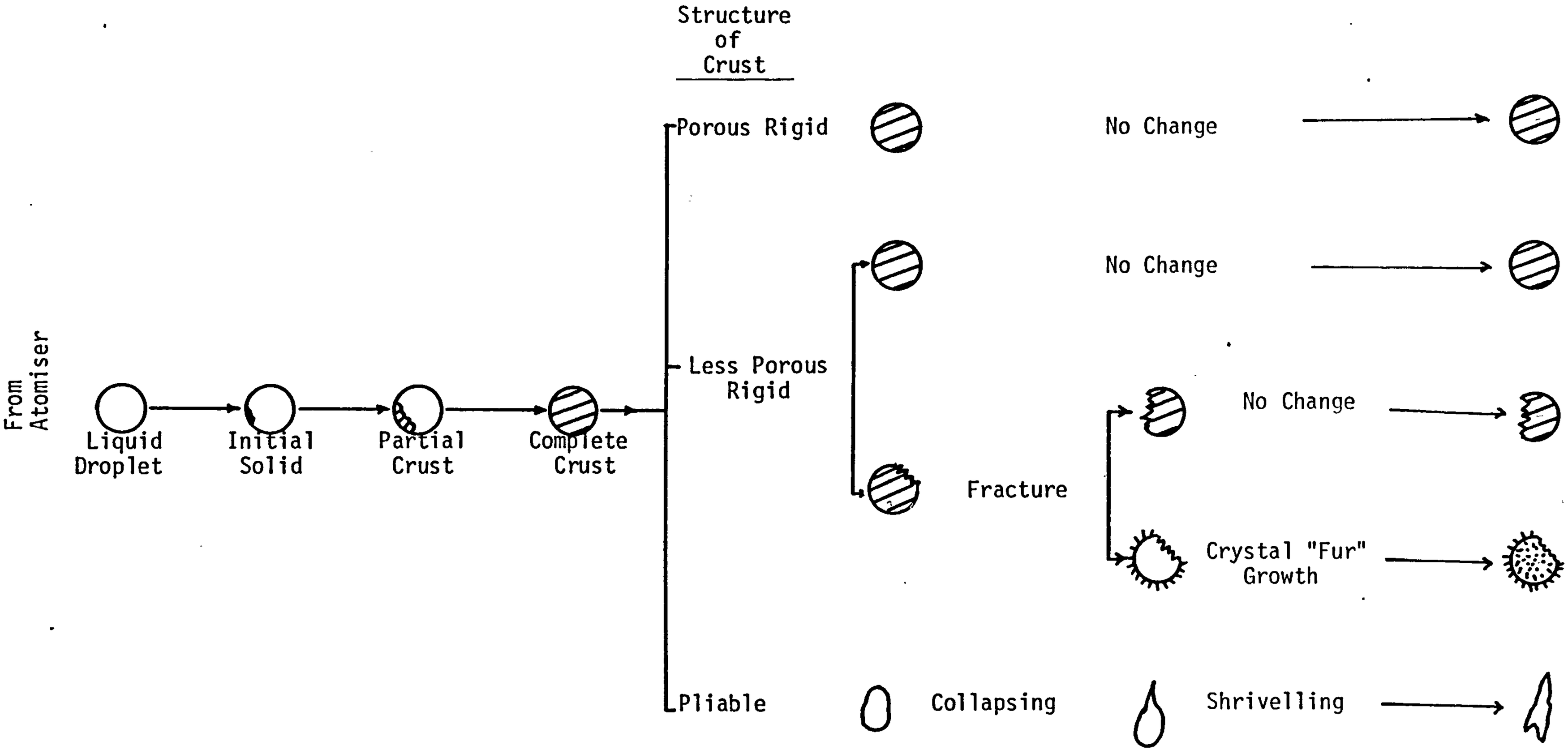

Fig. 1.2b Characteristics of droplet undergoing drying (drying air below boiling point)

(based on Charlesworth & Marshall 1960)

the drying chamber and the fine powder product is recovered in collecting equipment, while in single stage systems all the product is collected in the separation equipment.

The separation should be very efficient and very close to 100% especially if the dried material is harmful and also for efficiency in processing. For health reasons the level of any discharged particle through the exhaust should fulfil the regulations of the country where the dryer is operating. The powder is separated from the solvent either by gravity in which the product particles fall to the bottom of the chamber and are collected either by scrubber or an emptying valve. Also the separation can be obtained by a cyclone in which a centrifugal force applied on each particle will make the particles move away from the centre to the wall of the cyclone. Then the air flow is turned upward to the exhaust. The residence time of the air in the cyclone before leaving is important as it should be long enough for all the particles to move to the wall of the cyclone otherwise they will be pushed outside with the air flow to the exhausts. (Masters 1979, Lachman, Lieberman & Kanig 1970).

1.3.4 Pharmaceutical applications of spray drying

The applications of spray drying are increasing and spray drying is used in many industries such as the food industry, for making milk products, and fruit, vegetable and plant extracts, coffee, etc. Also spray drying is finding application in the ceramic and plastic industries (Masters 1979).

Spray drying has found use in the pharmaceutical industry because of the rapidity of drying and the unique form of the final product. Spray drying can thus be used by the pharmaceutical industry for drying heat-sensitive pharmaceuticals including many antibiotics, vitamins, enzymes,

yeasts, yaccines and plasma derivatiyes (Masters 1979). Recently interest has been concentrated on applying this technique to prepare powders with controlled particulate properties as the resulting particles are generally spherical in shape, possess a narrow size distribution, haye reduced bulk density and are hollow (Abdulrahman 1973). As a result, they are generally free flowing (Robinson et al. 1961) and dissolve rapidly (Kawashema et al. 1975, Kawashema & Takenaka 1974). Spray drying finds value in the modification of materials for use in tablet formulations by direct compression (Raff et al. 1961) to get different polymorphic forms of materials (Matsuda 1984) or obtain anhydrous and amorphous forms (Corrigan 1982).

Spray drying has also been successfully used to prepare microcapsules which provide solid particles of liquid droplets with an individual coat thereby modifying their physical, chemical or physiological characteristics. Speiser et al. (1973) prepared microcapsules of barbituric acid by spray polycondensation and Voellmy (1977) prepared microcapsules of phenobarbital using a similar technique. Takenaka et al. (1982) prepared solid particulates of theophylline-ethylenediamine complex (aminophylline) by spray drying. Kawashema et al. (1983) used a spray drying technique to prepare solid particulate of aminopyrine-barbital complex. Takenaka et al. (1981) studied the effect of cellulose acetate phthalate, colloidal silica and other excipients such as talc, on the polymorphism of spray dried microcapsulated sulphamethoxazole while Takenaka et al. (1980) spray dried an enteric coated microcapsule of sulphamethoxazole.

Spray drying was chosen in this work as an alternative technique to incorporate hydrophilic polymer and surfactant molecules with phenylbutazone and data will be presented and discussed in Chapters 3, 4 and 5 of this thesis.

1.4 Tableting

The art of compressing discrete solid particulate matter into a cohesive mass has been practised since the days of the ancient Egyptians. It was not until the mid nineteenth century however that medicinal use of this process was made when Brockedon (1843) took out a patent for shaping pills, lozenges and black leads by pressure in a die. In the U.S.A. McFerren (1874) and Dutton (1876) extended and improved on Brockedon's idea and obtained further patents for tablet compression machinery. Developments from this patent using the increasing amount of technology available now enables production rates in excess of 600,000 tablets per hour using the most modern machines. Initially the process was purely empirical, with little or no account being taken of the mechanisms involved, the only criterion for acceptability being production of a compact.

Fundamental research began in the 1920's mainly in the field of powder metallurgy, but quickly spread to other disciplines as the implications became more widely realised. Generally speaking two broad lines of investigation may be distinguished. (i) Studies of the distribution of forces at die and punch walls, and within compacts during compression (Higuchi 1954, Shotton & Garderton 1960, Fuhrer 1962, Shotton et al. 1963, Lewis & Shotton 1965, Leigh et al. 1967, Knoechel et al. 1967, Goodhart 1968) and (ii) analysis of the relationships between the applied pressure and the resulting density of compact (Heckel 1961a,b, Hersey & Rees 1970, Fell & Newton 1971, Cooper & Eaton 1962).

The former approach has involved the use of instrumental tableting machines of both single punch (e.g. Lewis & Shotton 1965, Shotton & Garderton 1960, Higuchi et al. 1954, Leigh et al. 1967 and Fuhrer 1962)

and multi-punch types (e.g. Shotton et al. 1963, Knoechel et al. 1967, Goodhart et al. 1968). The first published account of the instrumentation of a single punch tableting machine was given by Huguchi et al. 1954, who bonded a strain gauge onto the upper punch frame and a load cell onto the lower punch.

Because of the non-linear relationship between frame distortions and applied force, Shotton & Ganderton (1964) bonded strain gauges directly onto the punches, recording the forces on a U.V. recorder.

The force transmitted radially to the die wall was first measured by Nelson (1955) and Windheuser et al. (1963) who cut away a section of the die wall and bonded strain gauges on it. They reached the conclusion that materials which permitted good conversion of axial to radial pressure tend to form better tablets. A residual die wall pressure, after removal of the upper punch, was found by Higuchi et al. (1965). Instrumentation of this type has been reported by several workers (e.g. Leigh et al. 1967, Long 1960) who used it to record the compaction profiles of several materials, some of which were of pharmaceutical interest.

1.4.1 Mechanisms occurring during compaction

The several stages occurring during compaction could be listed as:-

i) filling the die
ii) densification by particles slippage
iii) elastic and plastic deformation
iv) cold welding with or without fragmentation (York 1978)

When a loose powder bed is subjected to a constant pressure, the pressure transmitted through the bed will decrease uniformally with the distance from the source. However, when the powder is filled in a die there are force losses due to extra forces which the upper punch has to overcome. These forces include die wall friction which is dependent on powder properties, the state of compaction and the interfacial condition between powder and die wall (see Fig. 1.3).

Fig. 1.3 Forces operating on a powder under compression

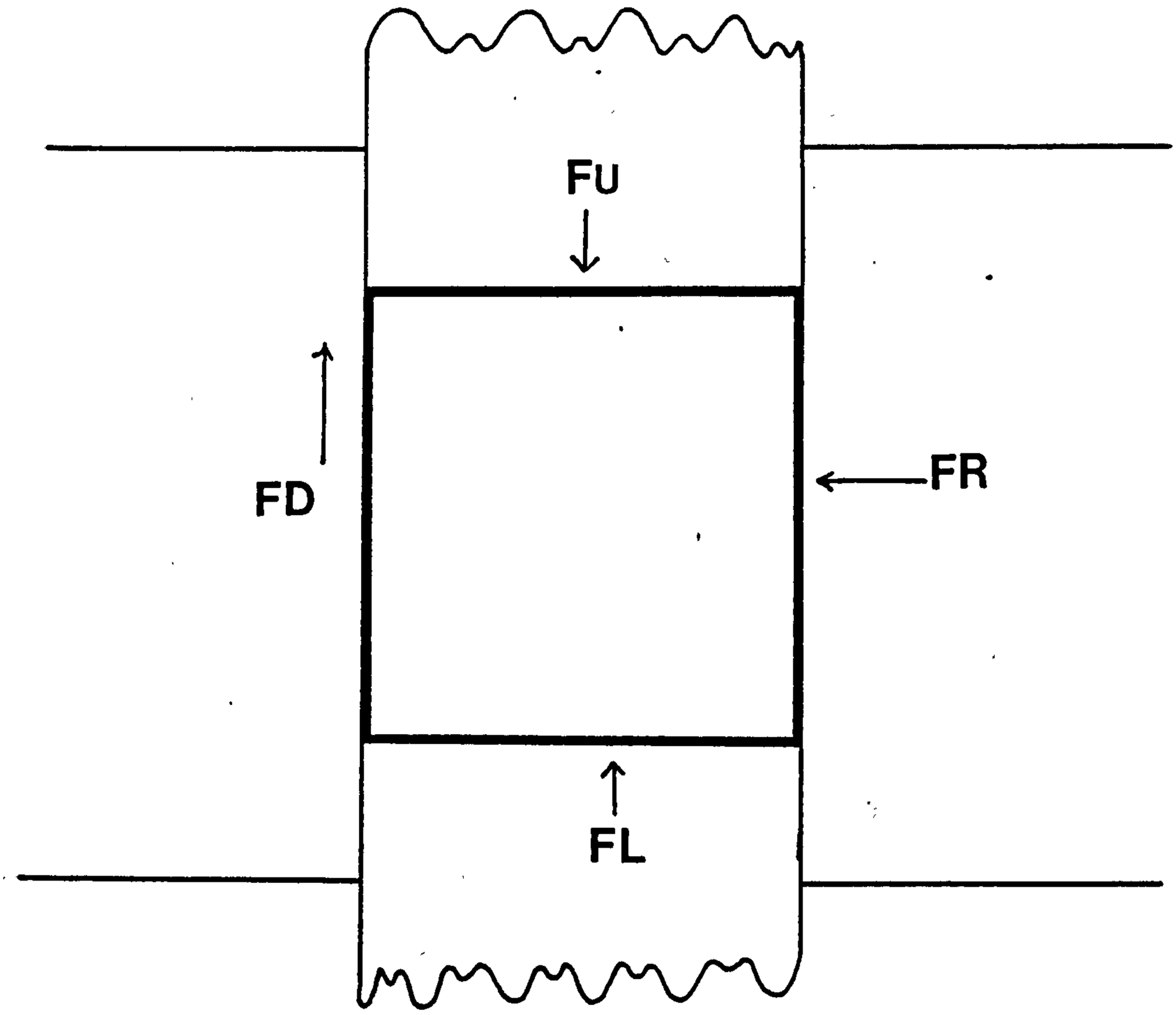

Where

Fu = The applied force by the upper punch

FL = Force transmitted to the lower punch

FR = Radial force

FD = Die wall reaction as die wall friction force

In powders and particulate solids friction usually occurs between the powder and the die wall which will induce the radial force, FR. Thus, some of the applied force will be transmitted to the die wall (FD) to overcome the radial force. Thus Fu = FL + FD.

For elastic materials, the elastic strain induced by the application of a load can be recovered by unloading the material. The change in dimension is generally attributed to the stretching of the atomic bonds and changes in the internal energy of the loaded and unloaded specimen (Stanley-Wood 1983). When a material undergoes a linear stress-strain relationship, the elastic characteristics of the material such as Young's modulus and Poisson's ratio can be calculated.

Plastic materials are materials which have non-recoverable strain on unloading when loaded beyond the elastic limit. The process occurs mainly because of the sliding of atoms over each other (Stanley-Wood 1983). The plastic deformation of materials occurs non-homogeneously by means of lattice dislocation within the crystal structure of materials (see Fig. 1.4). Some materials undergo fragmentation with increasing applied load.

1.4.2 Pressure/volume relationships

Many equations have been proposed to account for pressure/volume relationships during compaction (Kawakita & Ludde 1970, 1971). However, the equation developed by Heckel (1961a, 1961b) has been found particularly useful in numerous compaction studies (Hersey & Rees 1970, Hersey et al. 1972, Fell & Newton 1971, York & Pilpel 1973, Esazobo & Pilpel 1977, York 1978, De Boer et al. 1978, Rue & Rees 1978, Kurup & Pilpel 1978, Ho & Hersey 1980, Paronen & Juslin 1983).

Fig. 1.4 Representation of (a) Elastic deformation, (b) Plastic deformation and (c) Fragmentation of model powder particles during compression

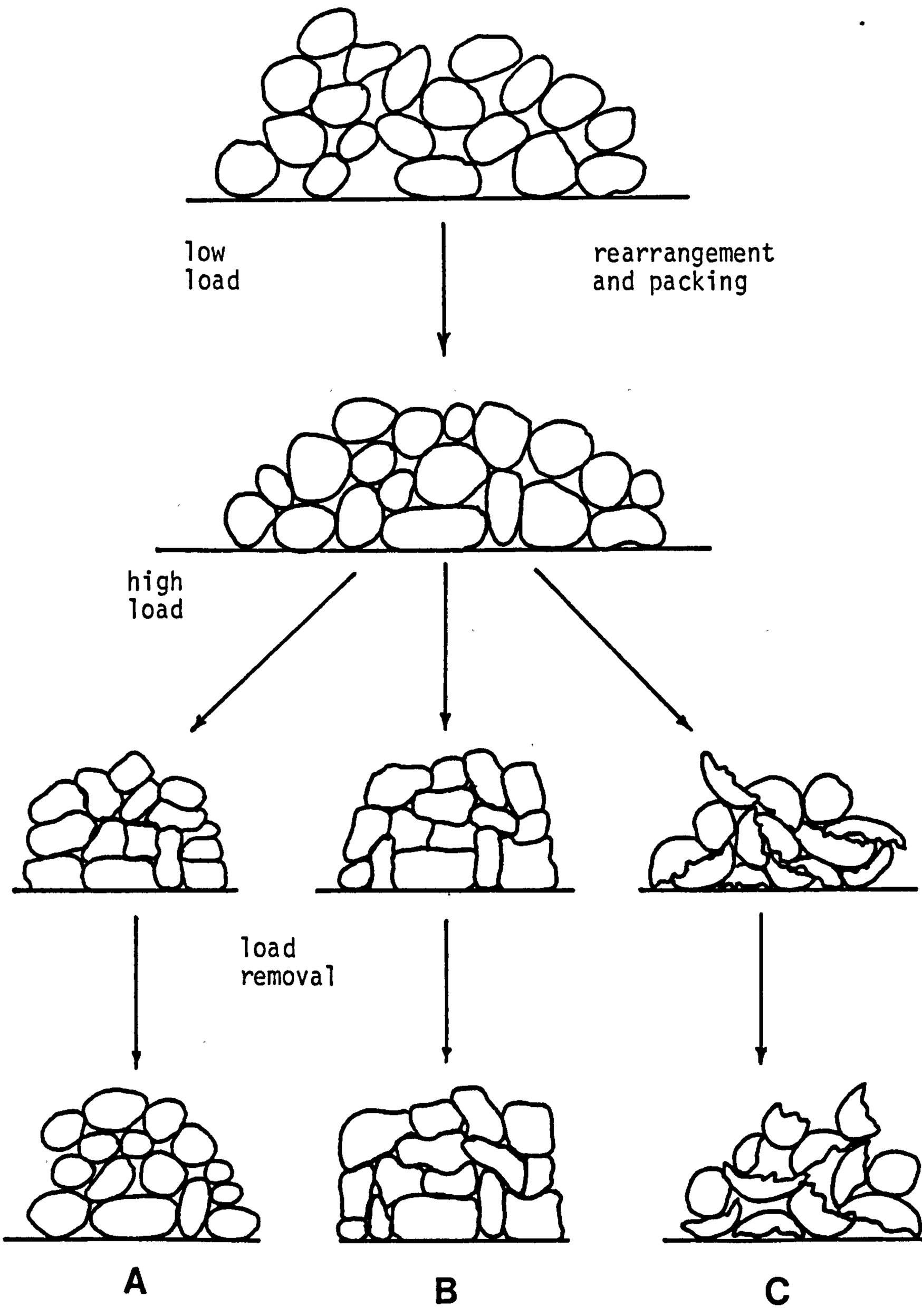

The Heckel equation essentially describes a first order relationship for the change in pore volume with pressure. The relationship is given by equation 1.1

$$\ln \frac{1}{1 - D} = KP + A \qquad 1.1$$

Where D is the density of the compact relative to the absolute density of the material being compacted

P is the applied pressure (Mpa)

$K = \frac{1}{Y}$ where Y is the yield pressure of the material

and A is a function of the original compact volume.

Several workers have however, expressed caution when analysing data by the Heckel equation (Rees & Rue 1978, York 1978); since the experimental conditions and method of measurement (e.g. within die or after removal following compaction) influence the numerical values of parameter derived from the analysis. Nevertheless, by standardising experiment procedures it is possible to use the data to compare the compaction behaviour of materials.

Hersey & Rees (1970) described two types of powder compaction behaviour when analysed according to the Heckel relationship. Type A and type B (see Fig. 1.5). Type A was observed for particles whose bulk density was dependent on initial particle size. Then under pressure the densification was due to particle rearrangement or slippage, followed by plastic deformation.

Type B was observed for materials that do not maintain the initial bulk density difference, due to particle size variation, have higher yield pressures and undergo consolidation by initial fragmentation to form a consistent packing followed by plastic deformation.

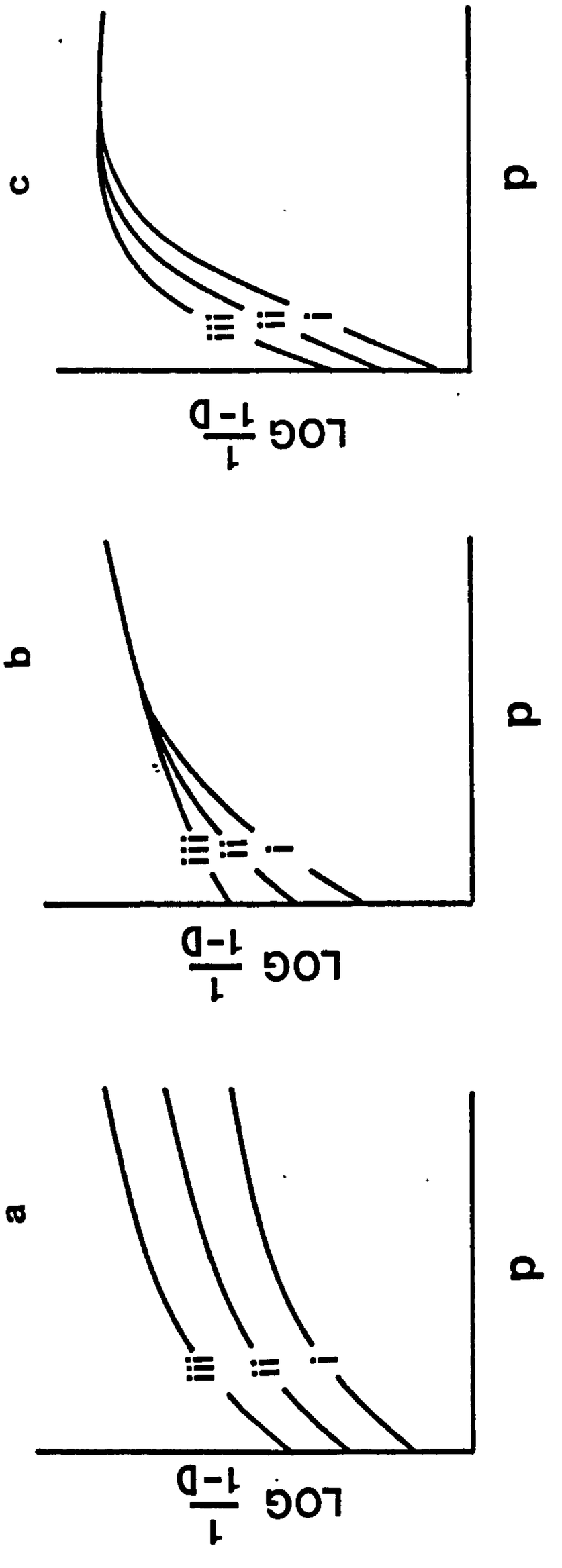

Fig. 1.5 Distinction between (a) Type A, (b) Type B and (c) Type C behaviour in Hendel plots. For types A and B behaviour lines i to iii refer to increasing particle size, while for type C behaviour, lines i to iii refer to increasing fatty acid concentration (Krycer et al. 1982)

A third type of behaviour, type C was distinguished by York & Pilpel (1973), showing a very rapid approach to limiting density for materials with very low yield pressures (see Fig. 1.5).

1.4.3 Force transmission

Early workers used the ratio of maximum lower to upper punch force or "R" value to study lubricant efficiency in tablet formulations (Nelson et al. 1954; Strickland 1959; Strickland et al. 1960) and axial pressure transmission across unlubricated beds (Shotton & Ganderton 1960; Shotton et al. 1963). The better the force transmission in an axial direction, the closer the "R" value approaches unity.

Since 1960 when Long elucidated the significance of radial versus axial pressure cycles, these plots have found widespread use in the evaluation of compaction data (Obiorah & Shotton 1976; Summers et al. 1976; Carless & Leigh 1974; Carstensen & Toure 1980; Carstensen et al. 1981; Carless & Sheak 1976). Long (1960) for model materials extended measurements to cover the complete compression cycle, including the removal and dissipation of pressure. Leigh et al. (1967) investigated pharmaceutical materials and suggested behaviour similar to three different types of theoretical compression patterns, namely an elastic body, a Mohr's body and a body with constant yield stress (see Fig.1.6). Further studies have attributed physical significance to each straight line of the pressure cycle plots showing differences between pharmaceutical powders (Carless & Leigh 1974; Davis et al. 1977) and various crystal forms (Summer et al. 1976).

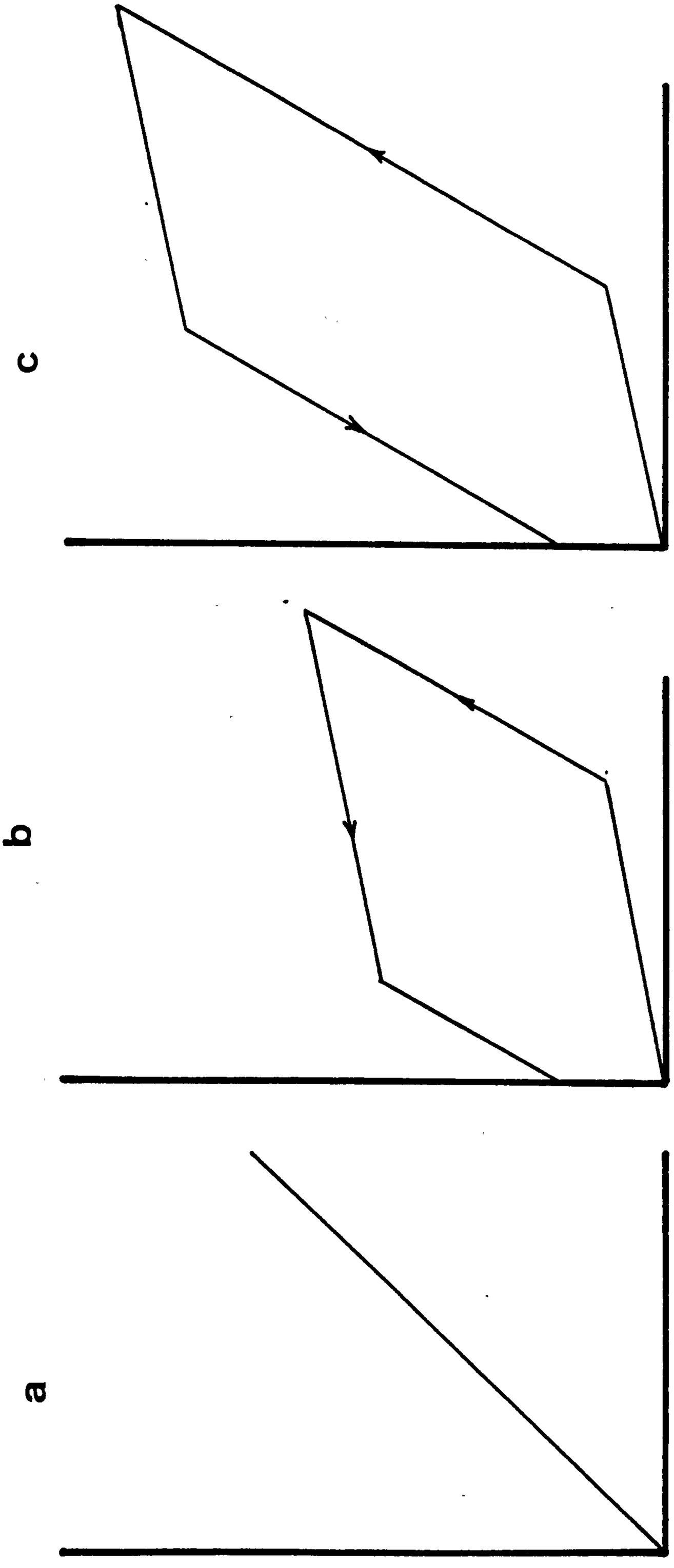

Fig. 1.6 Theoretical stress transmission plots (a) on elastic body, (b) a Mohr body and (c) a body with constant yield pressure

1.4.4 Stress relaxation

Stress relaxation is the decrease in the applied force which occurs when a compact is under static compression, due to plastic deformation of the compressed material into interstitial spaces. Various workers (Cole et al. 1975; Hiestand et al. 1977; Rees & Rue 1977) have used stress relaxation curves to compare the plastic flow of pharmaceutical powders under pressure. David & Augsberger (1977) derived the relationship:-

$$\text{In } \Delta F = \text{In } F_o - K^{11} t$$

where ΔF is the amount of force left in the viscoelastic region at time t; ΔF_o is the total magnitude of this force at t = 0 and K^{11} is the viscoelastic slope. By using the viscoelastic slope, K^{11}, these workers were able to quantify the degree of plastic flow. They found that materials with a higher viscoelastic slope exhibited a higher degree of plastic flow under compression and would form stronger compacts.

1.4.5 Tablet property evaluation

In terms of tablet property evaluation, several groups of workers have plotted tablet crushing force against mean compression pressure (Shotton & Ganderton 1960, 1961, Hersey et al. 1967, Rees & Hersey 1972, Shotton & Obiorah 1973), where the mean compaction pressure (Pm) is given by:-

$$Pm = \frac{Pa+Pb}{2} \qquad 1.2$$

and Pa and Pb are the maximum applied and transmitted pressures to the upper and lower punches respectively. A comparison of the relative slopes of crushing force against compression pressure plots has been used to give a qualitative indication of the tendency of materials to produce strong tablets (Krycer et al. 1982).

Rudnick et al. (1963) and Fell & Newton (1970), when describing the stress distributions within tablets subjected to diametrical compression tests, have shown that when suitable padding material is positioned between the tablet and the upper and lower plates, the tensile strength of the tablet can be calculated. It is essential to achieve such conditions when using this test as otherwise line loading may cause failure by compressive or shearing stresses.

By observation of the specimen after failure, three types of fracture have been reported (Rudnick et al. 1963; Fell & Newton 1970). They are shown diagrammatically in Fig.1.7 and are termed:-

i) compression or shear failure (producing irregular fragments)

ii) normal tensile failure (tablet fractures along loaded diameter into two halves)

iii) triple cleft failure (symmetrical split into four pieces).

A tensile break can therefore be confirmed by observing the failure pattern and such breaks could be calculated by the following equation:-

$$T_t = \frac{2P}{\pi D t_1} \qquad 1.3$$

where T_t = tablet tensile strength

P = is the load applied

D = tablet diameter

t_1 = tablet thickness

Fell & Newton (1970) have however shown that measured tensile strength differs when padding material is used compared with data obtained without padding, suggested that this causes doubt as to which value

Fig 1.7

FRACTURED TABLETS AFTER DIAMETRICAL COMPRESSION

Shear and Compressive Failure

Normal Tensile Failure

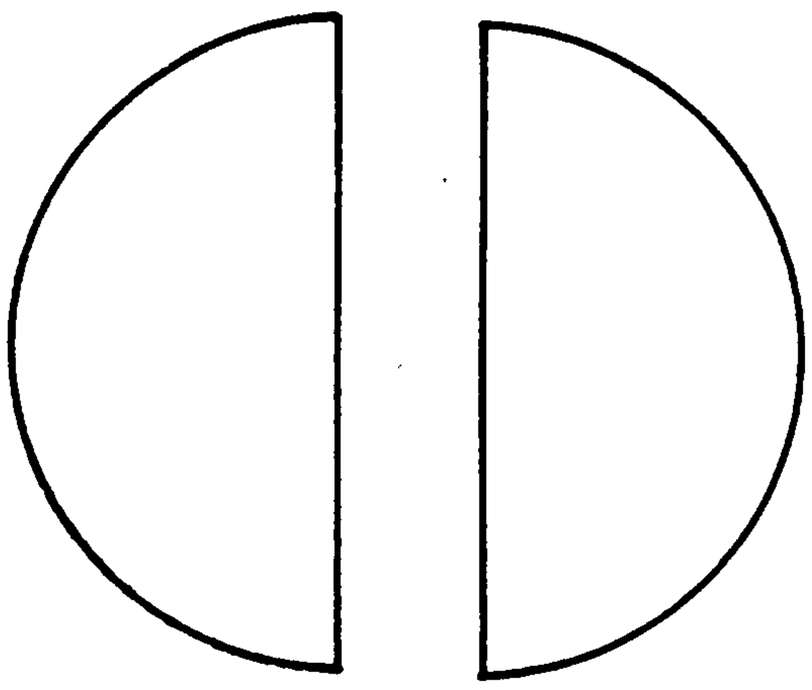

Triple Cleft Failure

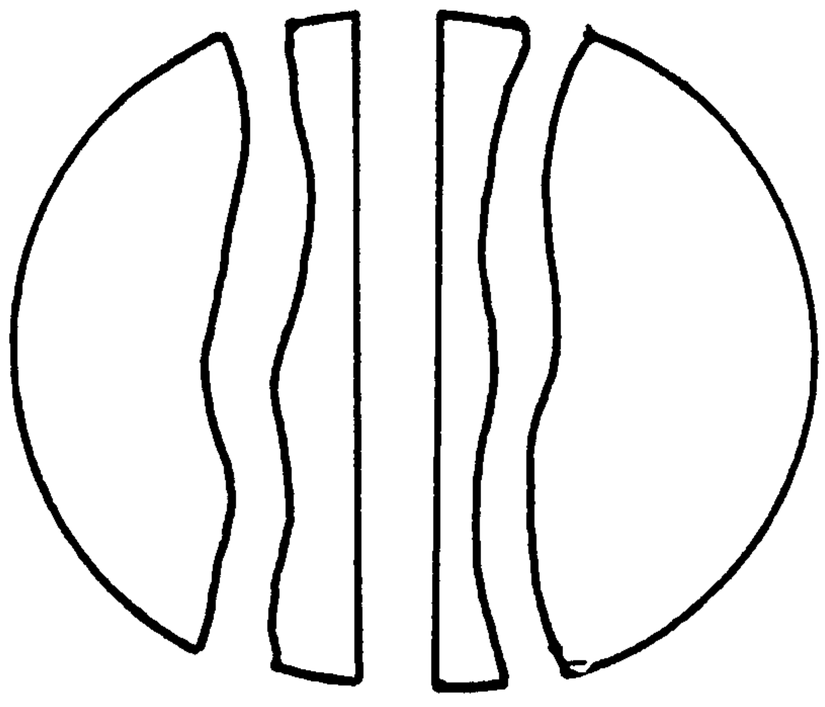

represent the true tensile strength. Rudnick et al. (1963) had previously commented that the tensile strength value is controlled by the test conditions and is true for each test. Thus, for comparison of different values and parameters, the test should be performed under the same conditions.

1.4.6 Tableting of modified materials

Several compaction studies have compared similar materials with various modifications. Varsano & Lachman (1966) found that potassium chloride crystals and granules behaved differently at lower compression loads than those of potassium citrate. They attributed this to inherent material properties rather than changes in particle size. York & Pilpel (1973) recognised a decrease in tablet tensile strength as the melting point of the fatty acid increased which was attributed to different amounts of interparticle bonding. Fell & Newton (1971), when studying spray dried and crystalline lactose, found that particle rearrangement was greater for smaller size fractions and that the yield pressure for spray dried samples was lower than that for crystalline materials. Summers et al. (1977) reported that the tensile strength of tablets prepared from metastable polymorphs of aspirin, barbitol and sulphathiazole was lower than for the stable form. This was attributed to the higher potential energy state of the metastable polymorph and weaker bonding, so the particle-particle bonds produced for the metastable were less than that for the stable form.

Since the physicochemical properties of materials can be advantageously modified by incorporating additives, it is appropriate to consider the further processing of these materials by tableting which is a widely used pharmaceutical operation. Thus the objective

of this part of the work was to examine the effect of incorporating small amounts of polymer into phenylbutazone on its compaction behaviour and tablet tensile strength together with a study of the effect of different material preparation techniques - direct crystallisation or spray drying - on these properties. The results, analysis and discussion of these experiments are presented in Chapter 7 of this thesis.

1.5 Materials selected for study

For this study phenylbutazone (PbZ) was chosen as a representative water insoluble drug. It was selected because:-

a) it exhibits an extremely low aqueous solubility

b) it is reported to exist in different polymorphic forms

c) it is thermally stable after melting which enables quantitative thermal analyses to be performed.

II Hydroxypropylmethylcellulose (H.P.M.C.)

This polymer was selected to be used as a carrier in this study because:-

a) it is a widely used hydrophilic polymer

b) it is approved for oral human use

c) it has not been used to our knowledge in previous solid dispersion studies

III Poloxamers

Poloxamers are a group of non-ionic surfactants having the general structure:-

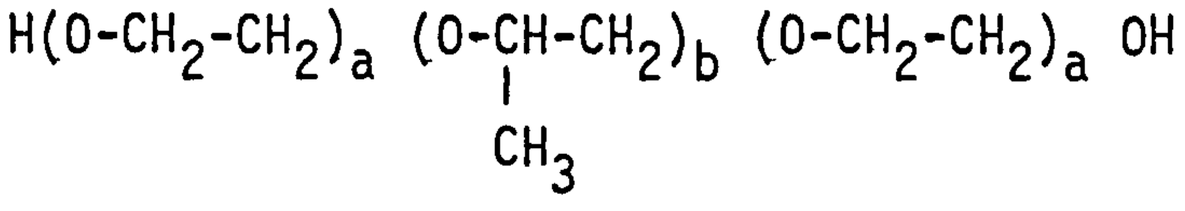

They were selected for use in this study because:-

a) they are non-ionic surfactants, so they would not have irritating effects when taken orally

b) a wide range of hydrophilic-libophilic balance is available within the group of compounds, due to differences in the polyoxypropylene-polyoxyethylene ratio.

The following chapters of the thesis present details of a study of the effects of incorporating polymeric additives into phenylbutazone using crystallisation and spray drying technique. Chapter 2 defines the materials used in the work and the experimental procedures followed.

Chapter 3 consists of three parts which present an evaluation of the spray dryer used, a study on the reported phenylbutazone polymorphs and a study on the effect of crystallisation rate on the polymorphism of phenylbutazone. The effects of presence of different amounts of H.P.M.C. and poloxamer on the physicochemical properties of phenylbutazone are presented in Chapters 4 and 5 respectively.

In Chapter 6 a study of the stability of the prepared powder samples stored under controlled conditions is reported and Chapter 7 reports on examination of the tableting properties of both spray dried

and crystallised samples of phenylbutazone: hydroxypropyl methylcellulose systems.

Whilst detailed discussions are provided in Chapters 3 to 7 inclusive, a general discussion of the results is provided in Chapter 8, and general conclusions and suggestions for future work.

CHAPTER 2

CHAPTER 2

2.1 Materials

Phenylbutazone powder (BP), Approved Prescription Services Ltd., Cleckheaton. Batch No. 109173.

The degradation products of phenylbutazone:

4 hydroxyphenylbutazone	(G 28 455)
α carboxy-N-caproylhydrazobenzene	(GP 40 588)
N caproylhydrazobenzene	(G 30 184)
α carboxy-α-hydroxy-N-caproylhydrazobenzene	(G 28 454)
N (α-ketocaproyl)-hydrazobenzene	(GP 46 060)
α-hydroxy-N-caproylhydrazobenzene	(GP 46 062)

All supplied by Ciba-Geigy, Basel, Switzerland.

n-Heptane, analar grade, BDH Chemicals Ltd., Poole, England. Batch No. 10363.

2-Propanol, analar grade, BDH Chemicals Ltd., Poole, England. Batch No. 10224.

Absolute alcohol (BP), James Burrough, England, claim 99.86% minimum.

Butan-2-ol, analar grade, BDH Chemicals Ltd., Poole, England. Batch No. 10316.

Cyclohexane, analar grade, BDH Chemicals Ltd., Poole, England.

Methanol, H.P.L.C. grade, Rathburn Chemicals Ltd., Scotland.

Potassium dihydrogen orthophosphate, analar grade, BDH Chemicals Ltd., Poole, England.

Acetonitrile, H.P.L.C. grade, Rathburn Chemicals Ltd., Scotland.

Salicylic acid, analar grade, BDH Chemicals Ltd., Poole, England. Batch No. 10226.

Acetone analar grade, BDH Chemicals Ltd., Poole, England.

Hydroxypropyl methylcellulose (H.P.M.C.)U.S.P.

pharmacoat 603 (CPS 3) lot no.57-022

pharmacoat 606 (CPS 6) lot no.57-035

pharmacoat 615 (CPS 15) lot no.57-712

All supplied by Shin-Etsu Chemical Co.Ltd., Japan.

Polyoxyethylene-polyoxypropylene glycols poloxamer surfactants

poloxamer 188 lot no. C 12/CC

poloxamer 407 lot no. H 01/L5

poloxamer 338 lot no. H 23/L5

poloxamer 184 lot no. C 66/CC

poloxamer 181 lot no. H 97/L5

poloxamer 101 lot no. C 64/CC

All supplied by Ugine Kuhlmann, Manchester.

Silica gel self indicating BDH Chemicals Ltd., Poole, England.

All other reagents are laboratory grade unless otherwise stated and all water used was double distilled from an all-glass still.

2.2 Methods

2.2.1 Assay of phenylbutazone

The B.P (1980) assay procedure was used to assay the purity of phenylbutazone powder. 0.5gm accurately weighed of phenylbutazone powder was dissolved in 25 mls of acetone then titrated against 0.1 N sodium hydroxide using 0.5 ml of bromethymol blue as indicator until a blue colour was obtained which persisted for fifteen seconds. Blank tests were carried out using the same procedure omitting the phenylbutazone powder. This assay was also used to estimate the amount of phenylbutazone in samples after recrystallising with H.P.M.C. and poloxamer surfactants. All tests were carried out at least in duplicate.

2.2.2 Ultraviolet spectrophotometer calibration curve

A scanning U.V. spectrophotometer (SP 800 Unicam, Cambridge) was used to check the wavelength of maximum absorbence. A calibration curve of U.V. absorbence against known concentrations of phenylbutazone in 0.01N sodium hydroxide was prepared using solutions containing between 0.0002 to 0.002 mg % of phenylbutazone, and the absorbence E, of each concentration was measured using a second U.V. spectrophotometer (Cecil Instruments CE 292, Cambridge). Maximum absorbence E was observed at 264 nm and a graph of E at 264 nm was plotted against concentration (see Fig. 2.1).

2.2.3 Buffer solution

For solubility and dissolution experiments a buffer medium consisting of 0.68% w/v dihydrogen orthophosphate at pH 7.5 (adjusted using 1 N sodium hydroxide), was used.

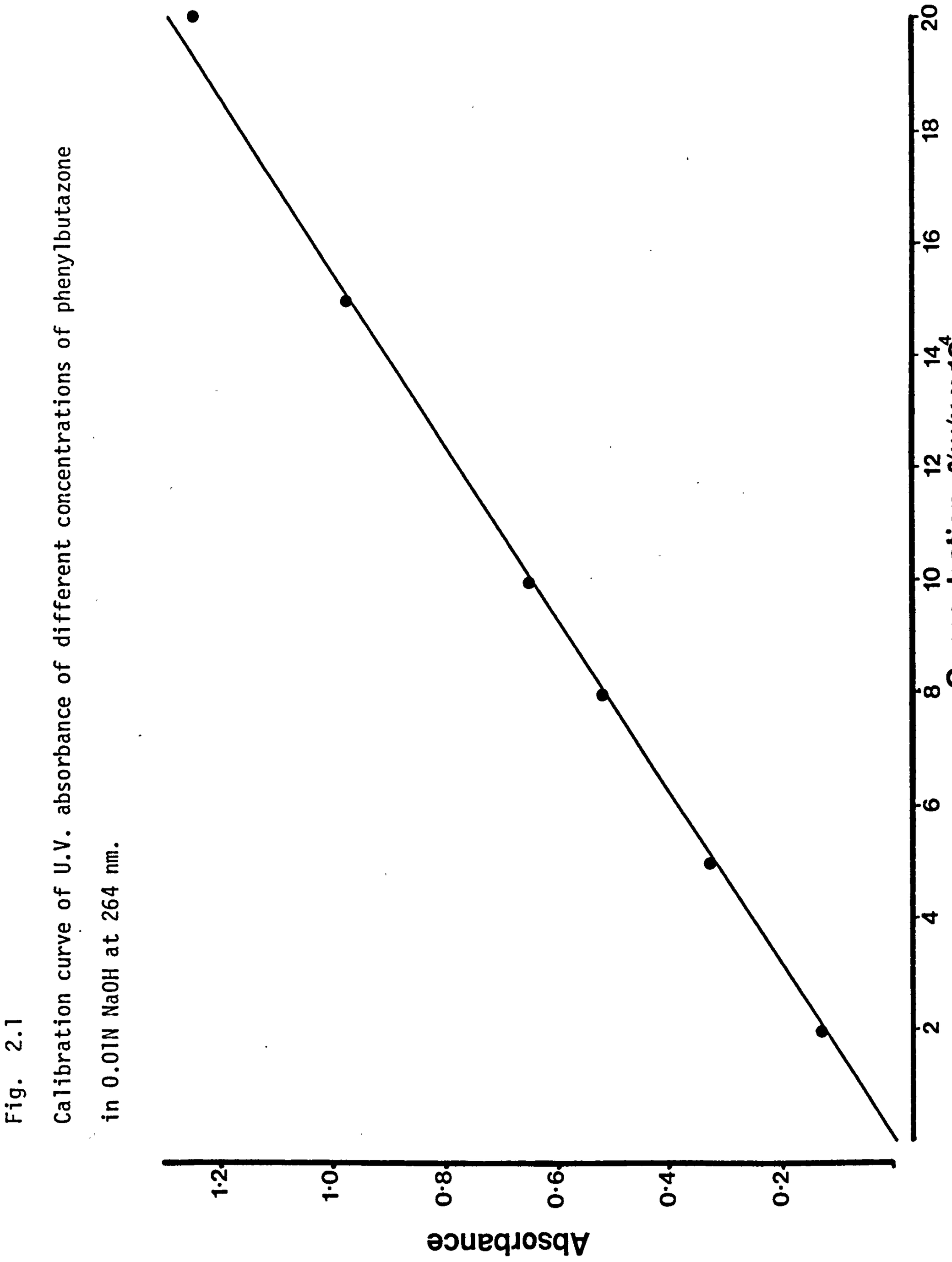

Fig. 2.1
Calibration curve of U.V. absorbance of different concentrations of phenylbutazone in 0.01N NaOH at 264 nm.

2.2.4 Solubility and intrinsic dissolution

The determination of the equilibrium dynamic solubility of samples was carried out in a shaking water bath (Gallenkamp, England) at $37^{o}C \pm 0.1^{o}C$ using phosphate buffer. An excess amount of the powder (1 gm) was placed in 100 ml of the buffer solution in a 250 ml stoppered conical flask which was then placed in the shaking water bath. Sampling was carried out at definite times by taking 1 ml of the solution with a 1 ml glass grade A syringe and filtering through a membrane filter (Millipore size 0.45 mm, Millipore). The volume was then completed to 100 ml using 0.01N sodium hydroxide. The U.V. absorbence of resulting solutions was measured at wavelength 264 nm.

The equilibrium dynamic solubility was measured using the same procedure at 20^{o}, 37^{o}, 50^{o} and $60^{o}C$, so that the data could be analysed by the Van't Hoff equation (Florence & Attwood 1981) to obtain ΔH_s, the enthalpy of solution.

$$\text{Log } K = \frac{-\Delta H s}{2.303RT} \qquad 2.1$$

Where K = solubility (mg/100 ml)

R = gas constant

T = absolute temperature (^{o}K)

Plots of log K against $\frac{1}{T}$ gave straight lines with slope = $\frac{-\Delta H_s}{2.303}$ from which ΔH_s was obtained.

To overcome the problems of particle size and surface changes during powder dissolution, intrinsic dissolution was carried out for the supplied phenylbutazone and all the prepared samples using a Wood's apparatus (see Fig. 2.2). This is designed to maintain constant surface area of 1.57 cm^2 of compressed powder during dissolution. Samples for dissolution were prepared by placing the die on a smooth surfaced

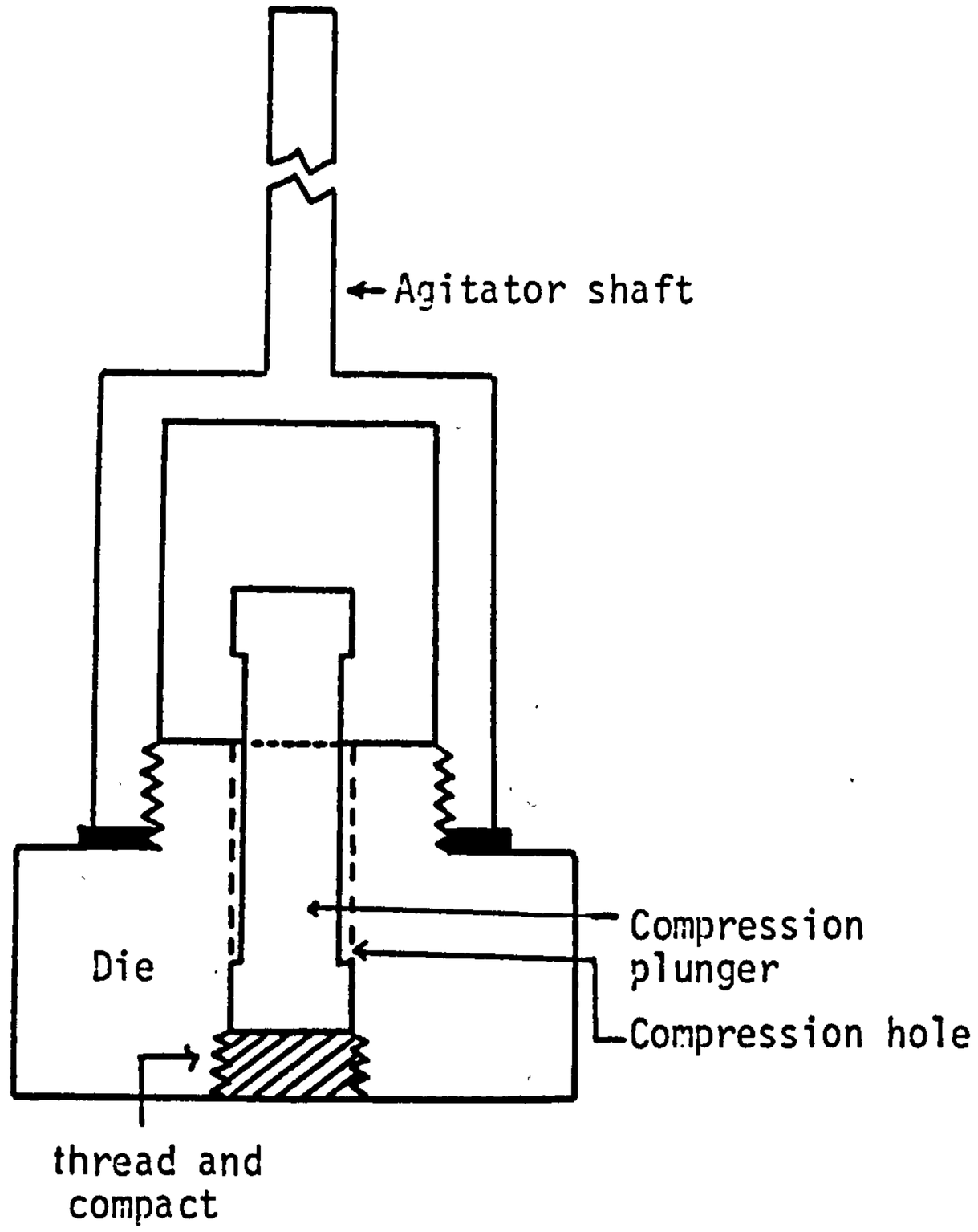

Fig. 2.2 Intrinsic dissolution testing apparatus

hardened stainless steel plate, then 300 mg of the powder previously sieved through a 200μm sieve was carefully layered into the hole in the die. The punch was then added and pressed using a manually operated hydraulic press (Apex PML) in a controlled manner to defined values of applied forces. The whole punch and die unit was attached to a rotating motor (Hieldolph RZPL, Germany) and placed in a constant positi in the dissolution medium which consisted of 600 mls of buffer solution in a one litre round-bottomed beaker at 37°C. Samples (10 ml) were taken at fixed time intervals and filtered using a membrane filter (Millipore size 0.45 mm). After each sampling, 10 ml of buffer at 37°C was added to keep the volume of the dissolution medium constant throughout the experiment.

The sample was then diluted to 100 ml using 0.01N sodium hydroxide and the concentration of drug released was measured using U.V. absorbence at 264 mM.

The dissolution rate of diffusion controlled process can be represented by the Noyes-Whitney equation (Florence & Attwood 1981) which may be written:-

$$\frac{dm}{dt} = K'A\ (C_s - C_o) \qquad 2.2$$

where $\frac{dm}{dt}$ = the rate of increase in the amount of material in solution

A = the area of the solvated tablet exposed to the dissolution medium

K' = the intrinsic dissolution rate constant

C_s = the maximum solubility

C_o = concentration of drug in solution at time t.

By having large receptor volume in comparison with the donor phase and ensuring "C_o" does not rise above approximately 10% of C_s, sink

conditions are achieved. In this situation the equation can be simplified to:-

$$\frac{dm}{dt} = K'.A \quad C_s \qquad 2.3$$

Since $M = V\ C_o$ where M = amount of material in solution and V = volume, the equation (2.3) can be written as

$$V\ C_o = K'.A\ C_s\ t \qquad 2.4$$

and $\frac{K'.A}{V}$ is the slope of the graphical representation of drug released against time.

For these experiments A, the constant surface area, could be calculated

$$A = 2\pi \quad (r)^2$$

$$1 = 2\pi \quad (0.5)^2 \quad = \quad 1.57\ cm^2$$

Thus the intrinsic dissolution constant (K') from compressed discs of prepared samples can be calculated using the expression:-

$$\text{Slope} = \frac{K'.A}{V} \qquad 2.5$$

However, for graphs of total drug released versus time this equation reducesto:-

$$\text{Slope} = K'.A$$

Initial experiments with compressed discs of as supplied phenylbutazone were carried out using speeds of rotation 60, 100 and 150 r.p.m. and compression force 175 KN. A second set of experiments using compression forces of 105 and 245 KN and rotation 100 r.p.m. was performed. Subsequent experiments were carried out at 100 r.p.m. and 175 KN.

2.2.5 Crystallisation of phenylbutazone

2.2.5.1 Preparation of polymorphism of phenylbutazone

Muller (1978) when preparing the α-polymorphic form of phenylbutazone (which as supplied, existsin the stable δ form), added water to a 2-propanol solution of phenylbutazone until the cloud point was reached. The solution was then warmed and allowed to cool rapidly. This procedure

was followed in this work and the resulting crystals were filtered using a sintered glass funnel and dried at 5°C under vacuum.

For the preparation of β-form, as reported by Muller (1978), samples were recrystallised by flocculating an ethanolic or n-heptane solution of phenylbutazone in water stirred at high speed.

Muller (1978) reported that the γ-form was prepared by heating the β-form to about 96°C then cooling down to 80°C, then reheating. An endothermic transition was observed on the D.S.C. thermogram at 105°C. Attempts were made using equivalent conditions in this work to isolate the γ-form of phenylbutazone.

2.2.5.2 Crystallising phenylbutazone with hydroxypropyl methylcellulose (H.P.M.C.).

a. Preparation of H.P.M.C. dispersion

The required amount of H.P.M.C. was added to one third of the total volume of water, preheated to 90°C and stirred with a glass rod until all the particles were wetted, then the remaining water was added cold with stirring. The warm solution was allowed to cool slowly to room temperature and a clear solution of required concentration was obtained.

b. Crystallising phenylbutazone with H.P.M.C.

The samples were prepared by dissolving 6 gms of phenylbutazone in 100 mls absolute alcohol at 60°C. The drug solution was then added to aqueous H.P.M.C. solutions containing H.P.M.C. concentrations of 0.01, 0.1, 1, 2 and 5% w/v. The formed crystals were left for one hour before collecting on a sintered glass filter and allowed to dry at room temperature under vacuum over self-indicating silica gel.

2.2.5.3 Crystallising phenylbutazone with polyoxyethylene-polyoxypropylene glycols (poloxamers)

The samples were prepared following the same procedure used to crystallise phenylbutazone with H.P.M.C. However, since the poloxamers are aqueous soluble they were dissolved directly in the water with simple stirring.

2.2.6 Crystal characterisation and polymorphic studies

2.2.6.1 Differential scanning calorimetry (D.S.C.)

Samples were analysed by thermal analysis using D.S.C. (DuPont 1090 thermal analyser and 910 differential scanning calorimeter, DuPont, Stevenage) (see Fig. 2.3).

The procedure involves heating the sample contained in an aluminium pan and a similar empty reference pan at a predetermined rate and over a predetermined temperature range. If a related change takes place in the sample the temperature of the sample lags (endotherm) or leads (exotherm) the reference pan temperature. The temperature difference between the sample and the reference is represented graphically in relation to the differential heat flow.

Heating rate is a very important factor affecting the melting point as well as the observation of polymorphic endothermic transitions. A series of different heating rates of 2, 5, 10, 20 and 50^{o}C/min was examined to identify the appropriate heating rate to be used for this study. (In this study the peak of melting endotherm was considered as the melting point of the tested sample). From this preliminary work, subsequent D.S.C. analyses were carried out using a standard heating rate of 10^{o}C/min and sample weight between 3-8mg over the temperature range 30-130^{o}C under nitrogen flow (10 ml/min) in a crimped aluminium pan with a pierced lid. The results were analysed using the DuPont

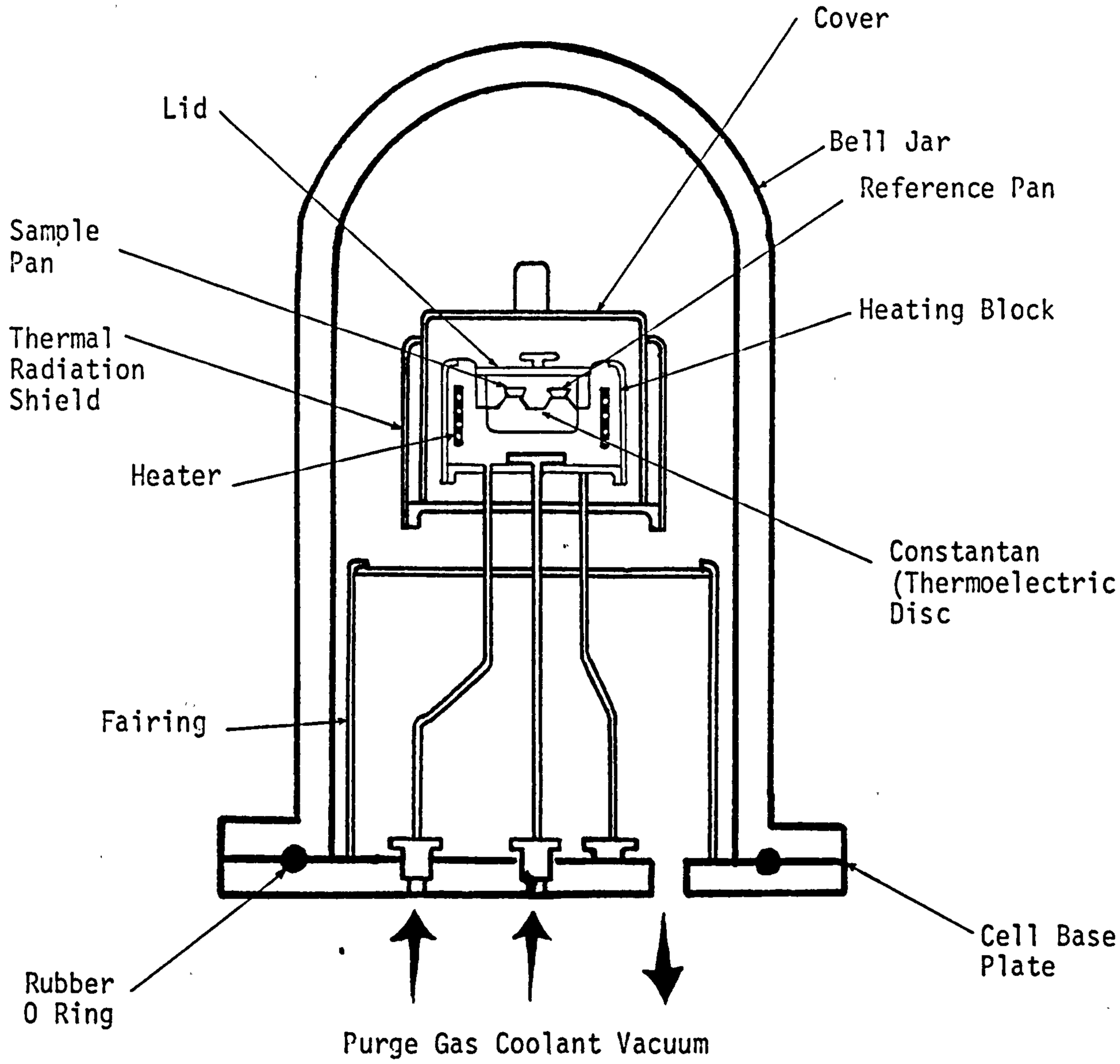

Fig. 2.3 Cross section of differential scanning calorimeter

interactive D.S.C. V.2 program to integrate the melting endotherms.

2.2.6.2 Determination of thermodynamic activation energy of the β-polymorph of phenylbutazone

The activation energy, Ea, of the transition endotherm for β-polymorph was calculated using the relationship after Kissenger (1975)

$$\frac{d \log \frac{\phi}{Tm^2}}{d \frac{1}{Tm}} = \frac{-Ea}{2.303R} \qquad 2.6$$

from the endothermic peak maximum temperature (Tm) observed after following different heating rates (ϕ) of 2, 5, 10, 15 and 20°C/min. The plot of log $\frac{\phi}{Tm^2}$ against $\frac{1}{Tm}$ gave a straight line with slope = $\frac{-Ea}{2.303R}$ from which Ea was calculated. R is the universal gas constant.

2.2.6.3 Thermogravimetry

The formation of solvates, and samples expected to form solvates or retain solvent, was investigated using a thermogravimetric analyser (DuPont 951 thermogravimetric analyser, DuPont, Stevenage). This consists of a microbalance with a sensitivity of $\pm 1 \times 10^{-2}$ mg. Samples (5-10 mg), loaded in the platinum cradle at one end of the microbalance arm, were heated at a programmed heating rate over a definite temperature range. Any weight losses, such as that due to the evolution of solvent, were recorded on the thermogram.

2.2.6.4 Powder X-ray diffraction

Samples for examination on an X-ray powder diffraction instrument (Philips PW 1120/00 with proportional detector probe, Holland) were prepared by filling powder into the cavity in the sample holder, then smoothing with a glass slide. The sample was then subjected to an X-ray radiation stream from a copper potassium-α electrode with wavelength of λ = 1.54059 A. The pattern was monitored on an attached

recorder (Philips, Holland) at a chart speed of 10 mm/min.

2.2.6.5 Infrared spectroscopy

The I.R. spectra of the samples were recorded on an infrared spectrophotometer (Pye Unicam SP 200, Cambridge) using nujol mulls.

2.2.6.6 Microscopy

a. Scanning electron microscope

Photomicrographs were obtained using a scanning electron microscope (Stereoscan 600, Cambridge Instruments, Cambridge) fitted with a back-scattered electron detector (K.E. Developments, Cambridge). All the samples were coated with gold (of thickness $\simeq$500Å) using a direct coating technique under vacuum (2×10^{-4} torr).

b. Optical microscope and particle sizing

An optical microscope with Olympus OM2 camera attachment was used to obtain photographs of the spray dried and crystallised phenylbutazone samples. The microscope was also used for sizing the spray dried samples using a calibrated linear graticule technique for measuring a linear dimension of particles in a constant direction. 600 particles were counted for each analysis.

c. Hot stage microscope

A zoom stereoscope microscope (Kyow, Tokyo) fitted with a hot stage attachment linked to a control unit (UTP Stanton Redcroft, London) was used to view the samples over a programmed temperature range to observe and record the melting point of the samples, and to monitor the physical changes occurring at any polymorphic transition. Samples were placed on a glass microscope cover slip, to minimise the heat difference between the sample and the heating plate.

All the samples were heated at $1^{o}C$/min.

2.7 Spray drying

Spray drying of phenylbutazone was carried out using a Büchi 190 mini-spray dryer (Büchi Laboratory Techniques Ltd., Switzerland) - see Fig. 2.4 - which operates on the principle of nozzle spraying with parallel flow i.e. the sprayed product and the drying air flow in the same direction.

The spray drying process was carried out by feeding the sample by means of a pump fixed on the top of the spray dryer, into the drying chamber in a very fine droplet form by means of an atomising air flow which was supplied from an air compressor. When the atomised small droplet was exposed to the hot temperature of the drying chamber (inlet temperature) the solvent evaporated rapidly leaving the dried powder. The powder and the solvent were transported to the cyclone separator by means of an aspiration force, and the solvent was separated from the dried product which collected in the sample collector. The solvent vapours were eliminated through the exhaust pipe.

2.7.1 Solvent used for spray drying

Aqueous ethanol was used as the spray drying solvent because phenylbutazone is virtually insoluble in water. A preliminary experiment to determine the solubility of phenylbutazone in aqueous ethanol and aqueous 2-propanol was carried out (see Fig. 2.5). The graphs show an increase in drug solubility with increasing alcohol component in the solvent system. From these results the concentration of 2% w/v phenylbutazone in 75% v/v ethanol in water was chosen for all spray drying processes.

Fig. 2.4 Buchi mini-spray dryer photograph

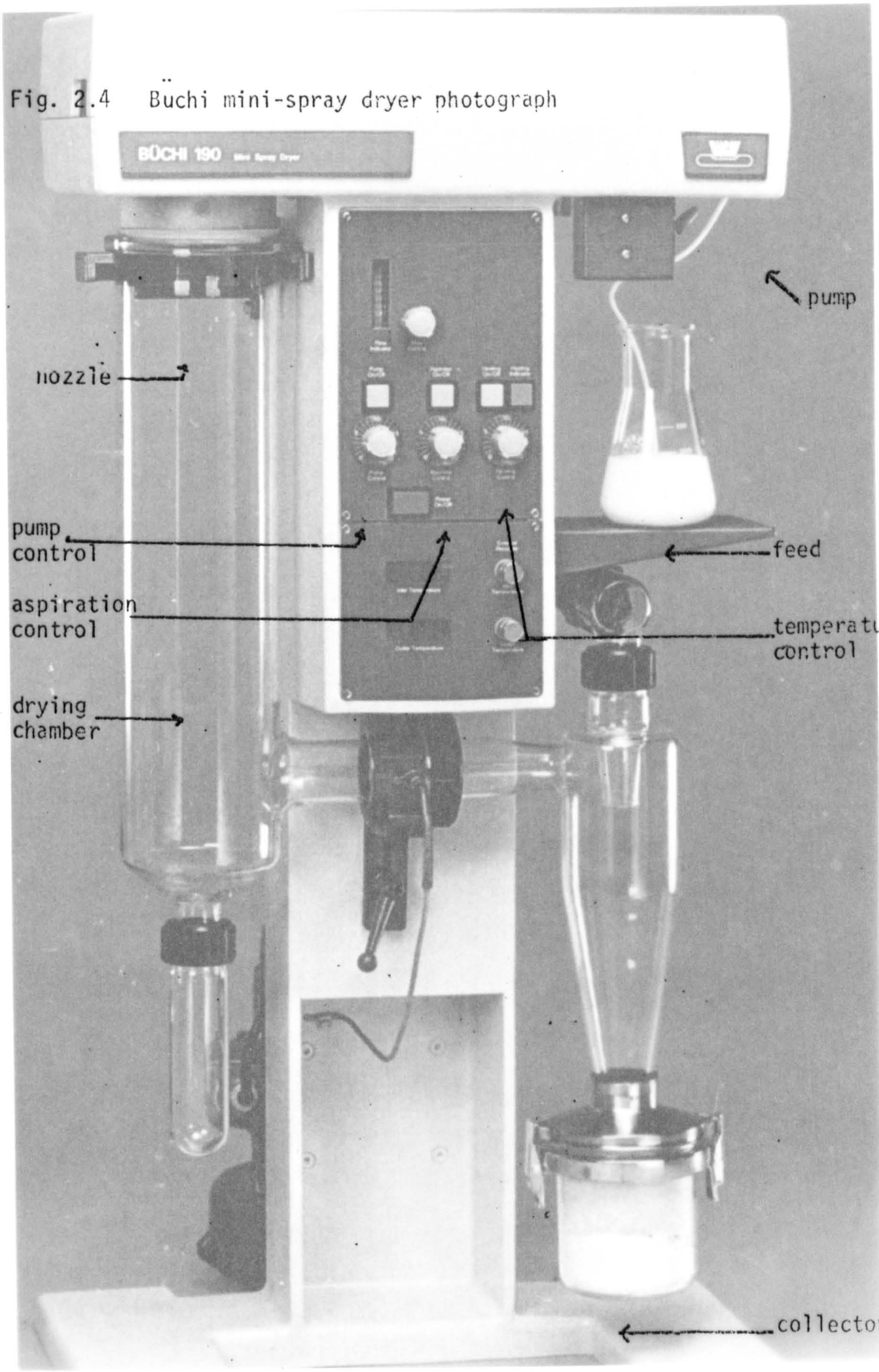

Fig. 2.5 Solubility of phenylbutazone in aqueous ethanol and 2 propanol mixtures at 25^{o} and $37^{o}C$.

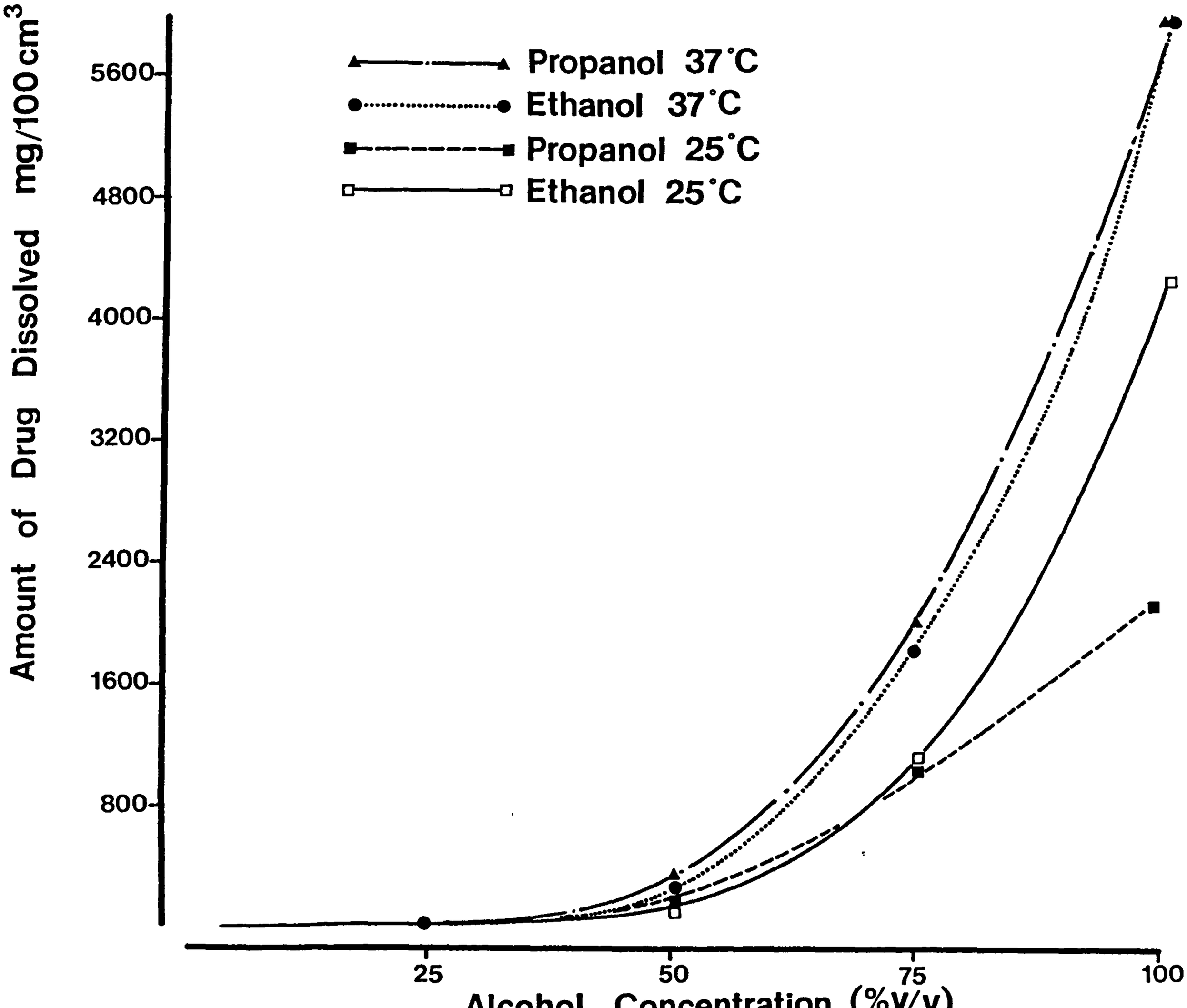

2.7.2 Spray drying of phenylbutazone

Solutions containing 2% w/v phenylbutzone in 75% v/v ethanol/water were spray dried using the Büchi mini-spray dryer. A full factorial analysis was carried out to assess the effect of the four monitored variables in the spray dryer (inlet temperature,pump rate, flow rate and aspiration rate) on the properties of spray-dried products such as particle size, per cent efficiency of process (i.e. $\left(\frac{\text{wt product}}{\text{wt phenylbutazone used}}\right) \times 100\%$) and number of peaks on the D.S.C. thermogram of prepared samples. Three levels of each variable were selected. For pumping rate 4 ml/min, 8 ml/min and 16 ml/min were employed and for flow rate 200, 400 and 600 l/h were selected. Aspiration rates (measured using an anemometer (Airflow Developments Ltd., High Wycombe, TA 3000))were 0.00823 m^3/sec, 0.00903 m^3/sec and 0.01060 m^3/sec. 100, 125 and 145^oC were the three inlet temperatures selected. In each run 200ml of 2% w/v phenylbutazone solution was spray dried and the outlet temperature (which is the temperature of the airstream containing the solid particles before entering the cyclone) was monitored. Efficiency of process as well as the particle size of the product were measured, and each run was carried out at least in duplicate.

2.8 High pressure liquid chromatography (H.P.L.C.)

2.8.1 Calibration curve for phenylbutazone and its degradation compounds

A high pressure liquid chromatograph with variable wavelength U.V. detector (Pye Unicam L.C. U.V. detector) was used. A 20µl sample was injected via a microsyringe (S.G.E. Type A-RN) to a Particil-10 ODS reversed phase column 25 cm x 4.6 mm internal diameter, packed by the pressurised slurry method in methanol.

Initially an attempt to reproduce the system reported by Fabre (1982) was made using an equivalent column. The mobile phase consisted of a degased 60:40 mixture of 0.1 M trimethomine citrate buffer (pH 5.25): acetonitrile. However this proved generally unsatisfactory since the column repeatedly blocked. One possible explanation is that the citric acid in the buffer which was used to adjust the pH crystallised inside the column causing blockage.

After screening other systems it was found that two solvent systems were required to resolve all seven materials (six breakdown products and phenylbutazone) (see Table 6.1). The first system used was methanol H.P.L.C. grade 58% v/v and double distilled water 42% v/v, for resolving, identifying and quantifying degradation products No.III, IV, V, and VI. The second system was 42% v/v methanol and 58% v/v water which resolved phenylbutazone and degradation product No.II. Degradation No.I was excluded because it was found to change slowly to No.III on dissolving in the solvent. In all cases analar grade salicylic acid was used as an internal standard. To obtain the calibration curve each of the degradation products and phenylbutazone was run at four concentrations 25µg, 12.5µg, 6.25µg and 3.125µg together with 10µg of internal standard in all samples at a flow rate of 2 ml/min, pressure 188±2 bars, detector sensitivity 0.08, and chart speed 10 mm/min. The absorbence was measured at 237µm and calibration curves were plotted see Figs. (2.6, 2.7, 2.8).

2.8.2 Testing the spray-dried samples

A number of spray-dried samples were selected to be tested by H.P.L.C. for presence of decomposition products. These samples were chosen to represent those prepared under the extreme conditions that phenylbutazone was exposed to during spray drying. These samples were

Fig. 2.6

Calibration curves of degradation product No.III and V of phenylbutazone from HPLC analysis.

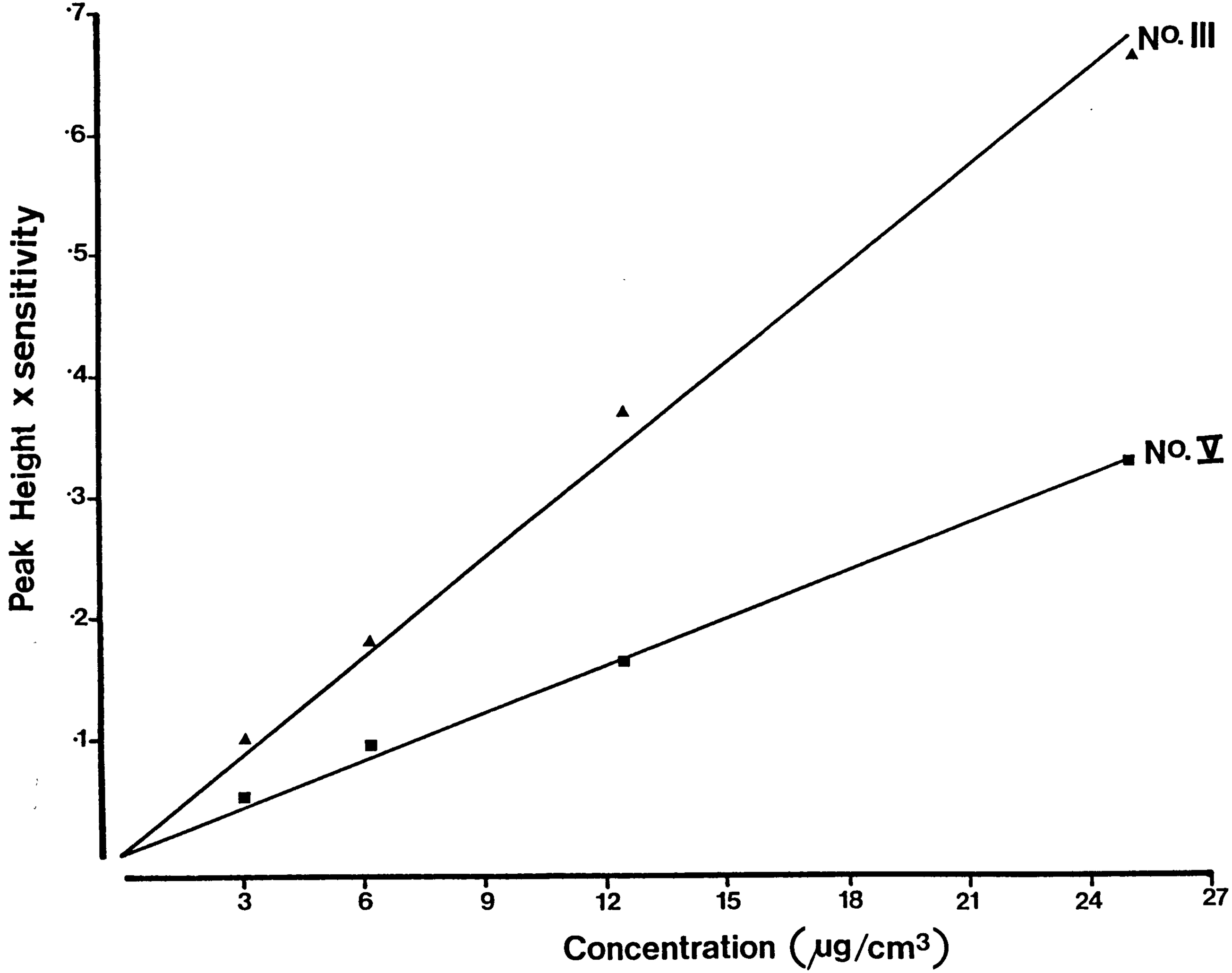

Fig. 2.7

Calibration curve of degradation product No.II from HPLC analysis.

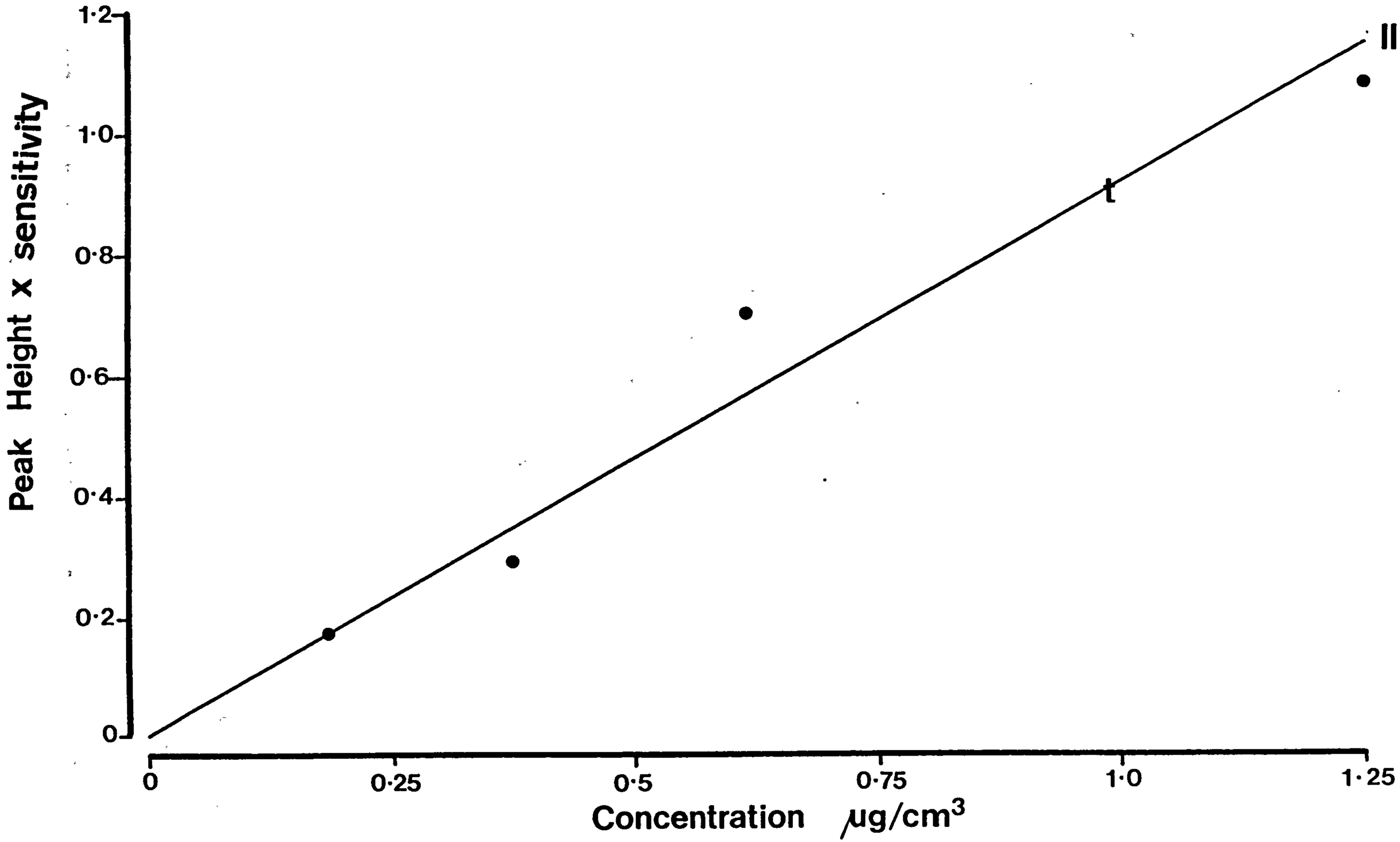

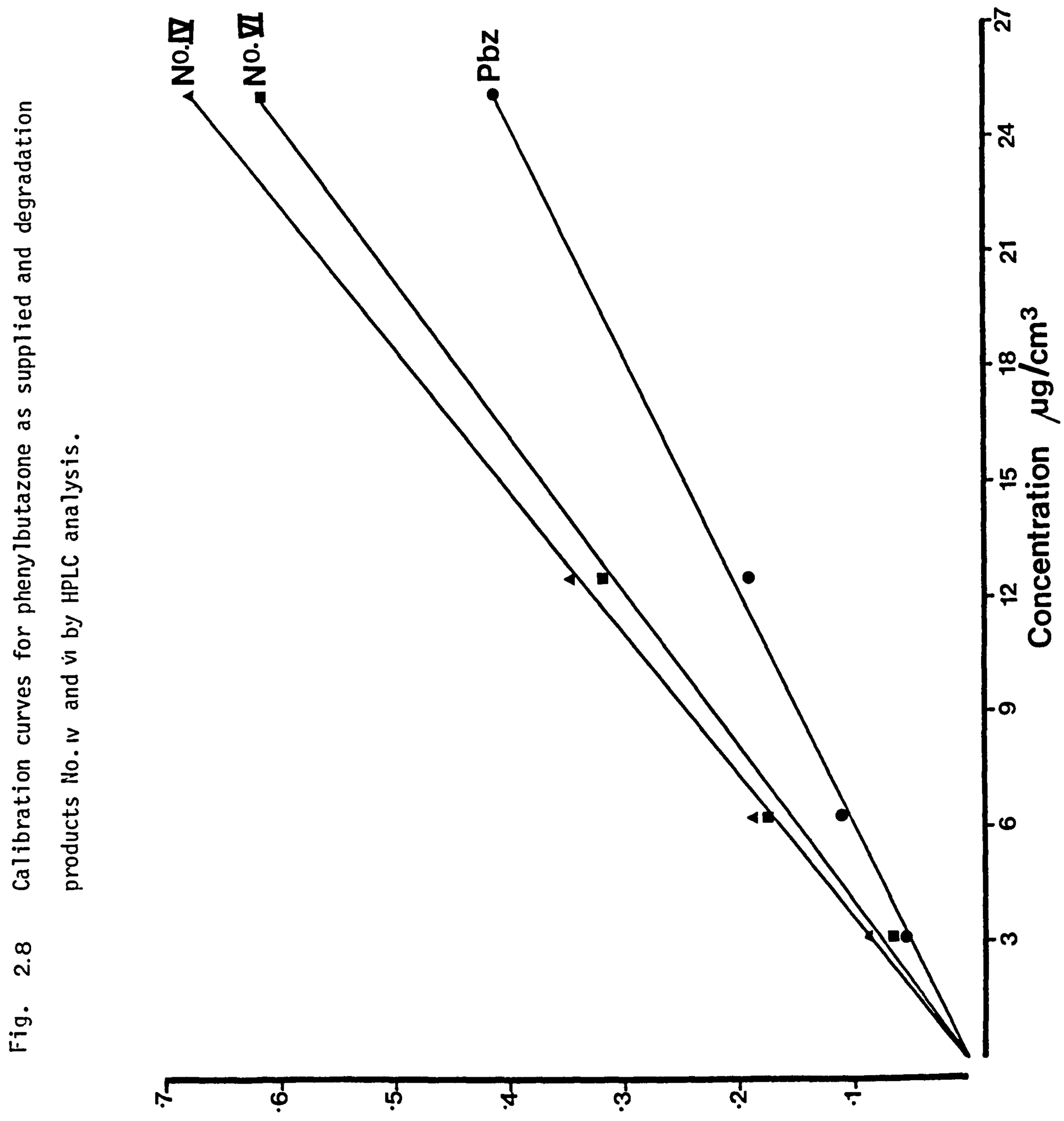

Fig. 2.8 Calibration curves for phenylbutazone as supplied and degradation products No.iv and vi by HPLC analysis.

analysed using the same conditions as those listed for calibration curve preparation.

2.9 Stability testing

Five samples were subjected to a stability testing programme.

2.9.1 Materials

the original as supplied phenylbutazone

phenylbutazone crystallised from 2% w/v HPMC solution (PHS4)

phenylbutazone spray dried from 2% w/v HPMC solution (PHR4)

phenylbutazone crystallised from 1% w/v poloxamer 188 solution (PPR3)

phenylbutazone spray dried from 1% w/v poloxamer 188 solution (PPS3)

2. 9.2 Method

Portions (3 gms) of these samples were each stored under four conditions - 20°C, 37°C and 50°C in sealed containers and also in open containers at 20°C and 40%±5% RH. The samples were tested for any degradatio or change inthermal behaviour using H.P.L.C. and D.S.C. initially and after 3 and 6 months to check any change in D.S.C. thermograms and H.P.L.C. profiles.

2.10 Tableting

2.10.1 True density measurement

The true density of the powder samples was measured using an air comparison pycnometer (Model 930, Beckman). By placing a known weight of powder in a sample bottle of known volume previously determined, the true density can be determined.

2.10.2 Instrumented tablet machine

Tableting was performed using a single punch tablet machine (Manesty Type E) fitted with ½" flat faced punches instrumented with load cells (Kistler Type 901) see Fig. 2.9a,b.The charge induced in the

Fig. 2.9a

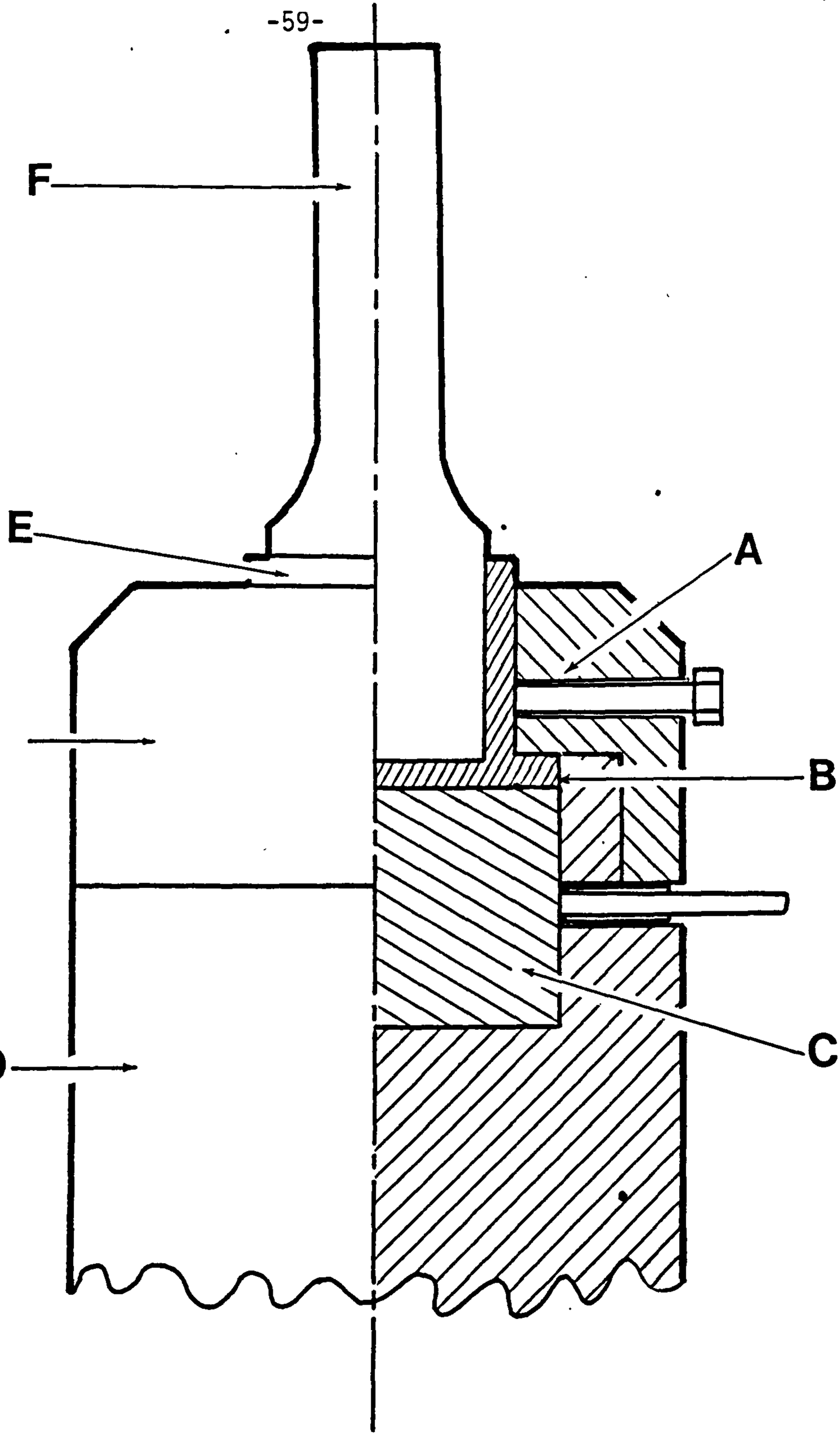

Instrumented tablet machine lower punch assembly

A - Piezo-electric load transducer
B - Force distributing washer
C - P.T.F.E. insulating plug
D - Lower punch
E - P.T.F.E. insulating sleeve
F - Lower punch holder

Fig. 2.9b

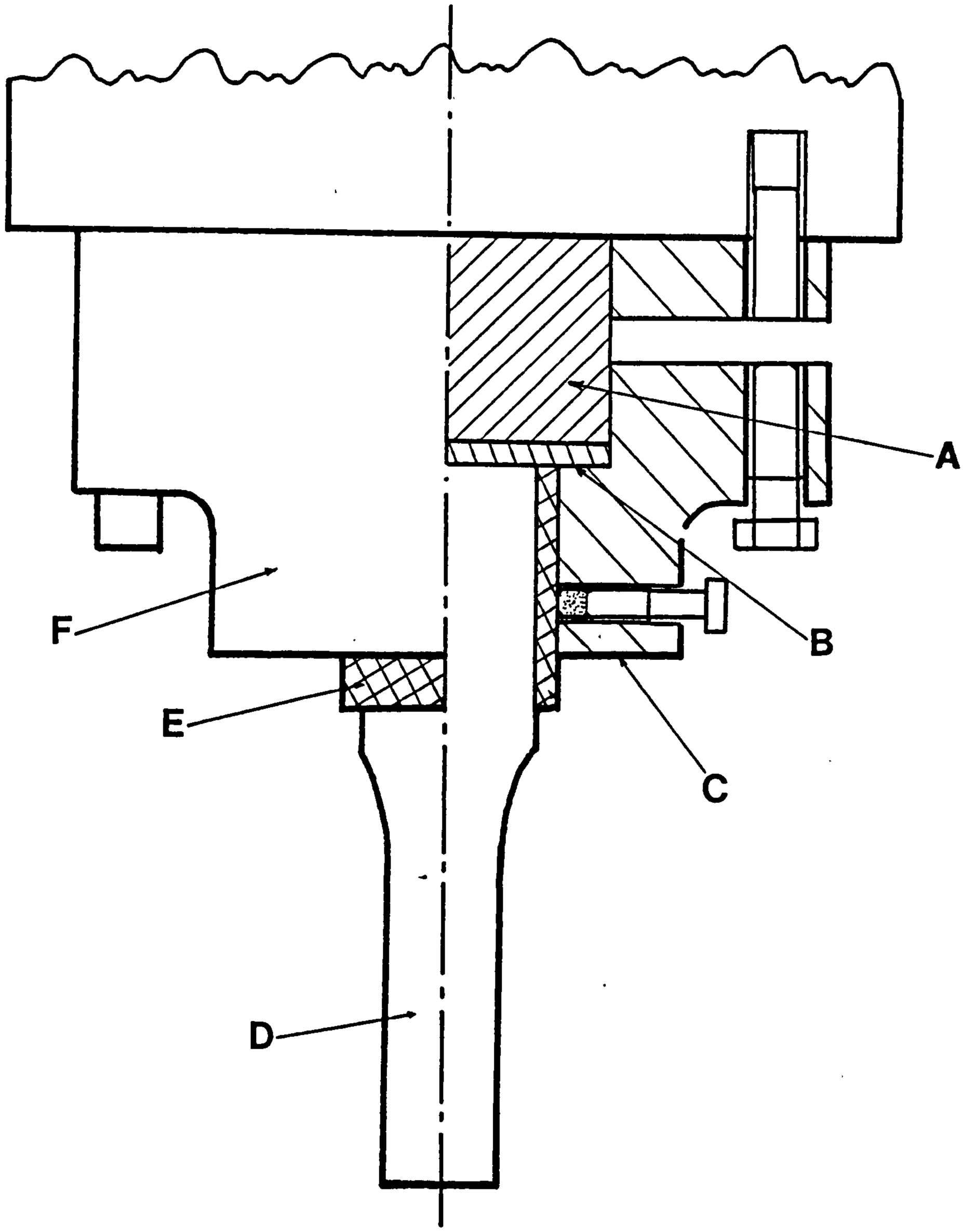

Instrumented tablet machine upper punch assembly

A - Piezo-electric load transducer
B - Force distributing washer
C - P.T.F.E. insulating plug
D - Upper punch
E - P.T.F.E. insulating sleeve
F - Upper punch holder

load cells which were positioned above the upper and below the lower punch during a compression gave signals proportional to the load, which were then amplified through the charge amplifiers (Kistler, Type 5006) and fed to a CP100 micro-computer (Comart Ltd., Winlingdon, England). The micro-computer has two floppy disc drives, each with a capacity of 390K bytes, which uses the CP/M operating system for the 8080 micro-processor .The computer was connected to a visual display unit, V.D.U., (Model 910, Teletype).

The voltage outputs from the charge amplifier connected to the load washers could not be fed and analysed directly by the computer as they must be converted to digital pulses. For this a Model-12 analogue to digital converter, ADC (Duel System Control, Cerforation, USA) was used (see Fig. 2.10). The output from the load cells could then be fed and stored in the computer which enabled interpretation of the maximal force applied to upper punch and the maximal force transmitted to the lower punch. Together with knowledge of the tablet weight and material density, the tablet volume, porosity and Heckel function could be calculated.

Calibration of the load washers involved using a third load washer independently mounted (Type 903A, Kistler) which was calibrated against a universal testing machine, T42 Orion calibrated to grade A standard. The upper punch load washer was then calibrated by applying the punch face against the calibrated load washer. The lower punch washer was subsequently calibrated against the upper punch washer by inverting a cylindrical stainless steel plug (diameter = 10m, height = 10mm), in the die and applying force via the upper punch. The relevant calibration curves are illustrated in Figs. (2.11, 2.12, 2.13).

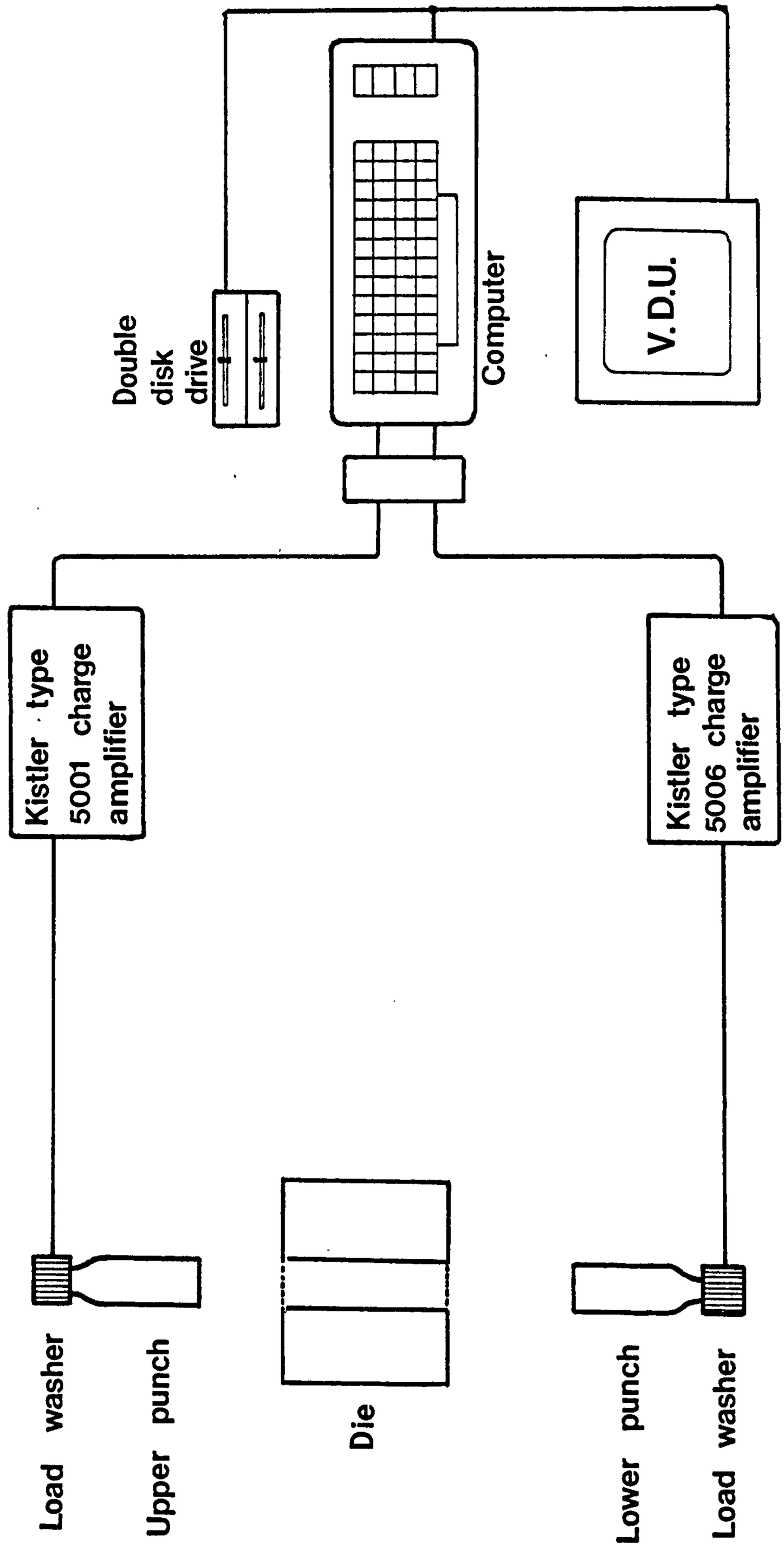

Fig. 2.10 Schematic representation of the connections of the tableting machine linkage to the computer and visual display unit

Fig. 2.11

Calibration curve for upper punch load washer.

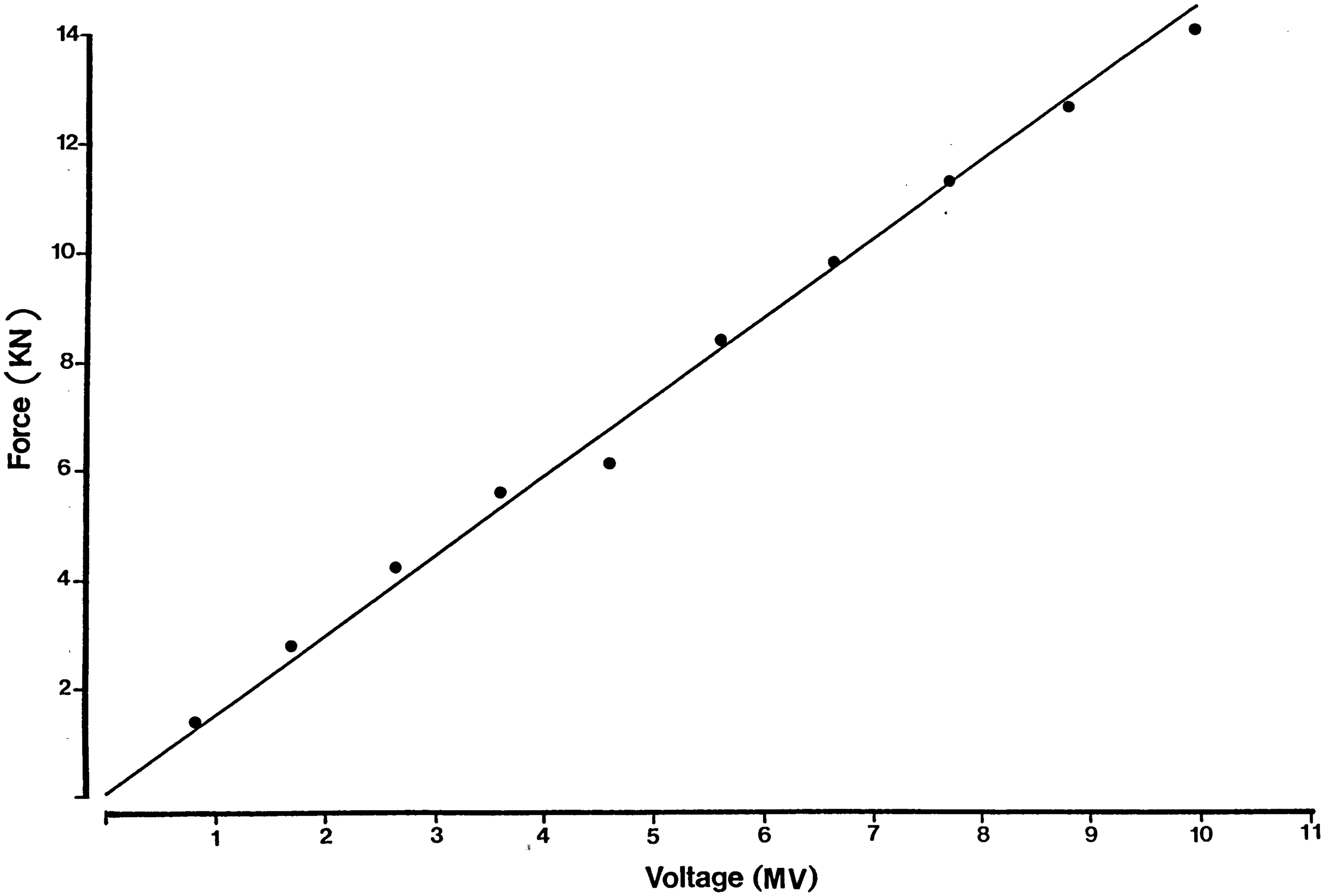

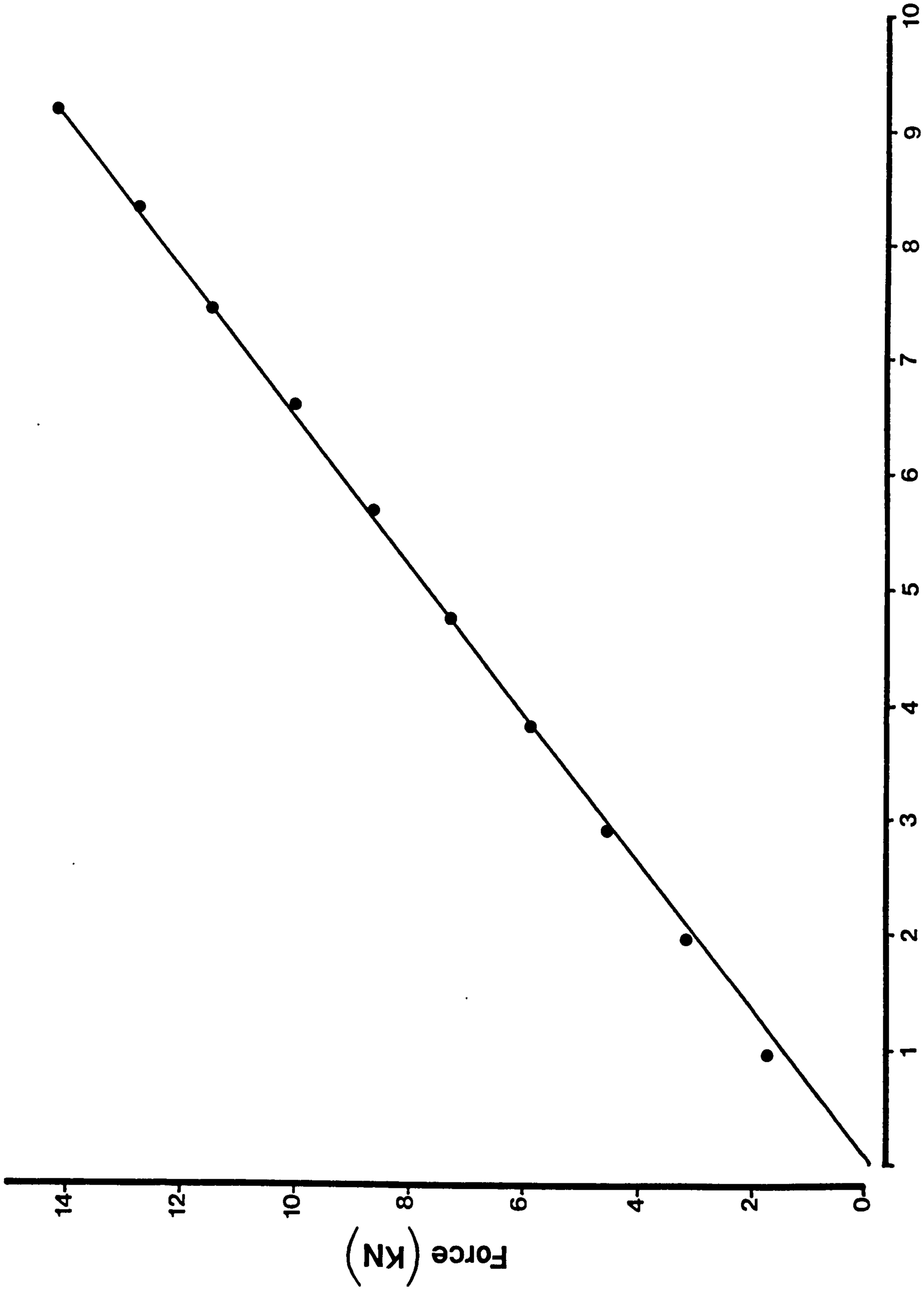

Fig. 2.12 Calibration curve for lower punch load washer.

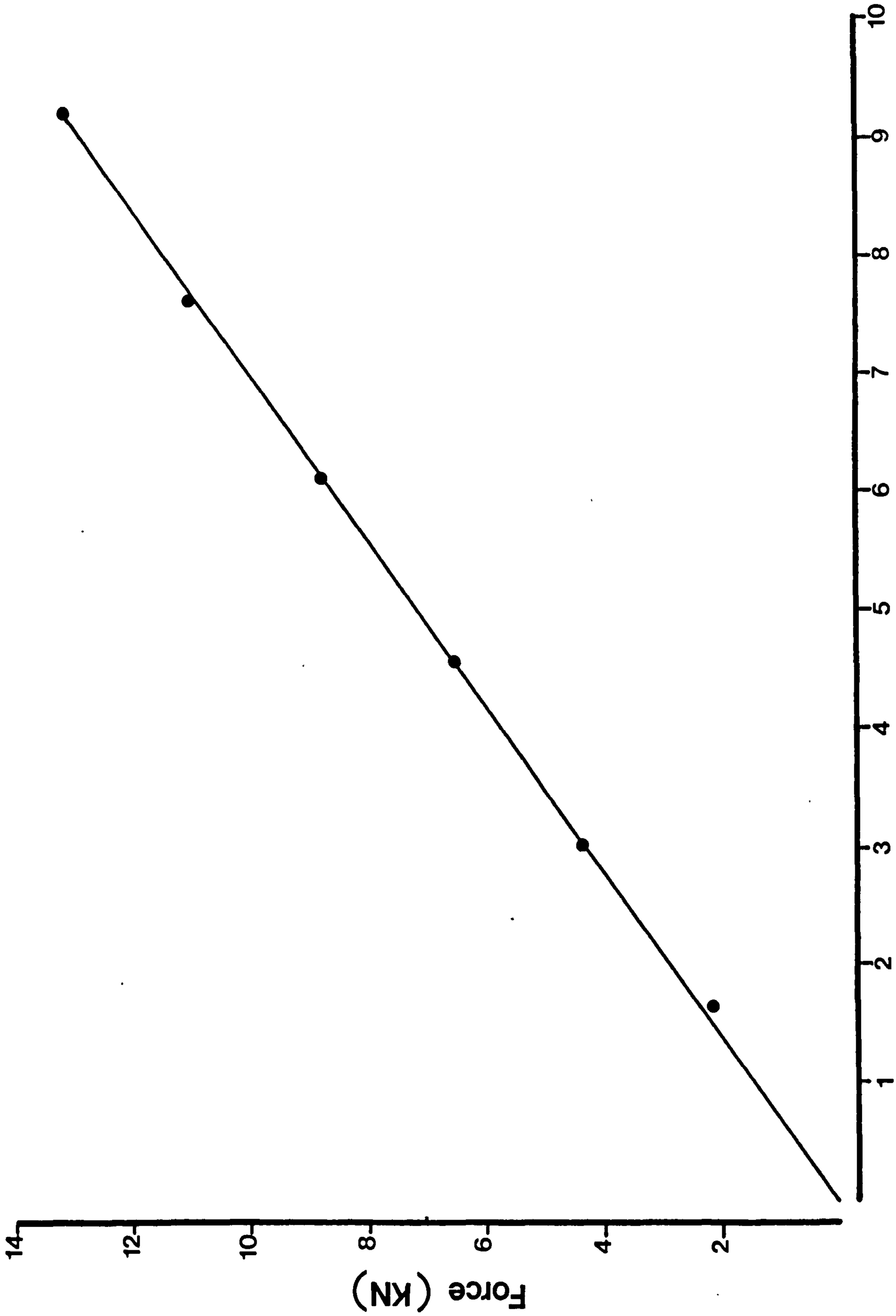

Fig. 2.13 Calibration curve for 903A calibrating load washer

To prepare tablets the powders were sieved through a 200μm sieve. The lower punch was lowered to its lowest position and 400 mg of the powder sample was carefully placed in the unlubricated die. The upper punch was positioned at its maximal height. The tableting machine was switched on for a single tablet press, then switched off immediately the upper punch had emerged from the die. After removal of each tablet, the punches and die were cleaned and wiped carefully by mechanical rubbing with a tissue. The thickness and diameter of the tablet were measured via a micrometer Type 130/5 (Mercer, England) to ±0.01 mm after ejection. The tablets were then left for 5 days under controlled environmental conditions, (20^{o}C and 40±5% RH). Then tablet thickness and diameter were remeasured. A minimum of five tablets were prepared at each compression force examined for all samples.

2.10.3 Tablet tensile strength

After storage for 5 days the crushing strengths of the tablets were measured using a Hebelein tester (Mod. 2E/205 - Switzerland). When the tablets were observed to break into two semi-circular sections after failure i.e. tensile failure, equation 2.7 was applied to estimate the tensile strength.

$$\text{Tensile strength} = \frac{2\text{x crushing force x } 9.81\text{x}10^{-6}}{\pi\text{x radius(m) x thickness(m)}} \quad \text{MPa} \qquad 2.7$$

A minimum of five tablets for each sample were examined.

CHAPTER 3

CHAPTER 3 - Spray drying of phenylbutazone and study of phenylbutazone polymorphism

3.1 The Büchi mini spray

3.1.1 Introduction

Spray drying is a useful technique for incorporating additives to drugs (Takenaka et al. 1980, 1981). As mentioned previously spray drying was used in this work as an alternative method of incorporating hydrophilic polymers with phenylbutazone. For this purpose the Büchi mini-spray dryer was used. The spray dryer has a number of operation variables. It was thought useful initially to study the effect of each variable on the performance of the spray dryer and to study the polymorphic transitions which might occur during spray drying, and the effect of spray drying on the stability of the product.

3.1.2 Evaluation of spray dryer

In an attempt to provide understanding of the effect of the operating variables on the performance of the spray dryer, a full factorial experiment was carried out at three levels of inlet temperature, pump rate, aspiration rate and two levels of flow rate (see Table 3.1). Experiments were carried out as given in Chapter 2.

3.1.2.1 Process efficiency

The process efficiency was defined as the percentage w/w of dried product recovered to the total amount of solid spray dried.

Analysis of the efficiency of the process data and calculation of the variance of the factorial experiments was carried out. However when the F-test (Moroney 1980) was applied to consider the interaction of the variables the F-figures were significant at all levels and further examination was not attempted (Moroney 1980). However when the results in Table 3.2 of each single variance were considered as a

Table 3.1 Efficiency of process and particle size of product under different conditions of spray drying process

Inlet Temperature	Aspiration rate (m^3/sec)	Pump rate (ml/min)	Flow rate (L/hr)	Outlet temp.	Efficiency of process % w/w	Run No.	Median Particle size in µm
		4	400	61°C	17.5%	28	17.0
			600	56°C	20.4%	1	28.5
	0.008232	8	400	51°C	0.5%	27	23.0
			600	50°C	26.5%	29	21.6
		16	400	38°C	12.3%	30	22.0
			600	36°C	16.0%	31	16.5
		4	400	62°C	32.5%	32	17.5
			600	60°C	22.5%	33	16.0
100°C	0.00903	8	400	55°C	11.0%	34	18.0
			600	53°C	12.5%	35	14.5
		16	400	39°C	15.0%	38	17.0
			600	38°C	17.5%	39	12.8
		4	400	64°C	32.0%	41	16.5
			600	63°C	21.0%	36	10.2
	0.0106	8	400	60°C	11.0%	43	20.0
			600	58°C	12.5%	44	16.0
		16	400	48°C	1.5%	42	18.5
			600	46°C	31.0%	37	14.5

cont ....

Table 3.1 cont ....

Inlet Temperature	Aspiration rate (m^3/sec)	Pump rate (ml/min)	Flow rate (L/hr)	Outlet temp.	Efficiency of process % w/w	Run No.	Median Particle size in µm
		4	400	65°C	18.0%	4	27.5
			600	62°C	16.0%	2	26.5
	0.008232	8	400	60°C	13.5%	45	25.5
			600	59°C	13.0%	46	14.0
		16	400	53°C	3.0%	47	18.0
			600	40°C	13.0%	48	14.0
		4	400	72°C	1.3%	49	16.5
			600	67°C	21.0%	50	19.0
125°C	0.00903	8	400	66°C	20.5%	40	14.5
			600	63°C	10.0%	57	15.0
		16	400	54°C	8.5%	57	18.0
			600	5o°C	9.0%	56	16.0
		4	400	79°C	19.5%	14	19.0
			600	78°C	22.5%	52	17.0
	0.0106	8	400	74°C	23.5%	53	21.0
			600	70°C	26.0%	54	19.0
		16	400	52°C	4.0%	55	21.0
			600	60°C	20.0%	51	16.5

cont ....

Table 3.1 cont ....

Inlet Temperature	Aspiration rate (m^3/sec)	Pump rate (ml/min)	Flow rate (L/hr)	Outlet temp.	Efficiency of process % w/w	Run No.	Median Particle size in µm
		4	400	83°C	20.0%	13	17.0
			600	81°C	23.0%	5	16.0
	0.008232	8	400	74°C	10.0%	15	39.0
			600	72°C	16.0%	18	22.0
		16	400	86°C	5.0%	8	33.5
			600	62°C	23.0%	7	24.0
		4	400	86°C	0.5%	23	20.0
			600	85°C	21.5%	19	17.0
145°C	0.00903	8	400	82°C	20.5%	58	27.0
			600	74°C	18.3%	11	17.0
		16	400	69°C	2.5%	24	25.0
			600	63°C	5.0%	20	22.0
		4	400	97°C	0.5%	21	40.0
			600	90°C	13.0%	26	28.0
	0.0106	8	400	85°C	2.0%	16	24.0
			600	81°C	22.0%	25	21.0
		16	400	73°C	9.5%	22	31.0
			600	72°C	8.5%	19	21.0

Table 3.2 Analysis of variance of process efficiency using factorial experiment results

Nature of Effect	Source	Sum of squares	d.f.	Variance estimate
Main factors	T	5.5	2	2.775
	A	0.18	2	0.09
	R	11.75	2	5.875
	F	7.8	1	7.8
Interaction between pairs of factors	T.A	4.6	4	1.15
	T.R	8	4	2
	T.F	1.5	2	0.75
	A.R	1.25	4	0.3125
	A.F	2.5	2	1.25
	R.F	0.8	2	0.4
Interaction between triplets of factors	T.A.R	4.76	8	0.595
	T.A.F	2.28	4	0.57
	T.R.F	2.98	4	0.745
	A.R.F	3	4	0.75
Interaction of all factors	T.A.R.F	12.2	8	1.525
Replication	Residual	7.05	54	0.13
Total		76.2	107	

Key:

T = inlet temperature

A = aspiration rate

R = pump rate

F = air flow

guideline for the effect on each processing variable, the pump and flow rates appear to have a more significant effect on the process efficiency as they show higher variance figures. This agrees with the practical point that increasing the pump rate increased the amount of feed per unit time. Increasing the flow rate will decrease the size of the droplet which needs a shorter time to dry. Thus the chance of the product not drying completely and sticking to the wall of the chamber increases, thereby reducing the process efficiency. The relatively low percentages of solid recovered are attributed to the small amounts used in these preliminary experiments and the fact that when spray drying the products tended to attach to the corners and wall of the glassware of the spray dryer. When larger batches of material were dried, efficiency figures increased.

3.1.2.2 Particle size of product

Analysis of the particle size data from the factorial experiments and application of the F-test produced significant results at all levels indicating that all four processing variables have an effect on the particle size of the product. However from Table 3.3 a rank order of variable influence on particle size emerges - aspiration rate>inlet temperature>flow rate>pump rate. Optical microscope analysis and photographs indicated that increasing the inlet temperature in general increases the size of the spray dried-particles (Fig. 3.1).

At the highest temperature used, particles do not exhibit conventional spherical shape, but branch irregularly. This appearance can be attributed to very rapid solvent evaporation from the sprayed droplets in the hot drying chamber causing irregular rupture of the droplet (flash drying) because there is a need for a very rapid solvent dissipation. This might be the same principle as in the case of rapid

Table 3.3 Analysis of variance of particle size using factorial experiment results

Nature of Effect	Source	Sum of squares	d.f.	Variance estimate
Main factors	T	83.2	2	41.6
	A	123.7	2	61.85
	R	3	2	1.5
	F	21.4	1	21.4
Interaction between pairs of factors	T.A	264	4	66
	T.R	120.9	4	30.225
	T.F	57.4	2	28.7
	A.R	98.7	4	24.675
	A.F	91.6	2	45.8
	R.F	87.9	2	43.95
Interaction between triplets of factors	T.A.R	166.2	8	20.775
	T.A.F	99.4	4	24.85
	T.R.F	14.3	4	3.575
	A.R.F	38.3	4	9.575
Interaction of all factors	T.A.R.F	136.4	8	17.05
Replication	Residual	208.03	54	3.85
Total		1625.11	107	

Key:

T = inlet temperature

A = aspiration rate

R = R pump rate

F = air flow

Fig. 3.1

Size distribution curves for samples of phenylbutazone spray dried under different conditions.

Crystallisation rate - 1>2>3>4

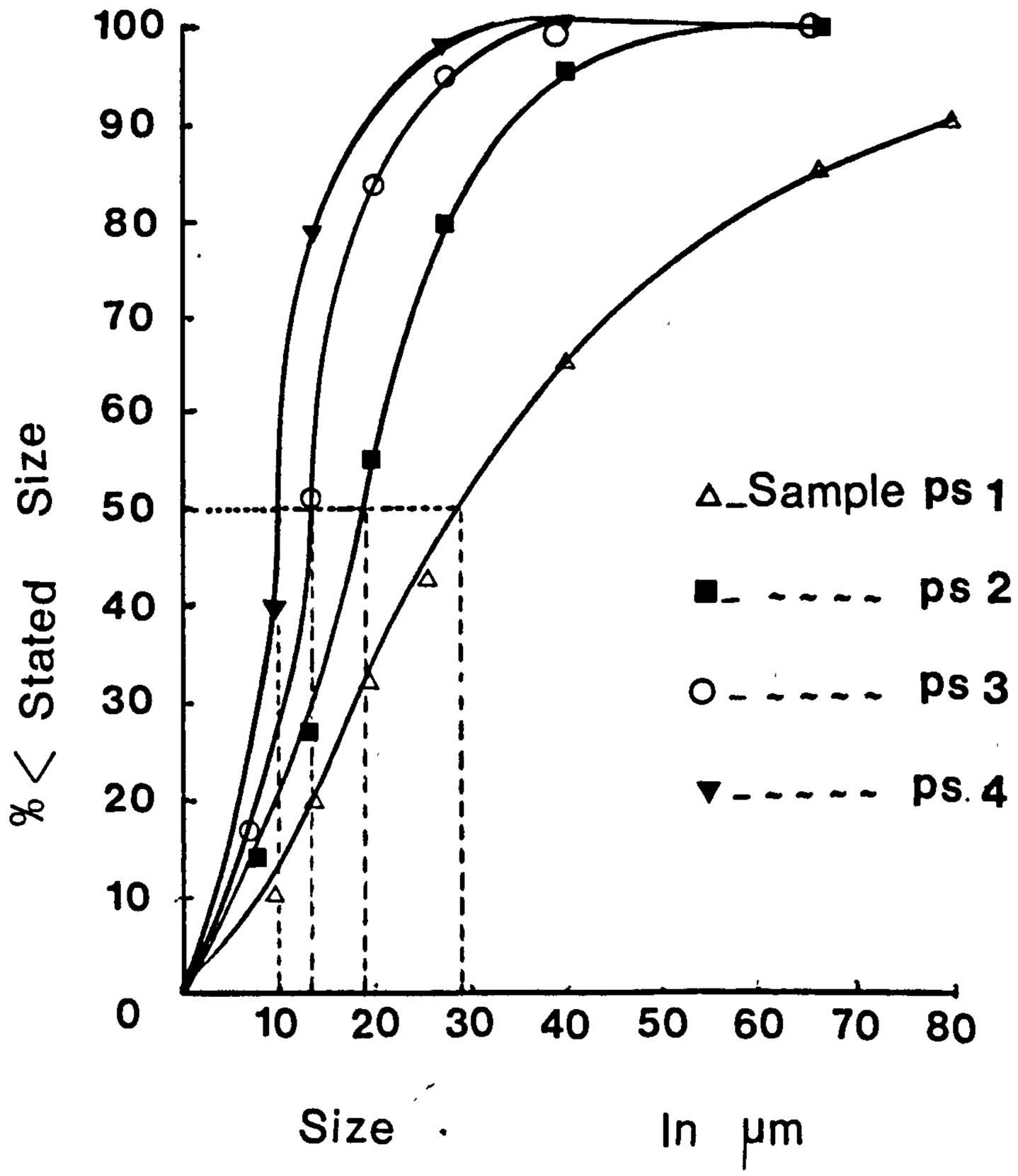

cooling crystallisation. There is need for a fast rate of heat dissipation and the elongated crystals provide a high surface area which is suitable for this purpose (Mullen 1972).

The flow rate plays a major role in controlling the particle size. In general increasing the flow rate decreases the particle size. The aspiration rate evacuates the drying chamber and therefore for a constant feeding rate there will be increased volume per droplet at higher aspiration rates, i.e. the chance for fine droplets to form bigger droplets by collision is reduced. Also at higher aspiration rates the time allowed for crystal growth is shorter resulting in smaller crystals.

3.1.3 Outlet temperature

Statistical analysis of the outlet temperature data resulted in large values of variance, and F-values. Thus all four operating variables contribute in determining the final outlet temperature. These results, presented graphically in Figure 3.2 indicate that:-

a) outlet temperature increases with increasing inlet temperature, aspiration rate and decreasing flow and pump rates,
b) increasing the pump rate increases the difference between inlet and outlet temperature,
c) the effect of pump rate on outlet temperature is more marked when aspiration rate is low and flow rate is high.

Figure 3.3 shows that there is a relationship between the outlet temperature and the thermal behaviour of the spray-dried phenylbutazone samples as indicated by the number of peaks on the D.S.C. thermograms. These transitions are attributed to the presence of polymorphic forms and will be discussed later in Section 3.2. It can be seen however that the additional transitions decrease with increasing outlet temperature.

aspiration rate 0.0106, air flow 400

aspiration rate 0.0106, air flow 600

aspiration rate 0.00905, air flow 400

aspiration rate 0.00903, air flow 600

aspiration rate 0.008232, air flow 400

aspiration rate 0.008232, air flow 600

aspiration rate 0.01060, air flow 400

aspiration rate 0.01060, air flow 600

aspiration rate 0.00903, air flow 400

aspiration rate 0.00903, air flow 600

aspiration rate 0.008232, air flow 400

aspiration rate 0.008232, air flow 600

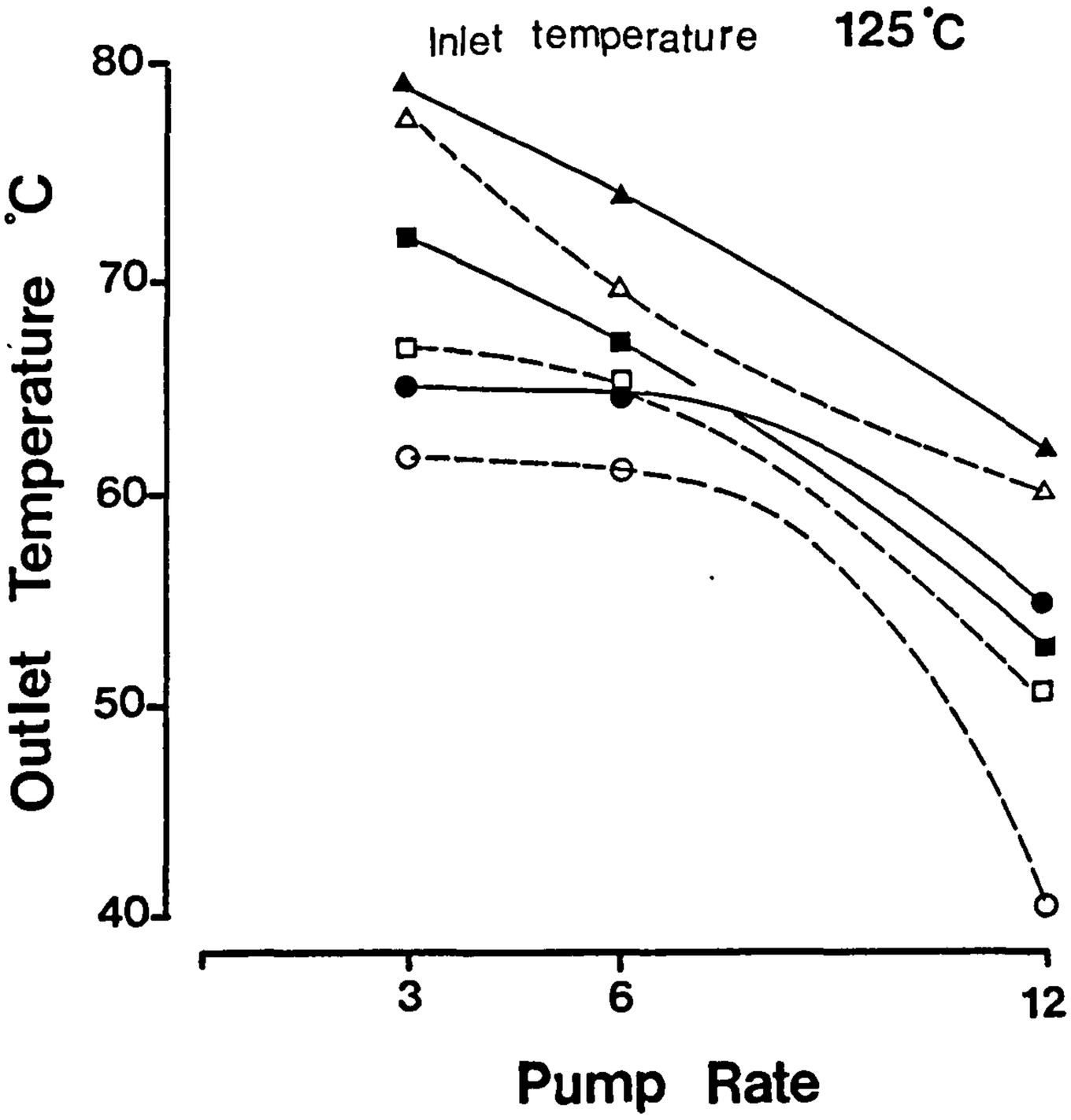

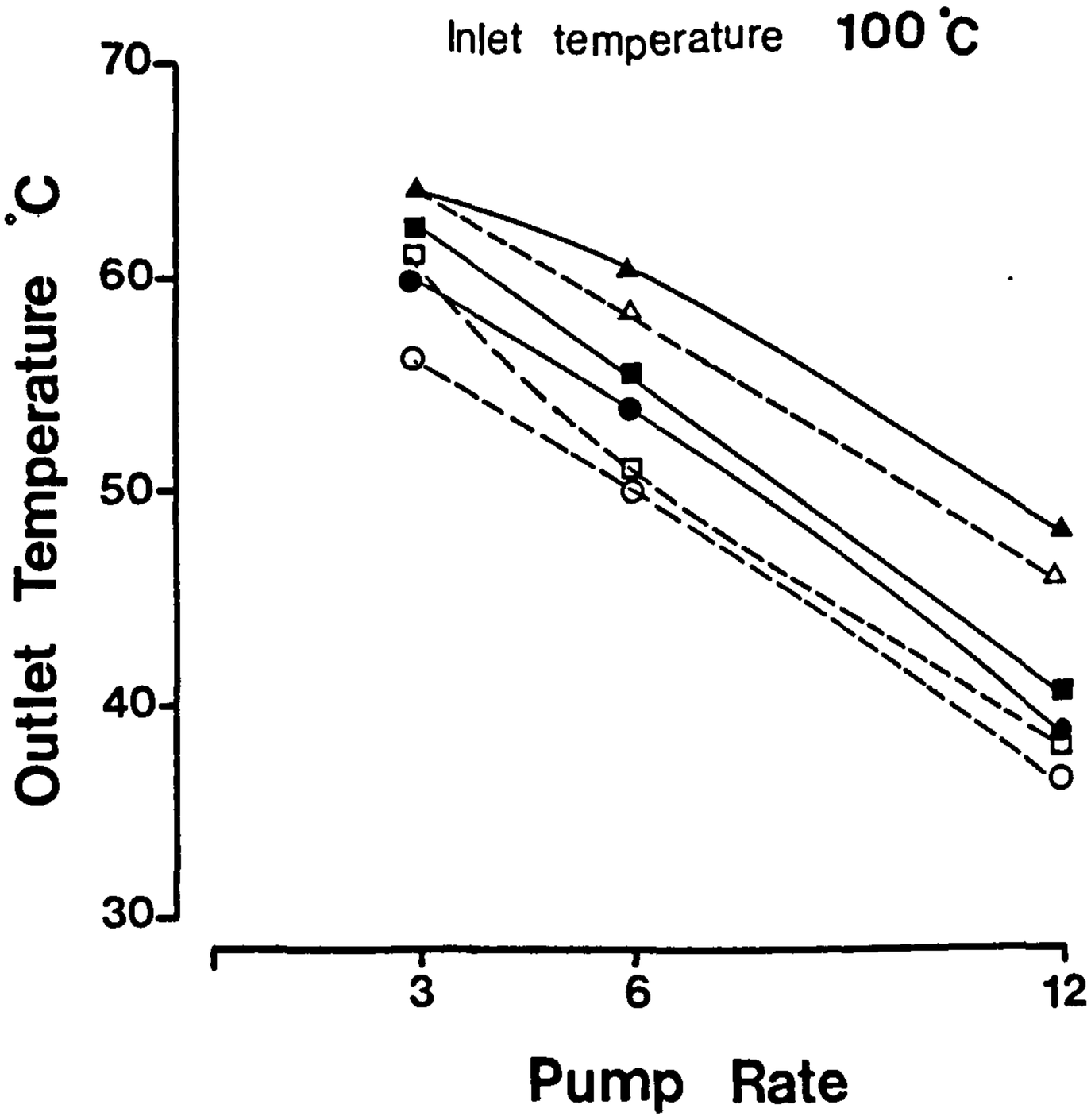

Fig. 3.2a The relationship between the four spray drying variables.

pump rate 4 ml/min, air flow 400

pump rate 4 ml/min, air flow 600

pump rate 8 ml/min, air flow 400

pump rate 8 ml/min, air flow 600

pump rate 16ml/min, air flow 400

pump rate 16ml/min, air flow 600

aspiration rate 0.0106, air flow 400

aspiration rate 0.0106, air flow 600

aspiration rate 0.00903, air flow 400

aspiration rate, 0.00903, air flow 600

aspiration rate, 0.008232, air flow 400

aspiration rate, 0.008232, air flow 600

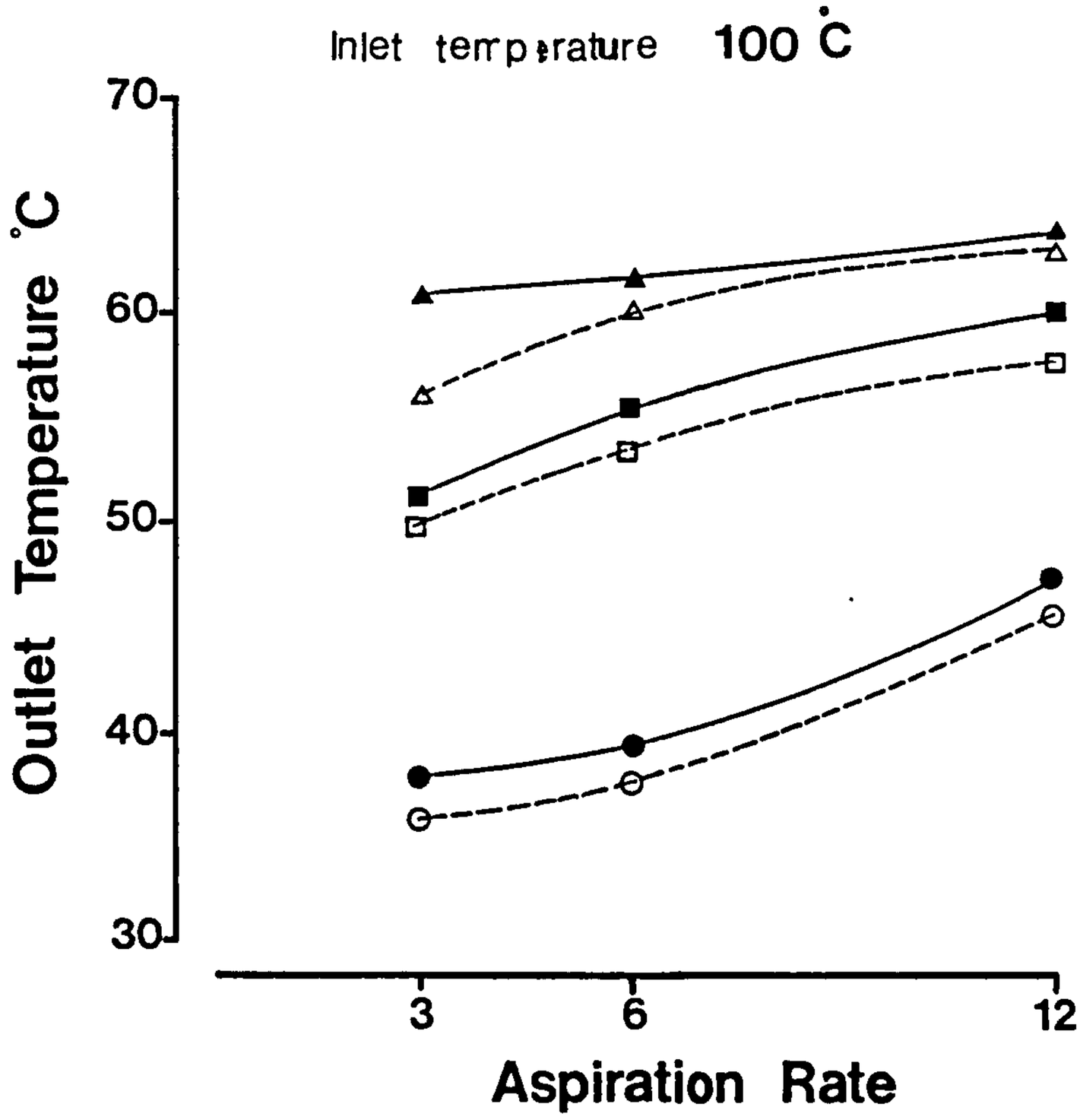

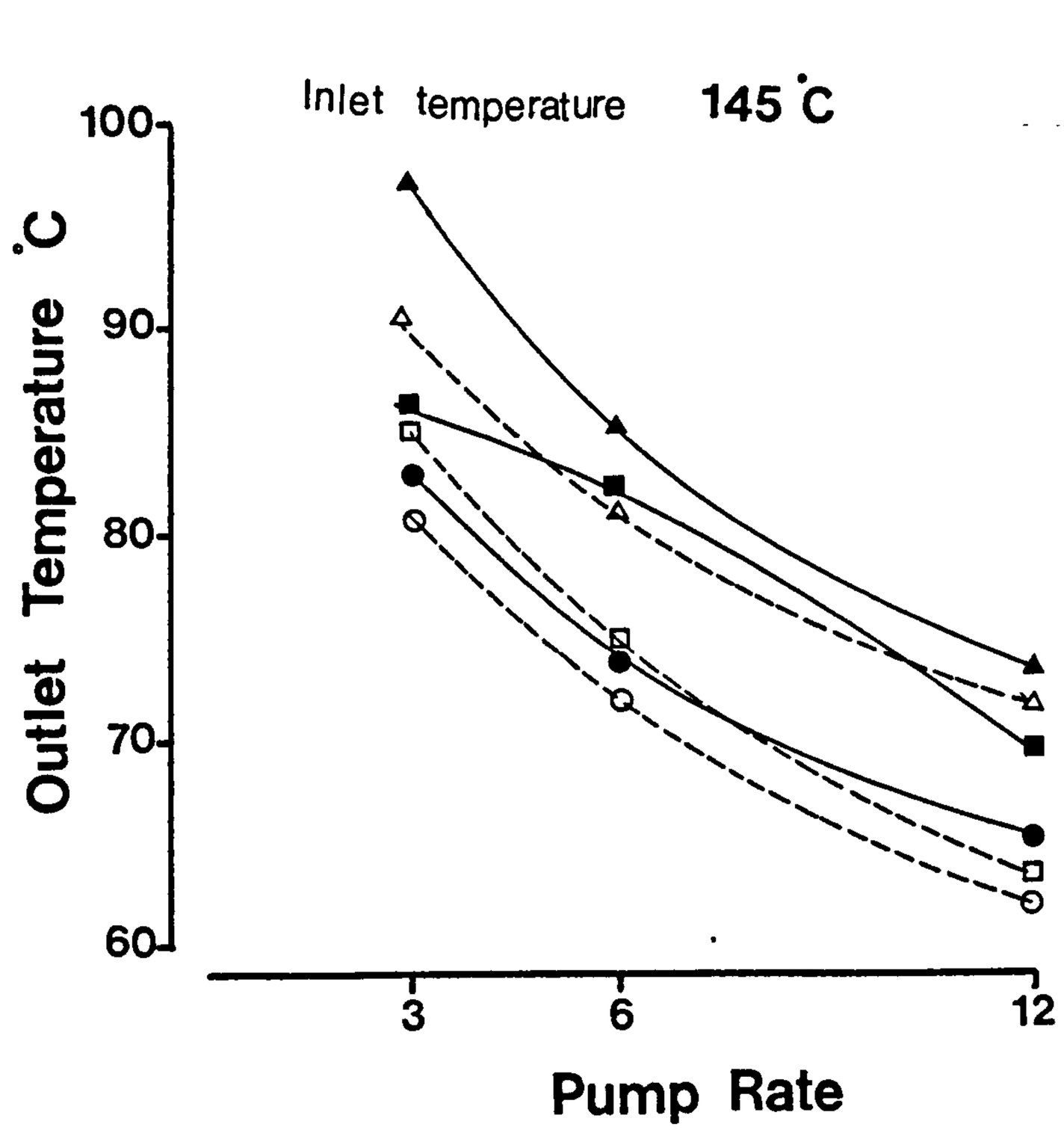

Fig. 32c The relationship between the four spray drying variables.

pump rate 4 ml/min, air flow 400

pump rate 4 ml/min, air flow 600

pump rate 8 ml/min, air flow 400

pump rate 8 ml/min, air flow 600

pump rate 16 ml/min, air flow 400

pump rate 16 ml/min, air flow 600

pump rate 4 ml/min, air flow 400

pump rate 4 ml/min, air flow 600

pump rate 8 ml/min, air flow 400

pump rate 8 ml/min, air flow 600

pump rate 16 ml/min, air flow 400

pump rate 16 ml/min, air flow 600

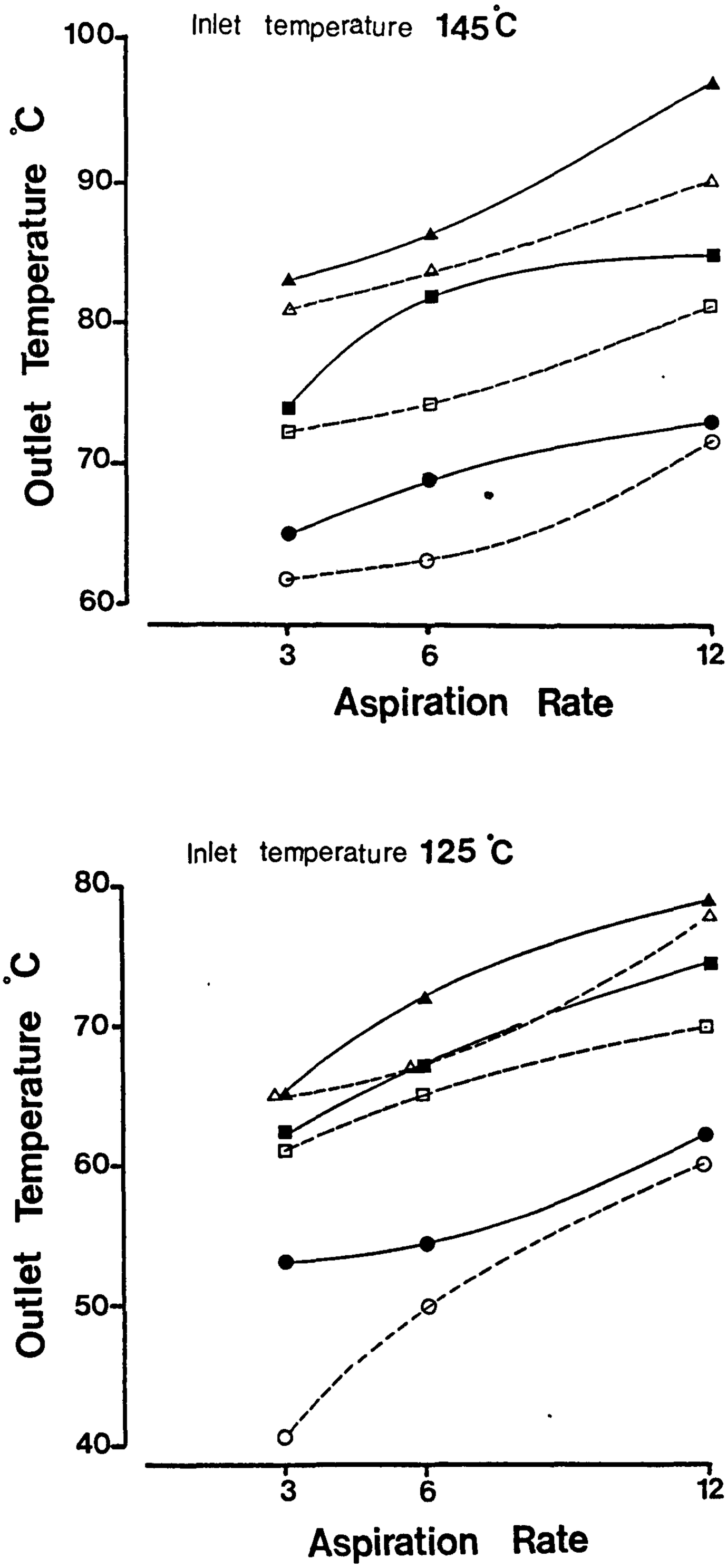

Fig. 3.2 d The relationship between the four spray drying variables.

Inlet Temperature	Outlet Temperature	D.S.C. Observation	Diagrammatic representation of D.S.C. thermogram	
100°C	36	3 separated endotherms	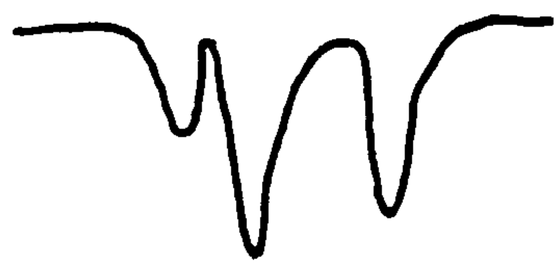	4
	56			
	62	2 endotherms 1 exotherm	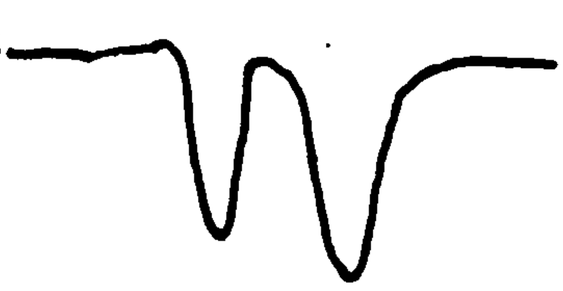	3
125°C	67	2 shoulders to broad single endotherm		5
	78	1 shouler 1 shoulder on single endotherm	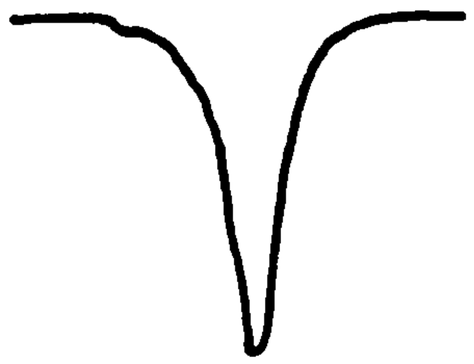	2
145°C	96	1 single endotherm equivalent to the original phenylbutazone	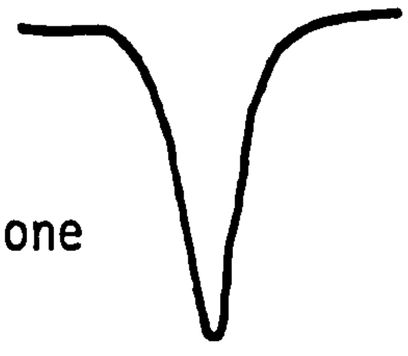	1

Fig. 3.3 Schematic representation of the effect of inlet temperature on outlet temperature and number of endothermic peaks on the D.S.C. thermogram.

3.1.4 Validation of the spray drying process

Figure 3.4 shows scanning electron photomicrographs of spray-dried sodium sulphite and shows regular spherical particles. This product was obtained using similar operation conditions to those used for spray drying phenylbutazone. The scanning photomicrographs show that the morphology of the spray-dried phenylbutazone samples (see Fig. 3.10) were not identical to the typical spherical spray-dried particles seen for sodium sulphite. The difference in particle morphology of the phenylbutazone is thus related to the specific features of phenylbutazone rather than the operation of the spray dryer or the procedure used.

3.1.5 Stability of phenylbutazone products after spray drying

Selected samples of spray-dried phenylbutazone (Table 3.4) were analysed by HPLC. For all samples a single peak corresponding to that of untreated phenylbutazone was observed. Thus spray drying phenylbutazone over the range of operating variables used in this study did not cause chemical degradation.

Fig. 3.4 Scanning electron microscope photomicrographs of spray dried sodium sulphite particles using the same procedure used to spray dry phenylbutazone

Fig 3.4

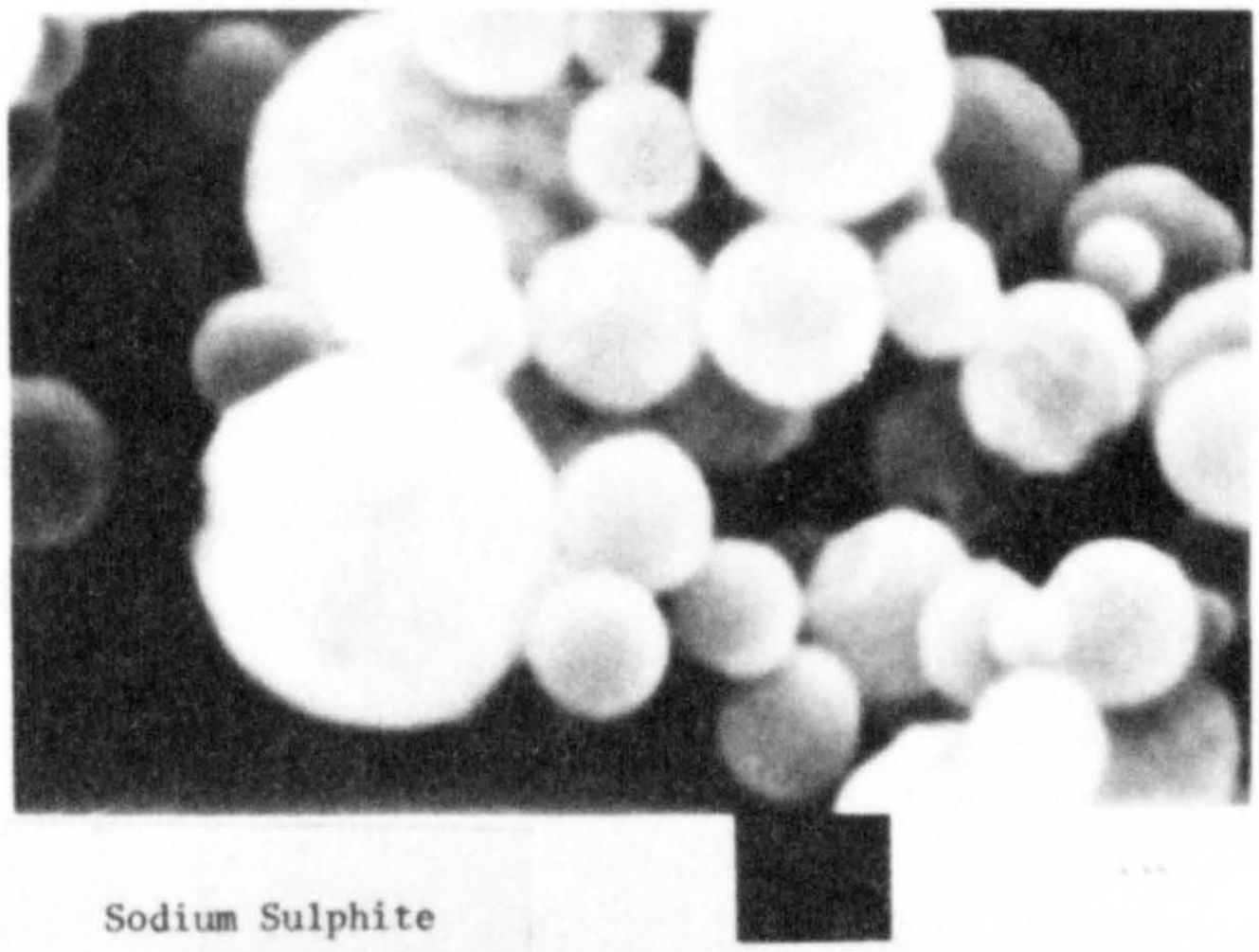

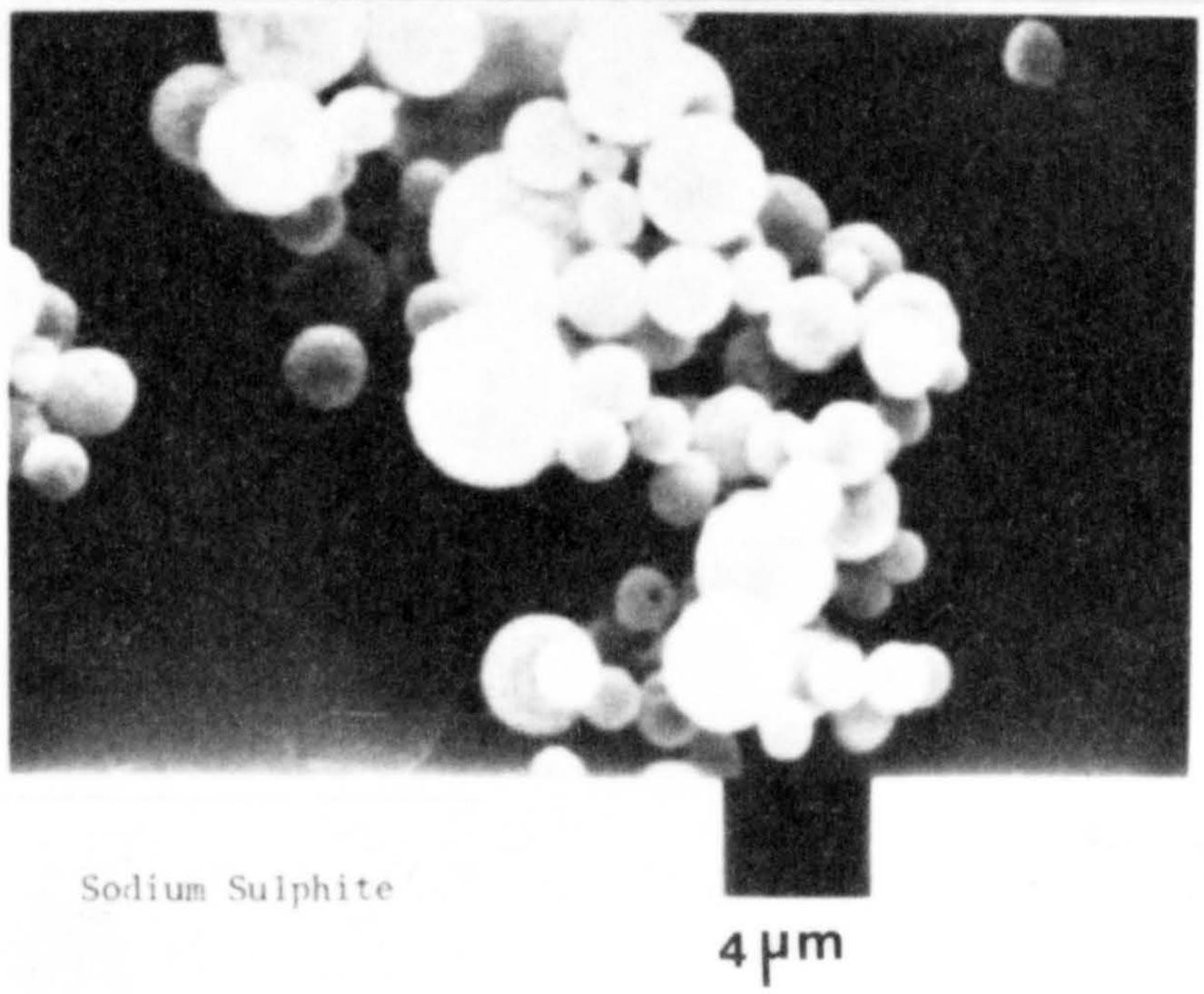

Table 3.4 Preparation conditions for spray dried phenylbutazone samples examined by H.P.L.C.

Sample No.	Inlet temperature (°C)	Outlet temperature (°C)	Flow rate (L/h)	Pump rate (ml/min)	Aspiration rate (m^3/sec)
1	100	38	600	16	0.00903
2	100	46	600	16	0.01060
3	100	63	600	4	0.01060
4	125	40	600	16	0.00823
5	125	60	600	16	0.01060
6	125	79	400	4	0.01060
7	145	63	600	16	0.00903
8	145	74	600	8	0.00903
9	145	90	400	4	0.01060

3.2 Polymorphism of phenylbutazone

3.2.1 Introduction

Phenylbutazone has been reported to exist in different polymorphic states. However there is confusion in the literature about the number of these polymorphs (see Table 3.5). Matsunaga et al. (1976) reported the existance of three polymorphic forms. Form I with a melting point of103^{o}C, Form II melting point at 93^{o}C solidifying immediately to remelt at 103^{o}C, and Form III which melts at 93^{o}C. Ibrahim et al. (1977) reported that phenylbutazone exists in four polymorphic forms - Form I prepared from isobutylalcohol melting at 80^{o}C, Form II prepared from cyclohexane melting at 90^{o}C, Form III which could be prepared from n-heptane and melted at 93^{o}C, and Form IV melting at 105^{o}C prepared from 2-propanol. Muller (1978) reported that Forms I and II mentioned by Ibrahim et al. were solvates (pseudopolymorphs) and also reported the existance of two new polymorphs. He obtained one of the new polymorphs, β form melting point at 95^{o}C, by adding water to ethanolic solution of phenylbutazone and also by melting and recrystallising the commercial phenylbutazone. Muller reported that the other new polymorph γ form could not be isolated.

Tuladhar et al. (1983) reported that phenylbutazone can exist in five polymorphic forms. Form A prepared from 2-propanol has a melting point of 105^{o}C. Form B, melting point 103^{o}C, was obtained by dissolving 5 gm of phenylbutazone in 100 ml of n-heptane and the solution was heated in a water bath at 90^{o}C then the solution was allowed to stand for 2-3 hours and filtered. Form C, melting point 96^{o}C, was obtained by dissolving 5 gm of phenylbutazone in 550 ml n-heptane and heating the solution in a water bath at 70^{o}C. The solution was then filtered and allowed to cool at room temperature for 2-3 hours. Form D, melting

Table 3.5 Reported melting points (^{o}C) of phenylbutazone polymorphic forms

Matsunaga et al. (1976)		Ibrahim et al. (1977)		Muller (1978)		Tuladhar et al. (1983)	
Form	M.P. (^{o}C)	Form	M.P. (^{o}C)	Form	M.P. (^{o}C)	Form	M.P. (^{o}C)
I	103	I	80	α	93	A	105
II	93, 103	II	90	β	95	B	103
III	93	III	93	γ	105	C	96
		IV	103	δ	107	D	94
						E	92.5

point 94°C, was prepared by allowing the filtered solution in C to cool at room temperature for 24 hours then filtering. Form E, melting point 92.5°C, was prepared by allowing the filtered solution of C form to cool in an ice bath for 2-3 hours then filtering. All the samples were allowed to dry under vacuum at room temperature.

The objective of this part of the work was to attempt to prepare the reported phenylbutazone polymorphs following procedures reported in the literature and to develop an understanding of the polymorphism of phenylbutazone which will assist in interpreting the changes occurring when preparing phenylbutazone samples containing polymeric additives by crystallisation and spray drying.

3.2.2 Experimental

3.2.2.1 Materials

The materials used were listed in Section 2.1.

3.2.2.2 Method

The commercial phenylbutazone (δ form) and the prepared polymorphs α and β' were subjected to the following tests: D.S.C., SEM, X-ray diffraction, solubility and dissolution rate, all according to the methods described in Chapter 2.

3.2.3 Results and discussion

The discrepancies in the number of polymorphic forms observed between workers could possibly be caused by different experimental techniques. In all previous works with D.S.C. different heating rates were used. However by heating samples of phenylbutazone at different heating rates (Fig. 3.5), different shapes of endotherms were obtained. For a fast heating rate of 50°C/min a broad endotherm is obtained, but as the heating rate was reduced the peak became sharper. In addition

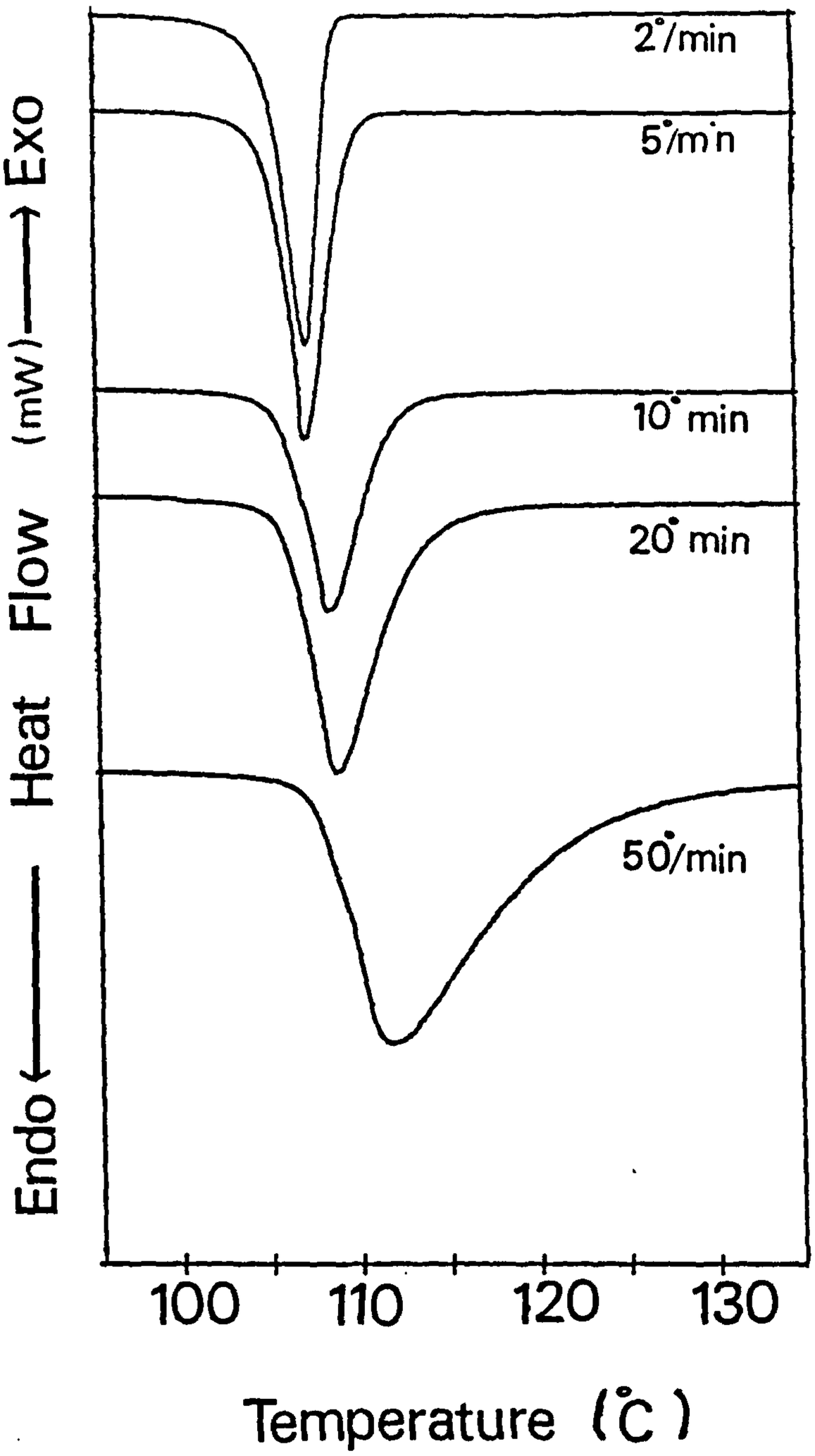

Fig. 3.5

The effect of heating rate on size and shape of melting endotherm of samples of phenylbutazone as supplied

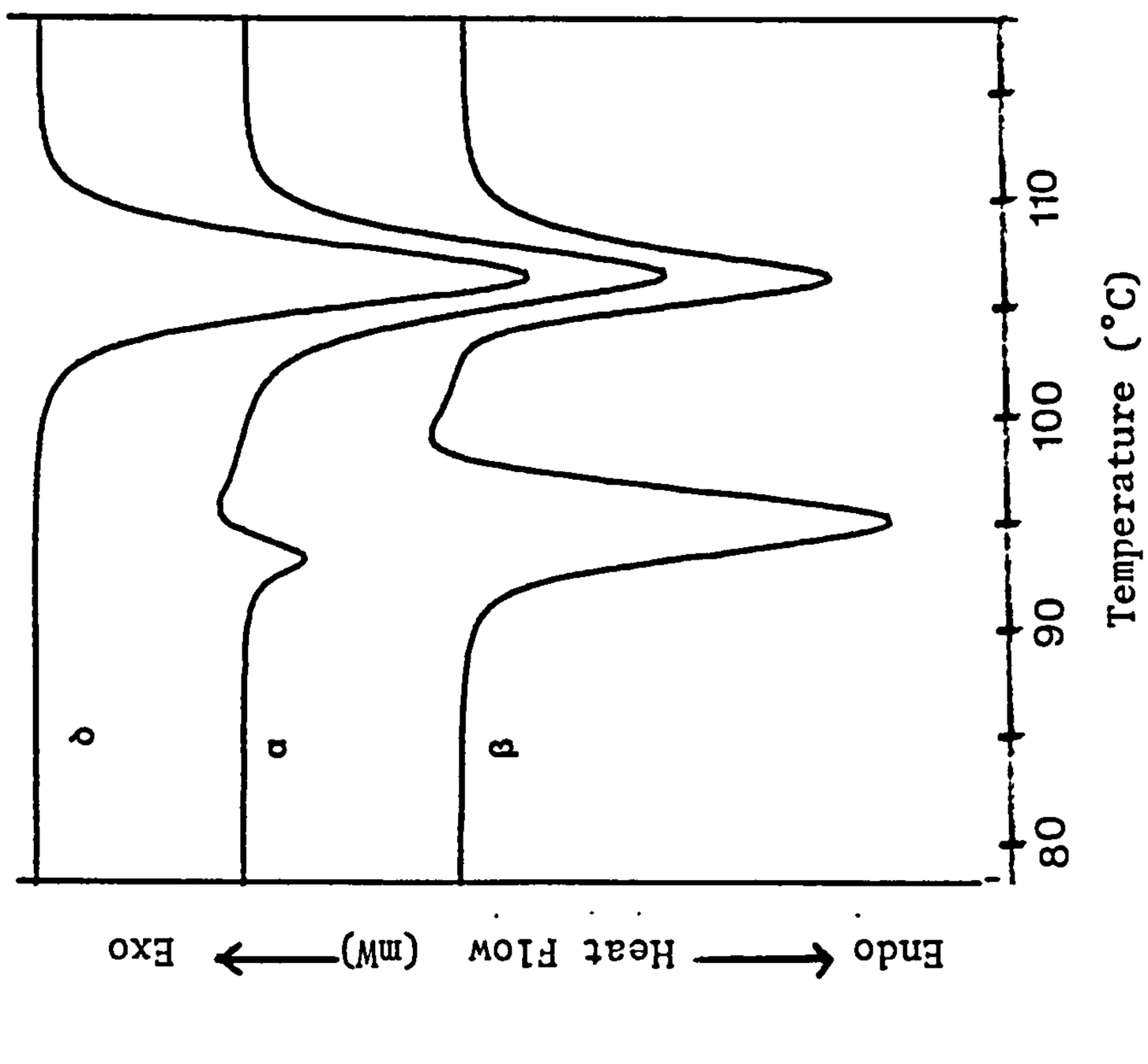

Fig. 3.6 The D.S.C. endotherms of phenylbutazone polymorphic forms obtained by crystallisation from different solvents (heating rate $10^{o}C/min$, sample size 5-9 mg and under nitrogen flow).

since thermal lag increases as heating rate increases, different peak melting points are found for different rates. Fast heating rates can also mask solid-solid transitions in polymorphic materials. In this study a standardised D.S.C. technique with heating rate of 10°C/min using samples in crimped pierced aluminium pans under an atmosphere of nitrogen was selected.

3.2.4 Characterisation of polymorphs

3.2.4.1 Differential scanning calorimetry (D.S.C.)

The D.S.C. thermograms of the prepared samples of phenylbutazone show that the stable form δ (the commercial form) exhibited one single endothermic peak at 107°C. The thermogram for the sample obtained by adding water to the 2-propanol solution of phenylbutazone until the cloud point then allowing the solution to cool (Ibrahim et al. 1977, Muller 1978) showed a small endothermic peak at 93°C on the D.S.C. thermogram followed by an exotherm at 95°C and remelt at 107°C (see Fig. 3.6). The first endothermic peak at 93°C, possibly the α form, was found to be very unstable on storage. The presence and magnitude of the endotherm at 93°C was found to be dependent upon preparative conditions such as the amount of water. Flocculating the n-heptane solution of phenylbutazone by adding water produced a sample with a melting point of 95°C and was termed the β form (Fig. 3.6).

The method of Kissinger (1957) was used to calculate the energy of activation from maximum peak temperature (Tm) for the transition of β polymorph to δ at different heating rates (Ø). From the plot of $\log \frac{Ø}{Tm^2}$ against $\frac{1}{Tm}$ a straight line was obtained with slope equal to $\frac{-EA}{2.303R}$ (Fig. 3.7) from which the heat of transition of β polymorph was estimated to be 796.6 KJ/mol which is in close agreement with the figure obtained by Muller (1978) (850 KJ/mol).

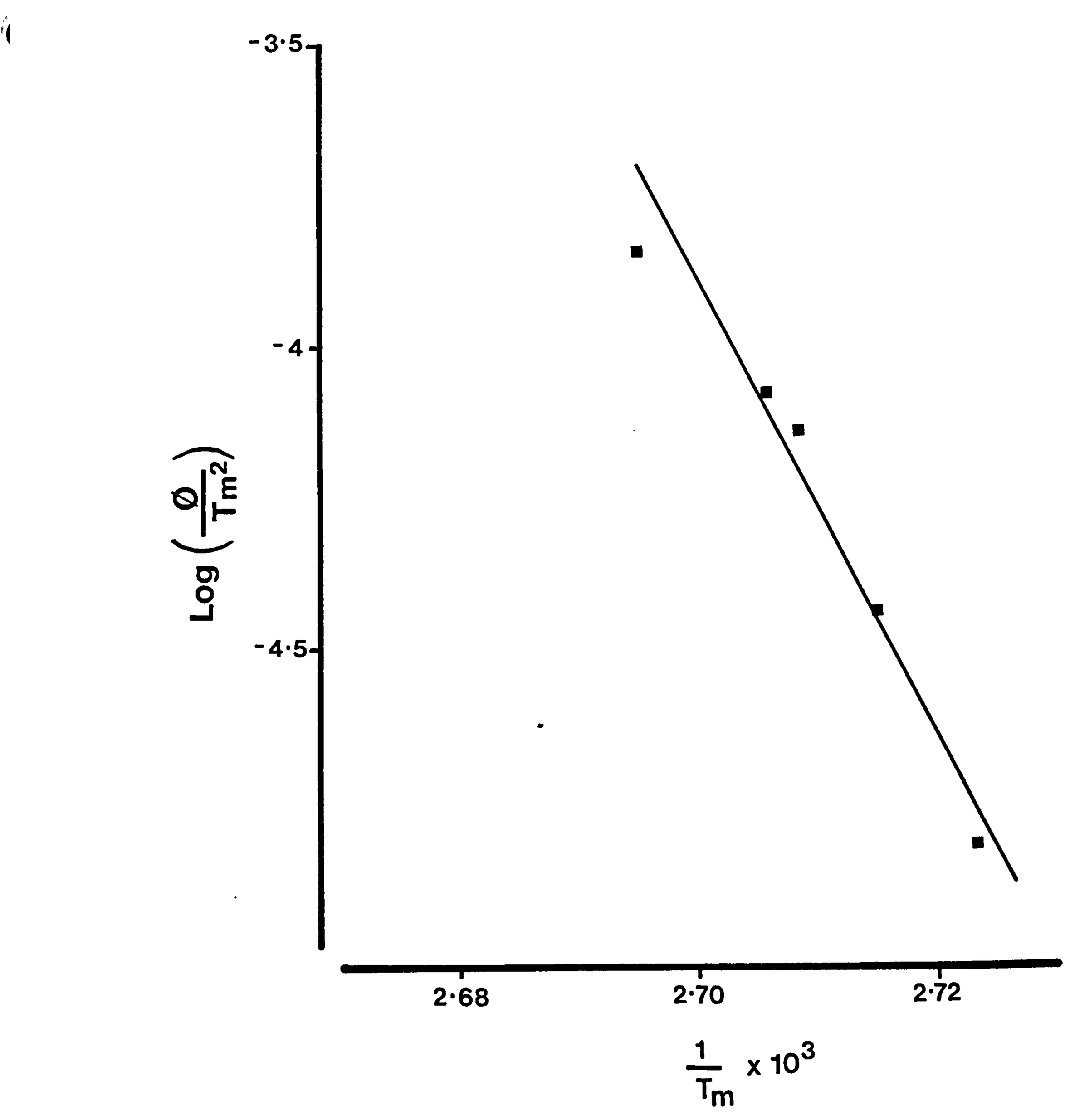

Fig. 3.7

Plot of the relationship of heating rate and peak maximum temperature, Tm, for the transition endotherm of β-polymorph in determining the thermodynamic activation energy E_a.

3.2.4.2 Scanning electron microscope

There were little observed differences in the morphology of the crystal of the different forms from scanning electron photomicrographs. All samples were shown to be needle-like with reduced length-to-width aspect ratio for the β form(Fig 3.7b).

3.2.4.3 Powder X-ray diffraction

The powder X-ray diffraction patterns for the β polymorph and the stable form δ are illustrated in Fig. 3.7a. Differences can be qualitatively characterised by the position of three main peaks in the diagram. The small differences between the results obtained and those in the literature (Table 3.6) might be due to the difference in packing of the powder bed.

The differences in X-ray patterns between the polymorphs are due to differences in the crystal spacing resulting from differences in molecular packing arrangement taking place during crystallisation.

3.2.4.4 Infrared spectrum

Only very minor changes at high wavelength regions in the i.r. spectra between the different forms were identified. Similar observations for the polymorphs of phenylbutazone have been reported by Muller (1978) and Ibrahim et al. (1977).

3.2.4.5 Solubility

The dynamic solubility of the isolated polymorphs was tested in buffer solution of pH 7.5 in a shaking water bath at 37°C. There was a major difference in the solubility between the metastable β polymorph and the δ stable form. The δ form showed an increase in concentration in solution with time until a maximum equilibrium concentration was reached after 48 hours (see Fig. 3.8). The β form exhibited a faster

Fig. 3.7a Powder X-ray diffraction patterns of phenylbutazone as supplied and samples spray dried at different crystallisation rates.

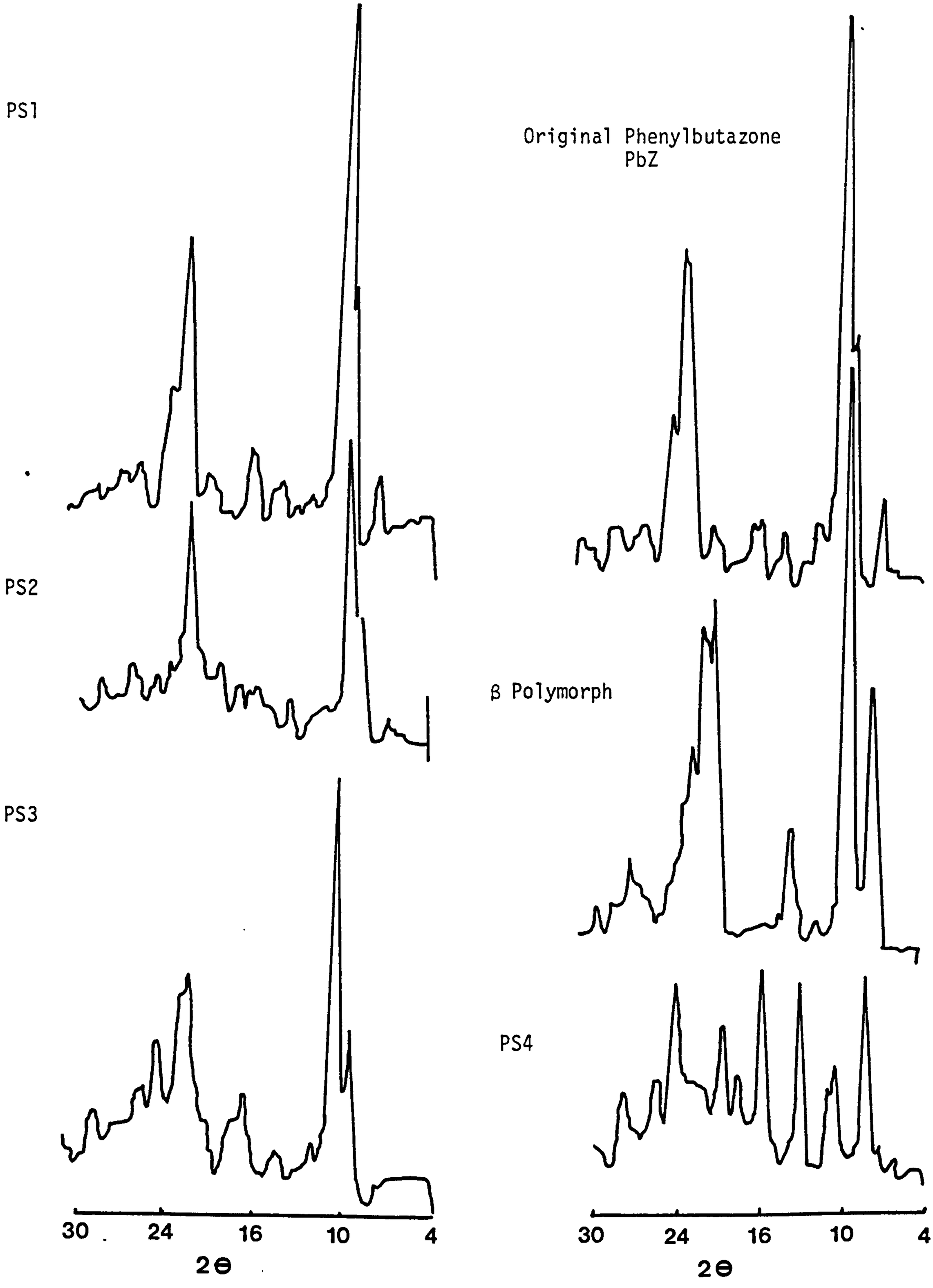

Fig. 3.7b Scanning electron microscope photomicrographs of phenylbutazone as supplied and β polymorph of phenylbutazone

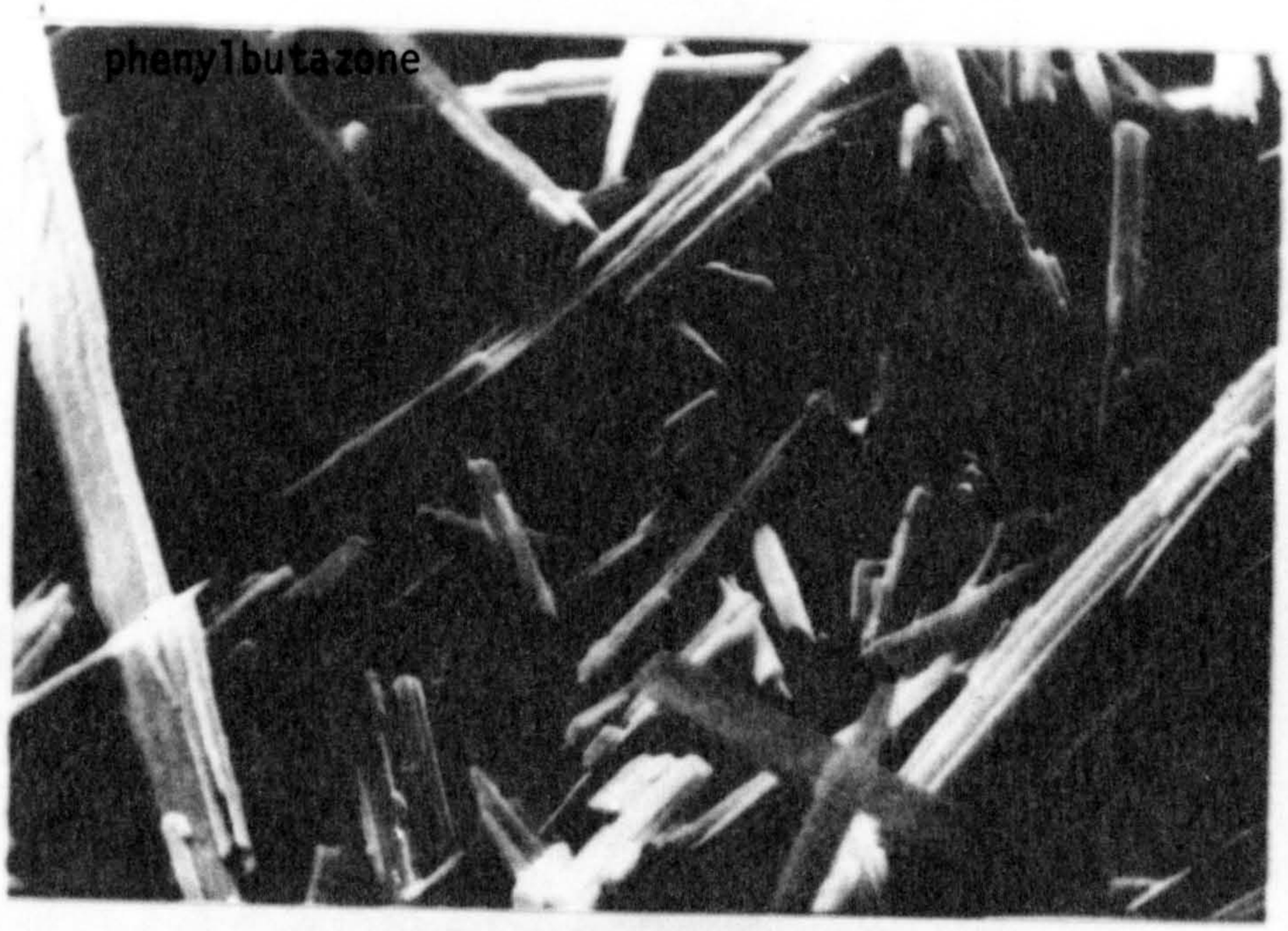

Pbz

20μm

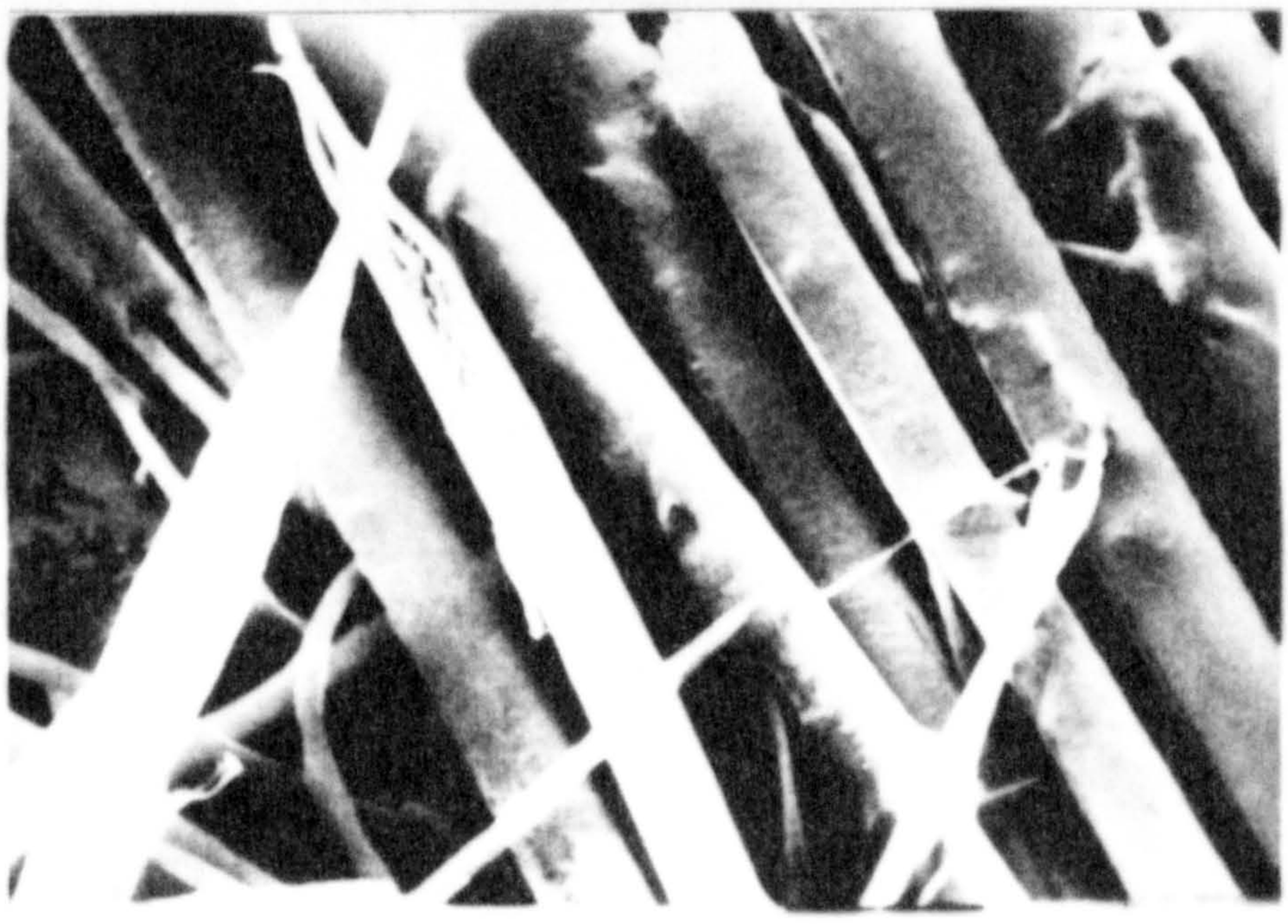

β-Polymorph

Table 3.6 X-ray diffraction patterns of the main peaks of phenylbutazone δ and β polymorphs

Polymorph	2θ Found	Muller 1978 Report	I/I_o
	8.1	7.9	100
δ	20.9	20.7	60
	6.95	7.05	9
	8.9	8.35	100
β	20.9	20.2	60
	7.1	7.05	40

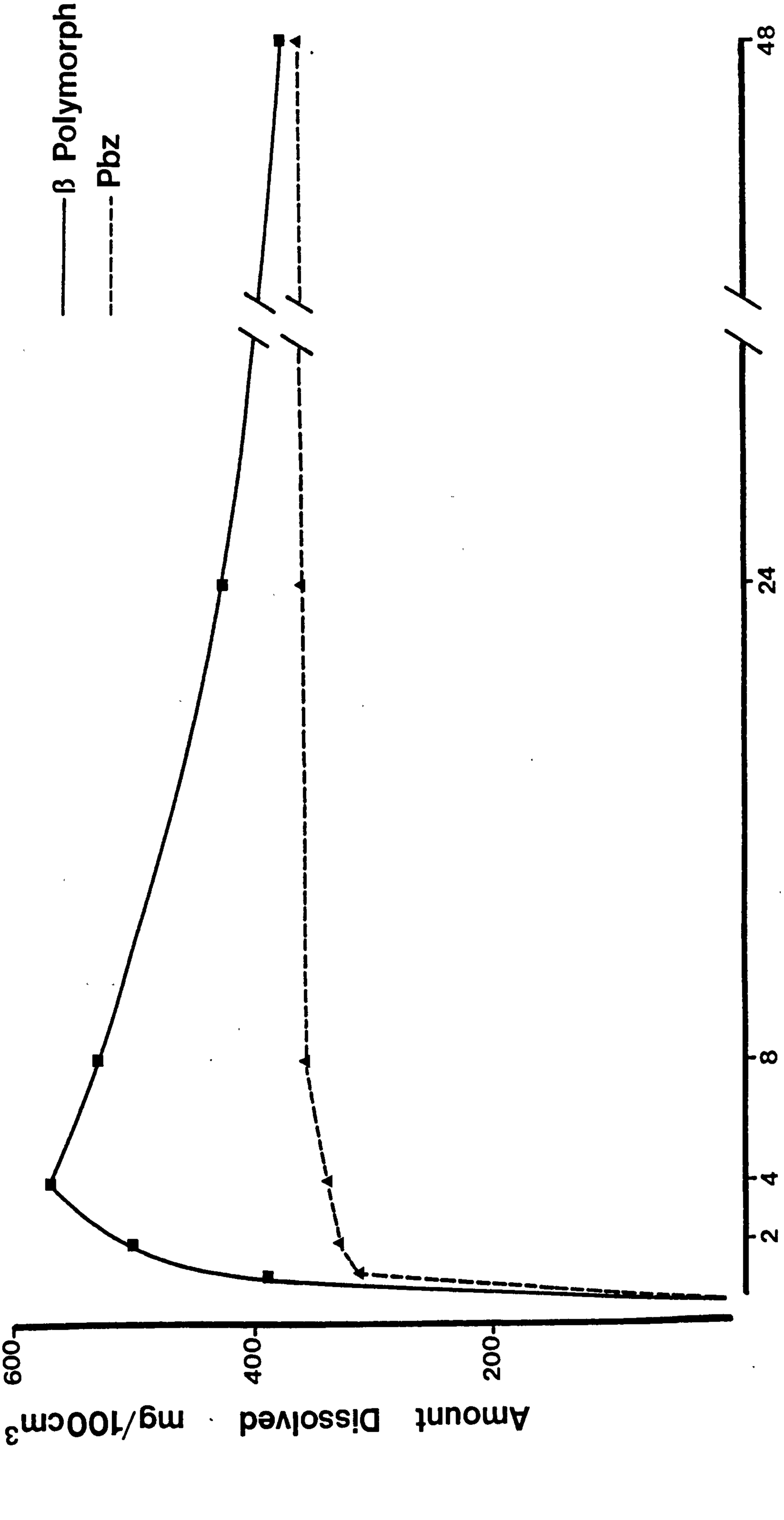

Fig. 3.8 The solubility curves for phenylbutazone as supplied (δ-form) and metastable β-form.

increase in solubility, with a peak solubility value occurring after 4 hours which was 1.8 fold higher than the maximal solubility shown by the stable δ form. The solubility profile then started to decrease with time until the equilibrium concentration exhibited by the δ form was reached after 48 hours. This peaking in solubility is a feature of metastable polymorphs (Carstensten 1980) which exhibit higher initial solubility than the stable form. This is due to higher free energy of the metastable polymorphs compared with the stable form. The solubility of each form depends on the ability of molecules to escape from the crystal to the solvent which is controlled by the free energy content of the crystal. The stable form possesses the lower free energy at a particular temperature and pressure, and therefore has the lower solubility or escaping tendency. However in solution polymorphism does not exist (Carstensten 1980), so the solution will be super-saturated with respect to the equilibrium dynamic solubility of phenylbutazone. As a result, excess solute molecules crystallise out of solution until the solution level of the stable form is reached.

3.2.4.6 Dissolution rate

The dissolution rates of the polymorphic forms were studied by determining their intrinsic dissolution rates using a Woods apparatus with constant surface area compressed discs. Since it was reported by Ibrahim et al. (1977) and Matsunaga et al. (1976) that polymorphic forms show some transition into the stable δ during compression, a study of the thermal behaviour of the compressed metastable β polymorph powder using the D.S.C. was done by compressing a disc of powder and taking samples of three parts of that disc (1) the inner face adjacent to the surface, (2) the outer face which will be in contact with the dissolution medium, (3) from the middle of the compact. The percentage

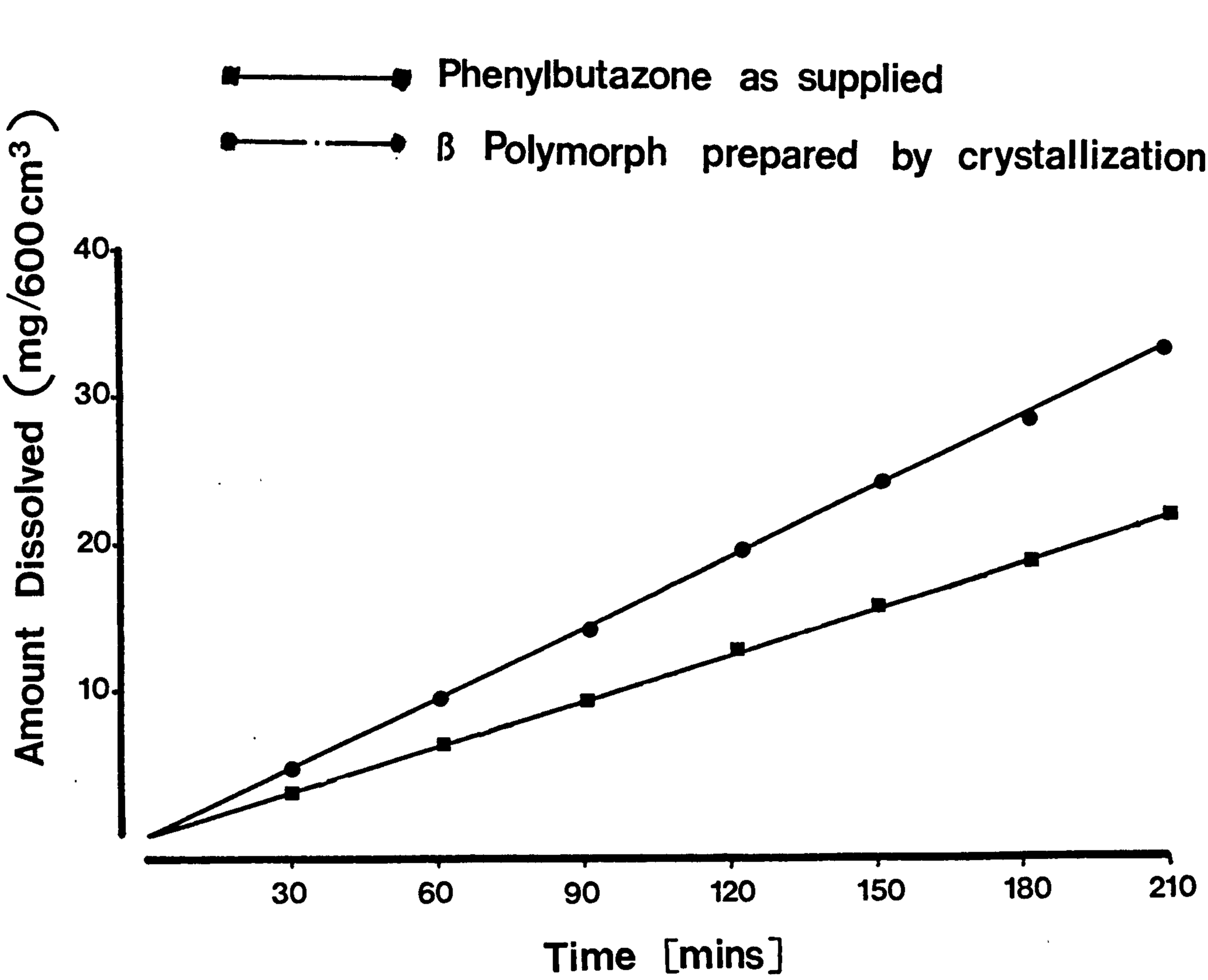

Fig. 3.9

Dissolution curves for phenylbutazone as supplied (δ-form) and β polymorph in buffer solution pH 7.5 at 37°C.

of transition to δ form taking place during compression, using the uncompressed powder as reference was then estimated from D.S.C. thermograms. It was found that the transition was higher at the inner face of(53%)and decreased towards the outer face in which the transition was found to be small (about 5.3%). Since the outer face was that exposed during dissolution tests, this transition effect was considered small enough to be disregarded for this test.

Figure 3.9 illustrates the dissolution rate curves obtained. The metastable β polymorph showed a 1.5-fold increase in dissolution rate compared with the stable δ form. As discussed above the metastable polymorph is at a higher energy level so molecules are expected to be able to leave the tablet surface to the solution more readily than the stable form. No peaking value in dissolution rate testing are observed because the dissolved amounts were only small fractions of the maximum solution levels of phenylbutazone in the dissolution medium.

3.3 The effect of crystallisation rate on the polymorphism and dissolution rate of spray dried phenylbutazone

3.3.1 Introduction

The polymorphism of water insoluble drugs can be used in formulations to modify the physicochemical properties of the drugs (Muller 1978; Ibrahim et al. 1977). When preparing polymorphs by crystallisation procedure, the nature of the solvent and the rate of crystallisation are critically important, with most studies concentrating on the former variable (Ibrahim et al. 1977, Muller 1978). In this study the effect of crystallisation rate on the polymorphism and dissolution rate of spray dried phenylbutazone has been examined.

As mentioned in Chapter 1, phenylbutazone was chosen as a model drug because:-

a) it has low aqueous solubility,

b) it exists in several polymorphic forms (see Section 3.2),

c) it is suitable for crystallographic studies using thermal analysis techniques and does not decompose after melting.

Different crystallisation rates using a Büchi mini-spray dryer were achieved by varying the inlet temperature, pumping rate, aspiration rate and air flow rate. As described in Section 3.1.2.1 a factorial experiment was performed to assess the effect of different levels of the four variables on the outlet temperature and thermal behaviour of the product which is an indication of the number and type of polymorphs present in the examined sample.

3.3.2 Experimental

3.3.2.1 Materials

The materials used were listed in Chapter 2,

3.3.2.2. Method

The samples prepared under different spray drying conditions (see Table 3.1 were examined by D.S.C., SEM, powder X-ray diffraction, hot stage microscopy, and solubility and dissolution rates were measured, all according to the methods described in Chapter 2.

3.3.3 Results and discussion

It was found earlier in this work that the outlet temperature, which corresponds to the drying temperature at the surface of the drying particles, is influenced by all four operating variables. For fast crystallisation rates, the outlet temperature is therefore high, and as the crystallisation rates become slower, the outlet temperature drops. From Fig. 3.3 Section 3.1, the effect of outlet temperature on the thermal behaviour of the spray-dried samples, represented by the number of peaks, can be divided into five regions. For the outlet temperature range 78°C to 96°C, the spray-dried samples exhibited a single endothermic peak at 107°C which corresponds with the endotherm obtained for the stable δ form of phenylbutazone. These samples were prepared at the highest outlet temperature and the fastest crystallisation rate.

As the outlet temperature decreased a small shoulder appeared on the melting endotherm. This effect was observed for the range of outlet temperature from 67°C to 78°C. As the outlet temperature and the crystallisation rate decreased, a second shoulder appeared on the endotherm widening the total peak. This effect was noticed for the

region of outlet temperature from 62°C to 66°C.

For the region of outlet temperature from 56°C to 61°C an extra discrete endothermic peak appeared at 95°C followed by an exothermic peak, which corresponds to that previously obtained for the β polymorphic form. For the lowest outlet temperature region of 36°C to 56°C, two additional endothermic peaks appeared on the thermogram at 94°C and 99°C each followed by an exotherm. This suggests the presence of at least two polymorphic forms in the sample.

Four samples from different regions were chosen for further investigations (see Table 3.7).

3.3.4 Characterisation of the samples

3.3.4.1 Scanning electron microscope

Figure 3.10 shows scanning electrophotomicrographs of the supplied phenylbutazone and the four samples selected for further study. The morphology of the spray-dried samples can be seen to be totally different from the original supplied phenylbutazone samples with the crystal shape changing from needle-like to irregular shapes. For sample PS1 branched and large particles were obtained and this appearance is attributed to droplet coalescence and rapid drying of the particles. As spray drying conditions became less severe the particle size of the product gradually became smaller and the particle shape became closer to the typical spherical spray-dried particles. This is evident in samples PS2, PS3, PS4 (see Fig. 3.10).

3.3.4.2 Hot stage microscope

The hot stage microscope was used to observe the changes during polymorphic transformation and the melting behaviour of the samples. Partial melt inside the crystal was detected for the sample PS3.

Table 3.7 Preparation conditions for spray dried samples PS1-PS4

Sample	Aspiration Rate (m^3/sec)	Pump Rate (ml/min)	Flow Rate (L/hr)	Inlet temperature ^oC
PS1	0.01060	16	400	145
PS2	0.01060	8	400	125
PS3	0.00903	4	600	100
PS4	0.01060	16	600	100

Fig. 3.10 Scanning electron microscope photomicrographs of samples PS1, PS2, PS3 and PS4

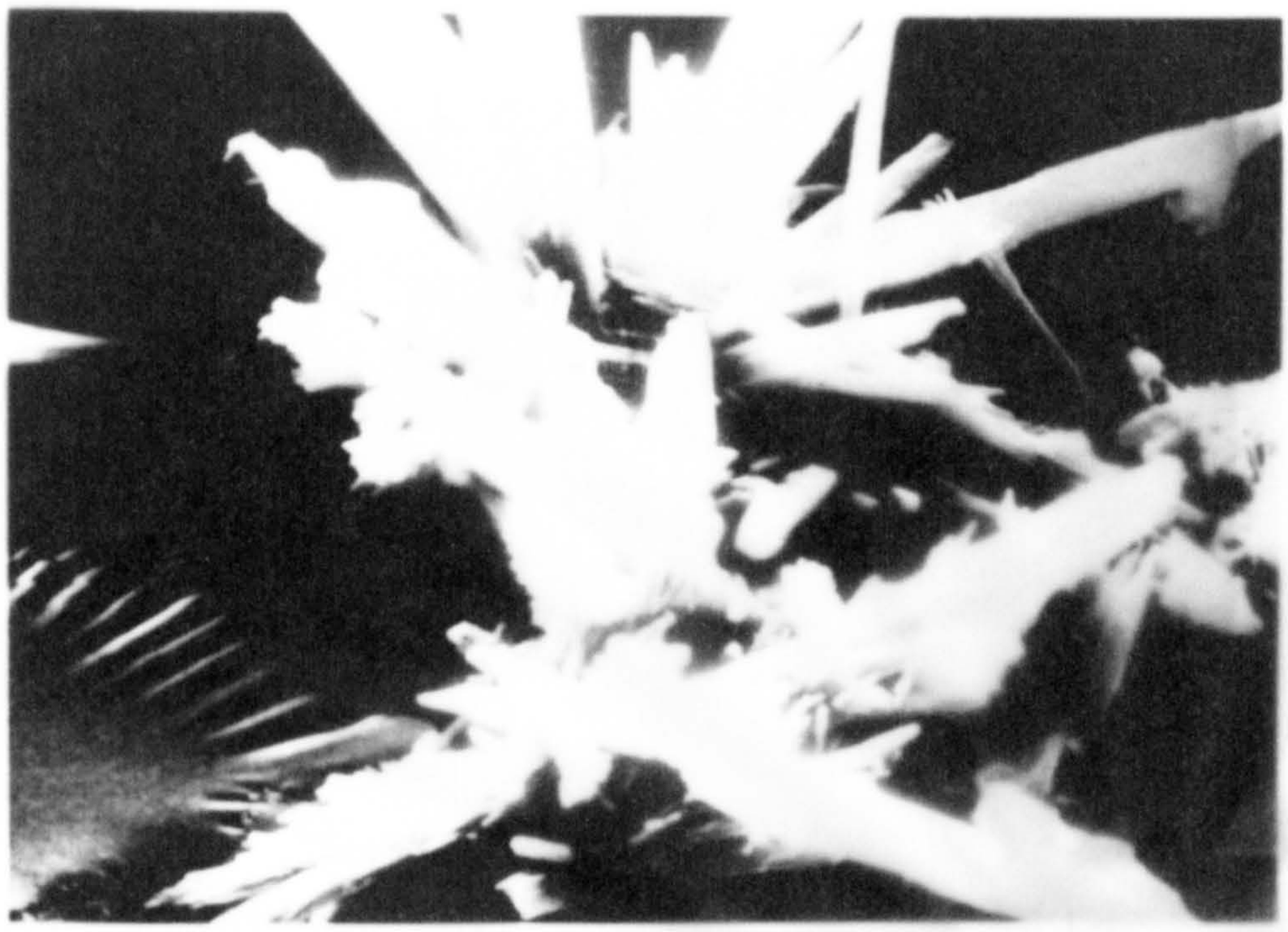

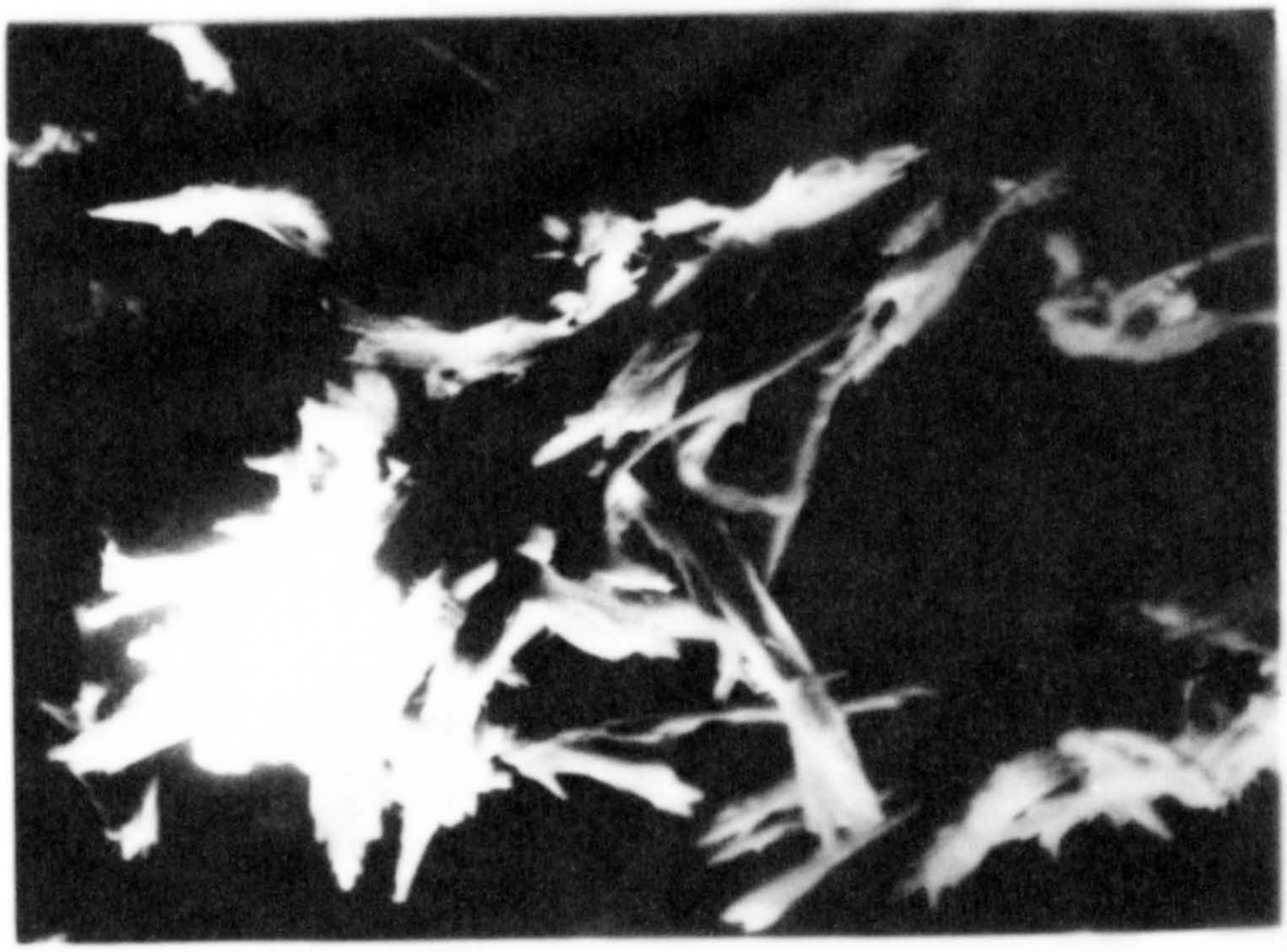

Fig. 3.10 Scanning electron microscope photomicrographs of samples PS1, PS2, PS3 and PS4

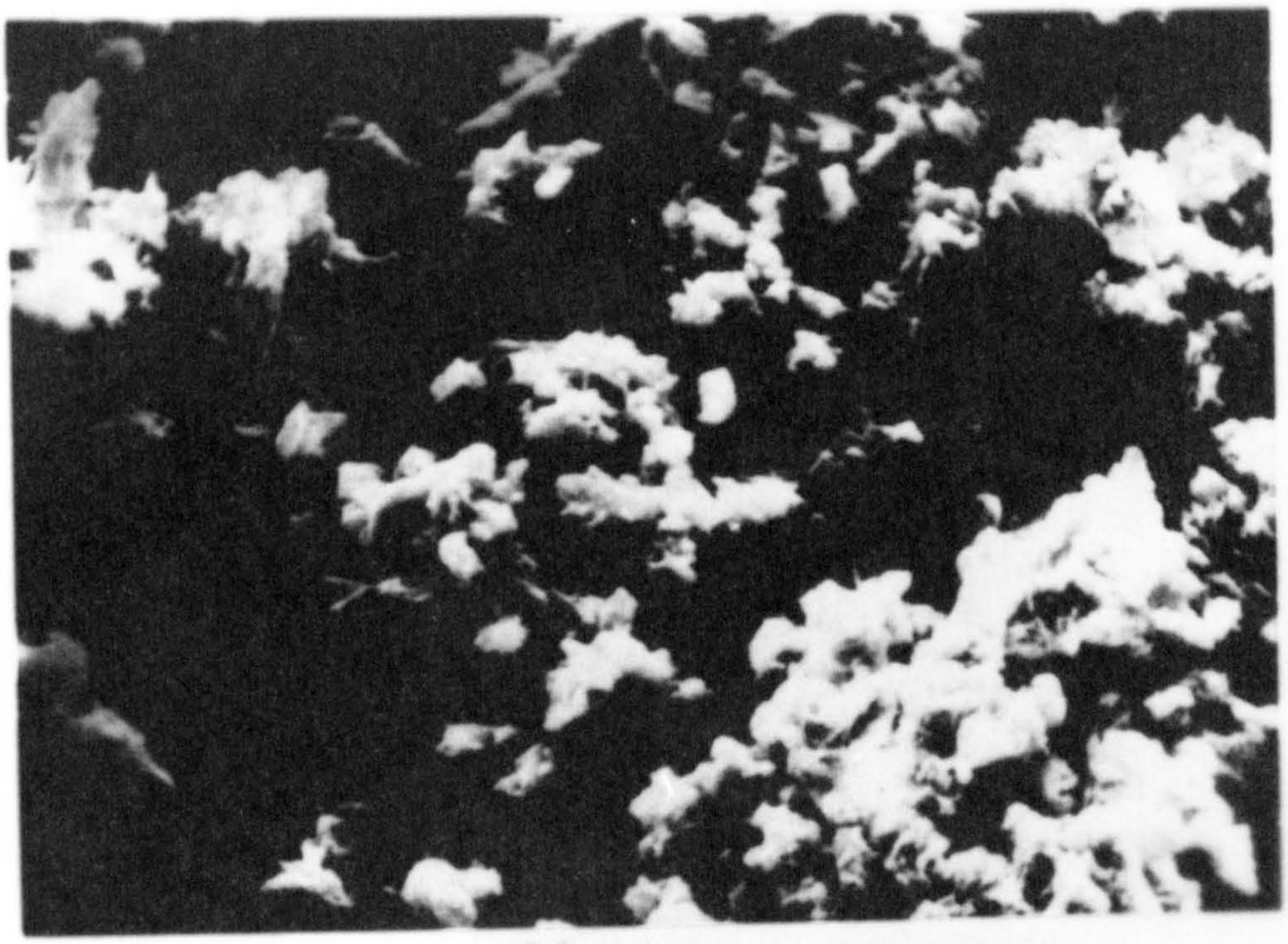

PS4

20 μm

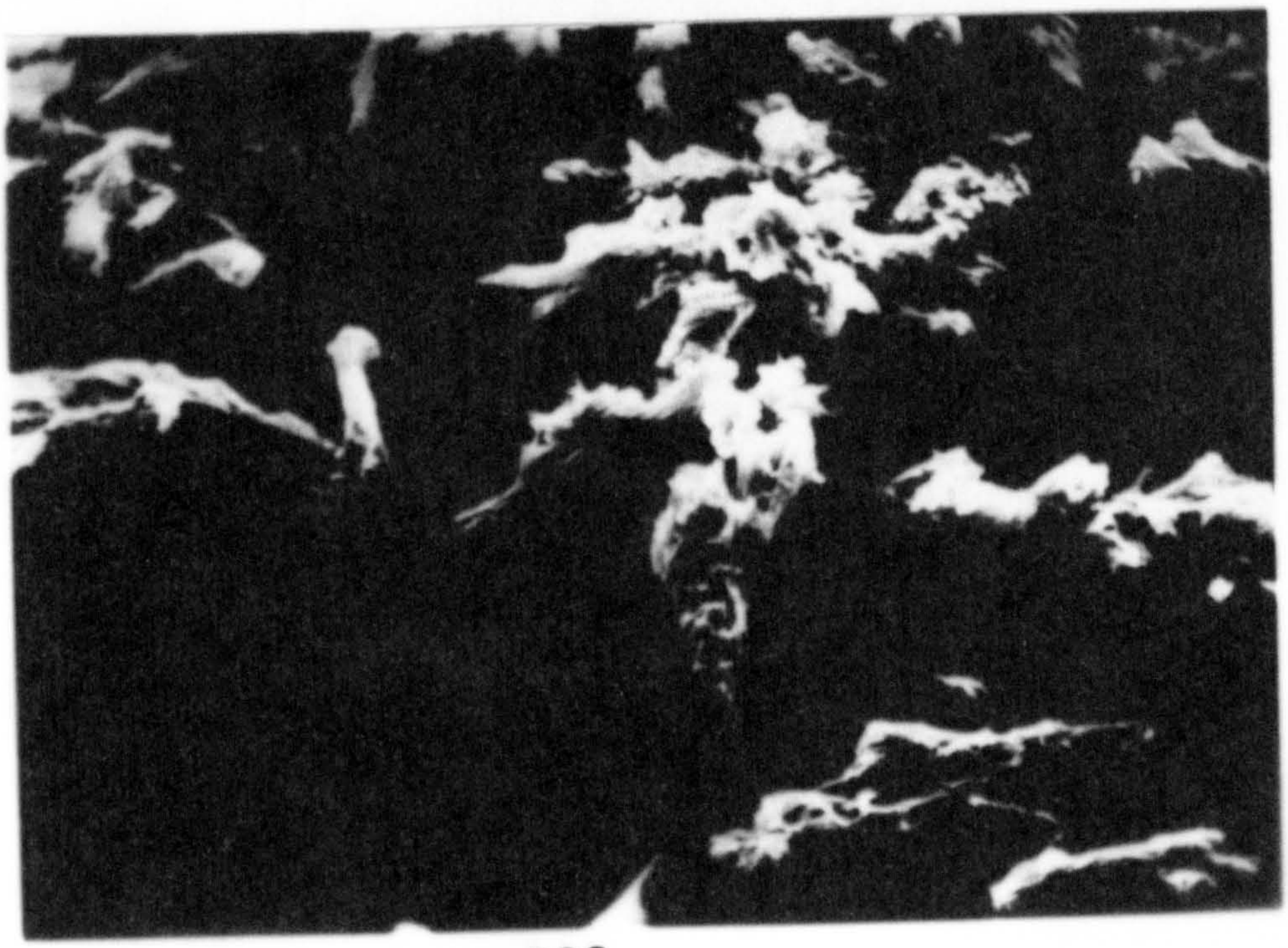

PS3

This effect was noticed at 95°C at a heating rate of 1°/min. The same effect was noticed for sample PS4, but for a wider temperature range (95-100°C)possibly due to overlapping of the melting of two polymorphs.

3.3.4.3 Differential scanning calorimetry

Figure 3.11 shows the D.S.C. thermograms of commercial phenylbutazone (δ form) and the four spray-dried samples. Original phenylbutazone and sample PS1 exhibited one single endothermic peak at 107°C, whilst sample PS2 showed a minor deviation at 95°C and small shoulder at 103°C on the endotherm. Sample PS3 gave an extra endothermic peak at 95°C followed by an exotherm at 97°C. This indicates the presence of a polymorph and corresponds to the β form. Sample PS4 exhibited two extra endothermic peaks at 95°C and 99°C each followed by an exothermic peak at 97°C and 101°C respectively indicating the presence of at least two polymorphs in this sample. Both samples PS3 and PS4 also gave the major endotherm at 107°C as observed in the original phenylbutazone and samples PS1 and PS2. Thus the D.S.C. thermograms show that at fast crystallisation rates metastable polymorphic forms were not formed, and the product has the same thermal behaviour as the stable commercial δ form. As the crystallisation rate decreased the number of metastable polymorphics formed increased.

3.3.4.4 Powder X-ray diffraction

The powder X-ray diffraction pattern for the stable δ form of phenylbutazone and the four spray dried samples are illustrated in Fig. 3.7a. Sample PS4 showed a totally different pattern from phenylbutazone δ form and the β polymorph with multi peaks at 6.4, 10, 14.6, 16, 19 and 24 degree of 2θ. This sample also gave two extra peaks

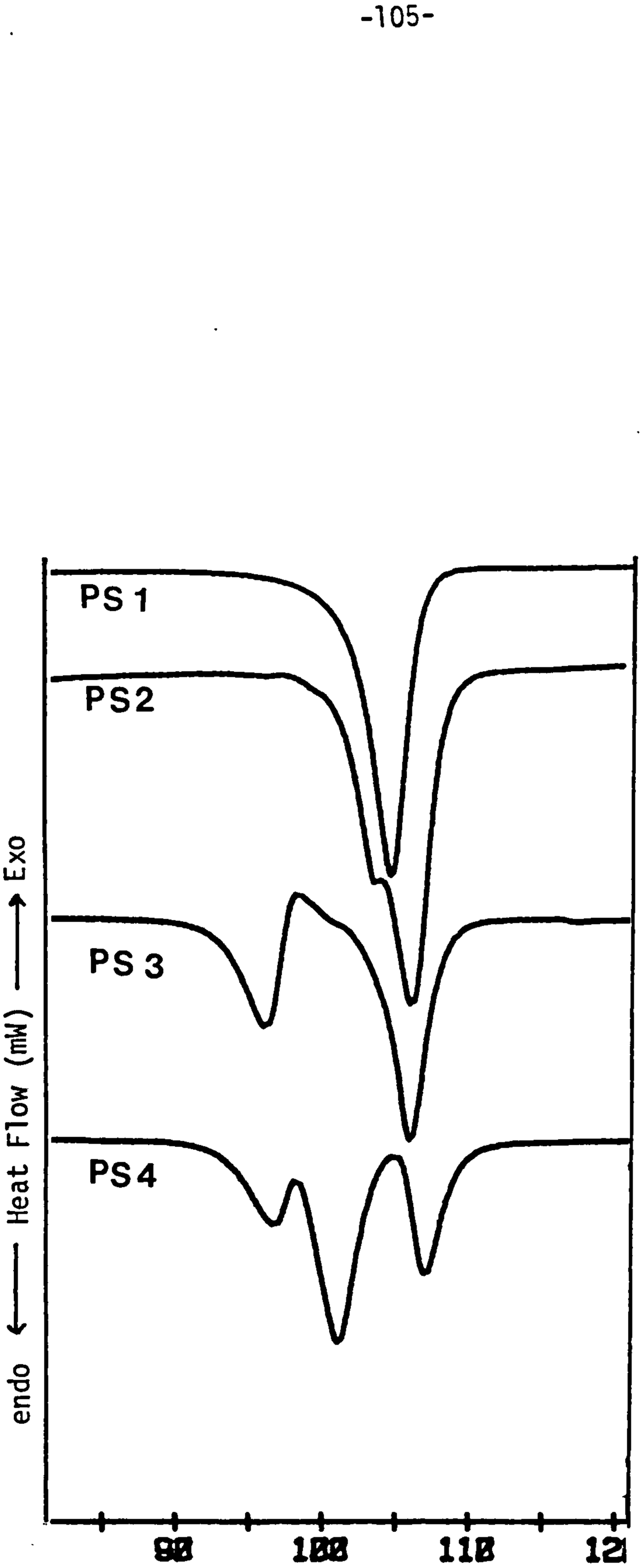

Fig. 3.11 The D.S.C. thermograms for samples PS1, PS2, PS3 and PS4 (heating rate 10°C/min, sample size 5-9 mg and under nitrogen flow)

on the D.S.C. thermogram which were thought to indicate the presence of two polymorphs. Sample PS3 gave an X-ray diffraction pattern similar to that shown by crystallised β polymorph which also showed on the D.S.C. thermogram an extra peak at 95°C. For sample PS2 only minor differences from the original X-ray pattern for phenylbutazone were observed. This sample exhibited a minor difference in the D.S.C. thermogram with a small shoulder on the melting endotherm. Sample PS1 was essentially the same as that observed for phenylbutazone δ form and had a very similar D.S.C. thermogram with a single endotherm at 107°C.

3.3.4.5 Solubility

The dynamic equilibrium solubility of the representative spray dried samples was examined in buffer phosphate of pH 7.5 at 37°C. Peak solubility was observed after 4 hours for all the spray-dried samples, followed by lower equilibrium values after 48 hours (see Fig. 3.13), and the height of the peak increased as the crystallisation rate reduced. This effect is attributed to the presence of polymorphic forms which initially showed metastable solubility prior to conversion to the stable form in solution. This is supported by the fact that the thermal behaviour of the samples observed by D.S.C. showed that as the crystallisation rate decreases the number of polymorphic forms present increased. The peak solubility figures agree with those reported by Matsuda et al. (1984). These workers tested the solubility of the spray-dried samples only for 5 hours. Matsuda et al. (1984) claimed that this peak values represent the limiting solubility of the samples and that the apparent equilibrium solubilities of β and α forms were not affected by time suggesting that they were not converted to δ form. This conclusion opposes the generally accepted mechanism of polymorphic

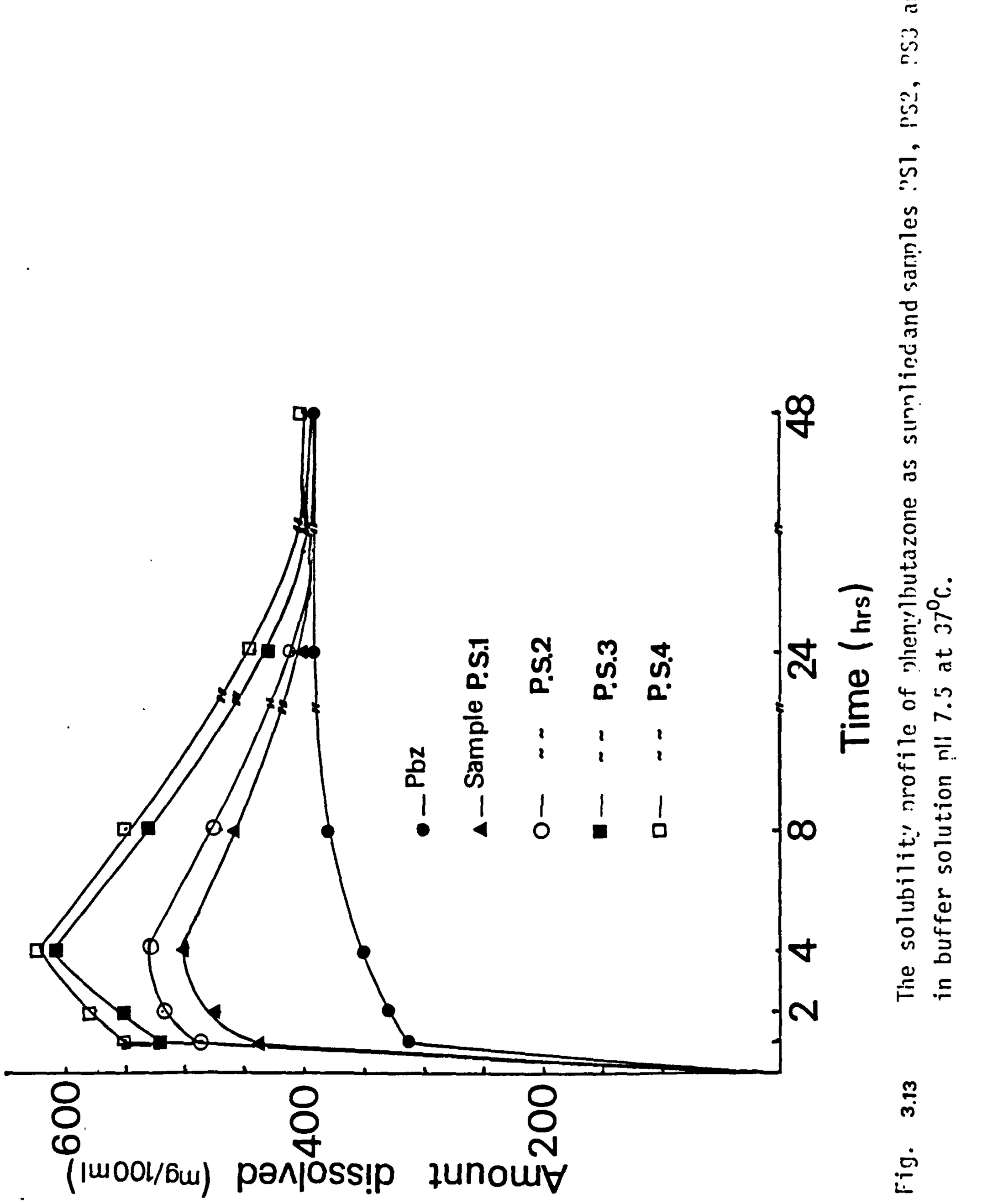

Fig. 3.13 The solubility profile of phenylbutazone as sum in buffer solution pH 7.5 at 37°C.

solubility behaviour, in that the metastable forms exhibit peaking solubility followed by conversion to the stable form and associated crystallisation from the super-saturated solution to the equilibrium solution of the stable form (Carstensten, 1980).

3.3.4.6 Dissolution rate

Dissolution rate data were obtained for compressed discs using a Woods apparatus to provide constant surface area in phosphate buffer pH 7.5 at 37°C (Fig. 3.14). Increases in dissolution rate over the supplied phenylbutazone were observed in the same sequence as that seen for solubility increases, i.e. samples PS4>PS3>PS2>PS1. The reason no peaking value was observed for dissolution rate data is attributed to the fact that the dissolved material had not reached the concentration level required for super-saturation with respect to the δ form.

It is interesting to note that sample PS1 showed an increase in dissolution as well as peaking effect in solubility curves, whilst the D.S.C. thermogram and X-ray diffraction pattern were similar to the original phenylbutazone β form. By integrating the area under the melting endotherm curve, the latent heat of fusion can be quantified It was found that the latent heat of fusion (see Table 3.8) was 10% lower than that for δ form phenylbutazone. This change might be due to the change in particle morphology and/or the presence of some amorphous drug after spray drying (Corrigan 1982).

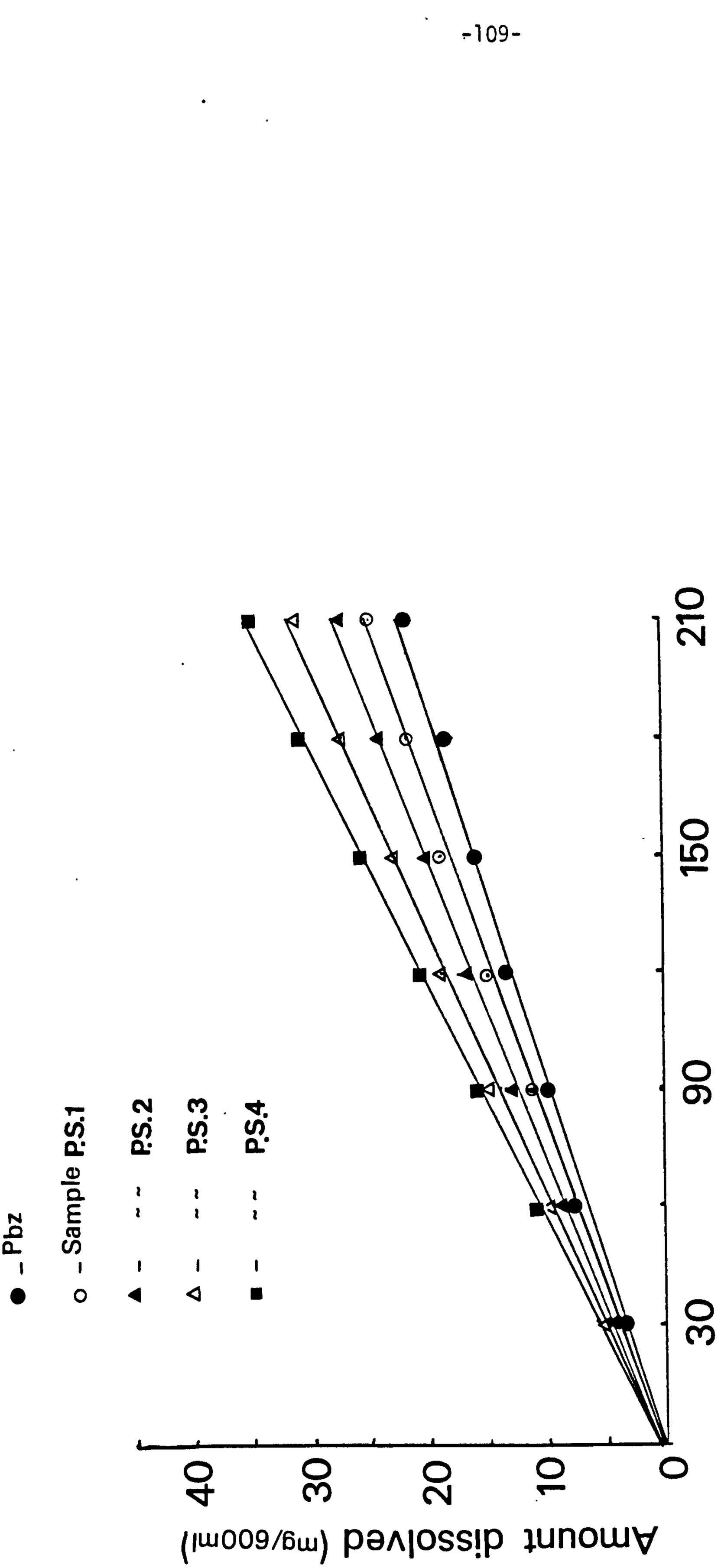

Fig. 3.14 Dissolution curves for phenylbutazone as supplied and samples PS1, PS2, PS3 and PS4 in buffer solution pH 7.5 at 37°C using Hoods apparatus.

Table 3.8 Heat of fusion for phenylbutazone as supplied and sample PS1

Sample	Heat of fusion ΔH_f KJ/mol
Pbz	27.00
PS1	24.31

3.4 Conclusions

1. The four spray dryer variables inlet temperature, pump rate, aspiration rate and flow rate were all found to contribute in controlling the spray dryer performance. Of the four variables examined, the inlet temperature and pumping rate had the largest effect on particle size and number of polymorphs in the product.

2. Three polymorphic forms of phenylbutazone were prepared and identified δ, the commercially available form, α form which was found to be very unstable, and the β form.

3. Dissolution rate of phenylbutazone β-polymorph exhibited 1.5 increase in dissolution rate compared with the original δ-form.

4. The rate of crystallisation was found to be important in influencing the number of polymorphs present in the spray-dried product. As the rate of crystallisation decreased the number of polymorphs formed increased.

5. No degradation of phenylbutazone occurred during spray drying.

CHAPTER 4

CHAPTER 4

4.1 The effect of H.P.M.C. on the physicochemical properties of phenylbutazone. Samples prepared by crystallisation and spray drying

4.1.1 Introduction

The use of hydrophilic polymers in the formulation of water insoluble drugs to enhance their dissolution rate has been widely studied (see Chiou 1969, Simonelli 1969, Gibaldi 1983). There are many ways of preparing the drug-polymer complex, including solid dispersion (Sekiguchi & Obi 1961), flocculating from alcoholic solutions (Naggar 1980) or spray drying (Takenaka et al. 1982).

Solid dispersions, the most popular technique used to make the drug-polymer complex, have been defined by Chiou & Riegelman (1971) as dispersion in the particular or molecular state of one or more very slightly soluble active ingredients in one or more water soluble inert excipient.

Solid dispersions can be obtained by two major procedures - melting or solvent evaporation (Anastasiadou 1982). Sekiguchi & Obi (1961) first used solid dispersions prepared by the melt method to increase the solubility of sparingly soluble drugs. They proposed the formation of eutectic mixture of a sparingly water soluble drug with hydrophilic carrier by melting the physical mixture of the drug and the carrier then cooling it to room temperature (Chiou 1969). Gibaldi (1968) showed that the magnitude of the increase in dissolution rate was a function of the ratio of the carrier to drug in the eutectic mixture; maximum rates were observed for the fusion mixtures containing very high proportions of carrier.

The solvent method was first reported by Tachibana & Nakamura (1965). This consists basically of dissolving the drug and the carrier in an organic solvent and evaporating the solvent. Numerous reports have subsequently been presented to explain the increase in dissolution rate of the treated drugs. Workers have suggested that the increase in dissolution rate is due to the decrease in particle size (Gibaldi 1968), eutectic mixture formation (Sekiguchi & Obi 1961), presence of glass transition (Chiou 1969), or the formation of high energy compounds (Simonelli 1969).

The main disadvantages of the solid dispersion method are the risk of decomposition of the drug and the possible evaporation of the components of the product by heat (Anastasiadou 1982). The method of flocculating the alcoholic solution of the drug in an aqueous solution of the polymer (Chiou 1976, Naggar 1980) was used in this study to reduce any possibility of decomposing the drug. This technique is thought to either coat each drug crystal with a film of polymer (Simonelli 1969) or create a complex with the drug via nucleophilic oxygen which is present in many polymers (Martin 1973).

Spray drying has also been successfully used to prepare microcapsules and provide solid particles or liquid droplets with an individual hydrophilic coat thereby modifying their physical, chemical or physiological characteristics. Speiser et al. (1973) prepared microcapsules of barbituric acid by spray polycondensation and Voellmy (1973) prepared microcapsules of phenobarbital using a similar technique. Then Takenaka & Kawashima (1982) prepared solid particulates of theophylline-ethylene-diamine complex (aminophylline) by spray drying and Kawashima (1983) reported a spray drying technique to prepare a solid particulate preparation of an aminopyrine-barbital complex. Takenaka & Kawashima (1981) studied the effect of cellulose acetate phthalate and colloidal

silica, and other excipients such as talc, on the polymorphism of spray dried microencapsulated sulphamethoxazole, while Takenaka et al. (1980) spray dried enteric coated microcapsules of sulphamethoxazole.

The objectives of this section of the work were: (1) to examine the effect of incorporating a hydrophilic polymer H.P.M.C., by crystallisation and spray drying, in phenylbutazone on the crystallographic and physicochemical properties of the resulting materials; and (2) to examine the influence of preparation process on the properties of the resulting products.

4.2 Experimental

4.2.1 Materials

The details of the materials used are listed in Chapter 2.

4.2.2 Methods

4.2.2.1 Crystallisation

The polymer was added to the drug by flocculating 100 ml of an ethanolic 6% w/v solution of the drug in 100 ml of an aqueous medium containing different concentrations of H.P.M.C. ranging from 0.01 to 5% w/v H.P.M.C. as reported in Section 2.2.6.2b. The dried crystals were crushed gently in a mortar and sieved through a 200μm sieve, then stored in a vacuum desiccator over self-indicating silica gel for the period of testing.

4.2.2.2 Spray drying

The amount of H.P.M.C. needed to produce the required H.P.M.C. level was dissolved in the aqueous part of the feed solution. Phenylbutazone was dissolved in absolute alcohol to give a 2% w/v solution. The two solutions were mixed and fed into the mini spray dryer operated under conditions previously found to produce a β-polymorph of phenylbutazone (i.e. inlet temperature 100°C, pump rate 4 ml/min., aspiration rate 0.00903 m^3/sec and flow rate 600 L/hr).

The materials prepared by crystallisation and spray drying were examined using the following techniques - D.S.C., SEM, powder X-ray diffraction, solubility and dissolution rate, all according to the methods described in Chapter 2.

4.3 Results and discussion

4.3.1 Incorporation of H.P.M.C. by direct crystallisation

H.P.M.C. was chosen in this study as it is a hydrophilic polymer, physiologically inert and suitable for human use. Also it is used in a wide range of coating formulations in film coating and controlled release preparations (e.g. Okhamafe 1983). However, it does not appear to have been used previously to prepare solid dispersions with water insoluble drugs to modify drug dissolution characteristics.

4.3.1.1 Assay of phenylbutazone - H.P.M.C. samples

An attempt to use HPLC to assay the two components in the phenylbutazone-polymer samples was made, but the procedure was not successful due to lack of reproducibility. The assay procedure subsequently used was that given in the B.P. (1980) to measure the phenylbutazone content in the drug-polymer sample. The untreated supplied drug containing 99.3% w/v phenylbutazone was used as the standard and other samples were related to it. The assay results (see Table 4.1) correspond approximately to the concentrations of H.P.M.C. used in the crystallisation liquor.

4.3.1.2 Differential scanning calorimetry

The prepared samples were tested by D.S.C. using aluminium crimped pans with pierced lids at a heating rate of $10^{o}C$/min under a flow of nitrogen gas of 10 ml/min. The D.S.C. thermogram of phenylbutazone (Fig. 4.1) crystallised without polymer exhibited.a single endothermic peak at $107^{o}C$, which corresponds to that of the untreated phenylbutazone. For the sample prepared from 0.01% w/v H.P.M.C. solution there is an extra small endothermic peak at $97^{o}C$ in addition to the endotherm at $107^{o}C$. The area of the new peak at $97^{o}C$ increased with

Table 4.1 Assay results of phenylbutazone and samples crystallised with H.P.M.C. containing solutions

Sample Code	Concentration of HPMC (% w/v in final crystallisation solvent)	% w/w of phenylbutazone in product *	Estimated % w/w of HPMC in samples
PbZ	0.0	99.30	0.00
PHR1	0.01	99.25	0.05
PHR2	0.1	99.10	0.20
PHR3	1.0	98.21	1.09
PHR4	2.0	97.10	2.20
PHR5	5.0	93.50	5.80

* Figures represent the arithmetic mean of three results

phenylbutazone crystallised with HPMC

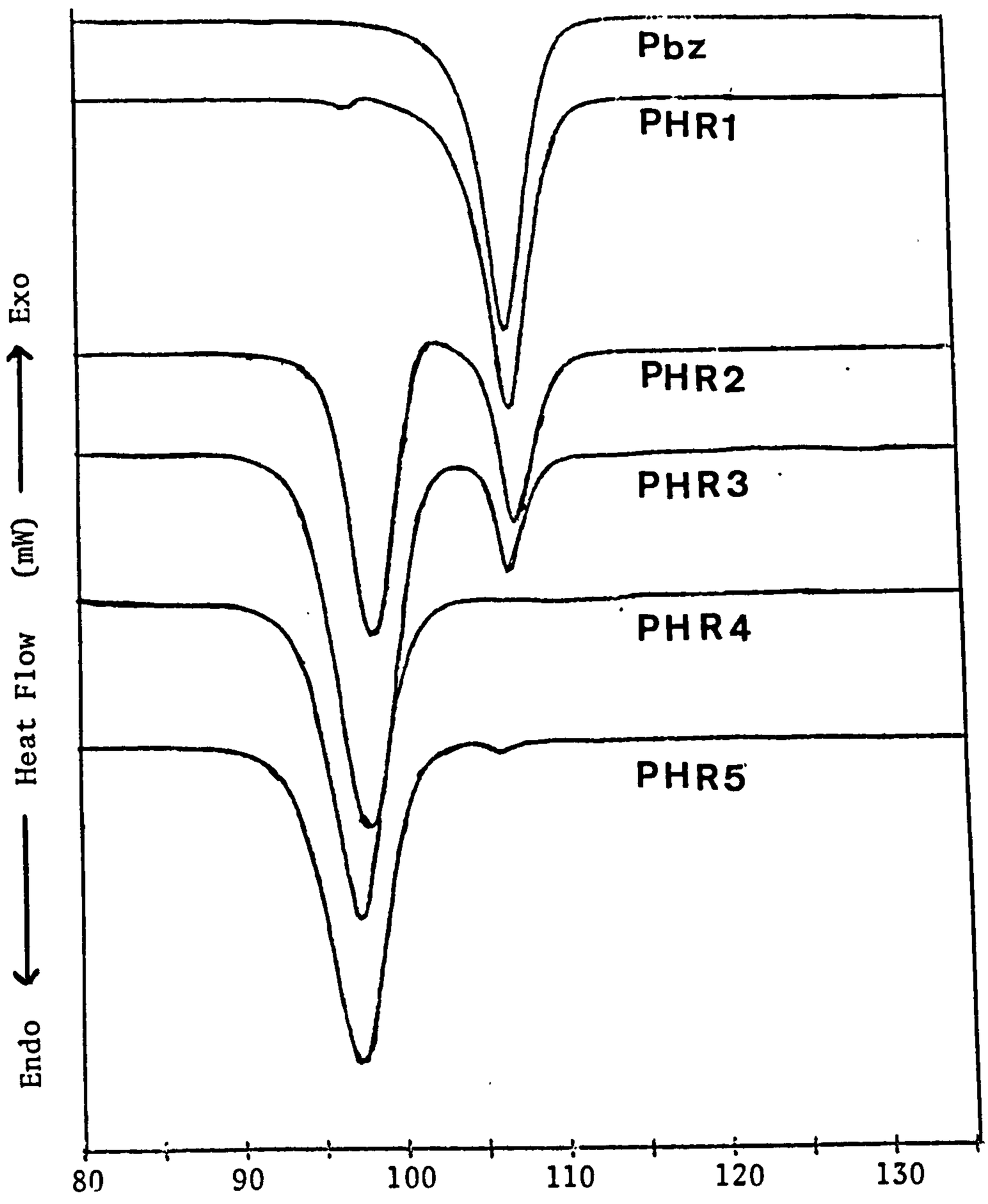

Fig. 4.1

D.S.C. for samples PbZ, PHR1, PHR2, PHR3, PHR4 and PHR5 (heating rate 10°C/min, sample size 5-9 gm and under nitrogen flow).

increasing H.P.M.C. concentration. Concurrent with the increase in the new peak at 97°C, the original endotherm at 107°C diminished up to H.P.M.C. concentration of approximately 2% w/w (see Fig. 4.1) when the endotherm at 107°C is completely absent. The peak at 97°C is not thought to be due to polymorphic transitions as:-

(a) the D.S.C. thermogram showed no exotherm between the two endothermic peaks at 97°C and 107°C even when scanned at lower rates. If the endotherm was due to a polymorphic transition an exothermic peak after the 97°C endotherm due to liquid recrystallisation would be expected.

(b) for sample PHR4 the peak at 107°C was completely absent. If it was due to a polymorphic transition the endotherm at 107°C should be present.

(c) no peaking values were observed in the dynamic solubility curves of the samples.

Previous data (Section 3.2 P. 94) showed the existance of peaking values in the dynamic solubility curves of polymorphic materials.

Table 4.2 shows the latent heat of fusion for the integrated endothermic peaks at 97°C and 107°C for all the samples. The latent heat of fusion at 97°C for sample PHR4 was 15% lower than that for phenylbutazone without H.P.M.C.

This, together with the 10°C shift in melting point, suggests the formation of a complex between the drug and the polymer possibly by hydrogen bonding,which could be called a 'high energy complex' (Simonelli et al. 1969). The major change in latent heat of fusion for the 107°C endotherm occurred between samples PHR1 and PHR2, whilst the major change in dissolution rate took place at the 1.09% w/w polymer level (see Fig.4.4)

Table 4.2 The latent heat of fusion (ΔH_f) of the two endothermic peaks at 97° and 107°C on the D.S.C. endotherm of phenylbutazone and crystallised samples containing H.P.M.C.

Sample Code	Concentration of HPMC Estimated (% w/w) of HPMC in samples	ΔH_f for original endotherm at 107°C (KJ/mol)	ΔH_f for new endotherm at 97°C (KJ/mol)
PbZ	0.00	27.00	0.00
PHR1	0.05	26.60	0.32
PHR2	0.20	9.71	18.90
PHR3	1.09	4.90	20.90
PHR4	2.20	0.00	23.30
PHR5	5.80	0.18	22.30

Fig. 4.2 Scanning electron microscope photomicrographs of samples PHR1, PHR2, PHR3, PHR4 and PHR5 phenylbutazone crystallised with HPMC

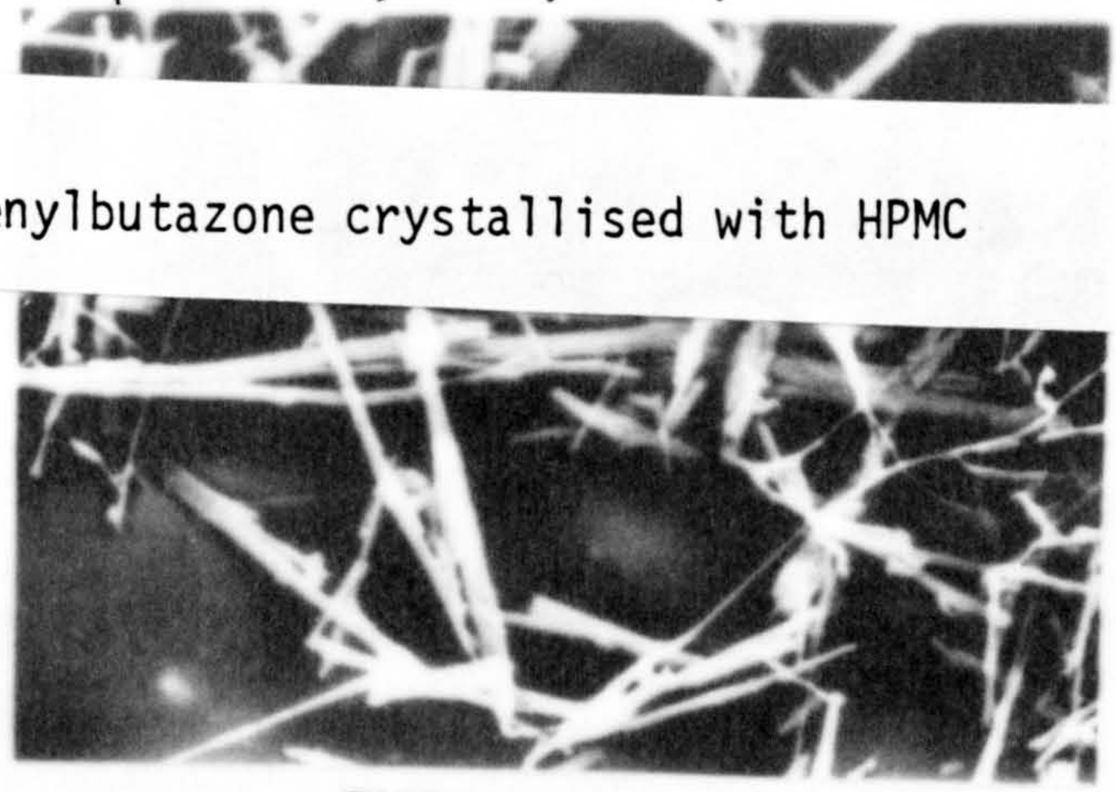

PHR1

PHR 2

PHR 3

20µm

Fig. 4.2 Scanning electron microscope photomicrographs of samples PHR1, PHR2, PHR3, PHR4 and PHR5

Fig 4.2

phenylbutazone crystallised with HPMC

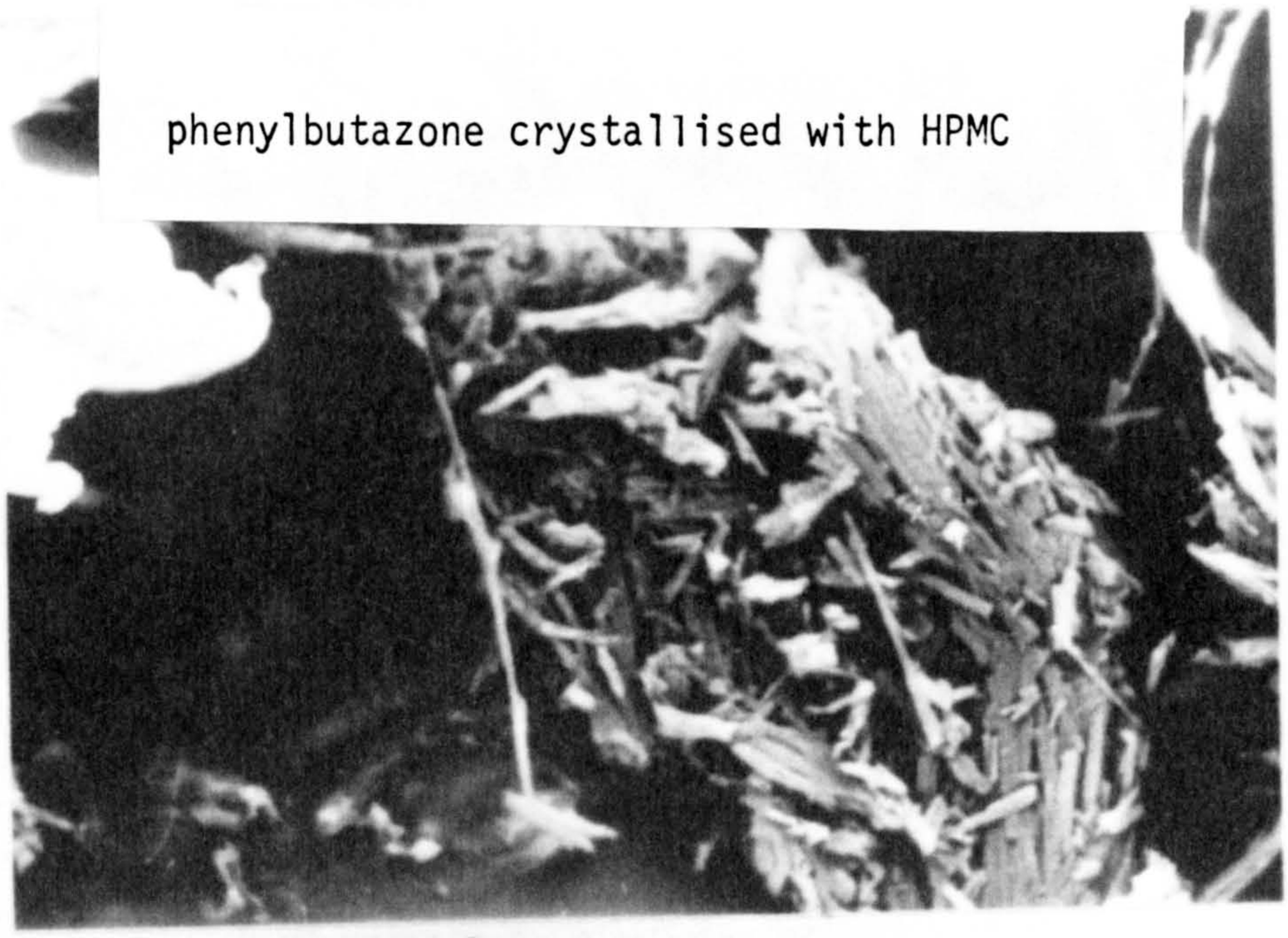

PHR 4

20 µm

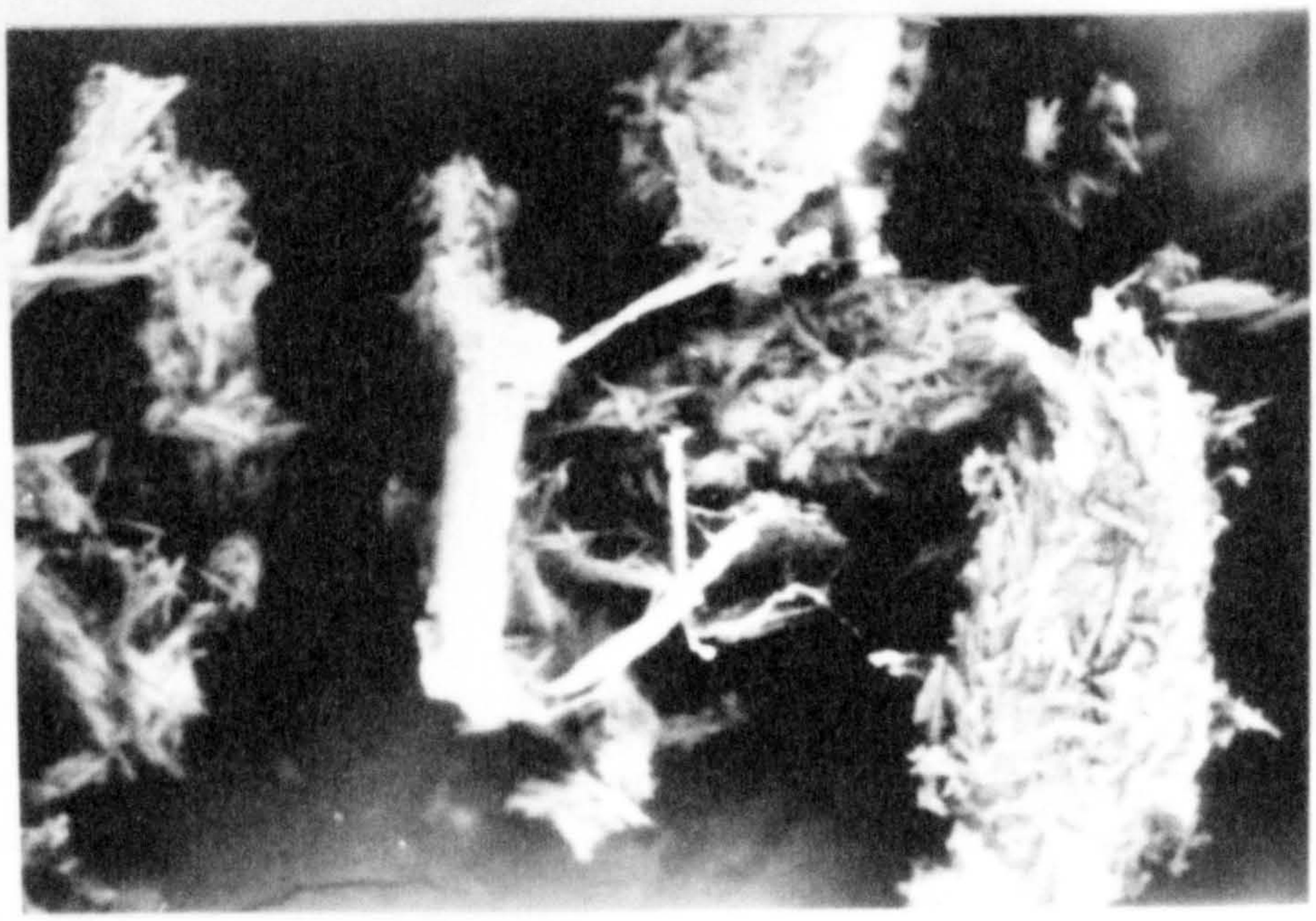

PHR 5

This might suggest that the change in dissolution rate was not primarily due to the change in crystal energy associated with the shift in melting point from 107°C to 97°C. Higher percentages of H.P.M.C. may be required to facilitate wetting of drug crystal surface prior to dissolution.

4.3.1.3 Scanning electron microscope

Samples were examined with the SEM for any change in particle morphology. The scanning electrophotomicrographs (Fig.4.2) indicate that the crystals retain their needle-like appearance, but the crystal length is reduced as the polymer concentration is increased. This observation is in agreement with Simonelli (1970) who reported that the rate of crystal growth is controlled by the polymer concentration. As the polymer concentration is raised the inhibition of crystal growth is increased. The observed decrease in crystal size is not thought to have influenced the increase in dissolution rate as postulated by Gibaldi (1968). This is because the decrease in crystal size increases with rising H.P.M.C. concentration whilst maximum increase in dissolution rate occurs at the 2.2% w/w H.P.M.C. level rather than the highest H.P.M.C. level studied, although other factors, such as changing viscosity of the diffusing layer,may be affecting observed dissolution rates.

4.3.1.4 Powder X-ray diffraction

Powder X-ray patterns were obtained (Fig. 4.3) by irradiating beds of the powder samples with a beam of X-ray radiation, using a diffractometer. All the crystallised samples containing H.P.M.C. showed peaks in the trace of 2θ versus I/Io indicating that the samples had some degree of crystallinity and were not amorphous. The

X-ray pattern for H.P.M.C. powder alone was obtained to establish that there were no peaks in the absorbing region for phenylbutazone. All the samples showed the same X-ray pattern except for the sample prepared from 0.01% w/v H.P.M.C. which was very similar to that of the original phenylbutazone. The major difference occurred in the region of 2θ between 16 and 24^{o} (see Fig. 4.3) in which the main peak at 22^{o} had reduced in size and divided into two peaks with the new peak at 2θ of 18^{o}. Small changes in the minor peaks could be attributed to the difference in packing during powder bed preparation.

However the X-ray diffraction traces indicate that all the samples are crystalline and not amorphous. The change in X-ray pattern, especially the peak at 2θ of 18^{o}, might be due to the presence of a phenylbutazone-H.P.M.C. complex.

4.3.1.5 Solubility

The results of the solubility experiments are listed in Appendix 2, Table 11. The equilibrium dynamic solubility was measured using a shaking water bath at 37^{o}C in phosphate buffer. There was a small increase of 1.2 fold in dynamic solubility for sample PHR4 compared with the original phenylbutazone with successive smaller increases in dynamic solubility with decreasing concentration of H.P.M.C. in the samples (see Table 4.3). The increase in solubility is attributed to the presence of high energy compounds in which phenylbutazone molecules require less energy to escape from the crystal lattice to go into solution than for those at lower energy levels.

4.3.1.6 Dissolution rate

Results from the dissolution rate experiments are listed in Appendix 2, Table 1-5. The dissolution rate for the samples was examined using Wood's apparatus in phosphate buffer. There was an increase in dissolution rate for samples crystallised with H.P.M.C.

TEXT CUT OFF IN ORIGINAL

Fig. 4.3 Powder X-ray diffraction patterns of phenylbutazone alone and samples crystallised from H.P.M.C. solutions.

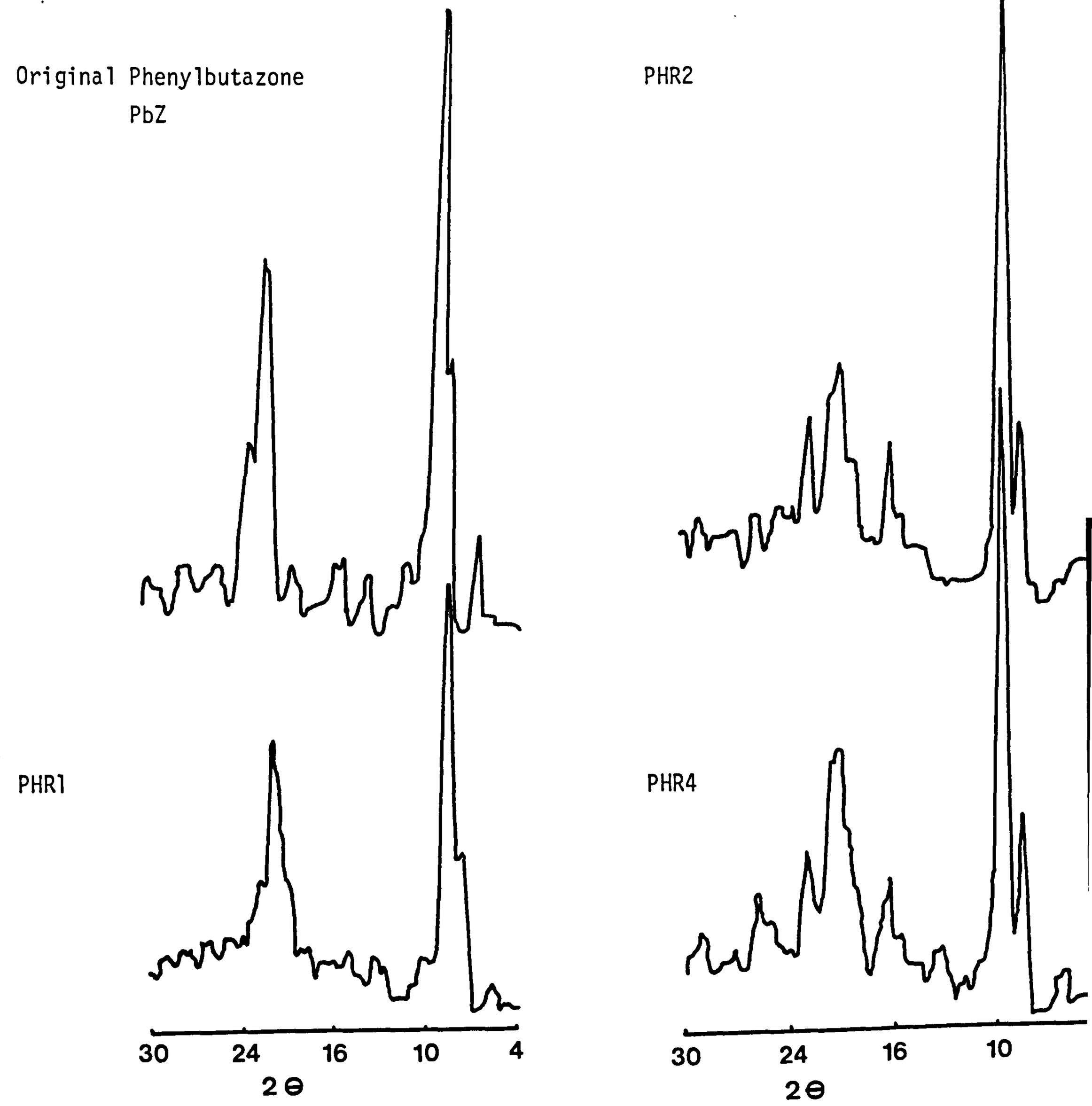

Table 4.3 The dynamic equilibrium solubility and intrinsic dissolution rate constant, $\hat{K}$, of phenylbutazone and samples crystallised from solutions containing different concentrations of H.P.M.C.

Sample code	Estimated % w/w of H.P.M.C. in samples	Sample Solubility (mgm/100 ml)	$\hat{K}$ ($mg/min/cm^2$)
PbZ	0.00	390	0.188
PHR1	0.05	400	0.250
PHR2	0.20	410	0.270
PHR3	1.09	430	0.290
PHR4	2.20	450	0.360
PHR5	5.80	440	0.410

compared with phenylbutazone alone (see Fig.4.4). Maximum increases occurred for sample PHR4, which contained 2.2% w/w H.P.M.C. Whilst samples prepared from the 5% w/v H.P.M.C. solution were shown in Section 4.3.1.2 to be composed completely of the high energy material, a decrease in dissolution rate is observed at this polymer level. This can be attributed to the polymer content in the sample reaching a limiting concentration such that the diffusion coefficient of the dissoluting tablet is modified which reduces the dissolution rate (Florence & Attwood, 1981). Alternatively, the polymer might modify the bulk viscosity of the dissolution medium reducing the dissolution rate (Braun & Parrott 1972, Kellaway & Najib 1983). However, when the amounts of H.P.M.C. dissolved in the dissolution media are calculated, the effect of bulk viscosity can be regarded as minimal.

The mechanism by which hydrophilic polymers work to increase dissolution rate is not well understood

but one possibility is that they reduce the hydrophobic barrier at the surface of the tablet by lowering the surface tension of the tablet which results in better wetting of the powder. Simonelli (1969) proposed that the polymer can act to improve the dissolution rate. He suggested that the dissolution of a complex can occur either by dissolving the intact complex in the dissolution medium with the drug then released from the complex, or by dissolving the bound drug from the surface by solvent interaction.

The increase in dissolution rate of phenylbutazone crystallised with H.P.M.C. is attributed to the formation of a high energy drug:polymer complex via hydrogen bonding. Thus the drug molecules require less energy to dissolve and the presence of the hydrophilic polymer could facilitate wetting. Simonelli (1969) suggested that coprecipitated

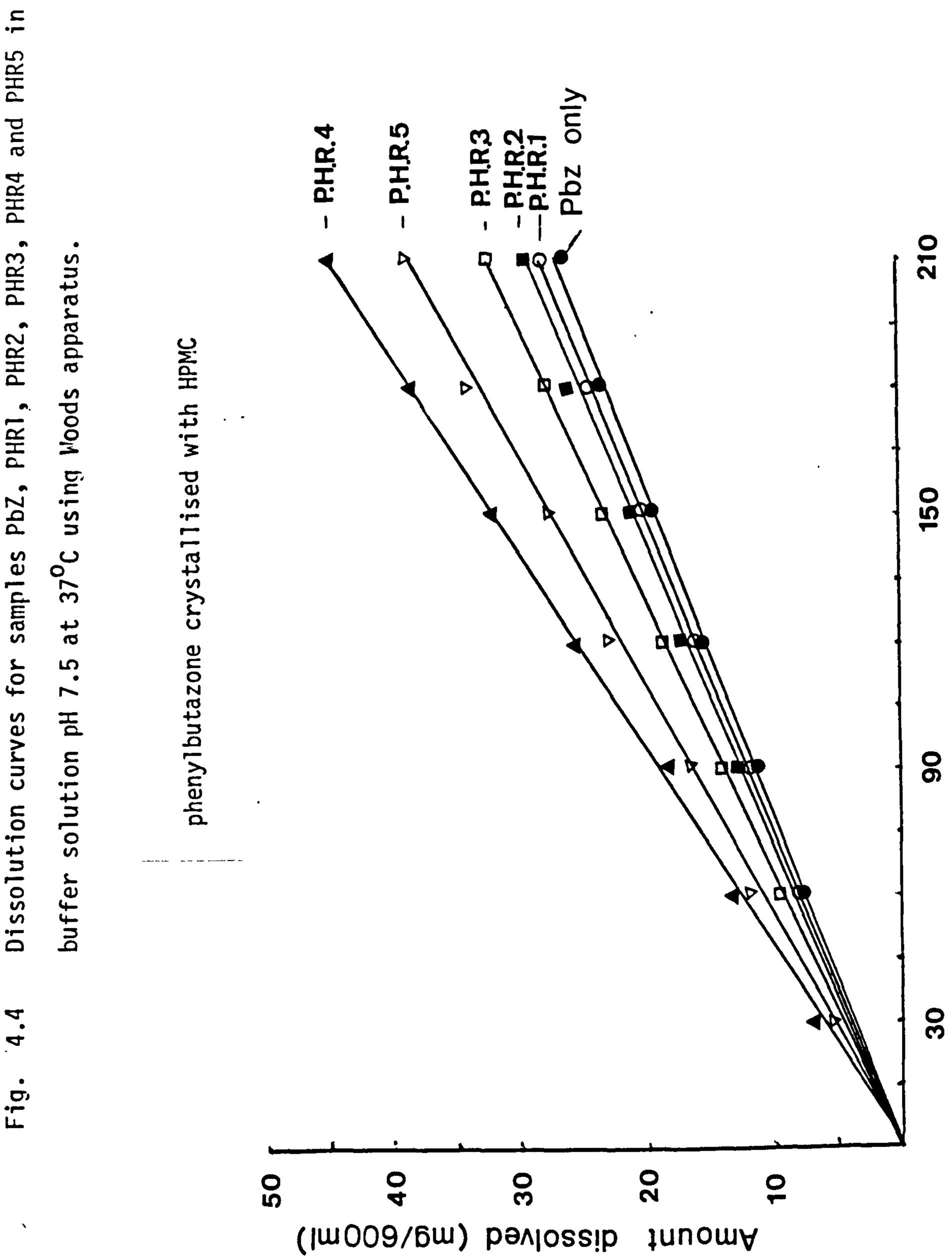

Fig. 4.4 Dissolution curves for samples PbZ, PHR1, PHR2, PHR3, PHR4 and PHR5 in buffer solution pH 7.5 at 37°C using Woods apparatus.

phenylbutazone crystallised with HPMC

sulphathiazole-polyvinylpyrrolidone formed high energy compounds. These high energy compounds were shown to be amorphous compounds due to distribution of the drug in a very fine crystal form through the drug:polymer complex. For phenylbutazone-H.P.M.C. complex the situation appears to be different.

Compounds melting $10^{o}C$ lower than the parent drug are formed and an increase in dissolution is associated with their presence, but they are crystalline in nature (see Fig. 4.3). However, a crystallographic change took place during crystallisation with the polymer as the compounds exhibited different X-ray diffraction patterns from the original δ form of phenylbutazone. All the samples containing H.P.M.C. exhibited the same X-ray diffraction pattern except for the sample at the lowest H.P.M.C. concentration.

If it is assumed that the complex is created by hydrogen bonding only and that a single hydrogen bond is created between one phenylbutazone molecule and one repeating unit in the H.P.M.C. polymer chain, then the mole fraction of each component in the complex would be 50% when maximally bonded and totally formed. The mole fractions of the components can be calculated according to the following equations:-

$$X_1 = \frac{n_1}{n_1+n_2} \qquad 4.1$$

$$X_2 = \frac{n_2}{n_1+n_2} \qquad 4.2$$

where X_1 the mole fraction of constituent 1

X_2 the mole fraction of constituent 2

and n_1 and n_2 are the number of moles of the constituent 1 and 2.

At 2.2% w/w H.P.M.C. concentration, when the δ form appears to be completely lost, the mole fractions of the components of the product are:-

$$\text{moles of H.P.M.C. repeating unit} = \frac{2.2}{265} = 0.008302$$

$$\text{moles of phenylbutazone} = \frac{97.1}{308.4} = 0.314851$$

$$\text{mole fraction of H.P.M.C. per repeating unit} = \frac{0.008302}{0.008302+0.314851} = 0.0257 = 2.57\%$$

$$\text{mole fraction of phenylbutazone} = \frac{0.314851}{000302+0314851} = 0.97431 = 97.43\%$$

The calculated fraction of H.P.M.C. required to cause the original δ form to be absent in the product is thus approximately twenty times smaller than the theoretical amount of 50%. The resulting structure would also be amorphous since periodicity of the phenylbutazone would be totally absent. Thus, since crystallinity is observed and much lower percentages of H.P.M.C. are required, additional interactions must be contributing to the proposed complex structuring.

It is also possible that the H.P.M.C. interferes within the arrangement of the phenylbutazone molecules in the lattice changing the angles of the crystals causing alteration of some phenylbutazone patterns e.g. the appearance of new peak on the X-ray diffraction pattern of 2θ at 18^{o}.

4.3.2 Incorporation of H.P.M.C. by spray drying

It was mentioned previously that when phenylbutazone was crystallised in the presence of H.P.M.C., a complex was formed. This crystalline complex was demonstrated to exist at a higher energy level than δ form phenylbutazone. Following on from this study it was of interest to examine whether phenylbutazone-H.P.M.C. complexes formed during spray drying which by comparison involves very rapid

crystallisation rates.

The operating conditions chosen for spray drying were those which produced a β-polymorph of phenylbutazone. Additional factors involved in selecting these conditions were:-

(a) the product obtained by spray drying under these conditions was of uniform particle size,

(b) the shape of the particles was the closest to the typical spherical spray-dried particles - observed in preliminary studies,

(c) these conditions produced a single polymorphic form, i.e. β-polymorph. Thus the effect of H.P.M.C. on the polymorphism of phenylbutazone during spray drying, could readily be monitored.

The product was assayed for phenylbutazone content in the drug: polymer samples using the procedure given in the B.P. (1980). The untreated supplied drug containing 99.3% w/w phenylbutazone was used as the standard and other samples were related to it. The assay results (see Table 4.4) indicate that the concentrations of H.P.M.C. in the products correspond closely to the amounts used in the feed solution to the spray dryer.

4.3.2.1 Differential scanning calorimetry

The D.S.C. thermograms of the products (see Fig. 4.5) were obtained by heating the samples in aluminium crimped pans with pierced lids, under nitrogen atmosphere, over the temperature range of 30-130^{o}C at a heating rate of 10^{o}C/min. For a sample of phenylbutazone spray dried alone, the thermogram exhibited an endothermic peak at 95^{o}C which corresponds to the β-polymorph, followed immediately by an exotherm

Table 4.4 Assay results of phenylbutazone and samples spray dried with H.P.M.C. containing solutions

Sample Code	Concentration of HPMC (% w/w) in the feed	% w/w of phenylbutazone in product *	Estimated % w/w of HPMC in samples
PbZ	0.0	99.30	0.00
PHS1	0.01	99.30	0.00
PHS2	0.1	99.21	0.09
PHS3	1.0	98.20	1.10
PHS4	2.0	97.40	1.90
PHS5	5.0	94.51	4.79

* Figures represent the arithmetic mean of three results

phenylbutazone spray dried with HPMC

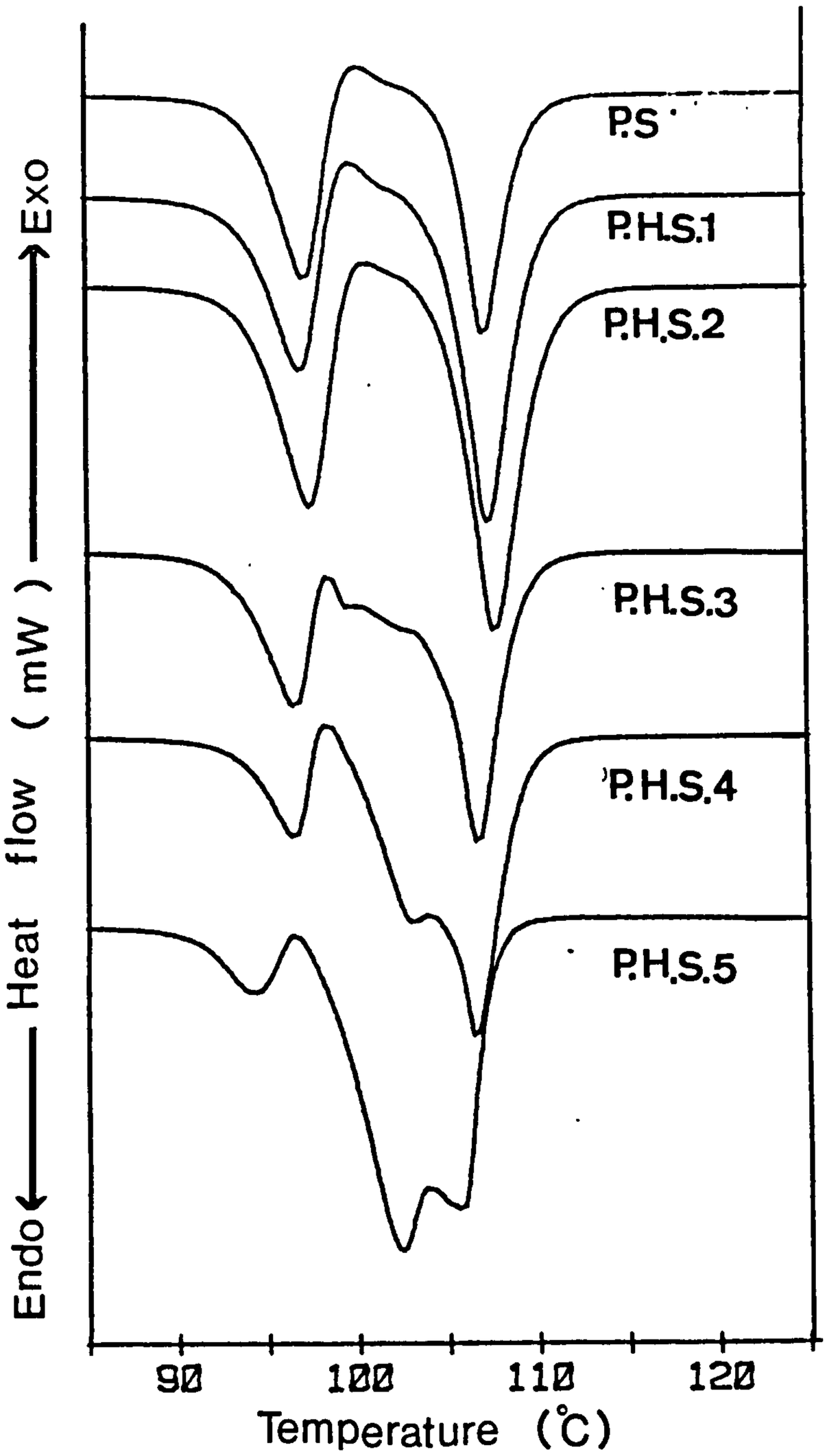

Fig. 4.5

D.S.C. for samples PS, PHS1, PHS2, PHS3, PHS4 and PHS5 (heating rate 10°C/min, sample size 5-9 mg and under nitrogen flow).

and the original phenylbutazone endotherm at 107°C (see Section 3.3 page105). Samples PHS1 and PHS2, containing the lowest two levels of H.P.M.C., exhibited the same thermograms as phenylbutazone spray dried alone, and no change was noticed on the D.S.C. thermogram.

For sample PHS3 in addition to the β-polymorph endotherm and exotherm, a small shoulder appeared at 102°C on the main melting endotherm. This shoulder became more distinct with increasing H.P.M.C. concentration until at the 4.79% w/w H.P.M.C. level (sample PHS5) it predominated over the endotherm at 107°C. Associated with the increase in shoulder at 102°C was a decrease in the endotherm at 95°C.

The presence of H.P.M.C. during the spray drying thus appears to have a two-fold effect on the thermogram. First,an extra and new endotherm starts to appear at 102°C which, for sample PHS5 dominates over the endotherm at 107°C. Second,H.P.M.C. appears to mask the formation of β-polymorph with the reduction in the endotherm at 95°C as the concentration of H.P.M.C. increases above 1% w/w. This latter observation is in contrast to that of Takenaka et al. (1981) who reported that spray drying sulphamethoxazole with cellulose acetate increased the polymorphism of sulphamethoxazole.

The endotherm at 102°C is thought to represent the melting of a drug:polymer complex as the X-ray diffraction pattern for these samples exhibited the new peak of 2θ at 18° which was shown by the complex prepared by conventional crystallisation (see Section 4.3) The difference in melting point and therefore structure of the complex prepared by spray drying compared with that obtained previously might be due to differences in preparation conditions, especially the rate of crystallisation.

4.3.2.2 Scanning electron microscope

Since all the samples were spray dried under the same conditions, samples were expected to have the same morphological shape and appearance. This was in fact observed and little change was noticed in the morphology of the product particles (see Fig.4.6).

4.3.2.3 Powder X-ray diffraction

Powder X-ray diffraction data for the samples showed that samples PHS1, PHS2 and PHS3 containing approximately 0.01%, 0.1% and 1% w/w H.P.M.C. gave the same X-ray diffraction pattern, which was very similar to that shown by the phenylbutazone spray dried alone, i.e. β-polymorph, with an additional new peak in the region of 2θ at 18^{o}. This peak was considered to be associated with the formation of a complex between the drug and the polymer (see Fig. 4.7) and be consistent with the interpretation of D.S.C. thermograms in Section 4.3.2.1.

For higher concentrations of H.P.M.C. the patterns changed, particularly in the area of 2θ between 24 and 30^{o}. The peak at 24^{o} decreased in size with increasing H.P.M.C. concentrations. Also the minor peaks in the area between 25-30^{o} diminished with increasing H.P.M.C. concentration. These observations support the suggestion that H.P.M.C. above 1% w/w concentration masked the formation of β-polymorph of phenylbutazone on spray drying.

The modified X-ray diffraction patterns also indicated that all the samples were crystalline in nature. Takenaka et al. (1981) reported that the reduced intensities of the X-ray diffraction patterns of the products with a high cellulose acetate phthalate concentration indicated increased amorphous nature. This is in contrast to the H.P.M.C.:phenylbutazone products as the intensity of

Fig. 4.6 Scanning electron micrographs of samples PHS1, PHS2, PHS3, PHS4 and PHS5

Fig 4.6

phenylbutazone spray dried with HPMC

PHS1

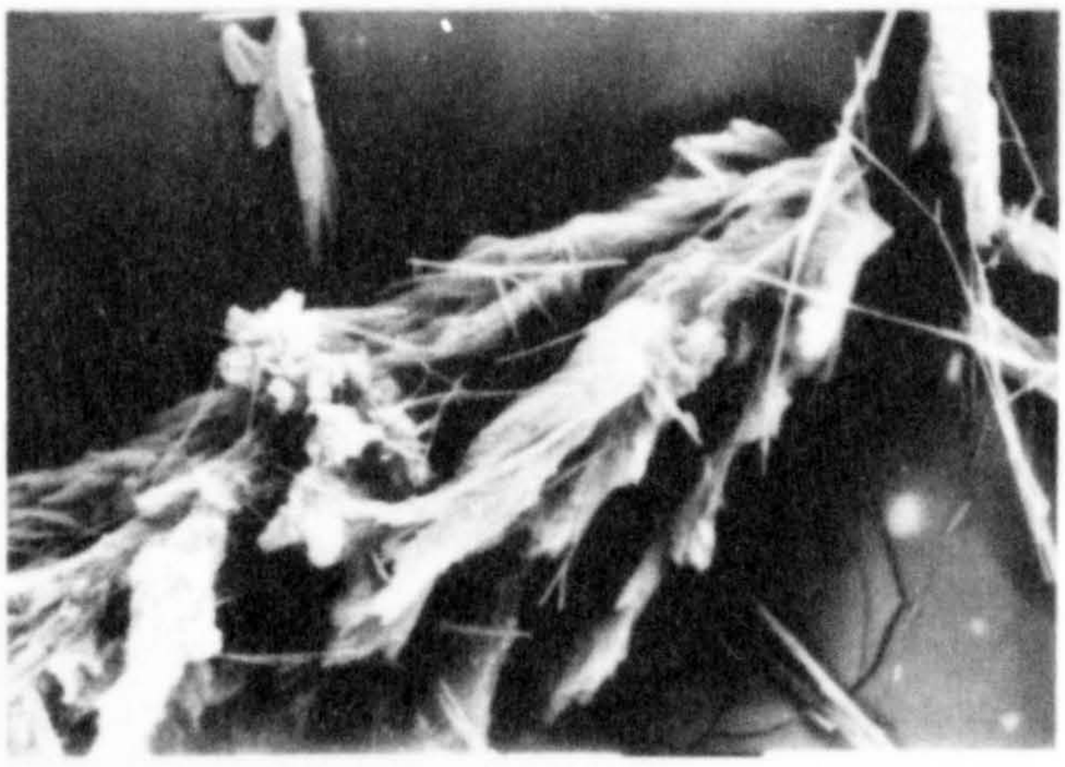

PHS2

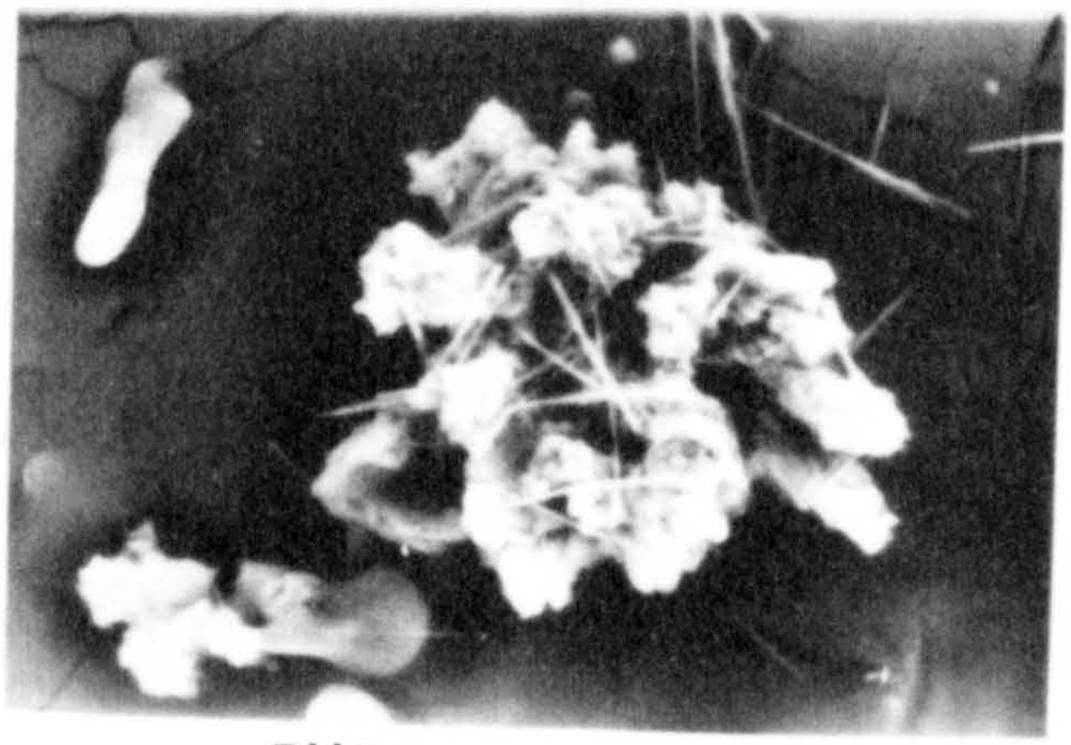

PHS3

20μm

Fig. 4.6 Scanning electron micrographs of samples PHS1, PHS2, PHS3, PHS4 and PHS5

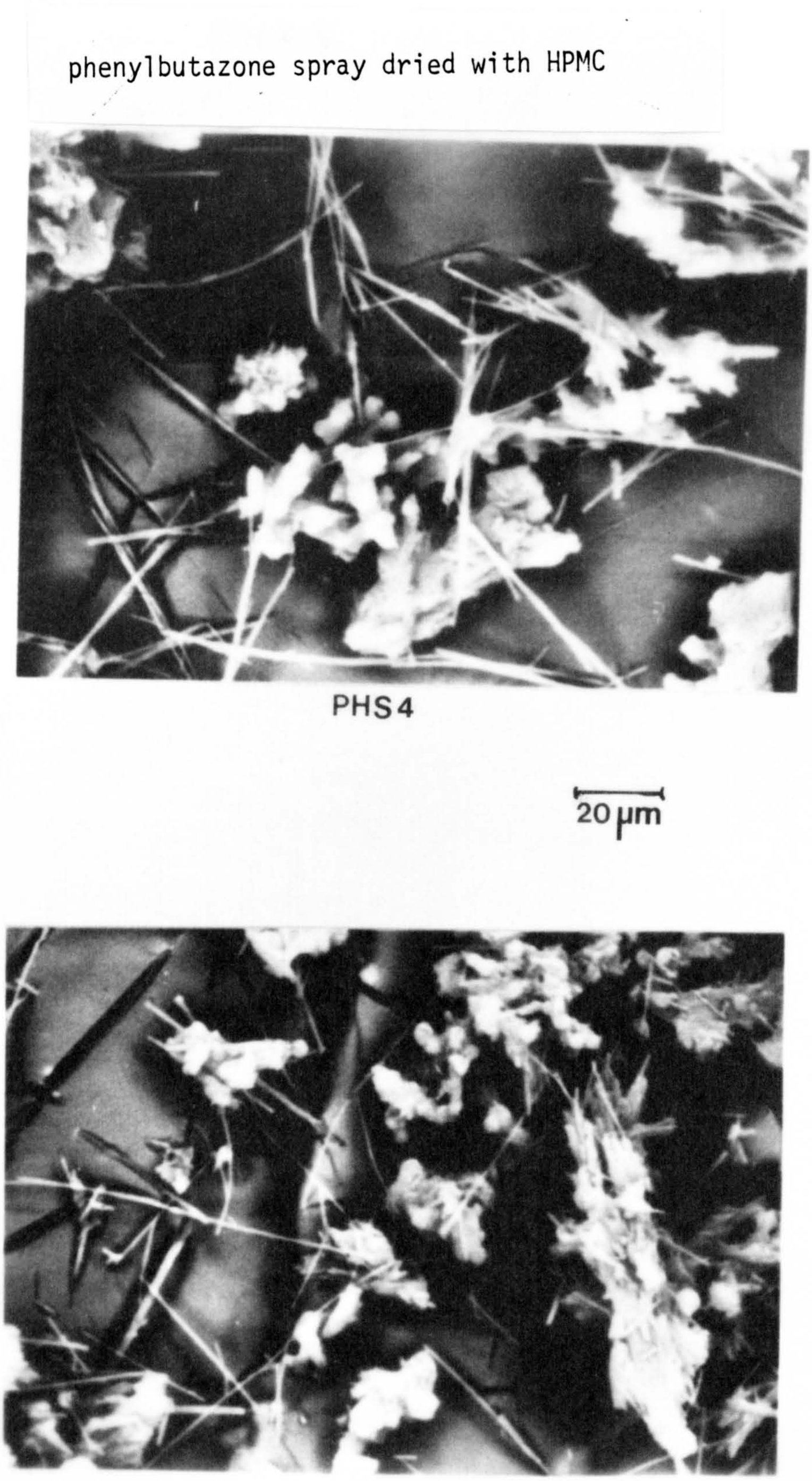

Fig. 4.7 The powder X-ray diffraction patterns of phenylbutazone alone and spray dried with H.P.M.C.

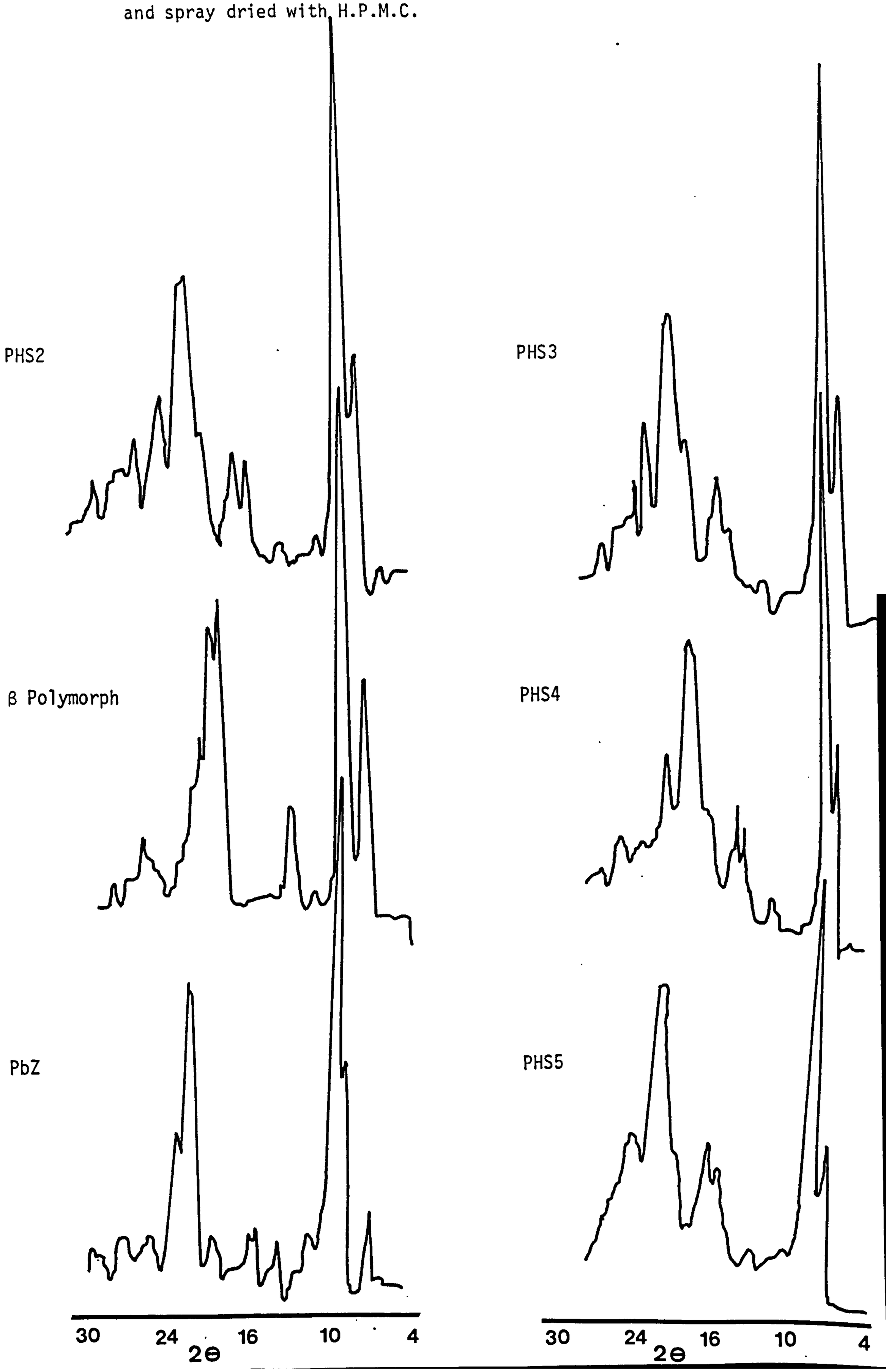

all the peaks below 2θ of 24° remained the same with only the minor peaks above 24°reduced in intensity with increasing H.P.M.C. concentration.

4.3.2.4 Solubility

The results of solubility experiments are listed in Appendix 2 Table 12.

The dynamic solubility of the samples was measured by placing excess of the powder in contact with buffer in a shaking water bath, as described in Chapter 2. As discussed in Chapter 3 polymorphic materials can be assigned two solubility values, peaking and equilibrium values.

Only small increases in maximal equilibrium solubility were observed for samples containing H.P.M.C. (see Table 4.5). An interesting change, however, occurred in the peaking solubility values. The spray-dried phenylbutazone without H.P.M.C. exhibited a peaking solubility value after 4 hours whilst for samples containing H.P.M.C. the time to reach peaking value was delayed and was achieved after 8 hours.

This observation is in agreement with Simonelli (1969) who suggested that the presence of polymer delays the conversion of metastable polymorph to the stable form. In addition the value of the peaking solubility decreased with increasing H.P.M.C. concentration in the samples, supporting the conclusion obtained from the D.S.C. thermograms that the presence of H.P.M.C. masks the formation of β-polymorph. The peaking value, which demonstrates the solubility of the metastable form, was reduced. Also the reduction in peaking value gives some support to the suggestion that the endotherm at 102°C on

Table 4.5 The dynamic peaking and equilibrium solubility, and intrinsic dissolution rate constant, $\grave{K}$, of phenylbutazone and samples spray dried with solution containing different concentrations of H.P.M.C.

Sample Code	Estimated % w/w of H.P.M.C. in sample	Solubility (mgm/100ml) Peak	Equilibrium	$\grave{K}$ (mg/min/cm^2)
PbZ	0.00	580	385	0.27
PHS1	0.00	560	400	0.28
PHS2	0.09	550	410	0.29
PHS3	1.10	540	415	0.33
PHS4	1.90	520	440	0.35
PHS5	4.79	500	435	0.37

the D.S.C. thermogram is not due to a polymorphic transition, but is associated with a phenylbutazone:H.P.M.C. complex.

The enthalpies of solution of the spray dried phenylbutazone-HPMC samples were estimated by determining the dynamic equilibrium solubility of the samples at different temperatures, applying equation (2.3), and plotting log solubility against $\frac{1}{T}$. Typical Vant Hoff plots (see Fig.4.8,4.9)gave linear graphs. Enthalpies of solution, ΔH_s, were then calculated from the slopes (see Table 4.6). The endothermic enthalpy of solution (ΔH_s) decreased with increasing H.P.M.C. concentration, which is an indication that the samples containing higher H.P.M.C. concentrations require less energy input to dissolve and are therefore less ordered. Also the fact that the endothermic value of enthalpy for the spray dried samples are less than those for samples recrystallised with H.P.M.C. (see Table 4.6) is an indication that the systems prepared by spray drying are generally less ordered than those made by conventional crystallisation. This is partly expected since the β-polymorphic form is present in the spray dried samples.

4.3.2.5 Dissolution rate

The results of the dissolution rate experiments are listed in Appendix 2, Table 6-10.

The dissolution ratesof the spray dried phenylbutazone with H.P.M.C. were determined using Wood's apparatus in buffer solution at 37^{o}C and sampling intervals of 30 minutes. It was shown previously (see Section 4.2) that when phenylbutazone was crystallised from a 2% w/v H.P.M.C. solution, the dissolution rate of the product was doubled (see Fig. 4.10 and Table 4.3). This was explained by the formation of a high energy complex between the drug and the polymer,

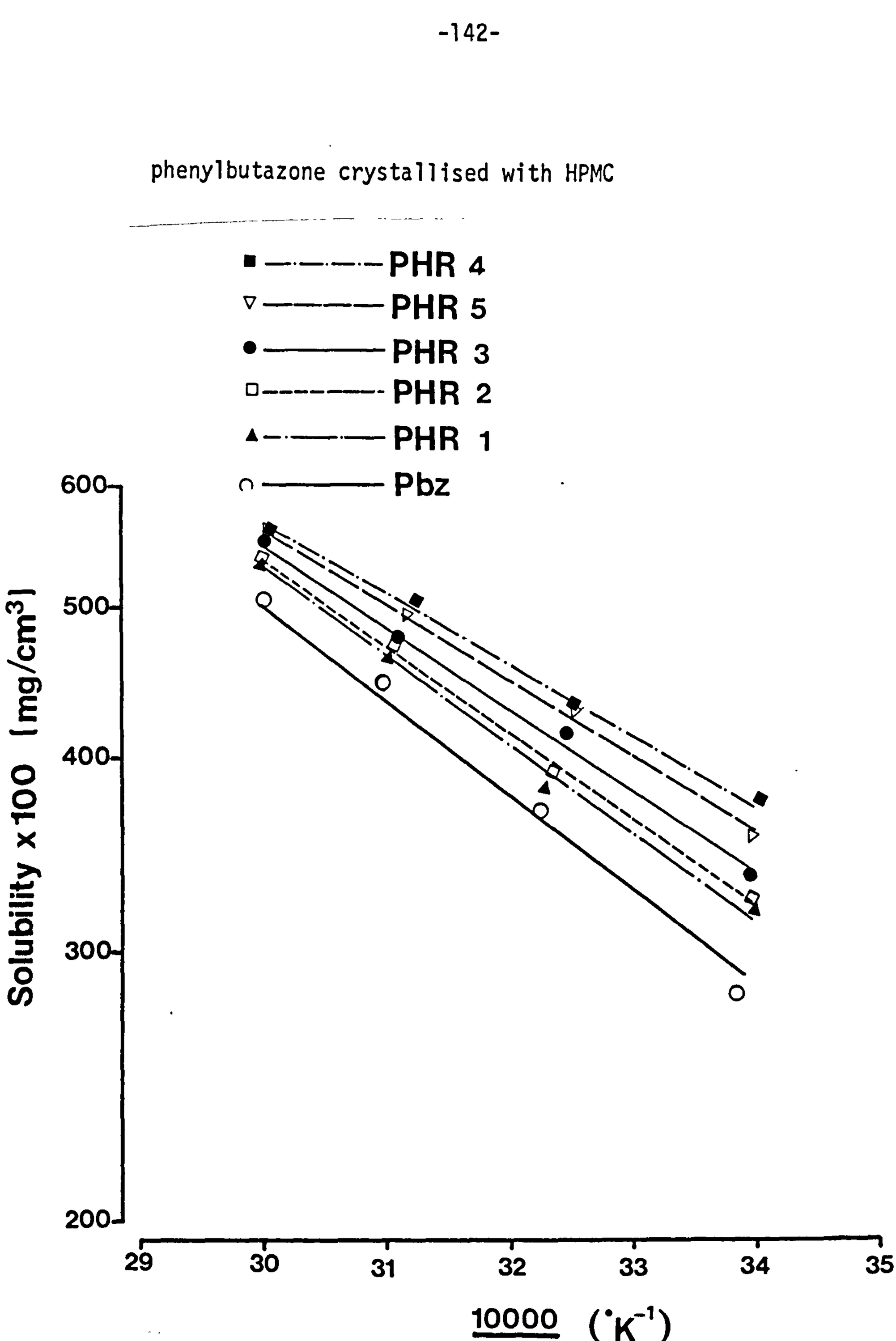

Fig. 4.8 Van't Hoff plots of the solubilities of the different forms of phenylbutazone alone and samples crystallised from solutions containing different concentrations of H.P.M.C.

phenylbutazone spray dried with HPMC

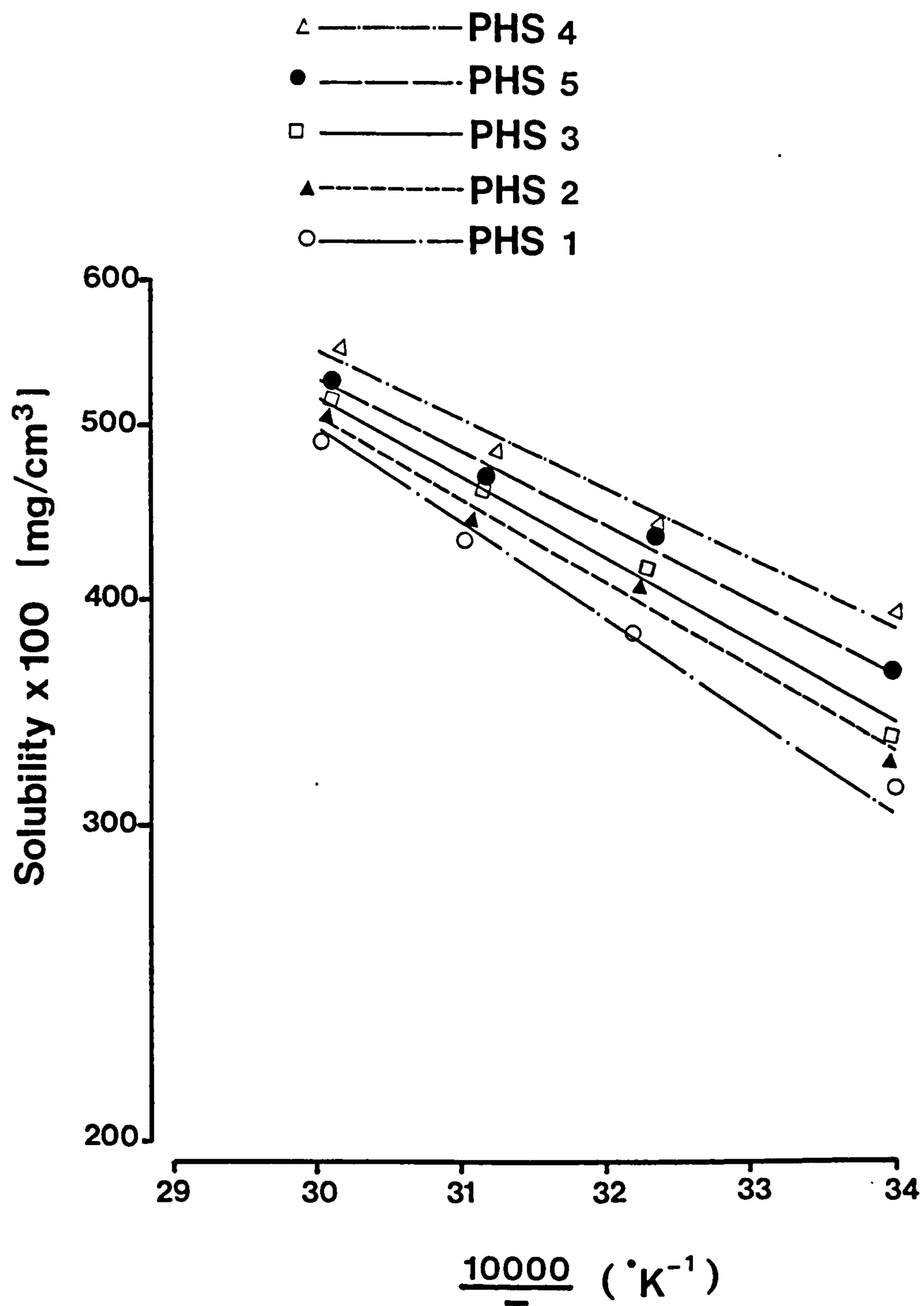

Fig. 4.9 Van't Hoff plots of the solubilities of the different forms of phenylbutazone spray dried with different concentrations of H.P.M.C.

Table 4.6 The enthalpy of solution (ΔH_s) for phenylbutazone crystallised and spray dried alone, and samples containing H.P.M.C. prepared by crystallisation and spray drying

Sample Code	ΔH_s (J/mol) of crystallised samples	Sample Code	ΔH_s (J/mol) of spray dried samples
PbZ	14.36	PbZ	12.46
PHR1	13.88	PHS1	11.96
PHR2	13.40	PHS2	11.00
PHR3	12.45	PHS3	10.53
PHR4	11.45	PHS4	9.85
PHR5	11.4	PHS5	9.80

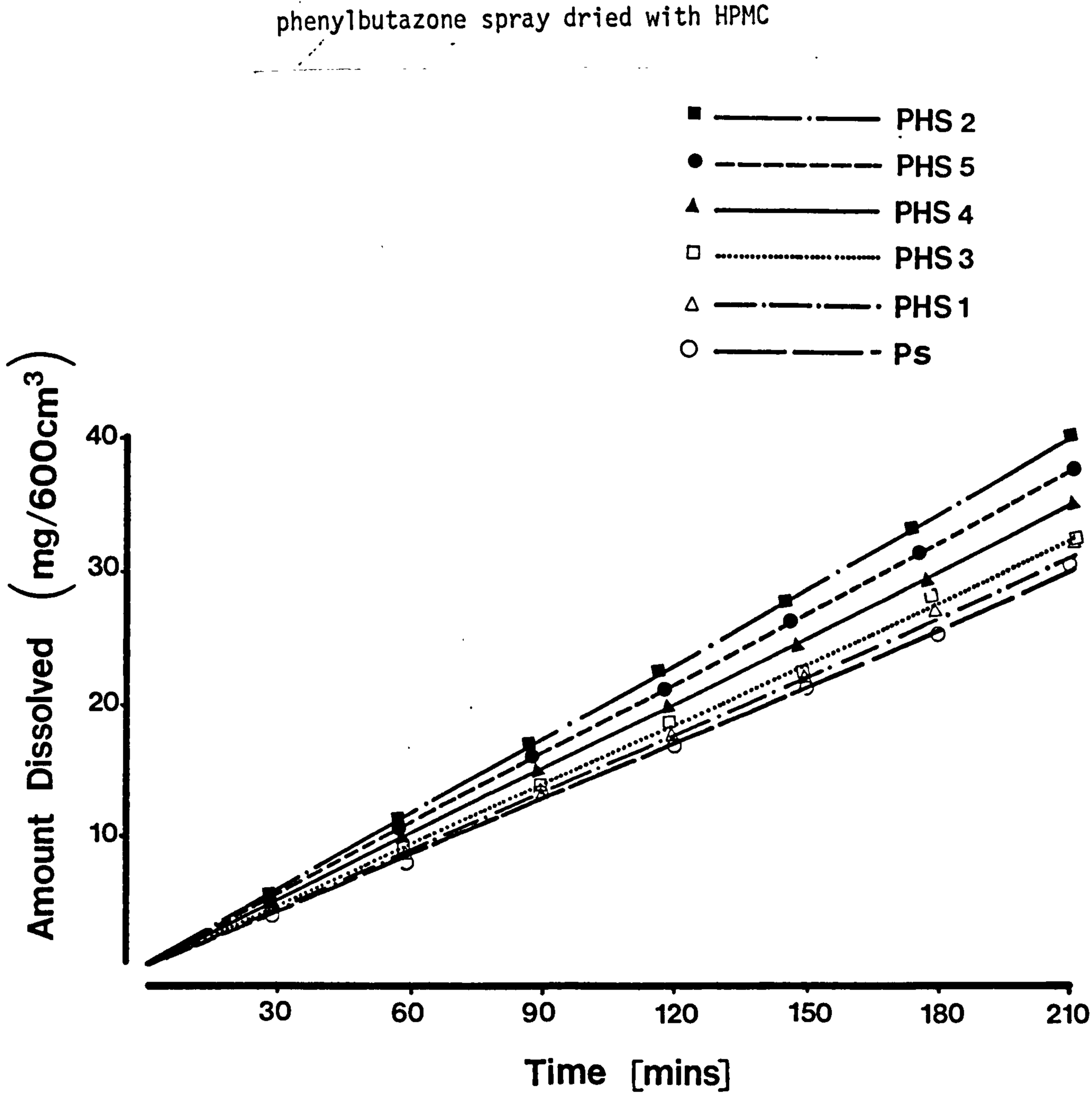

Fig. 4.10

Dissolution curves for samples PS, PHS1, PHS2, PHS3, PHS4 and PHS5 in buffer solution pH 7.5 at 37^{o}C using Woods apparatus.

the presence of the hydrophilic polymer also facilitating wetting. When phenylbutazone was spray dried from solutions containing the same concentrations of H.P.M.C. the optimal increase in dissolution rate was similar to that achieved by samples prepared by conventional crystallisation with approximately 2% w/w H.P.M.C. level exhibiting the highest dissolution rate. But for samples containing lower concentrations of H.P.M.C. the dissolution rate for equivalent samples prepared by spray drying was higher than for samples prepared by conventional crystallisation due to the presence of β-polymorph in the spray-dried samples. The similarity in dissolution for samples containing higher levels of H.P.M.C. adds support to the proposed mechanisms of effect of the polymer in that increases in dissolution rate can be attributed not only to the formation of high energy compounds, but also to the fact that the complexes or the presence of H.P.M.C., lowers the surface tension of the dissolving tablet, resulting in better wetting of the crystal surfaces. For sample PHS5 the dissolution rate was reduced as a result of changing the dissolution conditions either by modifying the diffusion coefficient at the surface of the dissolving tablet (Florence & Attwood 1981) or by increasing the bulk viscosity of the medium (Kellaway & Najib, 1983).

4.4 Conclusions

1. Phenylbutazone samples were prepared by conventional crystallisation and spray drying to contain H.P.M.C., which resulted in changes in the physicochemical and crystallographic properties of the drug.

2. Analysis of data from D.S.C. and X-ray diffraction indicated that a crystalline complex formed between the drug and H.P.M.C. in crystallised samples, the complex exhibiting a $10^{o}C$ lowering of melting point than the parent drug and producing an extra peak on the powder X-ray diffraction pattern of 2θ at 18^{o} compared with phenylbutazone. The drug:polymer complex produced a two-fold increase in dissolution rate which optimised at approximately 2% w/w H.P.M.C. level.

3. Spray-dried samples, prepared under conditions to form the β-polymorph, similarly demonstrated the formation of a complex between drug and H.P.M.C. with a melting point of $102^{o}C$ and an increase in dissolution rate of 100% was observed for samples containing 2% w/w H.P.M.C. The presence of H.P.M.C. also appeared to inhibit the formation of the β-polymorph.

4. The endothermic enthalpy of solution (ΔH_s) was found to be higher for the crystallised materials than the spray-dried indicating that the state of crystallographic order in two series of compounds was different with the spray-dried samples showing greater crystallographic disorder.

CHAPTER 5

CHAPTER 5 The effect of Poloxamer on the physicochemical properties of phenylbutazone prepared by crystallisation and spray drying

5.1 Introduction

The activity and physiological properties of water insoluble drugs can be modified by increasing their solubility and dissolution rate. Many trials have attempted to add a hydrophilic material to the formulation to increase its hydrophilicity. Materials, which include hydrophilic polymers (Simonelli et al. 1976) (see Chapter 4) and surfactants (Naggar et al. 1980, Elworthy & Lipscomb 1968) which are often referred to as surface active agents, are in general compounds which whilst soluble in a given liquid, tend to accumulate or be positively adsorbed at interfaces with air, another liquid, or a solid (Dittert 1974). The use of surfactants as solubilising agents to increase the solubility of sparingly water soluble drugs has been the subject of many studies in the last century (Attwood & Florence 1983).

Surfactants are thought to affect the dissolution rate of water insoluble drugs. One hypothesis states that by lowering the interfacial energy barrier between the drug and the dissolution medium, the drug is more readily wetted (Weintraub & Gibaldi 1969). This can take place by replacing the solid-air interface by a solid-liquid interface thereby increasing the available surface area for micellisation. Two factors should be considered when predicting the effect of the surfactant on the solid-liquid interface - the nature of the charge on the solid and the surfactant ion adsorbed by Van der Waal's forces. Thus when the surfactant is adsorbed to a non-polar solid, the surfactant is orientated with the hydrophilic group towards the aqueous solution thereby increasing the wettability. However when adsorption

takes place by charge interaction between the surfactant and the solid, e.g. by ion-exchange or ion-pairing, the surfactant will orient with the hydrophobic group toward the solution making it less wettable (Attwood & Florence 1981, Swarbrick 1965).

Another mechanism by which surfactants influence the solubility of water insoluble drugs is by micellisation. Micelles are aggregates of surfactant-molecules in the bulk of the solution. These aggregates form when the surfactant molecules in the solution are in excess concentration to that required to form a closely packed monolayer at the water-air interface. The surfactant molecules are not accommodated in the monolayer and aggregate to form micelles, which can be of various structures especially spherical (Dittert 1974). The lowest concentration at which micelles first appear is called the critical micelle concentration (CMC). The micelles are thought to form with the hydrocarbon portion inside the core (hydrophobic) and the hydrophilic portion towards the solvent. In the mechanism of entrapment of water insoluble drug molecules, the surfactant molecules accumulate in the interfaces between water and the drug. Then the hydrocarbon chains penetrate the interface to form weak bonds (adsorption) with the drug molecule and other surfactant molecules accumulate around the drug molecule to form micelles. This results in a marked increase in the apparent solubility of the drug in the medium thereby increasing the dissolution rate.

Most studies in this field have explained the influence of surfactant on dissolution rate by micellisation mechanisms. Schott et al. (1982) found that when octoxynol was added to the dissolution medium an increase in dissolution rate of prednisolone tablets was obtained, which was attributed to micellar solubilisation. Tusti et al.

(1982) also attributed the increase in dissolution rate of β-lactam antibiotics to drug-micelle complexes. Rees & Scott (1974) studied the solubility of salicylic acid in micellar solutions of polysorbate 20. All these workers used concentrations of surfactant above CMC and observed increases in solubility and dissolution rate were explained by micellar solubilisation.

Other workers have used concentrations of surfactants below CMC. Weintraub & Gibaldi (1969) studied the effect of premicellar surfactant concentration in the dissolution medium on the dissolution rate of aspirin tablets and observed a significant increase in dissolution rate. This effect, attributed to wetting, was found to increase as the concentration of the surfactant approached CMC. Taylor & Wurster (1965) found a significant increase in solubility and dissolution rate of prednisolone in sodium lauryl sulphate solutions, related to co-operative phenomena which facilitated the dissolution rate.

Several studies have examined the effect of the presence of surfactant by incorporating surfactant molecules into the drug crystals by recrystallising the poorly water soluble drug in an aqueous surfactant solution. Chiou et al. (1976) and Naggar et al. (1980), using this procedure, obtained an increase in dissolution rate, whilst increases were very small. The increases in dissolution rate were explained by lowering of the interfacial tension by the incorporated surfactant molecules which facilitated wetting. Levy & Gumtow (1963) used surfactants to counter the hydrophobic effect of tablet lubricants, such as magnesium stearate and a significant increase in dissolution rate was noticed.

Spray drying has also been used to incorporate surfactants into hydrophobic drugs (Matsuda et al. 1982).

This chapter reports a study of the physicochemical and dissolution properties of phenylbutazone samples prepared by conventional crystallisation and spray drying to contain different concentrations of non-ionic surfactants to examine the effects of the incorporated surfactant molecules. Since similar concentrations of surfactant (0.01%-5% w/w) and preparation techniques are used compared with those for H.P.M.C. in Chapter 4, a comparison between surfactant and hydrophilic polymer effects can be made. For this purpose an interesting class of non-ionic polyoxyethylene-polyoxypropylene block co-polymeric surfactants, or poloxamers, sold under the trade name of Pluronic were used.

The ability of the poloxamers to form micelles still remains the source of debate in the literature (Attwood & Florence 1983, Prasad et al. 1979). Mankowich (1954) concluded from light-scattering studies that polyoxyethylene co-polymer does not form micelles and Dwiggins et al. (1960) reached the same conclusion using ultra-centrifugation technique. Bell (1959) similarly reported that these co-polymer do not form micelles. However, Becher (1959) was the first to propose that ethylene oxide can form a CMC. Ross & Oliver (1959), when examining poloxamer 182, calculated the CMC to be 2.4%, whilst Sckmolka & Raymod (1965) reported a CMC of 0.0014% for the co-polymer of lowest HLB and 0.0037% for that of highest HLB. The discrepancy between workers concerning the existance and value of CMC's can be attributed to the different techniques used to prepare and assess the materials.

The objective of this study was to examine the effect of incorporating poloxamers on the physicochemical properties of phenyl-butazone in particular the crystallographic structure, solubility and

dissolution rate. Since the technique of incorporating the poloxamer into the drug crystals was thought to have an effect on the products, the samples were prepared by both conventional crystallisation and spray-drying techniques. The spray-drying conditions employed have been shown in Chapter 3 Section 1 to produce the β-polymorph of phenylbutazone and thus it was also of interest to study the effect of poloxamer surfactant on the formation of the β-polymorph of phenylbutazone.

5.2 Experimental

5.2.1 Materials

Poloxamer 188 was used to study the influence of surfactant on the solubility and dissolution rate of phenylbutazone. Poloxamers 338, 188, 184, 181 and 101 were used to study the effect of changing the surfactant chain length on dissolution rate. All the poloxamers were used as received. The other materials used are listed in Chapter 2.

5.2.2 Method

5.2.2.1 Crystallisation

The crystals were prepared by flocculating a solution of phenylbutazone (6 gms) in 100 mls of absolute alcohol, with 100 mls of distilled water containing the required surfactant concentration. The resulting crystals were dried in a vacuum desiccator over silica gel for 72 hours. The dried crystals were gently triturated in a mortar then sieved through a 200 µm sieve and kept in the vacuum desiccator over silica gel over the period of testing.

5.2.2.2 Spray drying

The feed solution was prepared by dissolving phenylbutazone and the required poloxamer concentrations (0.01-5% w/w) with respect to the amount of phenylbutazone, in aqueous alcohol (75% w/v) solvent, and spray dried as mentioned in Chapter 3 Section 3, using conditions which gave β-polymorph of phenylbutazone when spray dried alone (as for sample PS3).

The resulting samples were tested by D.S.C., powder X-ray diffraction, SEM and for solubility and dissolution rate, all according to the methods described in Chapter 2.

Table 5.1 The assay results of phenylbutazone samples recrystallised with poloxamer 188

Sample Code	Concentration of HPMC (% w/v) in final crystallisation solvent	% w/wt of phenylbutazone in product *	Estimated % w/w Poloxamer 188 in product
PbZ	0.00	99.30	0.00
PPR1	0.01	99.29	0.01
PPR2	0.1	99.21	0.09
PPR3	1	98.24	1.06
PPR4	2	97.30	2.00
PPR5	5	93.56	5.74

* Figures represent the arithmetic mean of at least three determinations.

Fig. 5.1 Scanning electron photomicrographs of samples PPR1, PPR2, PPR3, PPR4 and PPR5

Fig 5.1

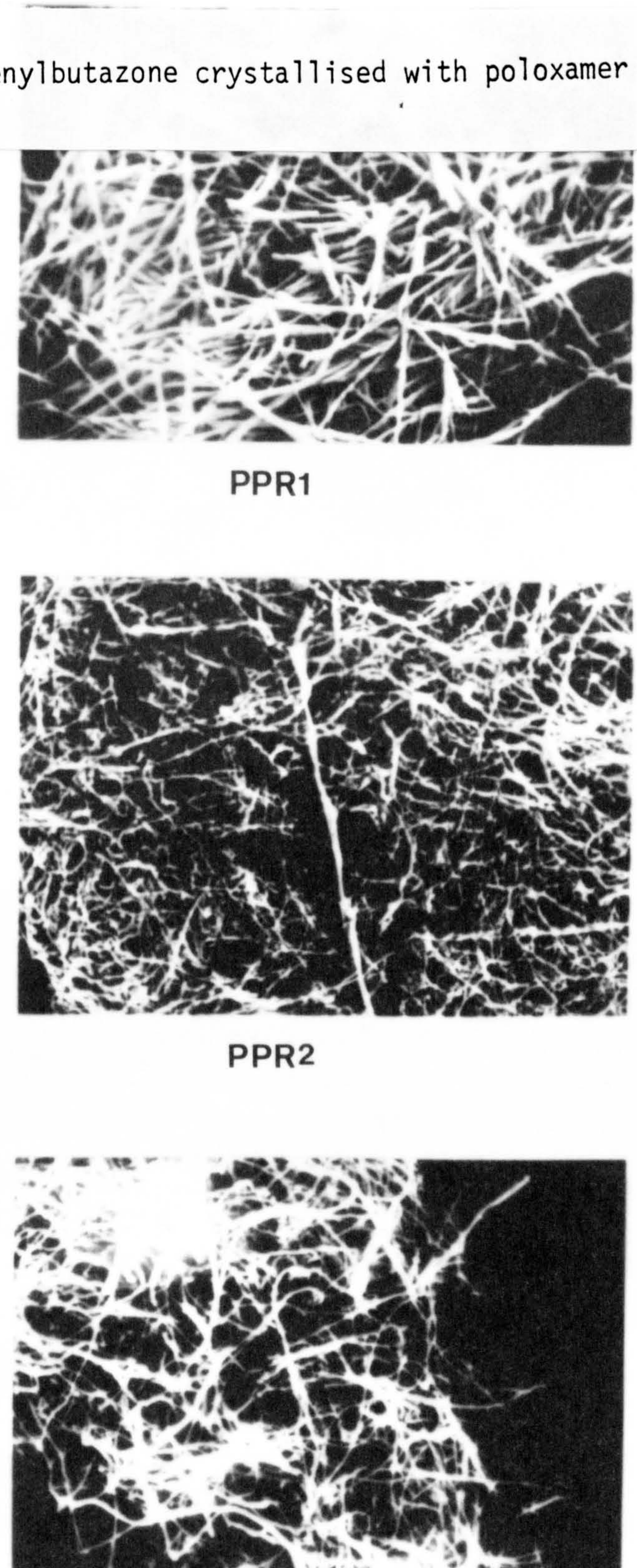

Fig. 5.1 Scanning electron photomicrographs of samples PPR1, PPR2, PPR3, PPR4 and PPR5

Fig 5.1

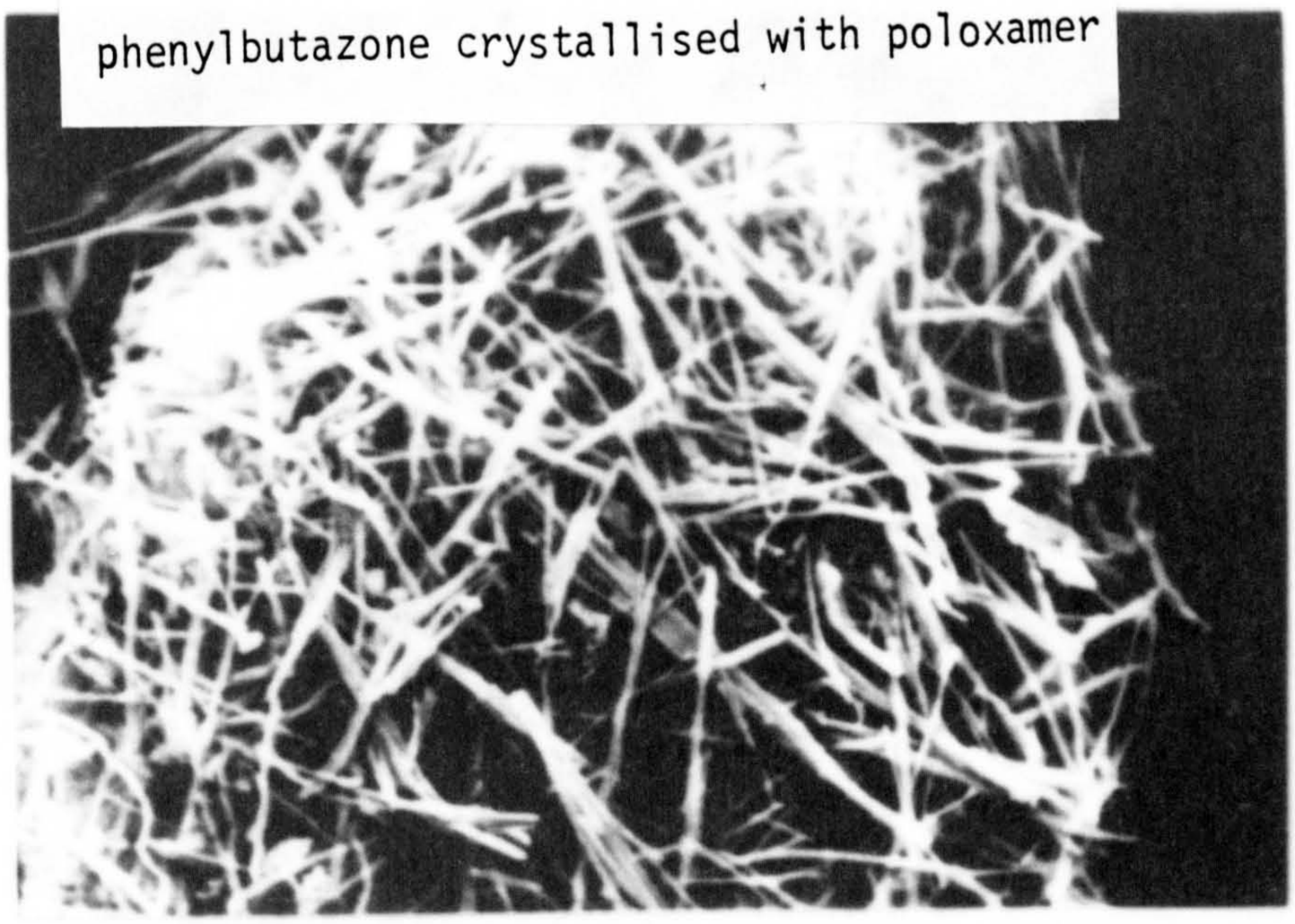

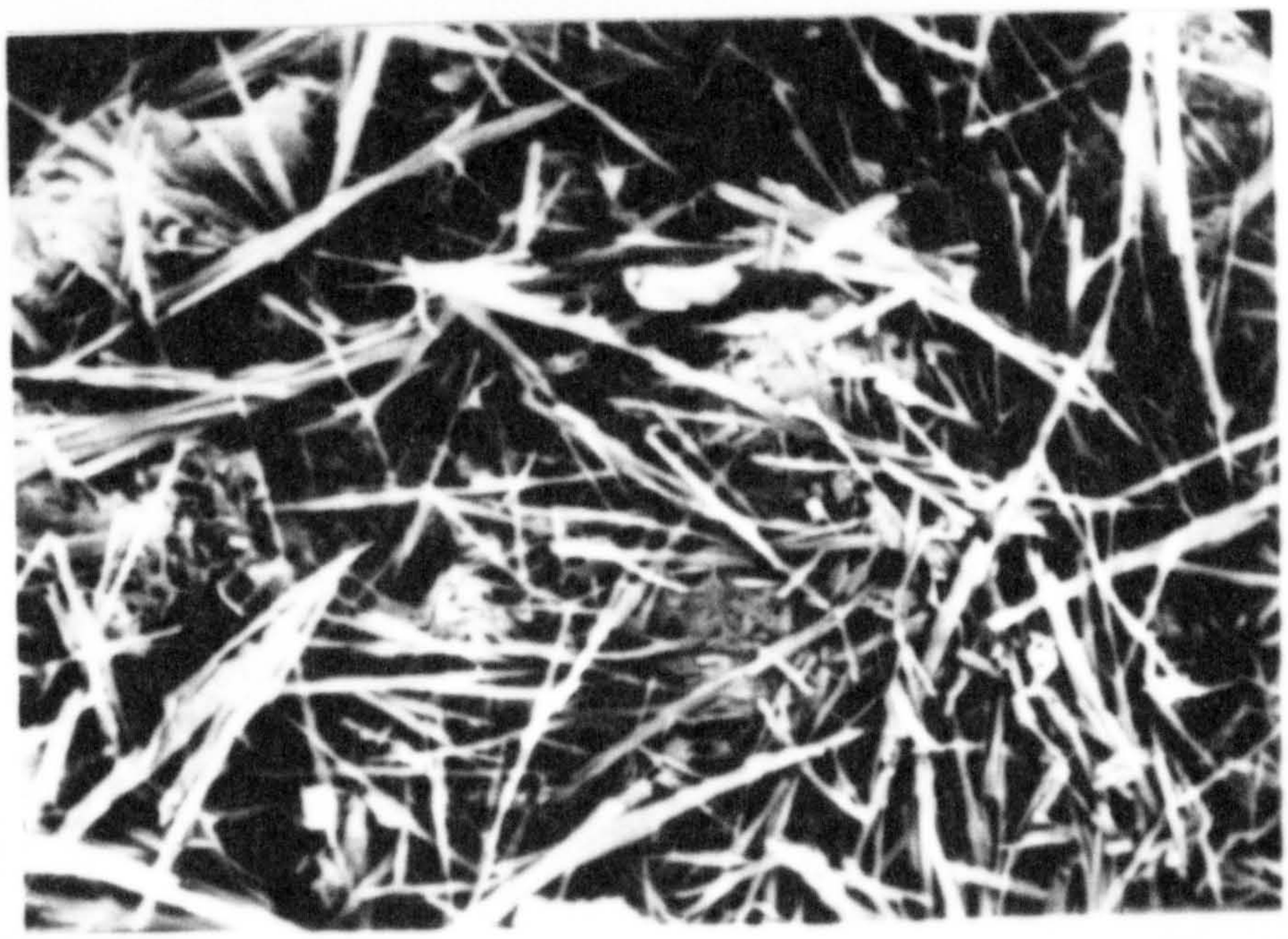

5.3 Results and discussion

5.3.1 Incorporating surfactant by direct crystallisation

5.3.1.1 Assay of the samples

It was mentioned in Section 4.4, that it proved difficult to estimate the amount of H.P.M.C. present in the samples directly, and H.P.M.C. concentrations were calculated by difference after assaying the amount of phenylbutazone content of samples using the B.P. (1980) assay. The same procedure was used to determine the amount of poloxamer 188 in the samples (see Table 5.1). The assay results show that the uptake of poloxamer by the drug was similar to the concentration present in the crystallisation medium with the exception of the 5% w/v level, where a higher concentration appeared to be taken up by the sample PPR5. This might be due to preferential and enhanced adsorption at higher concentration levels of poloxamer.

5.3.1.2 Scanning electron microscope

Microphotographs of the crystallised phenylbutazone from poloxamer 188 solutions (see Fig. 5.1) indicate that whilst slight thinning of the crystals needles can be seen, no major change occurred in the morphology of the crystals when compared with recrystallised phenylbutazone.

5.3.1.3 Differential scanning calorimetry

The thermograms of the samples of phenylbutazone crystallised in the presence of poloxamer 188 were obtained by D.S.C. using crimped aluminium pans with pierced lids under nitrogen flow. All the samples exhibited a single endothermic peak at 107^{o}C (see Fig. 5.2). This suggests the presence of surfactant during the crystallisation process did not result in different polymorphic forms or complex formation.

phenylbutazone crystallised with poloxamer

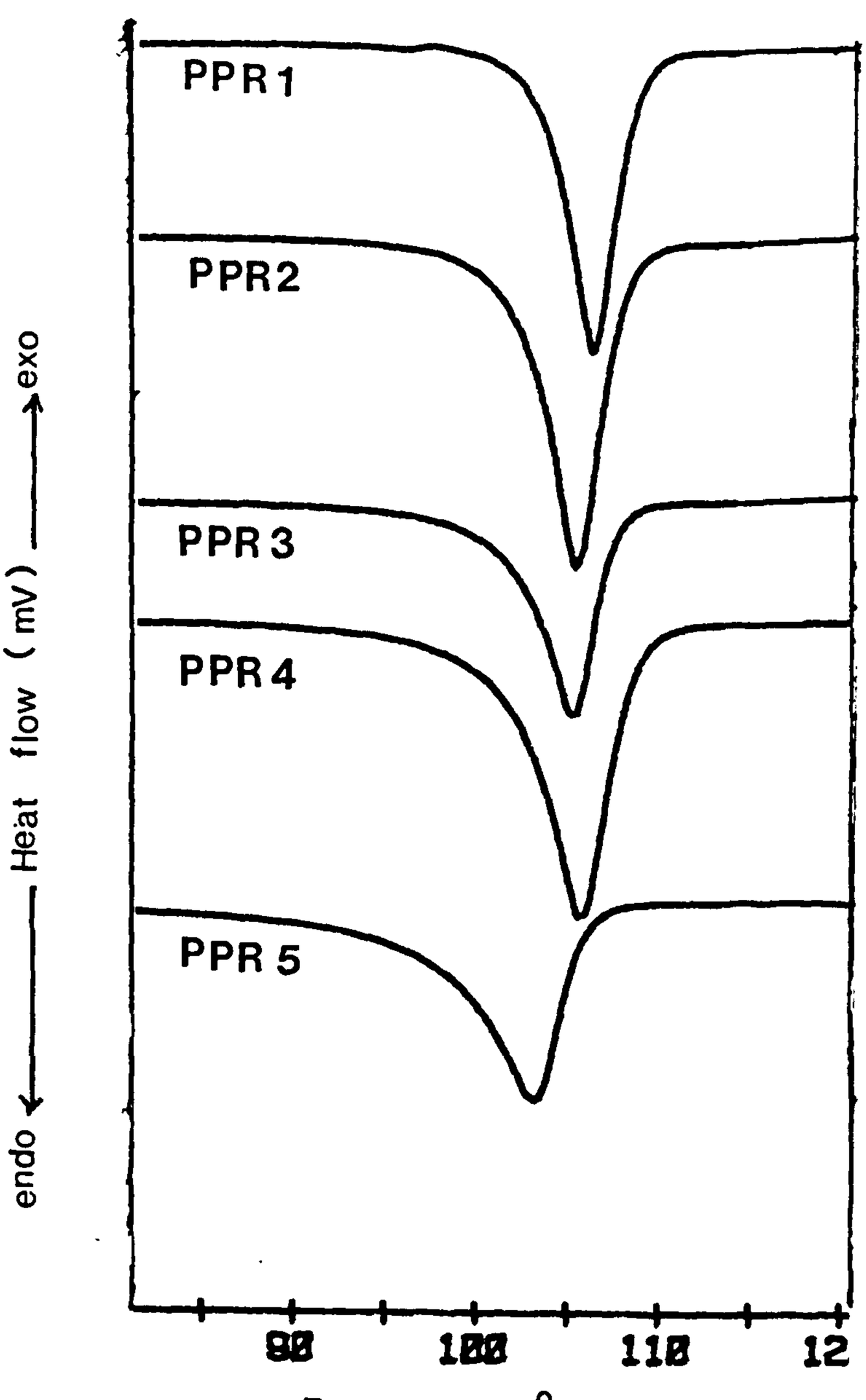

Fig. 5.2 D.S.C. endotherms for samples PPR1, PPR2, PPR3, PPR4 and PPR5 (heating rate 10°C/min sample size 5-9 mg and under nitrogen flow)

Table 5.2 Melting point and heat of fusion of phenylbutazone crystallised with different concentrations of poloxamer 188

Sample Code	Estimated (% w/w) concentration of poloxamer 188 in sample	Melting Point (^{o}C)	Heat of fusion ΔH_F(KJ/mol)
Pbz	0.00	107	27.00
PPR1	0.01	106.3	26.8
PPR2	0.09	105.8	26.0
PPR3	1.06	105.5	24.6
PPR4	2.00	105.3	22.6
PPR5	5.74	103	15.8

Fig. 5.3 The powder X-ray diffraction patterns for phenylbutazone crystallised from solutions containing poloxamer 188.

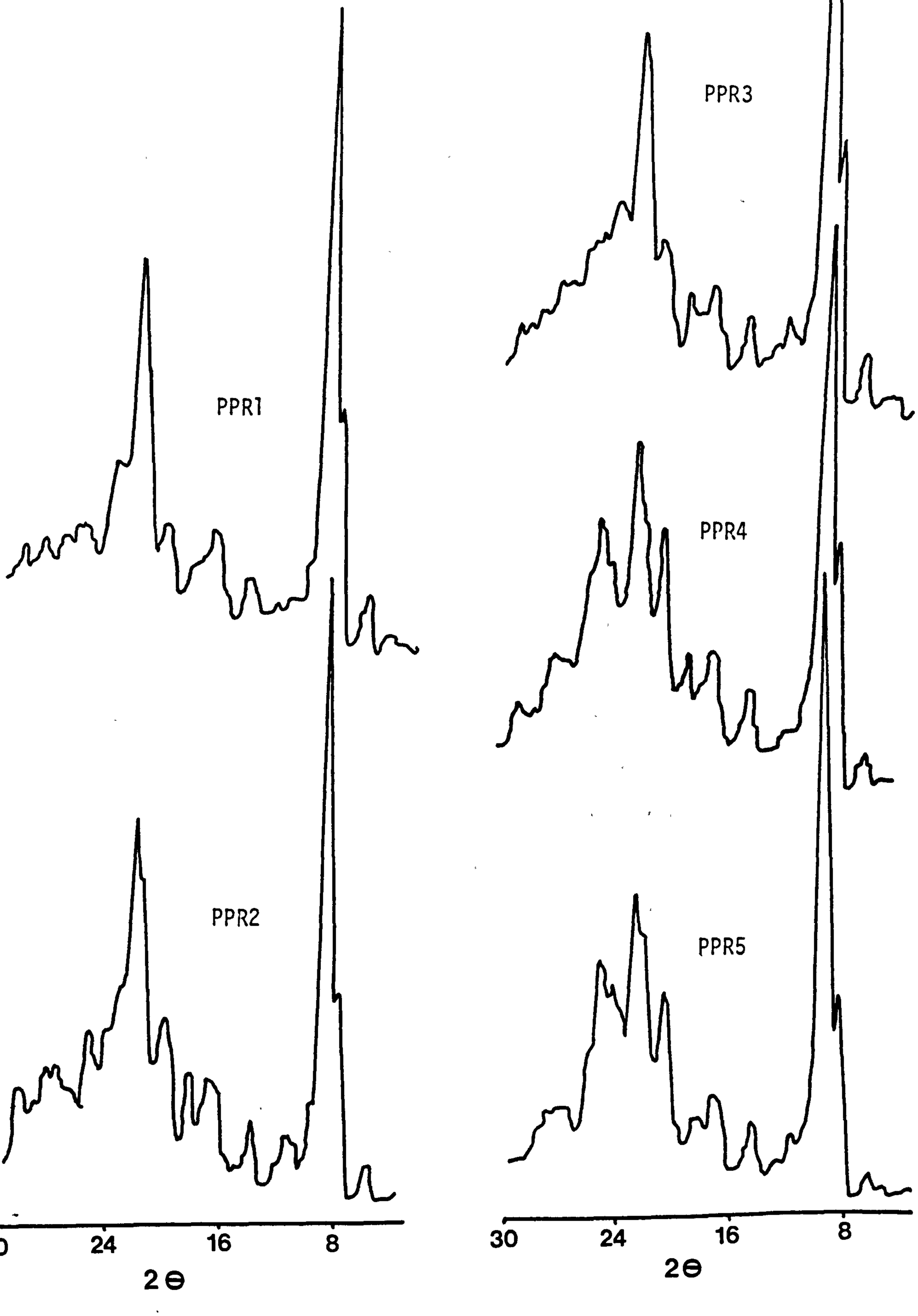

This observation agrees with that reported by Chiou (1976) for sulphathiazole, prednisone and chloramphenicol crystallised with polysorbate 80.

The latent heat of fusion (ΔH_f) of the samples decreased with increasing surfactant concentration, and was accompanied by a small decrease in melting point of the samples (see Table 5.2). These data suggest that the surfactant molecules are taken into the drug crystals in a manner which does not result in a major change in the crystal form. Blaine(1982) (DuPont publications) reported that the higher the concentration of impurities in the sample, the lower its melting point and the broader its melting range and this trend is observed in Table 5.2. The surfactant molecules thus appear to act as impurities, possibly forming a solid-solutions system at low levels of incorporation.

5.3.1.4 Powder X-ray diffraction

The powder X-ray diffraction data for the samples of phenylbutazone crystallised in the presence of poloxamer and the poloxamer 188 flakes alone (see Fig. 5.3) were obtained by bombarding prepared powder beds. The poloxamer 188 flakes alone exhibited two peaks in the region of 2θ at 16.4 and 21.2^{o}, the same region where phenylbutazone peaks were expected (see Chapter 3. P92). The X-ray pattern of the crystallised phenylbutazone with different concentrations of poloxamer 188 showed no major change in the number and positions of the main peaks exhibited by phenylbutazone alone, except for the emergence of two new peaks at 2θ, 16.4 and 21.2^{o}. The size of these two peaks increased with increasing poloxamer 188 concentration and correspond to the peaks observed for poloxamer alone. The similarity in the powder X-ray diffraction traces between the samples and the original phenylbutazone supports the suggestion proposed from analysis of D.S.C.

data that when phenylbutazone is crystallised in the presence of polyoxamer, physical adsorption and/or solid solution formation were the dominant mechanisms and major changes in crystal form or complex formation were absent.

5.3.1.5 Solubility

Data for solubility experiments are listed in Appendix 3 Table 16.

The equilibrium dynamic solubility of the phenylbutazone-polyoxamer samples were measured by placing excess of the powder (1 gm) in contact with 100 ml of buffer solution of pH 7.5 in a shaking water bath at 37^{o}C. The presence of the surfactant in the crystallised samples of phenylbutazone did not appear to have a great effect on the maximal solubility compared with the control sample of pure drug as the maximum increase obtained was 1.2 fold. This increase in solubility rose with increasing surfactant concentration until the 1% w/w level was reached: beyond this level no further increase was observed (see Table 5.3). (Maximum increase in dissolution rate was also obtained at the 1% w/w : poloxamer level.)

A small increase in solubility has been reported by Finholt & Solvage (1968) when studying the influence of polysorbate 80 on the solubility of phenacetin (1.26 fold). Also Naggar et al. (1980) observed small changes in solubility of phenylbutazone crystallised with polysorbate 80. Both groups of workers also noticed major increases in dissolution rate, and concluded that the increase in dissolution rate was due to a small extent on its solubilising powder (Finholt & Solvage 1968). The small increase in solubility with increasing surfactant concentration indicates that poloxamer do not solubilise phenylbutazone in micelles which tends to support the conclusion of Mankowich (1954) that the polyoxyethylene copolymers do not form micelles, and that the increase in solubility and

Table 5.3 The dynamic equilibrium solubility and intrinsic dissolution rate constant, $\grave{K}$, of phenylbutazone and samples crystallised from solutions containing different concentrations of poloxamer 188

Sample Code	Concentration of HPMC (% w/v) in final crystallisation solvent	Estimated % w/v poloxamer in sample	Sample solubility mgm/100ml *	$\grave{K}$ (mg/min/cm^2)
PbZ	0.00	0.00	380	0.188
PPR1	0.01	0.01	405	0.364
PPR2	0.1	0.09	435	0.478
PPR3	1	1.06	460	0.569
PPR4	2	2.00	458	0.569
PPR5	5	5.74	460	0.569

* Figures represent the arithmetic mean of at least two determinations.

dissolution rate is due to facilitating wetting and lowering of the interfacial tension.

5.3.1.6 Dissolution rate

Data from the dissolution rate experiments are listed in Appendix 3 Table 1-5.

The dissolution rate of phenylbutazone-poloxamer samples was determined using a Woods apparatus. An increase in dissolution rate with increasing concentration of surfactant added during the crystallisation process was observed up to an optimal concentration of 1% w/v surfactant which gave the highest dissolution rate. Higher surfactant concentrations had no further effect on the dissolution rate (see Fig. 5.4 & Table 5.3).

Although poloxamers have been widely studied, considerable confusion exists in the literature over the exact nature of their colloidal behaviour and in particular whether micelles are formed (Attwood & Florence 1983, Prasad et al. 1979). Whilst some workers suggest that micelles are not formed (Mankowich 1954, Dwiggins 1960) or only formed at high surfactant concentration (Ross & Oliver 1959) others proposed that micelles are produced (Becher 1959, Prasad 1979).

The influence of surface active agents on the dissolution rate of relatively water insoluble drug may involve several mechanisms. The surfactant decreases the interfacial energy barrier between the drug and dissolution medium allowing the drug to be wetted more completely and readily thereby effectively increasing the available surface of the solid for dissolution. Alternatively, when the concentration of the surfactant increases above the critical micellar concentration (CMC) the apparent solubility of the drug in the medium may markedly increase by means of micellar solubilisation thereby

phenylbutazone crystallised with poloxamer

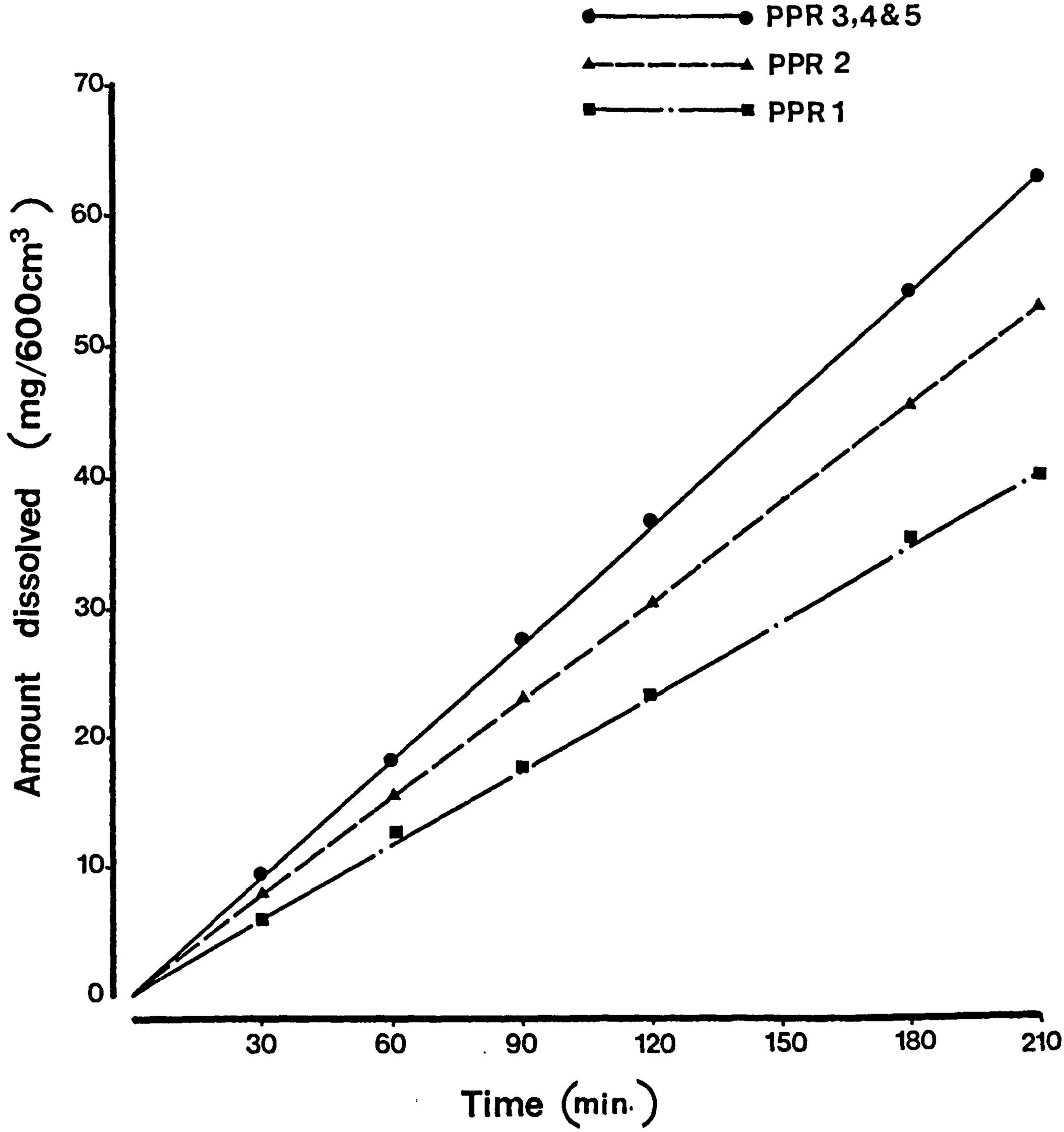

Fig. 5.4

Dissolution curves for samples PPR1, PPR2, PPR3, PPR4 and PPR5 in buffer solution pH 7.5 at 37°C using Woods apparatus.

effecting an increase in dissolution rate (Weintroub & Gibaldi 1969). Any change in solubility due to micellar solubilisation causes an increase in the difference between the saturation solubility (Cs) and solubility of the given time (Co) i.e. (Cs-Co) and any change in this ratio will lead to an increase in the dissolution rate (Parrott & Shama 1967, Bates et al. 1966).

Whilst no significant change in dynamic equilibrium solubility was achieved for these samples, a 3-fold increase in dissolution rate was observed which is attributed to a facilitated wetting process rather than solubilisation. The increase in wetting is achieved by lowering the interfacial tension between the substance and dissolution medium which results in a low contact angle (Matsuda et al. 1982). It is also possible that the surfactant might increase the solubility of the drug in the diffusion layer during dissolution (Naggar et al. 1980). The same suggestion was raised by Chiou (1976) who reported that the presence of the surfactant inside and/or outside the crystals might enhance the solubility of the drug in the diffusion layer during the dissolution process. Also Levy & Gumtow (1963) found that sodium lauryl sulphate increased the dissolution rate of a compressed tablet of salicylic acid and they attributed this increase to improved wetting which was achieved by lowering the interfacial tension of the tablet by the surfactant. In the present work the limiting increase in dissolution rate at 1% w/v poloxamer level might correspond to the concentration which produces optimal wetting possibly achieved by adsorbing poloxamer to the drug crystal. Additional surfactant molecules would not provide a further effect with respect to dissolution rate.

Parrott & Sharma (1967) studied the dissolution rate of benzoic acid in the presence of different surface active agents in the dissolution medium and found that the dissolution rate increased with increasing surfactant concentration until a maximum rate was obtained. The maximum was followed by a decrease in dissolution rate with higher surfactant concentrations. A similar observation was reported by Elworth & Lipscomb (1968), when studying the dissolution rate of griseofulvin, and by Naggar et al. (1980), who studied phenylbutazone dissolution in the presence of polysorbate 80. All these workers attributed the decrease in dissolution rate following the maximum to changes in dissolution medium viscosity by the surfactant causing increase in the diffusion layer thickness and thus reducing the dissolution rate. However, Finholt & Solvage (1968) observed that at a certain level, addition of more polysorbate 80 has very little effect on the dissolution rate of phenacetin, but no explanation for this effect was given. Collett & Tobin (1977, 1979), in a study of solubilisation of poloxamer systems, found that the poloxamer solubilising power depends on the structure of the solubilisate for less hydrophobic drugs, the solubility increasing with increasing oxyethylene content. For the more hydrophobic the solubility decreases with increasing oxyethylene content.

In the present work for phenylbutazone-poloxamer systems, the limiting dissolution rate is attributed to optimal wetting ability at 1% w/w level. The levelling at 1% w/w poloxamer concentration could be attributed to adsorption of poloxamer molecules to the drug crystals' surface. Addition of more poloxamer beyond 1% w/w did not result in adsorbing further surfactant molecules to the drug crystals. The physical adsorption hypothesis is supported by data from D.S.C.

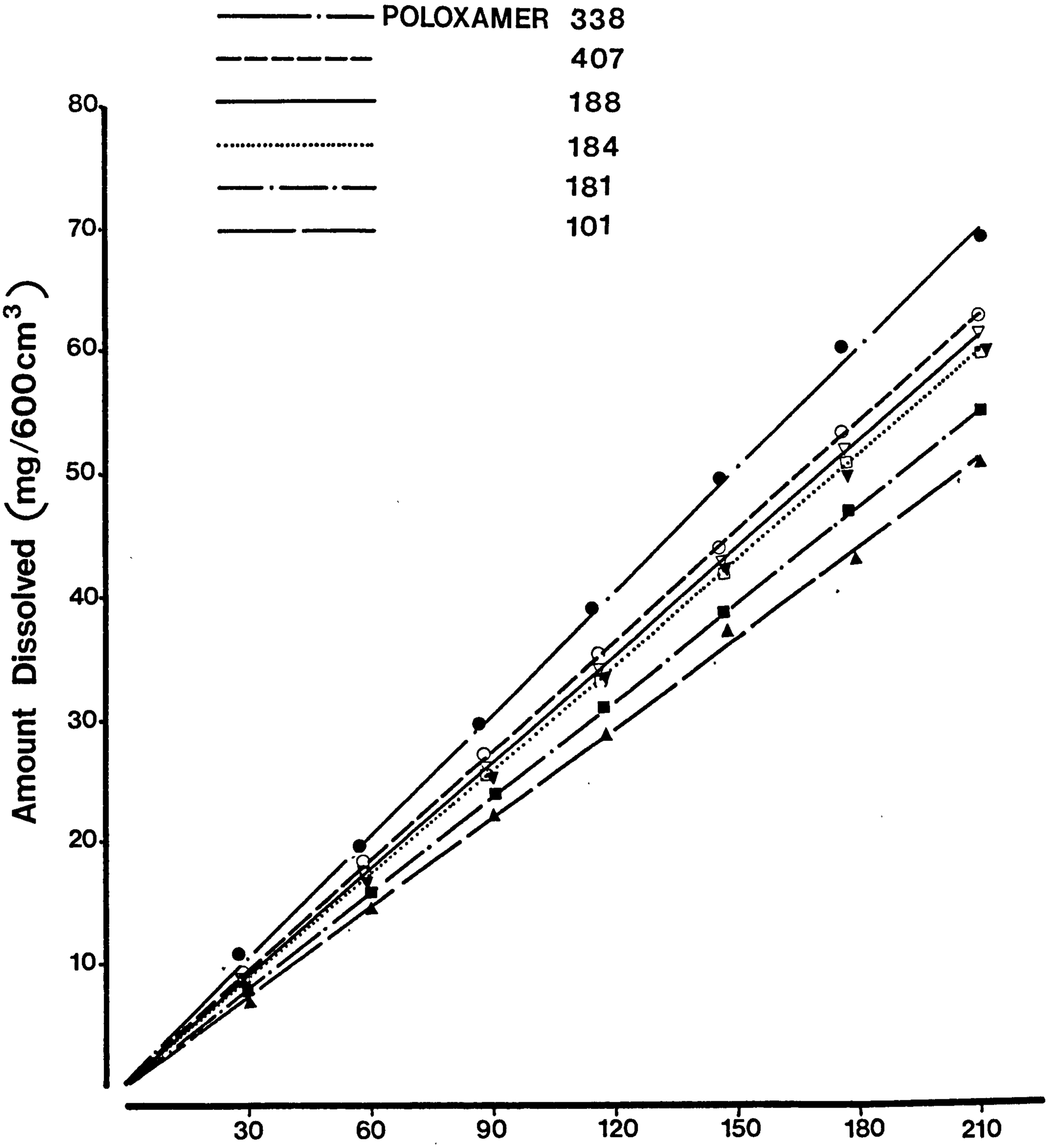

Fig. 5.5 Dissolution curves for samples of phenylbutazone crystallised from solutions containing 1% w/v of poloxamer - 338, 407, 188, 184, 181 and 101

and X-ray diffraction studies, while the viscosity effect in this case is unlikely since a reduction in the dissolution rate was not observed.

To examine the effect of oxyethylene and oxypropylene content of poloxamer on dissolution rate, a series of six different poloxamers was examined. Three of the surfactants were selected to have the same oxypropylene content with the amount of oxyethylene content varying for all the selected poloxamer i.e. in increasing HLB sequence. The samples of phenylbutazone with the different type of poloxamer were prepared by the same crystallisation procedure used before and the amount of poloxamer added each time kept constant at 1% w/v level in the crystallising liquor. The dissolution rate data for these samples (see Fig. 5.5) showed an increase in dissolution rate with increasing oxyethylene concentration in the sample. The rank order of poloxamer in increasing the dissolution rate was 338>407> 188>184>181>101. This observation is consistant with the conclusions drawn by Attwood & Florence (1983) that the solubility of the hydrophobic drug 4-hydroxyocetanilide increased in aqueous poloxamer solutions with increasing oxyethylene content of the polymer.

5.3.2 Incorporation of poloxamer by spray drying

5.3.2.1 Assay of spray dried phenylbutazone-poloxamer samples

Table 5.4 shows the results for the spray dried phenylbutazone-poloxamer samples obtained by the B.P. assay procedure for phenylbutazone. The poloxamer content was obtained by subtracting from the pure drug assay figure, and the assay results indicate that the spray dried samples contain amounts reasonably close to the theoretical concentrations of Poloxamer 188 used.

Table 5.4 Assay results of phenylbutazone samples spray dried from feed solutions containing poloxamer 188

Sample Code	Concentration of poloxamer (% w/v) in final crystallisation solvent with respect to phenylbutazone concentration)	% w/w of phenylbutazone in product *	Estimated % w/w Poloxamer in sample
PbZ	0.00	99.30	0.00
PPS1	0.01	99.30	0.00
PPS2	0.1	99.22	0.08
PPS3	1.0	98.25	1.05
PPS4	2.0	97.56	1.94
PPS5	5.0	94.69	4.61

* Results are the arithmetic mean of at least three individual assays.

Fig. 5.6 Scanning electron photomicrographs of samples PPS1, PPS2, PPS3, PPS4 and PPS5

Fig 5.6

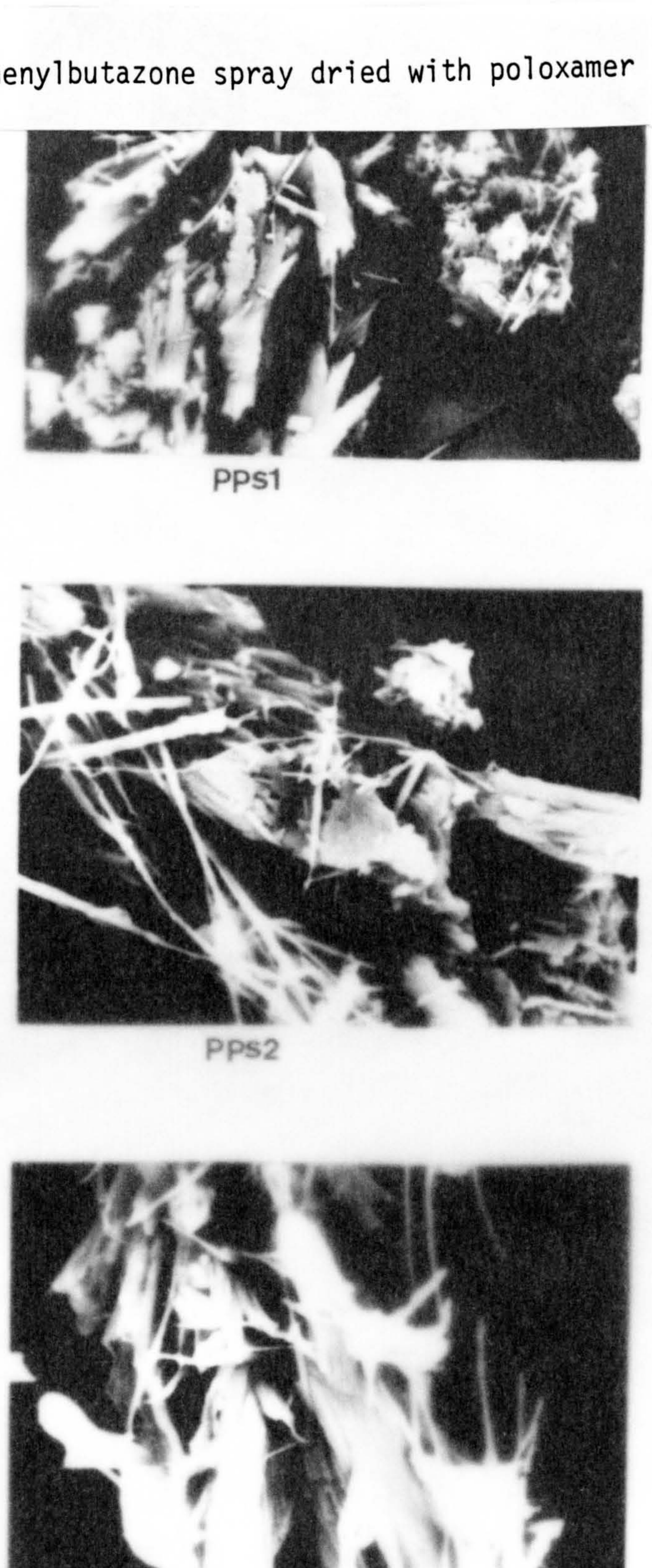

Fig. 5.6 Scanning electron photomicrographs of samples PPS1, PPS2, PPS3, PPS4 and PPS5

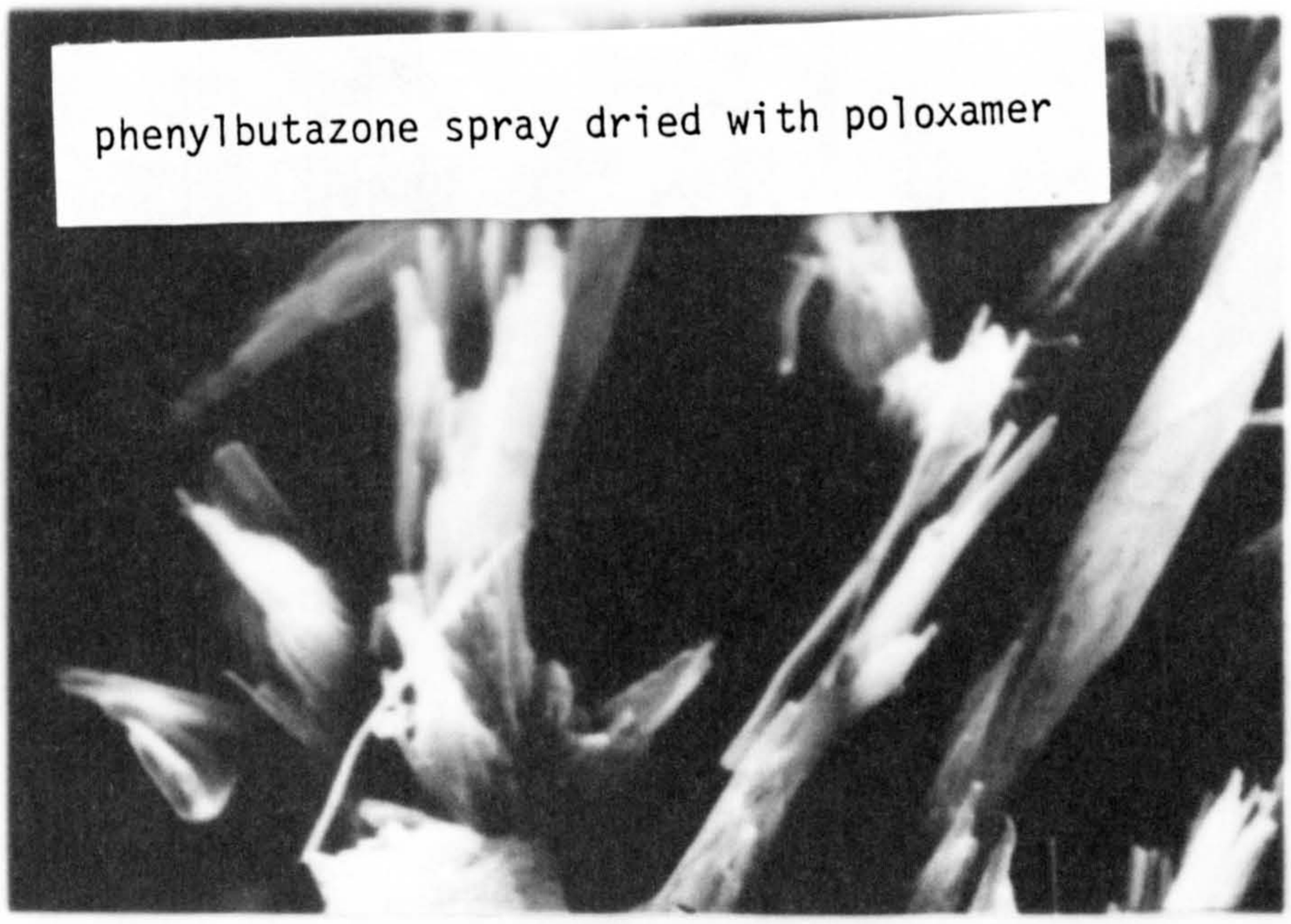

5.3.2.2 Scanning electron microscope

The scanning electron photomicrographs were obtained for the spray-dried samples using the Steroscan 600 electron microscope. The photomicrographs showed no change in the morphology of the spray-dried samples in the presence or varying the amount of poloxamer added (see Fig. 5.6). This was expected as all the samples were spray dried under the same spray drying conditions. Matsuda et al. (1982) used scanning electron photomicrographs to trace the location of surfactant added during the spray drying process and claimed that the micrographs indicate that the surfactant formed a thin layer over the crystal surface. No such feature can be seen in Fig.5.6.

5.3.2.3 Differential scanning calorimetry

The samples were tested for thermal behaviour using differential scanning calorimetry in crimped aluminium pans with pierced lids under nitrogen flow at a heating rate 10^{o}C/min over the heating range 20 to 130^{o}C. The thermogram of the spray dried samples containing phenylbutazone only exhibited two melting endotherms, the first endotherm at 95^{o}C which corresponds to β-form and the second at 107^{o}C which is the original melting endotherm for δ phenylbutazone (see Fig. 5.7). This was expected, since as mentioned previously the spray drying conditions chosen were those which produced the β-polymorph.

All the spray-dried samples containing phenylbutazone and different concentrations of poloxamer 188 gave endotherms which are similar to the endotherms shown by the samples containing β-polymorph. This result leads to the suggestion that the presence of poloxamer 188 within polymorphic materials does not prevent the formation of polymorphic forms when the conditions are selected to form the poly-

Fig. 5.7 D.S.C. endotherm for samples PS, PPS1, PPS2, PPS3, PPS4 and PPS5 (heating rate 10°C/min sample size 5-9 mg and under nitrogen flow)

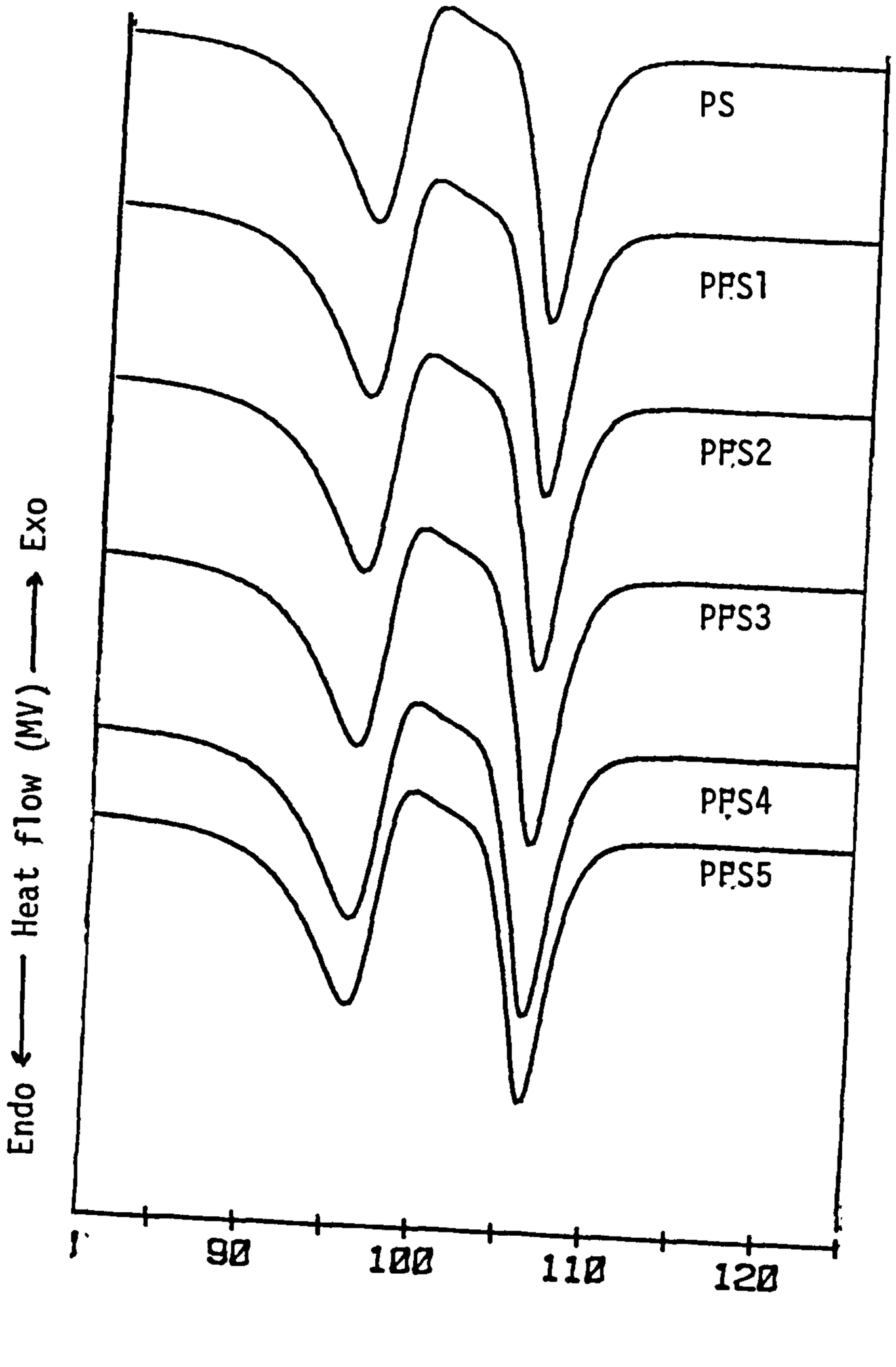

Fig. 5.8 Powder X-ray diffraction patterns of poloxamer 188 alone and phenylbutazone sample spray dried with poloxamer 188 solutions.

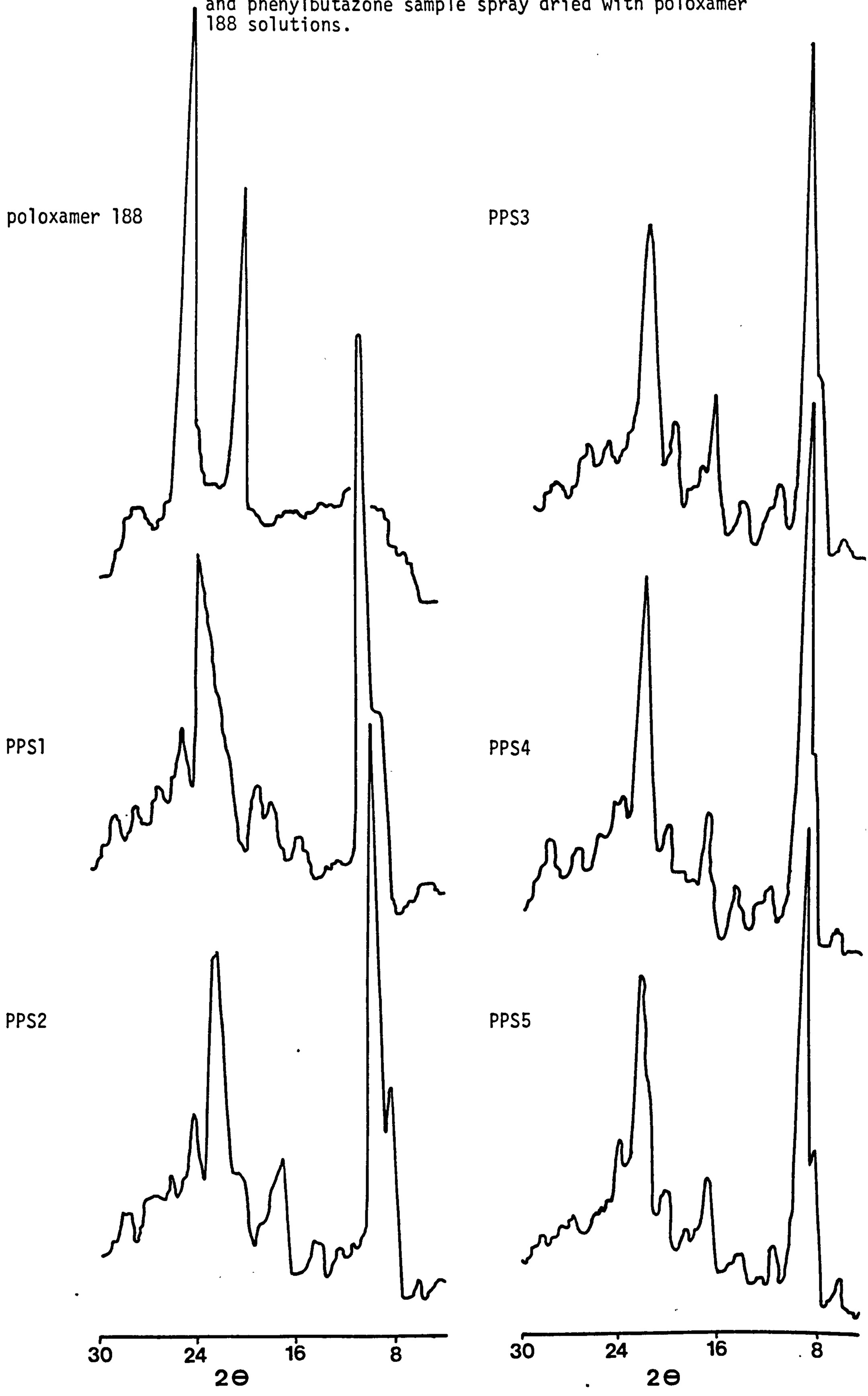

morphs. Also, as concluded in Section 5.1.3. the presence of poloxamer 188 does not appear to initiate the formation of alternative polymorphs, which is in agreement with Chiou's (1976) observation. This finding i.e. the lack of interference with polymorphic formation, supports the suggestion that poloxamers when incorporated into the samples, are adsorbed physically onto the surface of the crystals. This is in contrast to the effect of H.P.M.C. on phenylbutazone, where a complex was thought to form between the polymer and phenylbutazone.

5.3.2.4 Powder X-ray diffraction

Powder X-ray diffraction scans were obtained by bombarding a bed of powder samples with X-ray radiation. The resulting X-ray diffraction patterns for all the samples were very similar to that obtained for the β phenylbutazone polymorph, with the main peaks at 2θ of 10^{o}, 16.2^{o}, 23^{o} and 24.2^{o} (see Fig. 5.8). At higher concentrations of poloxamer 188, a small peak at 2θ 23.2^{o} appeared which is an indication of the poloxamer peak, whilst the second poloxamer peak at 2θ, 24.2^{o} appeared to overlap with the phenylbutazone peak at 2θ of 24.2^{o}. The similarity between X-ray patterns for all the samples containing poloxamer agrees with the previous suggestion that poloxamer does not interfere with polymorphic formations, or form a complex with phenylbutazone.

5.3.2.5 Solubility

The result of the solubility experiments are listed in Appendix 3 Table 17.

The solubility of the spray-dried samples of phenylbutazone-poloxamer 188 were tested by placing an excess weight of the samples (1gm) in 100 ml of buffer of pH 7.5 in a shaking water bath at 37^{o}C. The solubility showed a peaking value after 4 hours followed by a steady decline towards an equilibrium value (see Table 5.5).

Table 5.5 The peak and equilibrium solubility and intrinsic dissolution rate constant, $\hat{K}$, of phenylbutazone and samples spray dried with different concentrations of poloxamer 188, at 37°C

Sample Code	Estimated % w/w poloxamer in sample	Peaking solubility values (mg/100 ml)	Samples equilibrium solubility values (mg/100 ml)	$\hat{K}$ (mg/min/cm^2)
PbZ	0.00	580	390	0.364
PPS1	0.00	580	440	0.469
PPS2	0.08	574	440	0.532
PPS3	1.05	578	460	0.569
PPS4	1.94	580	456	0.569
PPS5	4.61	578	460	0.569

The peaking value was similar for all the samples tested indicating that all the samples have similar β-polymorphic content. This further supports the conclusion reached from the D.S.C. thermograms and powder X-ray diffraction studies that the presence of poloxamer does not interfere with or change the β polymorphic formation.

Maximal or peaking solubility is attributed to the super-saturated solution at peaking metastable solubility subsequently recrystallising to the stable δ form. The presence of poloxamer molecules do not affect the peaking time in contrast to the presence of H.P.M.C. When the metastable polymorph starts to convert to the stable form, the solubility started to decline to an equilibrium value. This showed a slight increase over the value obtained for the β-polymorph of phenylbutazone, with the increase reaching a plateau at concentrations of approximately 1.0% w/w and above (see Table 5.5)

5.3.2.6 Dissolution rate

The dissolution rate data of the spray-dried samples of phenyl-butazone-poloxamer were obtained for a compressed disc of the powder using a Woods apparatus in phosphate buffer at 37°C and are listed in Appendix 3 Table 5-10.

The dissolution rates of the spray-dried samples were very similar to the samples prepared by crystallisation i.e. there was an increase in dissolution rate up to 1% w/w poloxamer concentration (see Fig. 5.9 & Table 5.5). Incorporating polyoxamer above 1% w/w has negligible effect on the dissolution rate. This is attributed to improved wetting in the presence of poloxamer and the limitation at 1% w/w could be attributed to the same reasons mentioned in Section 5.3.1.6.

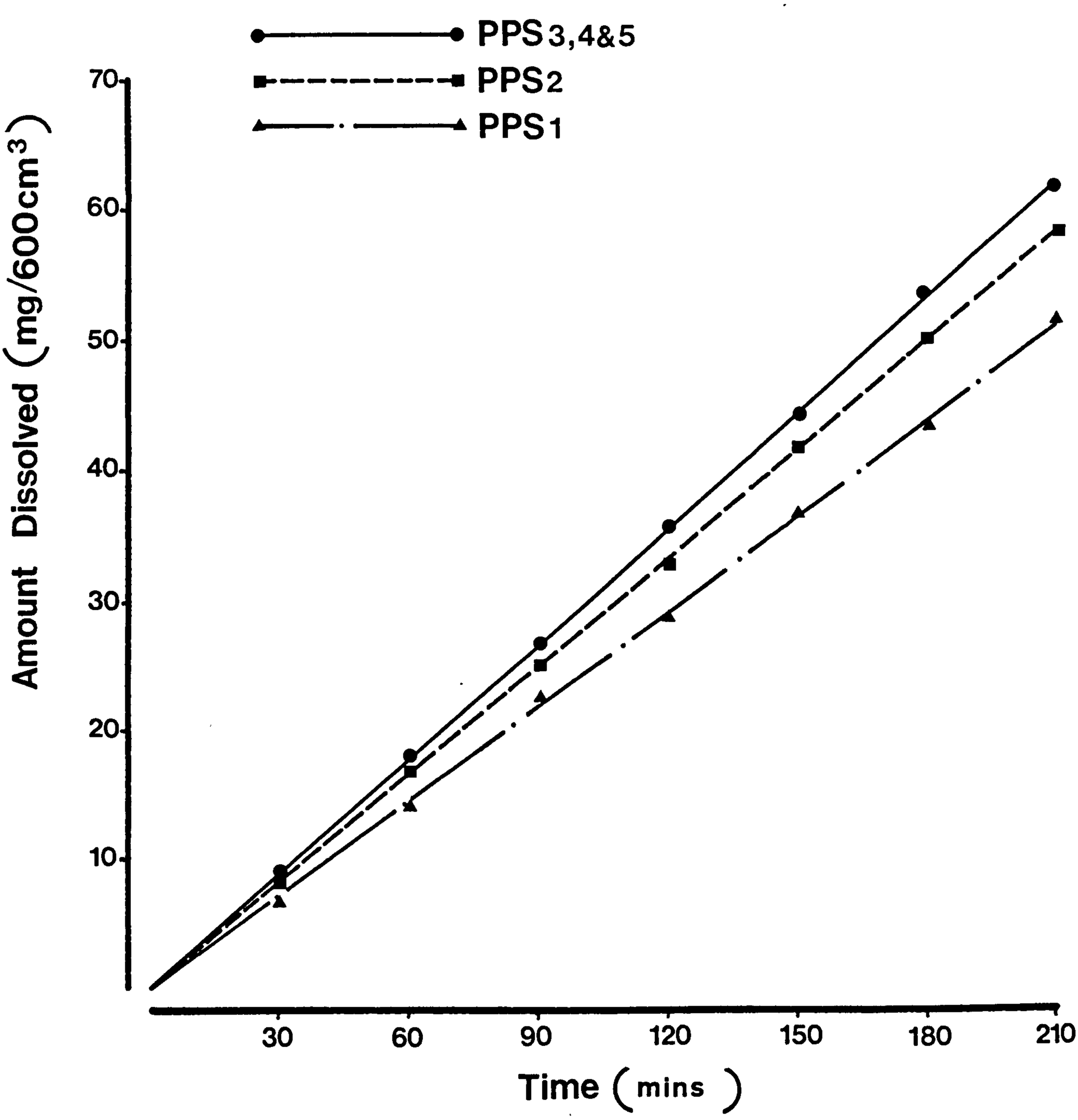

Fig. 5.9

Dissolution curves for samples PPS1, PPS2, PPS3, PPS4 and PPS5 in buffer solution pH 7.5 at 37°C using Woods apparatus.

It is interesting to note that the samples prepared by spray drying which are β polymorph and samples prepared by conventional crystallisation gave the same limiting value of dissolution rate at the same poloxamer concentration despite the difference in the crystal state of the samples (β and δ) and the difference in preparative conditions. Thus the optimal wetting effect exerted by poloxamer dominates over any effect obtained by the change in crystal polymorph.

5.4 Conclusions

1. When poloxamer 188 was incorporated into phenylbutazone crystals a 3-fold increase in dissolution rate for both crystallised and spray-dried samples was obtained, with optimal increases obtained at approximately 1% w/w poloxamer concentration.

2. The increase in dissolution rate was thought to be obtained by facilitating wetting through lowering the interfacial tension, as the increase in solubility was relatively small.

3. No complex appeared to form between the surfactant and the drug molecules and the poloxamer 188 molecules were thought to be primarily physically adsorbed to the crystal surface.

4. The presence of poloxamer did not inhibit or initiate the formation of polymorphism.

CHAPTER 6

CHAPTER 6 Stability testing of phenylbutazone samples containing polymeric additives

6.1 Introduction

The life of a pharmaceutical product is the maximal length of time expected to pass between the manufacture and the last sale of the preparation. This time or shelf life, is usually calculated by the manufacturers and enables an expiry date to be listed on the container (Carstenston 1980). Shelf life can be defined as the time required for the drug level in a product stored at room temperature ($25^{o}C$) to degrade to 90% of its labelled potency (Ditter 1974). Degradation can result from many factors, but the major problems are environmental parameters such as temperature, light, oxygen and moisture (Florence & Attwood 1981). These factors cause either physical or chemical degradation through different reactions. A particular problem is hydrolysis which is the reaction of water with ions of weak acids and weak bases, and solid dosage forms are usually very susceptible to the moisture content of the atmosphere in the containers in which they are stored (Florence & Attwood 1981). Oxidation, which is the result of removal of an electron from the molecule, is not easy to assess during storage, but its effect could be eliminated by adding antioxidant. The effect of temperature is important and useful, as increasing the temperature generally accelerates degradation. The effect of temperature on the rate of decomposition may be described by an empirical equation proposed Arrhenius (Florence & Attwood 1981).

$$\text{Log } K''' = \log A' - \frac{E'_a}{2.303RT} \qquad 6.1$$

where K''' is the degradation rate

A' is the frequency factor

$E_a^{`}$ is the degradation activation energy

T is the absolute temperature

R is the universal gas constant.

A plot of log $K^{''}$ as a function of reciprocal temperature should be linear with a slope of $-E_a^{`}/2.303R$ from which $E_a^{`}$ may be calculated (Florence & Attwood 1981).

The degradation rate constant at any storage temperature may be extrapolated from measurement at a series of elevated temperatures where the reaction was accelerated by elevating the temperature. This finding is very useful in predicting the shelf life of a product.

Several groups of workers have studied the effect of aging on the physicochemical properties of compressed tablets. Ewe (1934) used the changes in crushing strength with aging as an indication to predict change in drug activity. Burlinson & Pickering (1950), Bergman & Bandelin (1965) used the disintegration time to predict changes in drug properties with aging, as they noticed an increase in disintegration time with aging. But Horhota et al. (1976) found that neither crushing strength nor thickness and diameter bear any relationship to changes in dissolution rate, and he found that there was a substantial change in dissolution efficiency occurring without any change in hardness or tablet size. This finding was confirmed by Lausier et al. (1977). Alam & Parrott (1971) found that aging increases the disintegration time, and crushing strength, and dissolution time of tablets granulated with acacia, whilst tablets granulated with polyvinylpyrrolidone (PVP) were stable at room temperature and only very slight increases in disintegration time were observed after one year. Mattok et al. (1971) found that dissolution

time increased with aging of acetaminophen and the blood level resulting from administration of old tablets was lower than for the freshly prepared tablets. Ondari et al. (1984) studied the dissolution rate of four types of compressed tablets, the dissolution time increasing with age for all four types.

The effect of aging on solid dispersions has also been examined. El Banna et al. (1974) found the dissolution rate of fused phenobarbitone-urea decreased with age and they attributed this to the coarsening of the eutectic mixture. Other workers such as Ford & Rubinstein (1979), Chiou & Niazi (1971) found a decrease in dissolution time with aging of the solid dispersion of sulphathiazole-urea which related to the conversion of metastable polymorphic form II of sulphathiazole to the stable form I, whilst Chiou & Riegelman (1969) could not find any change in dissolution time for griseofulvin-polyethyleneglycol 600 systems when stored at room temperature for six months. Even the diluent used in tablet manufacture such as spray dried lactose and dextrose tends to harden with age causing increase in disintegration times. This effect was greater for lactose than dextrose and dissolution rate was also decreased with both additives (Duvall et al. 1965).

The effect of aging on phenylbutazone tablets has been studied by several workers' groups including Barrett & Fell (1975), Matsui et al. (1978) and Naggar et al. (1980). These workers studied the effect of aging on phenylbutazone tablet alone or with additives and the results showed decreasing dissolution rate with aging.

The degradation of phenylbutazone alone has been examined by several workers including Awang et al. (1973), Kata (1974), Beckstead et al. (1968) & Awang et al. (1976). However the method used to detect

and trace the degradation point was different between groups. Most of the workers (Awang et al. 1973,1976, Kata 1974) used a thin layer chromatography (TLC) technique reported by Beckstead et al. (1968). This technique is useful in separating the degradation products for further analysis, such as NMR, but the risk of oxidation on the plate can be accelerated by the presence of iron in the silica coating. An alternative method reported by Watson et al. (1973) was to use gas liquid chromatography (GLC). This method was thought to be more accurate and faster. However the limitation for this method is that the injection point was kept at 230^{o}C which might cause further degradation after injecting the samples or break down the degradation to be assessed.

Fabre et al.(1982) recently reported the use of high pressure liquid chromatography (HPLC) which was claimed to be more reliable in assessing phenylbutazone degradation due to the absence of risk of oxidation and no heat required. Also the technique was fast, so in this study HPLC was chosen.

The objective of this study was to apply an accelerated test using elevated temperatures to assess the effect of the presence of the additive and the change of the crystallographic nature of phenylbutazone on the stability of phenylbutazone.

6.2 Experimental

6.2.1 Materials

A high pressure liquid chromatograph with a variable wavelength U.V. detector, a 20µl loop injection, and reversed phase column were used. Phenylbutazone, the pure drug and six degradation products, I-VI, and supplied by Ciba-Geigy (see Table 6.1), were all used as received. Salicylic acid (analar grade) was used as the internal standard. Solvents used were methanol HPLC grade and double distilled water prepared from an all-glass still. The samples PHR4, PHS4, PPR3 and PPS3 were used.

6.2.2 Method

6.2.2.1 Stability testing for phenylbutazone with additives

The stability testing was carried out for the samples of phenylbutazone PHS4, PHR4, PPS3 and PPR3. The test was carried out by placing 3 gm of the powder of each sample in 20 ml glass bottles with rubber lined metal screw lids, four bottles for each sample. The sealed bottles were kept at 20°C, 37°C and 50°C. Another bottle was kept at 20°C and left open and exposed to a relative humidity of 45%±5% RH. The samples were tested initially and at three and six months, to check any change in D.S.C. thermograms and H.P.L.C. profiles.

6.3 Results and discussion

Fabre et al. (1976), using an HPLC technique, mentioned three degradation compounds (Nos. I , II and III see Table 6.1) and used a degassed 60:40 mixture of 0.1 M trimethamine citrate buffer (pH 5.25)-acetonitrile as mobile phase. An attempt to follow the same system was not successful, as blockage of the chromatographic column occurred. One possible cause of blockage is that the citric acid used adjusting the buffer pH tends to crystallise.

An alternative mobile phase was examined in which two systems are required to resolve and identify phenylbutazone and the breakdown products (Table 6.1). The first system consisted of a degassed mixture of 58/42 methanol HPLC grade, with double distilled water, and the second system is a degassed mixture of 42/58 methanol/water, using salicylic acid analar grade as internal standard in both systems (see Figs. 6.1 & 6.2).

6.3.1 Calibration curve

Five decomposition products were analysed using HPLC and four concentrations of each were injected into the column. Degradation product No. I was found to be very unstable during analysis, gradually changing to No. III after dissolving in the solvent. Thus No. I was excluded from further experiments. For breakdown product No. II , one tenth of the concentration of the other samples, was used to bring it within the scale reading. Calibration curves were linear passing through the origin.

6.3.2 Stability testing of phenylbutazone-polymeric additive samples

As illustrated in Fig. 6.3(Awang 1973), oxidation of phenylbutazone at the tertiary C4 results in 4-hydroxyphenylbutazone (No. I)

Table 6.1 List of phenylbutazone degradation products

Degradation Name	Number	Structure
4-hydroxyphenylbutazone	I	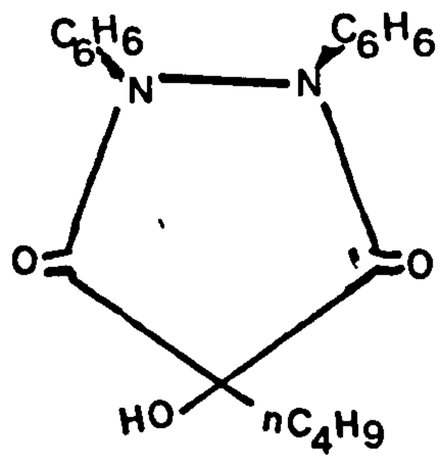
α-carboxy-α-hydroxy-N-caproyl-hydrazobenzene	II	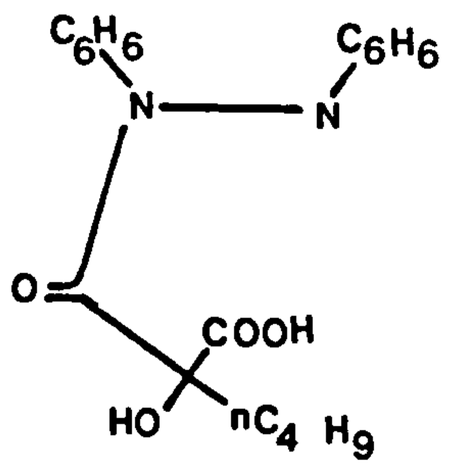
α-carboxy-N-caproylhydrazobenzene	III	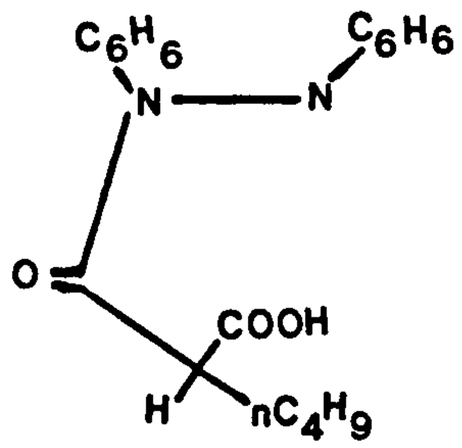
α-hydroxy-N-caproylhydrazobenzene	IV	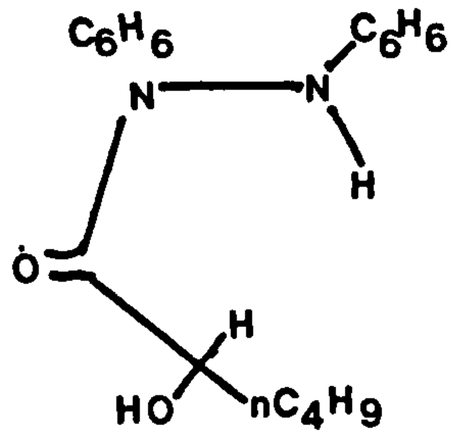
N-caproyl-hydrazobenzene	V	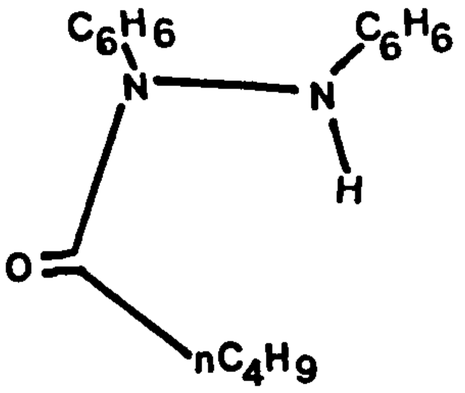
N-(α-ketocaproyl)-hydrazobenzene	VI	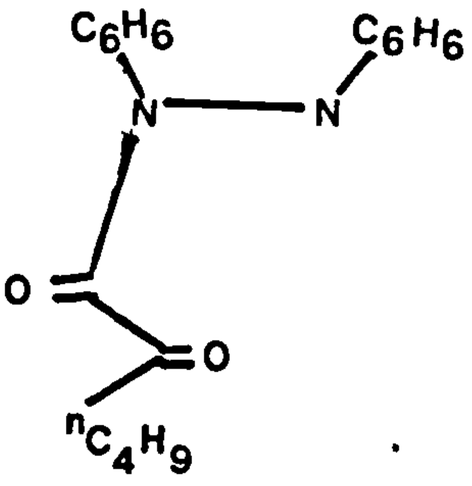

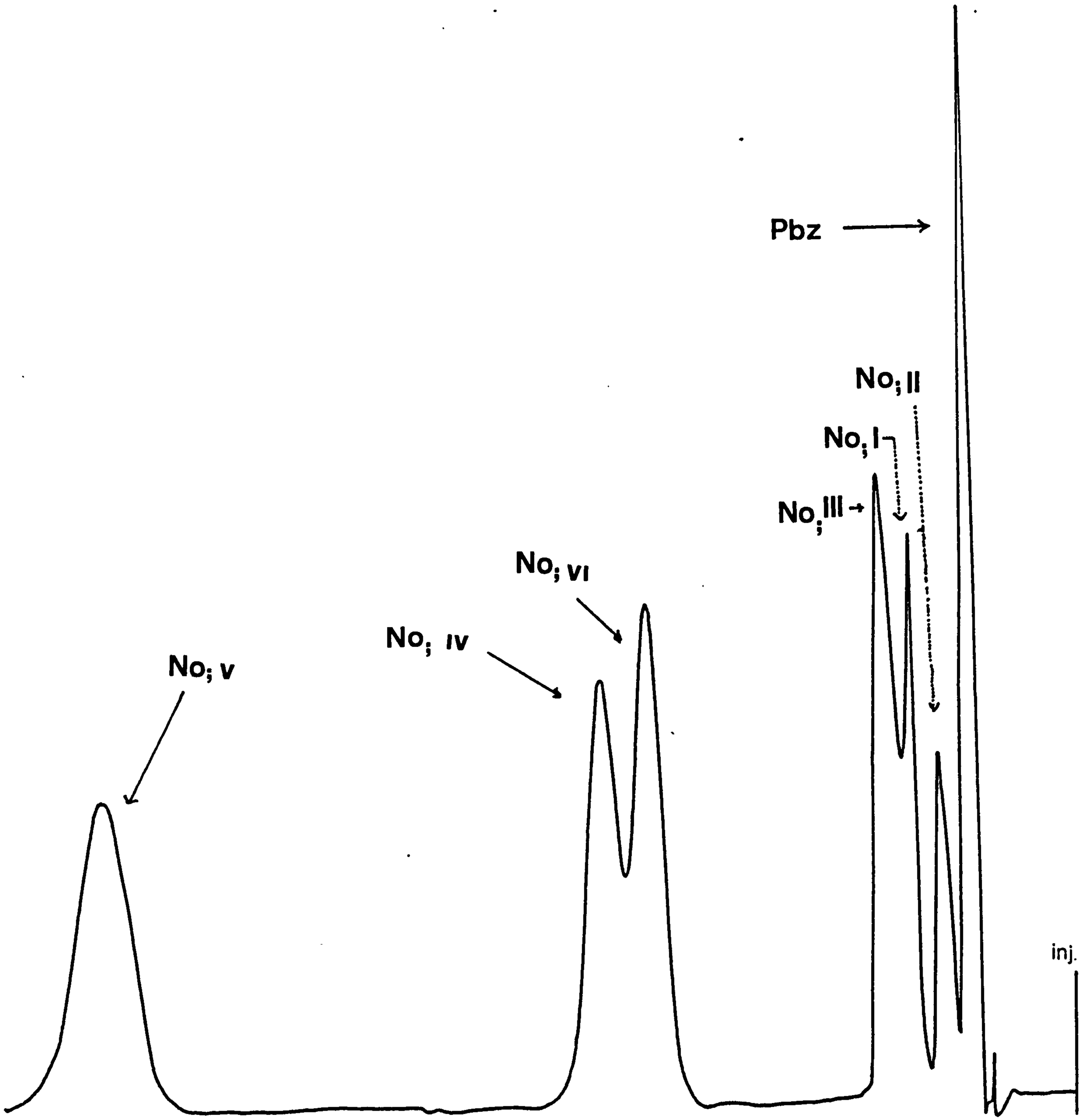

Fig. 6.1

Solvent system one (58/42 ethanol/water) for HPLC analysis to separate phenylbutazone and degradation products III,IV, V and VI

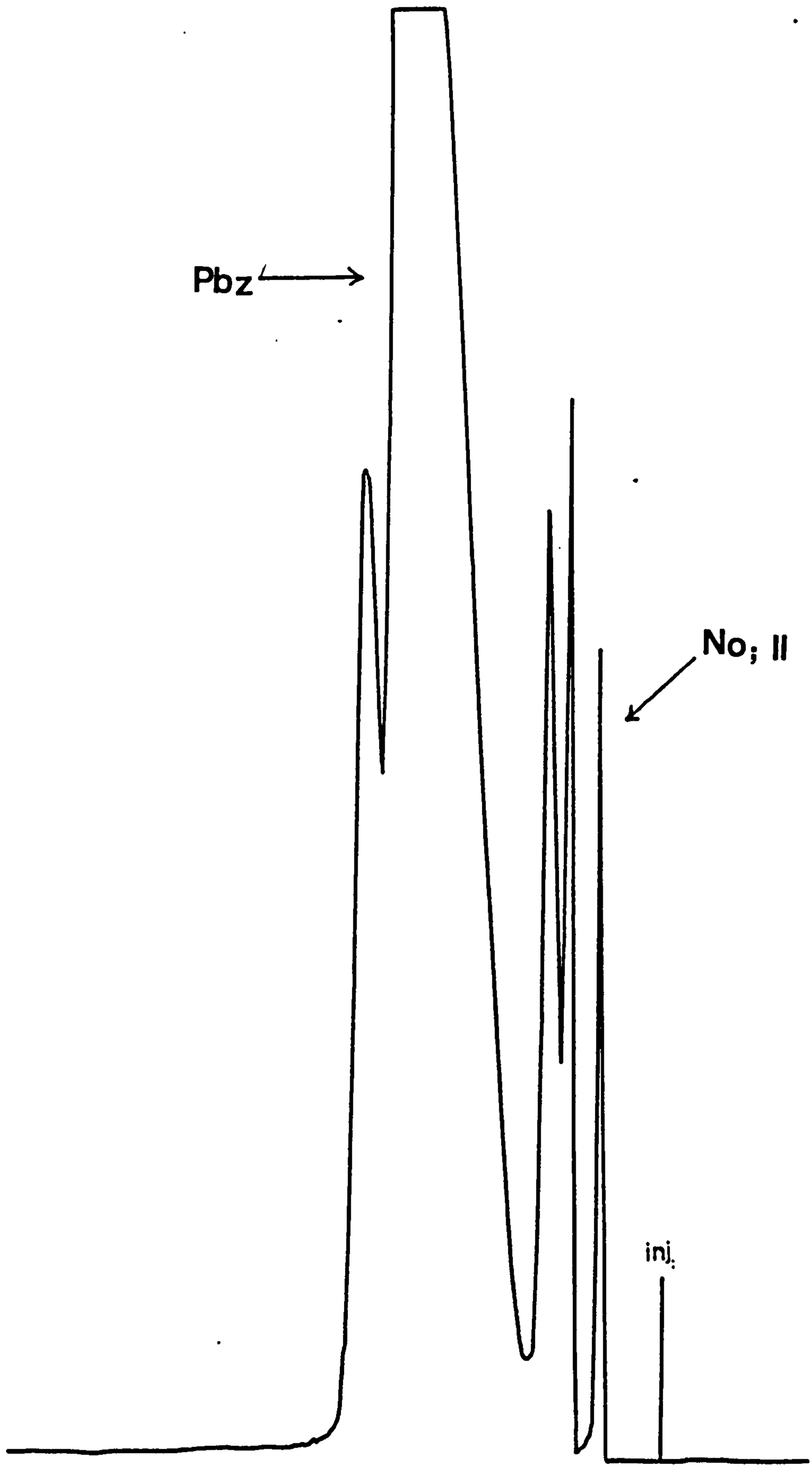

Fig. 6.2 Solvent system two (42/58) methanol/water for HPLC to separate phenylbutazone degradation No.II

Fig. 6.3 Degradation sequence of phenylbutazone

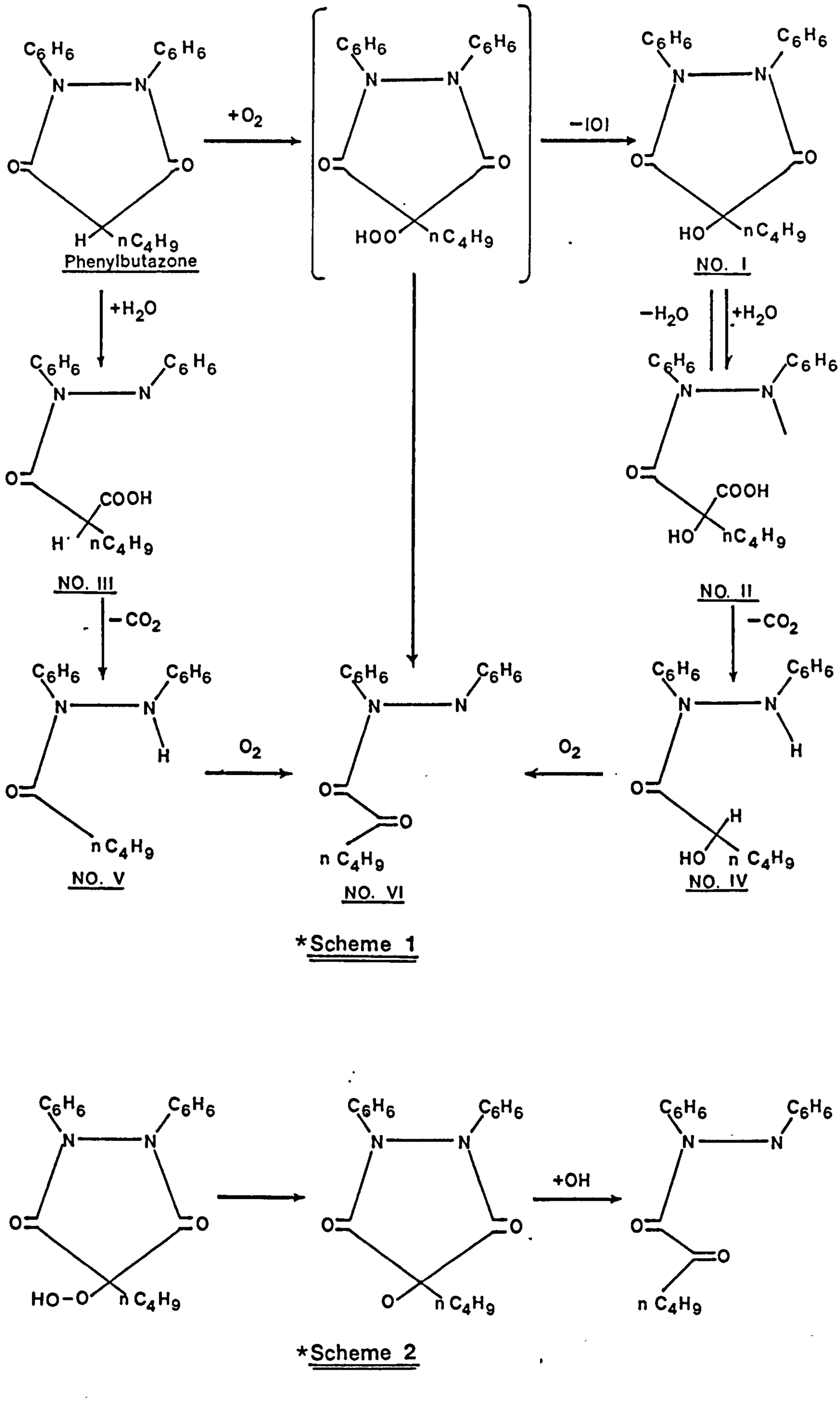

*Scheme 1

*Scheme 2

* From Awang et al. 1973

which was found to be unstable converting to α-carpoxy-α-hydroxy-N-caproyl-hydrazobenzene (No. II), just after dissolving it in mobile phase. The detected amount of II increased with successive injections of I. This agrees with the sequence in the degradation scheme as product II is the result of hydrolysis of I. The reaction occurs so fast that product I can be regarded as very unstable. Awang et al. (1973) were in fact unable to isolate I and this observation has also been reported by Veibel et al. (1958). Product I however was obtained by Awe & Kierner (1963) and was made available for this study by Ciba-Geigy.

Powelezyk & Wachowlok (1969) reported that I was the major degradation product in phenylbutazone suppositories. Awang et al. (1973) related this to the hydrophobic nature of the bases with which phenylbutazone was compounded in the formulations studies. Hydrolysis product I results in cleavage of the C-N amide bond and yields the degradation product α-carpoxy-α-hydroxy-N-caproyl-hydrazobenzene (II), while hydrolysis of phenylbutazone results in degradation product - carpoxy-N-cabroylhydrazobenzene (III) which was reported by Matsui et al. (1978) to be the major degradation product in phenylbutazone-antacid formulations. Schmid (1970) also reported that product III is the major degradation product of phenylbutazone in aqueous solution. The observation in this study that product III was the only degradation product found in the stability testing of phenylbutazone with polymeric additives is consistent with these reports.

The presence of an electron withdrawing group will facilitate decarboxilation and loss of carbon dioxide (Hine 1962), so the loss of carbon dioxide from degradation products II and III will lead to further degradation resulting in product α-hydroxy-N-caproyl-hydrazobenzene (IV),

and N-caproyl-hydrazobenzene (V) successively. When IV and V are further oxidised degradation product N(α-ketocaproyl)-hydrazobenzene (VI) is obtained.

6.3.2.1 H.P.L.C.

The stored samples were tested for the presence of any degradation product in the samples when exposed to the adverse conditions. The retention times of the peaks were examined to determine the type of the degradation and the size of the peak to calculate the concentration of the degradation product.

The result of analysing the samples after three and six months indicated that the pure phenylbutazone tested as received without any further purification or additives, was stable during the testing period at all the temperatures studied (see Table 6.3). This agrees with Matsui et al. (1978) who reported that unformulated drug was stable at 60°C.

Results also indicated that there was one degradation product α-carboxy-N-caproyl-hydrazobenzene (III) (see Fig. 6.4 & Table 6.2). This is consistent with the report of Matsui et al. (1978) that α-carboxy-N-caproyl-hydrazobenzene was the major degradation product in the phenylbutazone-antacid tablets. Also Powelezyk & Wachowiak (1969), who studied the aqueous injection solution of sodium salts of phenylbutazone, found this compound to be the major degradation product.

All the samples were stable at 20°C after three months when kept in both closed and open containers, although traces of product III were present in open samples presumably due to access of some moisture. The degradation product started to appear clearly for samples stored at 37°C and was more pronounced for samples stored at

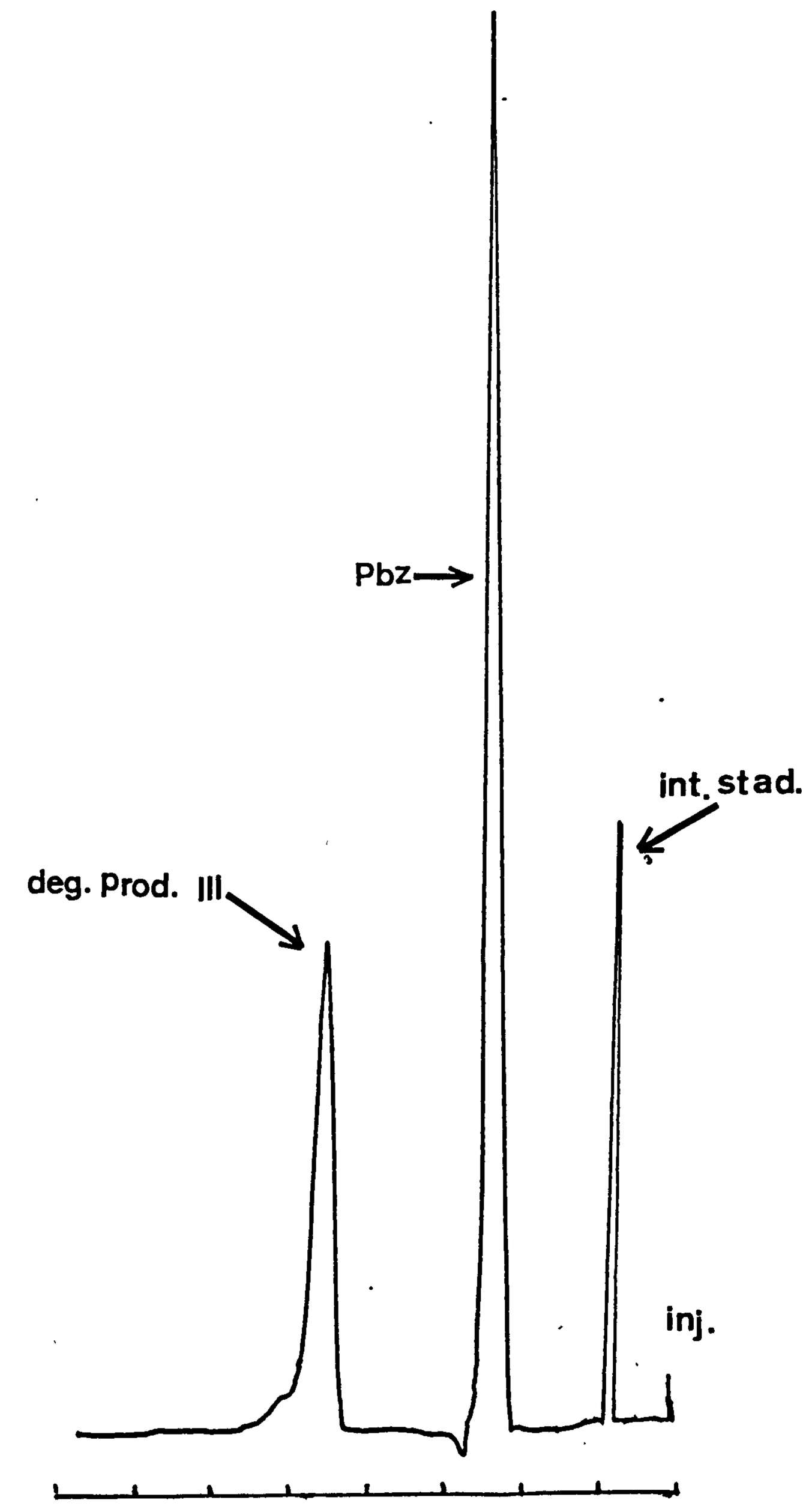

Fig. 6.4

Representative HPLC trace for phenylbutazone and degradation product of the stored phenylbutazone samples.

Table 6.2 The stability testing of phenylbutazone with additive and the concentration of degradation product III (% w/w)

	0 Months	3 Months				6 Months			
Sample		Stored at 50°C	Stored at 37°C	Stored at 20°C Open	Stored at 20°C Closed	Stored at 50°C	Stored at 37°C	Stored at 20°C Open	Stored at 20°C Closed
PHR4	0.0%	13.0%	3.8%	0.0%	0.0%	18.0%	6.3%	3.1%	<1.0%
PHS4	0.0%	4.4%	2.1%	0.0%	0.0%	10.0%	3.2%	2.9%	<1.0%
PPR3	0.0%	33.0%	17.4%	0.8%	0.0%	54.5%	20.5%	3.3%	1.4%
PPS3	0.0%	15.6%	5.9%	<0.0%	0.0%	20.0%	8.4%	3.0%	1.1%
PbZ	0.0%	0.0%	0.0%	0.0%	0.0%	0.0%	0.0%	0.0%	0.0%

50°C (see Fig. 6.5).

When analysing the samples after storage for six months, increased amounts of III were noticed, but no additional decomposition product was detected. For samples stored at 20°C, the presence of degradation product III was detected with reduced amounts for samples in sealed containers.

The moisture levels are likely to differ slightly between samples due to both the sample preparation conditions, conventional crystallisation or spray drying involving different temperatures and rates of crystallisation, and also the different affinity of the polymer additive for water molecules causing samples to release moisture during elevated temperature storage which will facilitate hydrolysis of phenylbutazone.

6.3.2.2 Differential scanning calorimetry

The effect of age and storing the sample at different temperatures influenced the thermal behaviour of some of the samples. For phenylbutazone pure drug, no change has been observed in its melting endotherm during the testing period for all storage conditions. The same was observed with crystallised samples containing poloxamer 188.

For samples prepared by spray drying, changes were observed in the endotherm at 95°C, the effect depending on the additive. For the samples spray dried with poloxamer 188 the peak at 95°C completely disappeared for samples stored at all the storage temperatures, this effect being noticed after storage for three months (see Fig. 6.6). The peak at 95°C is attributed to the β-polymorph which is a metastable form, so with time and elevated temperature reversion to the stable δ form could occur. For samples spray dried with H.P.M.C. there was a

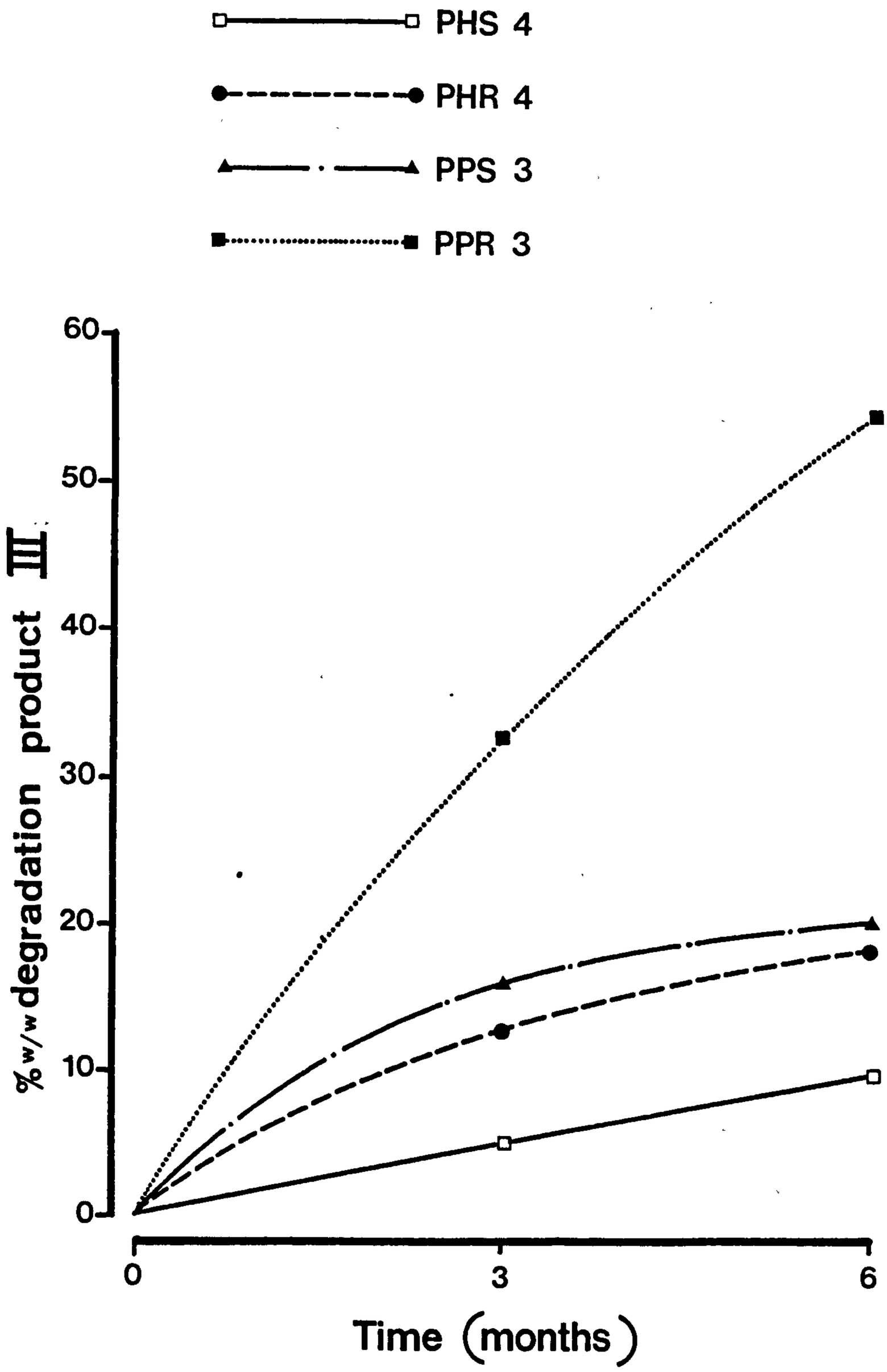

Fig. 6.5

Graphical representation of the percentage of degradation product III with time for tested materials, stored at 50°C

reduction in size of the peak at 95°C and the reduction increased with increasing storage temperature and with time. After three months the 95°C endotherm was present for all the samples, but after six months it completely disappeared for sample stored at 50°C, with samples exhibiting a single endotherm at 107°C.

The difference in rate of solid-solid transition and decreasing the peak size at 95°C between samples spray dried with poloxamer 188 and H.P.M.C. can be explained by the fact that for poloxamer 188 no reaction or complexation appeared to occur between the drug and polymer. The presence of polymer is therefore unlikely to interfere with the rate of conversion of metastable polymorph to the stable form which is initiated with elevated temperature. However, for samples spray dried with H.P.M.C., previous discussion (see Chapter 4) suggested that H.P.M.C. formed a complex with the drug and it is suggested that this complexation retards the solid-solid transition.

For samples crystallised with H.P.M.C. the samples at time (zero) exhibited a single endothermic peak at 97°C, but with increased time and temperature the δ-peak at 107°C started to appear. As it increased the peak at 97°C decreased, although after six months the 97°C endotherm was not completely absent. This effect could be explained by the high energy complex between the drug and H.P.M.C. starting to breakdown and liberate phenylbutazone alone. Elevated temperature appears to have accelerated this breakdown.

Fig. 6.6 The D.S.C. thermograms for samples of phenylbutazone with additives stored at 50°C

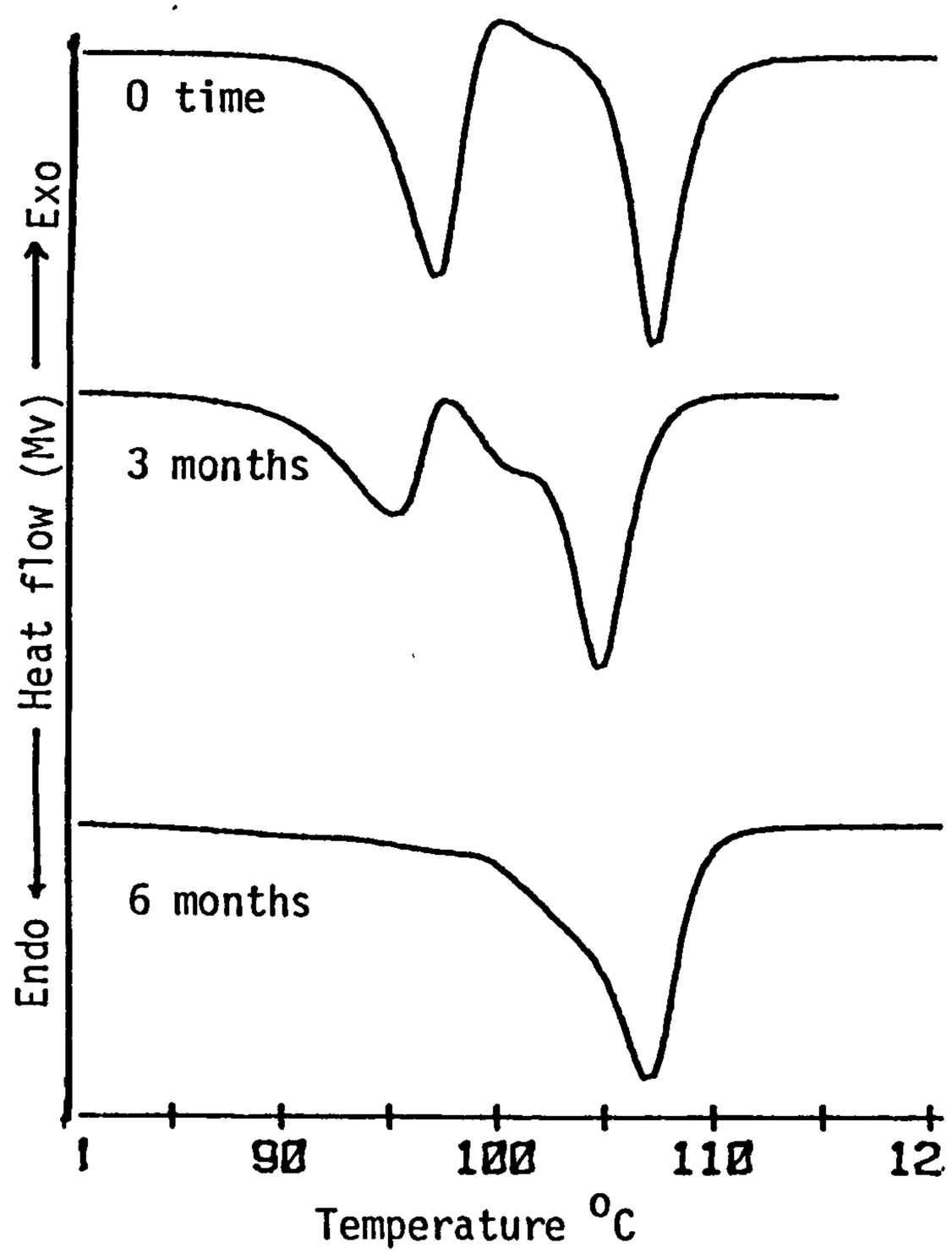

PHS4

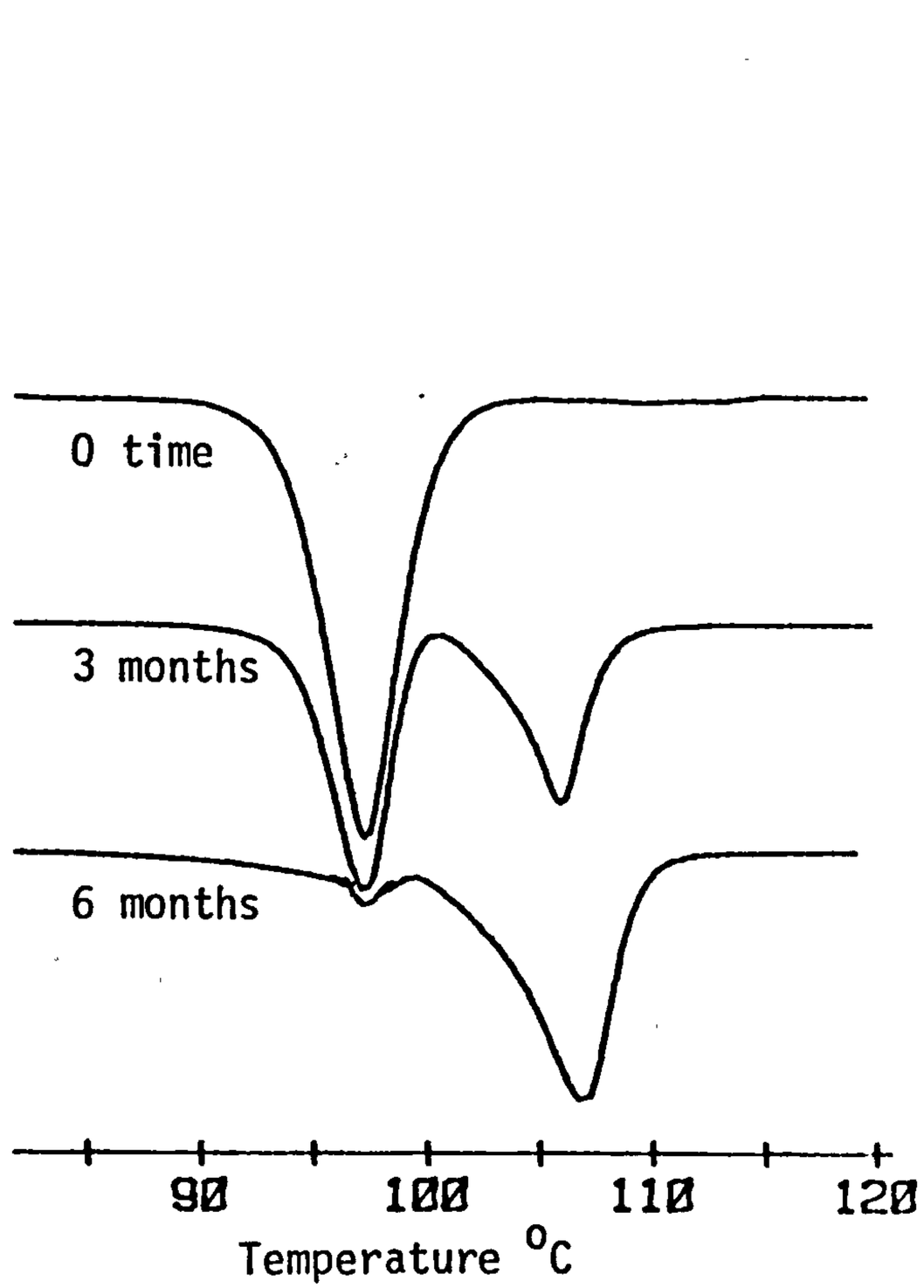

PHR4

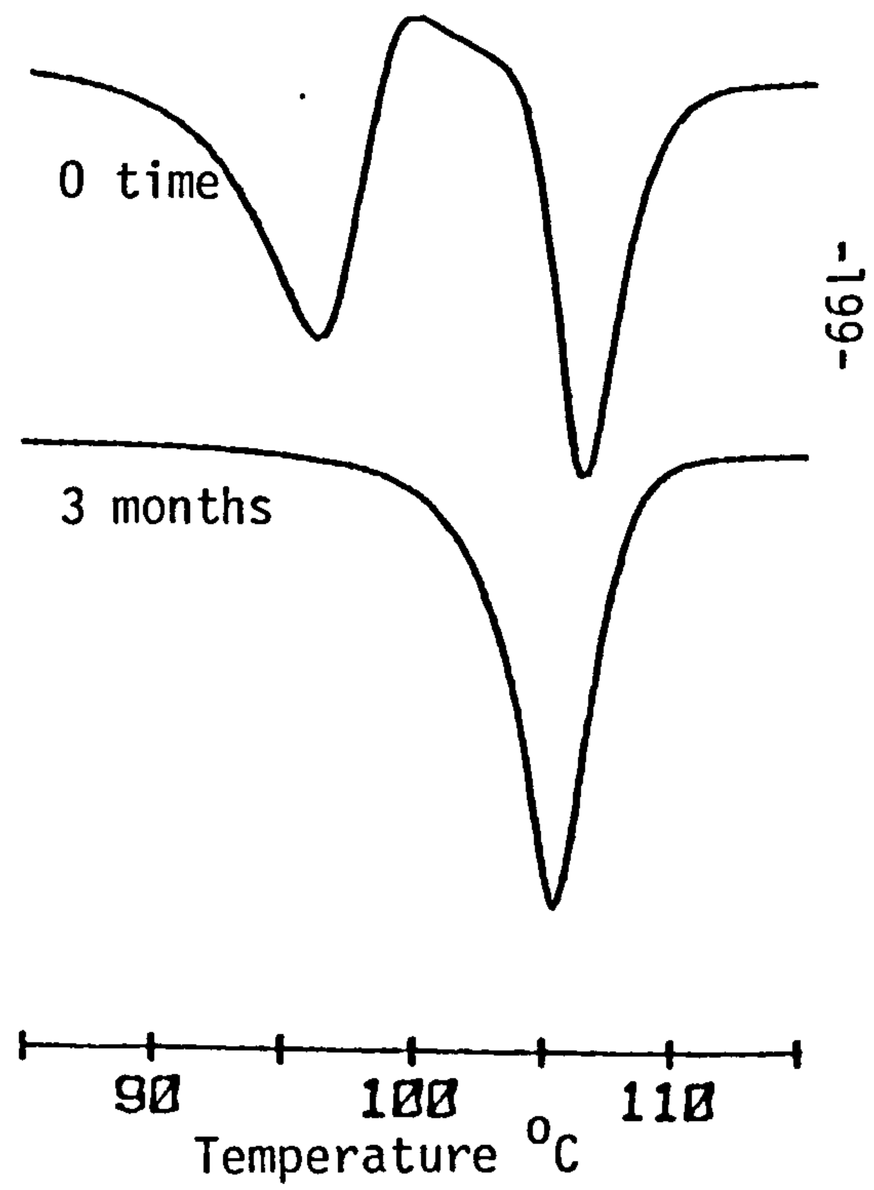

PPS3

6.4 Conclusion

1. From the study it was found that HPLC was a reliable, useful and fast technique for examining and detecting the degradation product of phenylbutazone. The stability study showed that phenylbutazone was stable during the period of study even when stored at $50^{o}C$.

2. A degradation product appeared when samples of phenylbutazone containing either H.P.M.C. or poloxamer 188 were stored.

The product was found to be α-carpoxy-N-caproylhydrazobenzene (degradation product No. III) which was present due to the hydrolysis of phenylbutazone.

3. The study revealed that the type of additive and the way of preparing the samples played a major role in initiating the degradation process. This was seen for samples having the same additive but prepared by different processes. Samples prepared by conventional crystallisation showed higher concentration of degradation product than those prepared by spray drying, whilst samples containing poloxamer 188 showed higher concentration of decomposition product than those containing H.P.M.C.

4. The D.S.C. thermograms showed that solid-solid transition occurred in the samples on storage and the presence of H.P.M.C. tended to slow down this transition.

5. Elevated temperature appeared to cause the proposed complex between H.P.M.C. and phenylbutazone to be broken.

CHAPTER 7

CHAPTER 7 Tableting of spray-dried and crystallised phenylbutazone samples containing H.P.M.C.

7.1 Introduction

Previous chapters of this thesis have considered the physico-chemical and crystallographic of modified phenylbutazone samples. It is also of relevant interest to consider the processing characteristics of the phenylbutazone:polymer samples. This chapter considers aspects of the tableting behaviours of prepared samples of phenylbutazone, PS, PHS2, PHS3, PHS4, PHS5, PHR2, PHR3, PHR4 and PHR5.

Tableting is a widely used process in the pharmaceutical industry and has been used in this work to represent a relevant aspect of pharmaceutical processing.

Powder compaction data have been analysed according to the Heckel pressure, volume relationship (Heckel, 1961).

In addition, force transmission through the bed of powder was measured to assess changes in frictional effects during compression and to monitor a property of the prepared compact, dependent upon both material and processing conditions, tablet tensile strength was determined.

7.2 Experimental

7.2.1 Materials

The materials used were phenylbutazone as supplied (PbZ), Ps, PHS2, PHS3, PHS4, PHS5, PHR2, PHR3, PHR4 and PHR5.

7.2.2 Method

The samples were prepared using techniques described in Chapter 2. Tableting and analysis of data were carried out using techniques described in Chapter 2.

7.3 Results and discussion

7.3.1 Heckel plot analysis

Data from the ejected compressed tablets which are listed in Appendix 4 Tables1-10, plotted according to the Heckel equation gave curves which exhibited two distinct sections. The first curved section is attributed to initial packing and rearrangement of the powder particles under low pressure. The second part of the curve gave straight lines where the reciprocal of the slope can be taken to equal the mean yield pressure K_1 (see Figs. 7.1 & 7.2).

Table 7.1 lists values of mean yield pressure for the various samples studied. For the spray-dried materials, it can be seen that the estimated values of yield pressure for all samples containing H.P.M.C. gave similar figures (mean 93.5 MPa) suggesting that major changes in the yield pressure of the β form prepared did not occur when up to 5% w/w H.P.M.C. was included into phenylbutazone. There is however a downward displacement of the curves with increasing H.P.M.C. concentration. Further analysis of the Heckel relationship enables density changes occurring during the rearrangement stages to be estimated (see Fig. 7.3).

Table 7.1 lists calculated values of packing fraction F_A packing fraction F_B and it can be seen that as the amount of H.P.M.C. present in the phenylbutazone sample increases, the density change due to particle rearrangement and repacking decreases. Since only minor differences in particle size and shape occur between samples, the principle causative factor is attributed to increased cohesion between particles due to the presence of the polymer in the samples.

Table 7.1 Values of K_1, the mean yield pressure; ρ_{FA}, densification due to die filling and particle slippage and rearrangement; ρ_{FO}, initial powder packing fraction; ρ_{FB}, densification due to particle slippage and rearrangement.

	Crystallised samples					Spray dried samples			
Sample	K_1 (MPa)	ρ_{FO}	ρ_{FA}	ρ_{FB}		K_1 (MPa)	ρ_{FO}	ρ_{FA}	ρ_{FB}
PbZ	142.28	0.090	0.980	0.890	PS	89.81	0.128	0.860	0.732
PHR2	143.71	0.092	0.886	0.788	PHS2	92.12	0.130	0.840	0.710
PHR3	145.10	0.095	0.860	0.765	PHS3	92.12	0.132	0.720	0.588
PHR4	147.40	0.131	0.800	0.669	PHS4	94.42	0.143	0.581	0.435
PHR5	156.61	0.134	0.660	0.526	PHS5	94.03	0.145	0.480	0.335

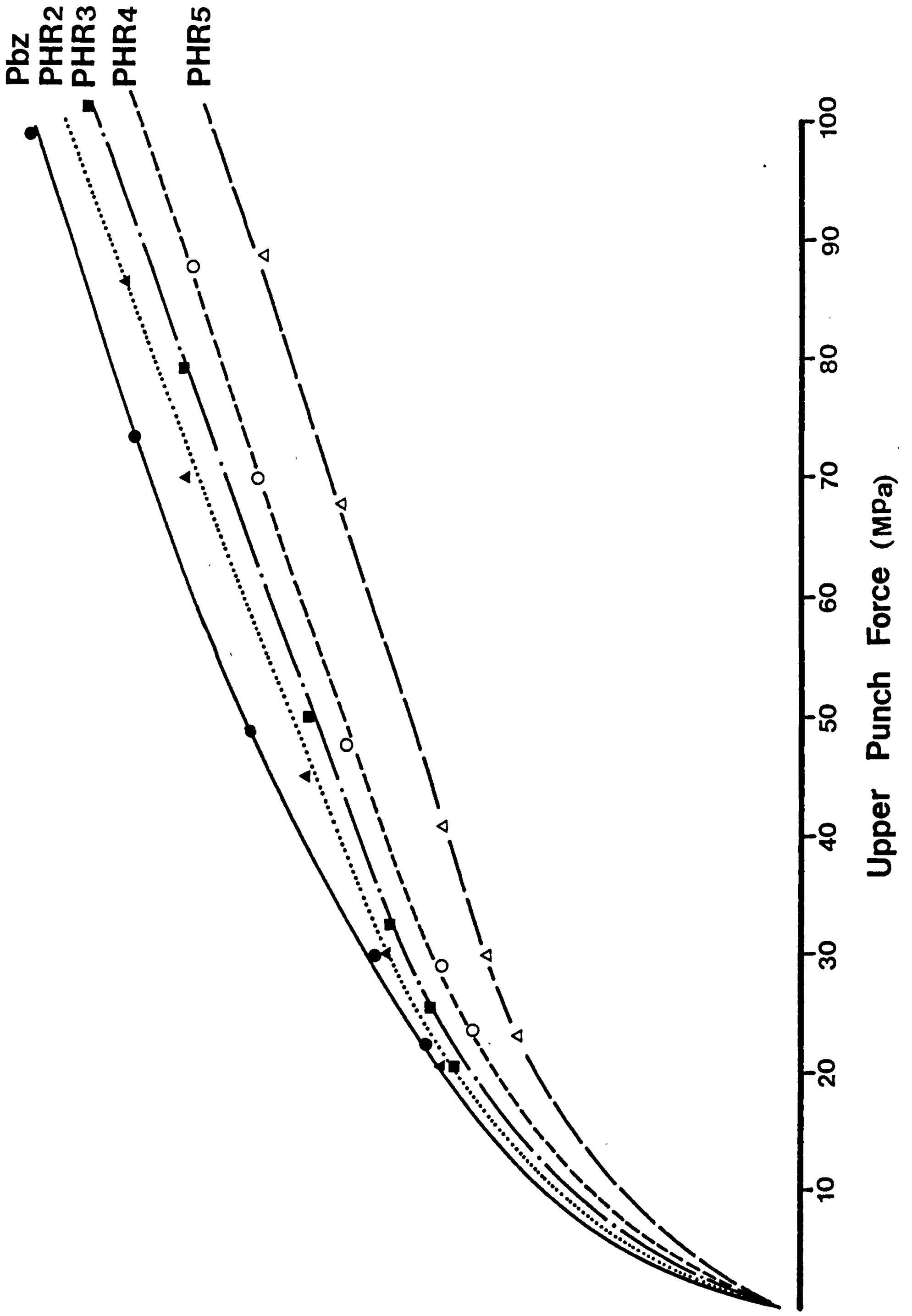

Fig. 7.1 Heckels plot for phenylbutazone crystalline as supplied (δ-form) and samples crystallised from solutions containing different concentrations of H.P.M.C.

Fig. 7.2 The Heckel plot of phenylbutazone spray dried alone and samples spray dried to contain different concentrations of H.P.M.C.

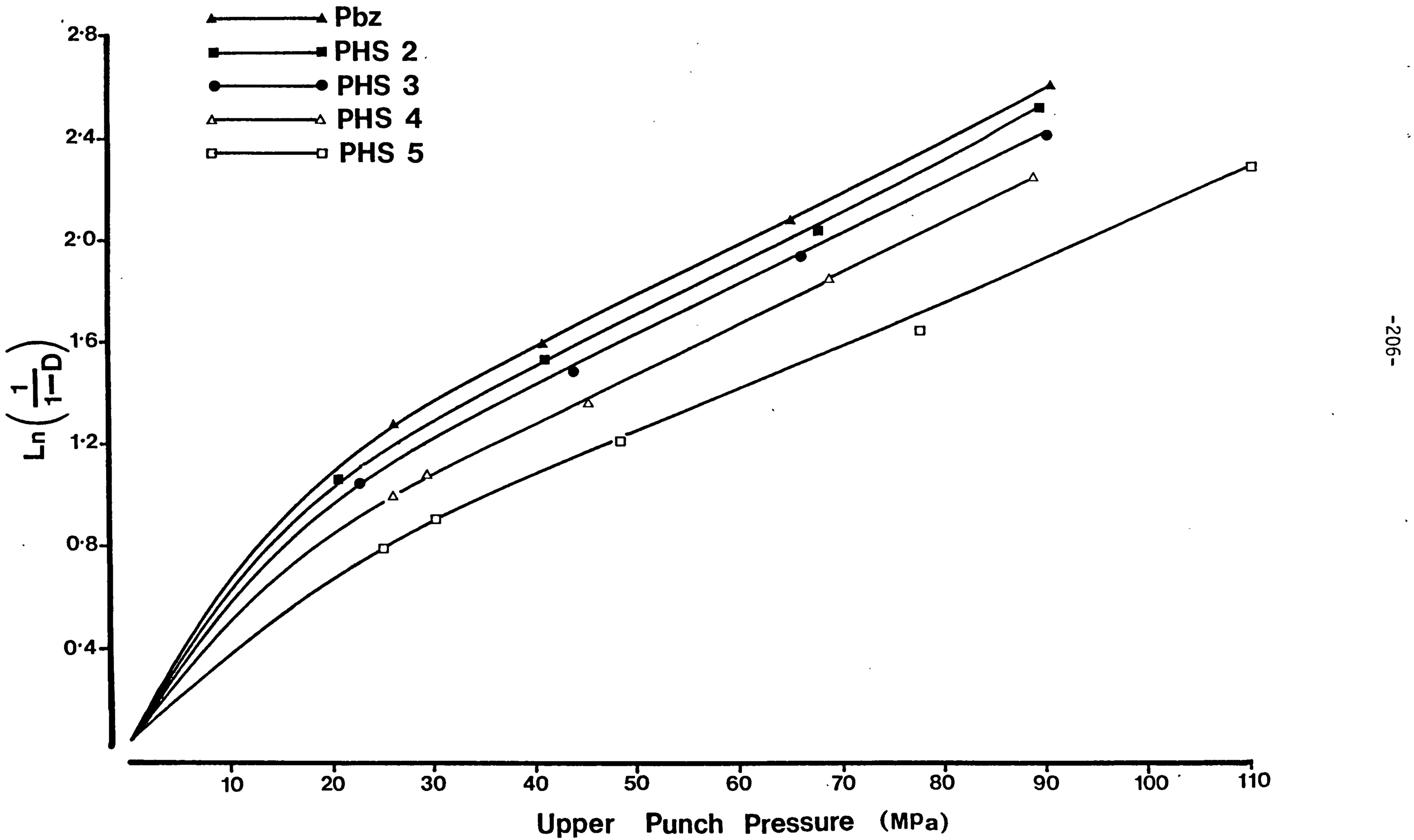

A similar family of curves was obtained for the samples prepared by conventional crystallisation. The linear portions are again similar in slope, although there is a trend of increasing value of mean yield pressure as the concentration of H.P.M.C. in the sample increases (see Table 7.1). Also as the concentration of H.P.M.C. in the sample increases, the curves are displaced downwards. This again suggests that the presence of H.P.M.C. increases the cohesiveness of the powder samples.

Table 7.1 also shows that the mean yield pressure for the crystallised material without H.P.M.C. was greater than that obtained for the spray-dried phenylbutazone without H.P.M.C., which follows the observation of Fell & Newton (1971) for lactose samples, who reported that the yield pressure for spray-dried lactose was lower than that for the crystalline lactose. In the case of spray-dried phenylbutazone the yield pressure and onset of linear section occurred at a higher pressure than for the material prepared by conventional crystallisation.

The bulk density and linear onset effects can be attributed to differences in the shape, morphology and crystallographic character of the materials. In the case of the crystallised phenylbutazone, the stable δ polymorphic form is present and the particles were needles, which will need comparatively higher pressures for packing and rearrangement to overcome interparticle friction forces compared with the more spherical spray-dried particles. The higher yield pressure for the crystallised sample can partly be attributed to the fact that samples exist in the stable δ form whilst the spray-dried phenylbutazone is in the β-metastable form, and partly due to other crystallographic and morphological differences between samples.

Fig. 7.3a Graphical representation of Heckel equation for samples of phenylbutazone, crystalline and spray dried.

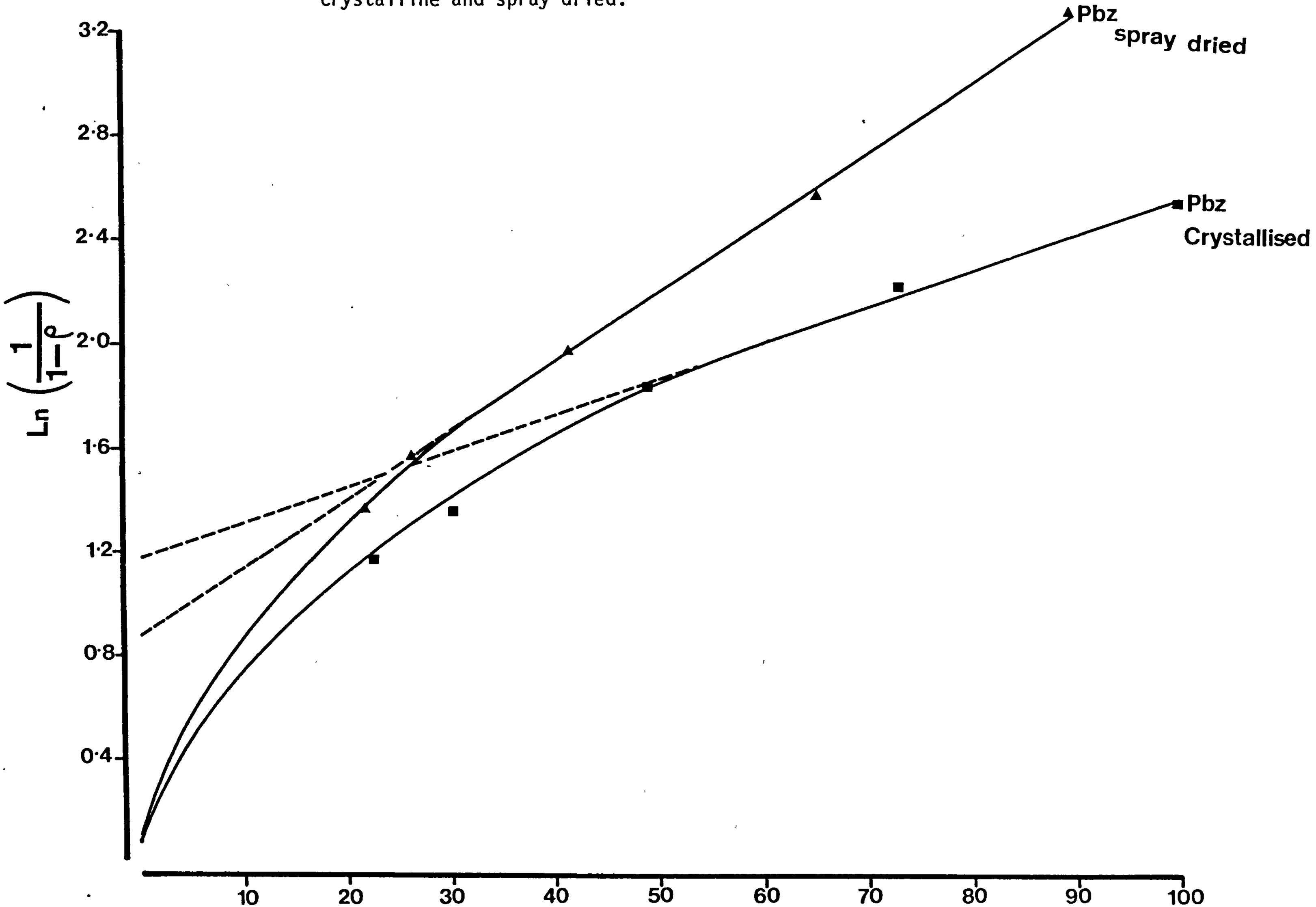

7.3.2 Force transmission

The force transmission $\frac{FL}{Fu}$ is defined in this study as the ratio of maximum force transmitted to the lower punch (FL), to the maximum force applied to the upper punch (Fu). The lower the ratio, the greater the force loss due to friction, primarily between particles and die wall but also interparticulate friction particle rearrangement, heat gain and bonding. Data from the instrumented tablet of maximum upper and lower force are listed in Appendix 4 Tables 1-10. Fig. 7.4 & 7.5 show plots of $\frac{FL}{Fu}$ versus final tablet porosity for crystallised and spray-dried samples. The curves show that the amount of force loss at equivalent porosity for the two series of materials were very similar. Fig. 7.6 shows that the force loss decreased steadily with increasing amounts of H.P.M.C. up to 2% w/w concentration then at 5% w/w H.P.M.C. concentration, a much improved transmission of applied forces took place. It thus appears that whilst the presence of higher concentrations of H.P.M.C. increases interparticle cohesion die wall friction is reduced, and the nature, morphology and crystal form of the phenylbutazone does not seem to be important in this change in frictional character.

7.3.3 Tablet tensile strength

From the Heckel plot discussed earlier it was concluded that the spray-dried materials were more plastic (i.e. had lower mean yield pressure value), compared with the crystallised materials. Also the addition of polymer reduced the extent of particle packing, rearrangement and generally particles with polymer were thought to be more cohesive making it easier for the particles to form bonds on compression.. The tensile strength data for the sample examined are listed in Appendix 4 , Table 1-10. Using these data (Fig. 7.7 , 7.8)

Fig. 7.4 Force transmission ratio versus final tablet porosity for samples of spray dried phenylbutazone alone and spray dried samples containing different concentrations of H.P.M.C.

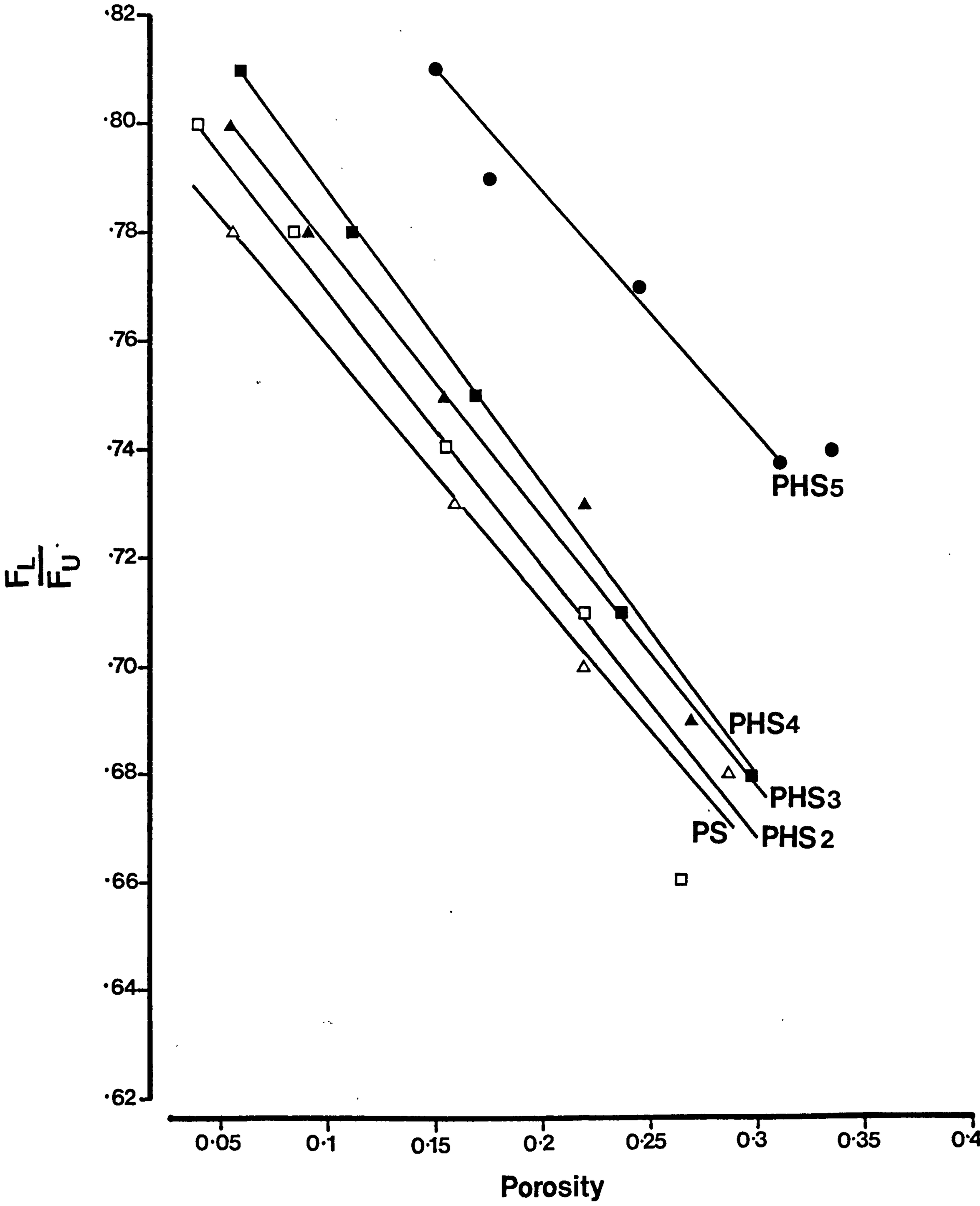

Fig. 7.5 Force transmission ratio against final tablet porosity for phenylbutazone as supplied and samples crystallised from solutions containing different concentrations of H.P.M.C.

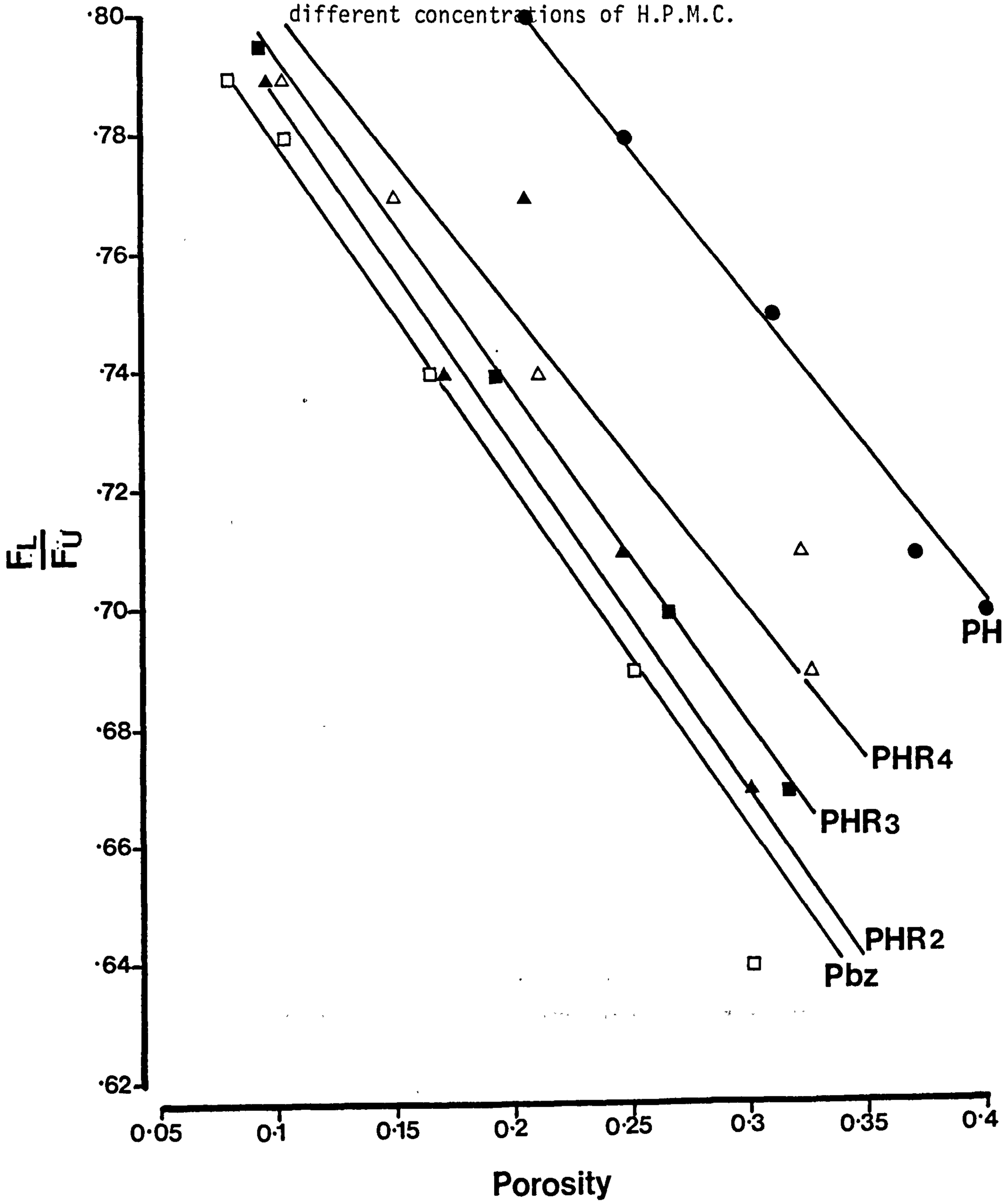

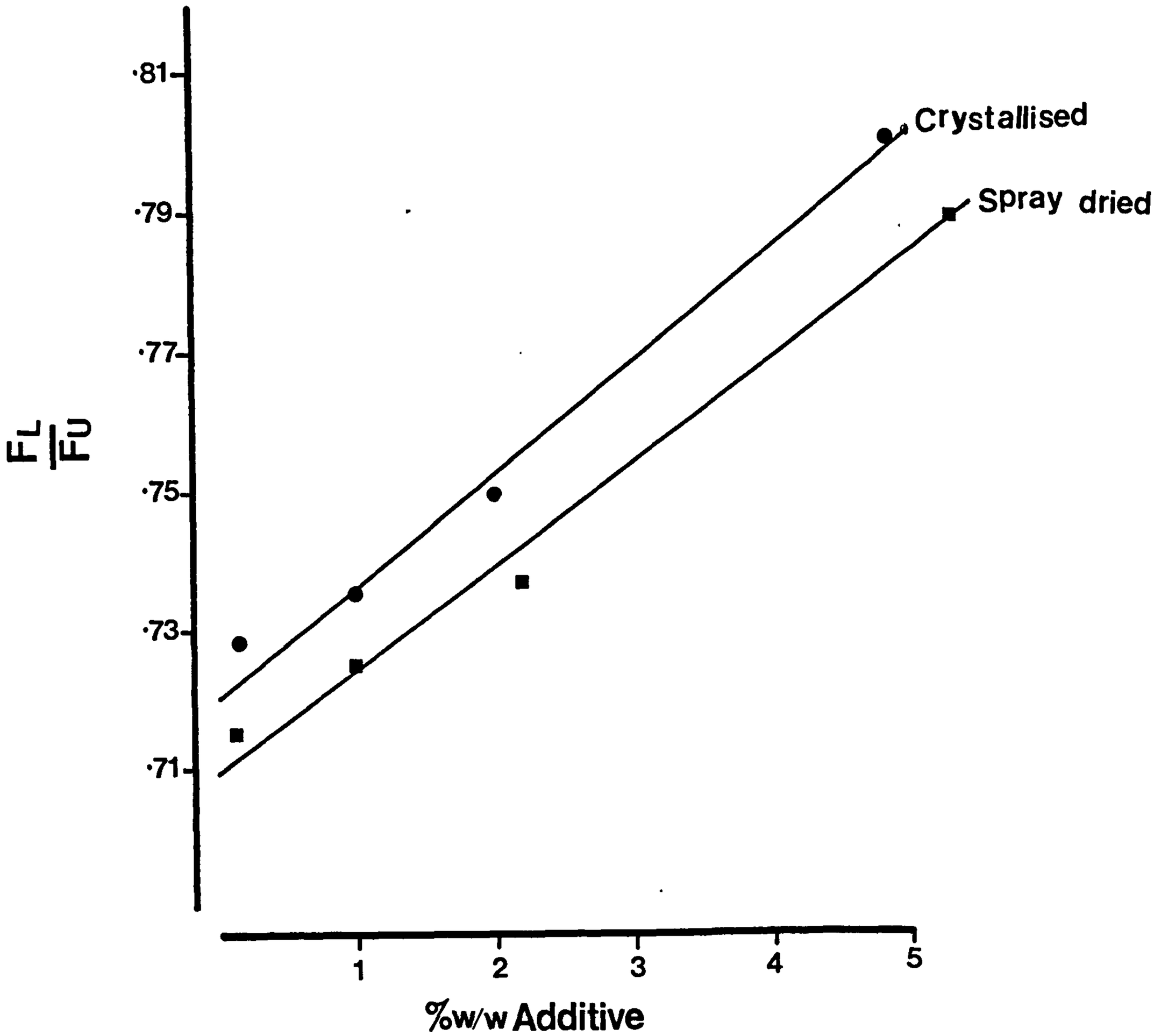

Fig. 7.6

Relationship between force transmission ratio and H.P.M.C. concentration in samples at constant tablet porosity of 0.2 (20%).

demonstrated differences between the spray-dried and the conventional crystallised materials. Whilst both groups exhibit increases in tensile strength with increasing concentration of H.P.M.C. added, for similar porosity values the tensile strength of compacts from conventional crystallisation procedures are significantly higher.

The form of the curves is different between the spray dried and crystallised materials, with the former showing an exponential increase in tensile strength as the porosity decreases compared with an apparent linear function for the crystallised materials. It is possible that the spray-dried spherical-like particles fracture and/or breakdown extensively at higher pressures to achieve low porosities and which creates new, clean surfaces in close proximity which would lead to increased bonding.

Fig. 7.8 shows the change in tablet tensile strength of a fixed porosity of 0.2, chosen to minimise extrapolation of data, and to approximate to conventional tablet porosity figures. The graph confirms that the tablets prepared from phenylbutazone samples containing H.P.M.C. prepared by conventional crystallisation have values of tensile strength approximately three times larger than equivalent spray-dried samples. Whilst the spray dried materials contain the β polymorph of phenylbutazone, they also have different shape and morphology, all factors which could contribute to this effect. An additional factor could be the nature of the distribution pattern of the H.P.M.C. within the spray-dried and crystalline materials. A surface matrix of H.P.M.C. would facilitate polymer-polymer contact and since H.P.M.C. is plastic in nature, deformation could readily occur leading to bonding between particles. However,

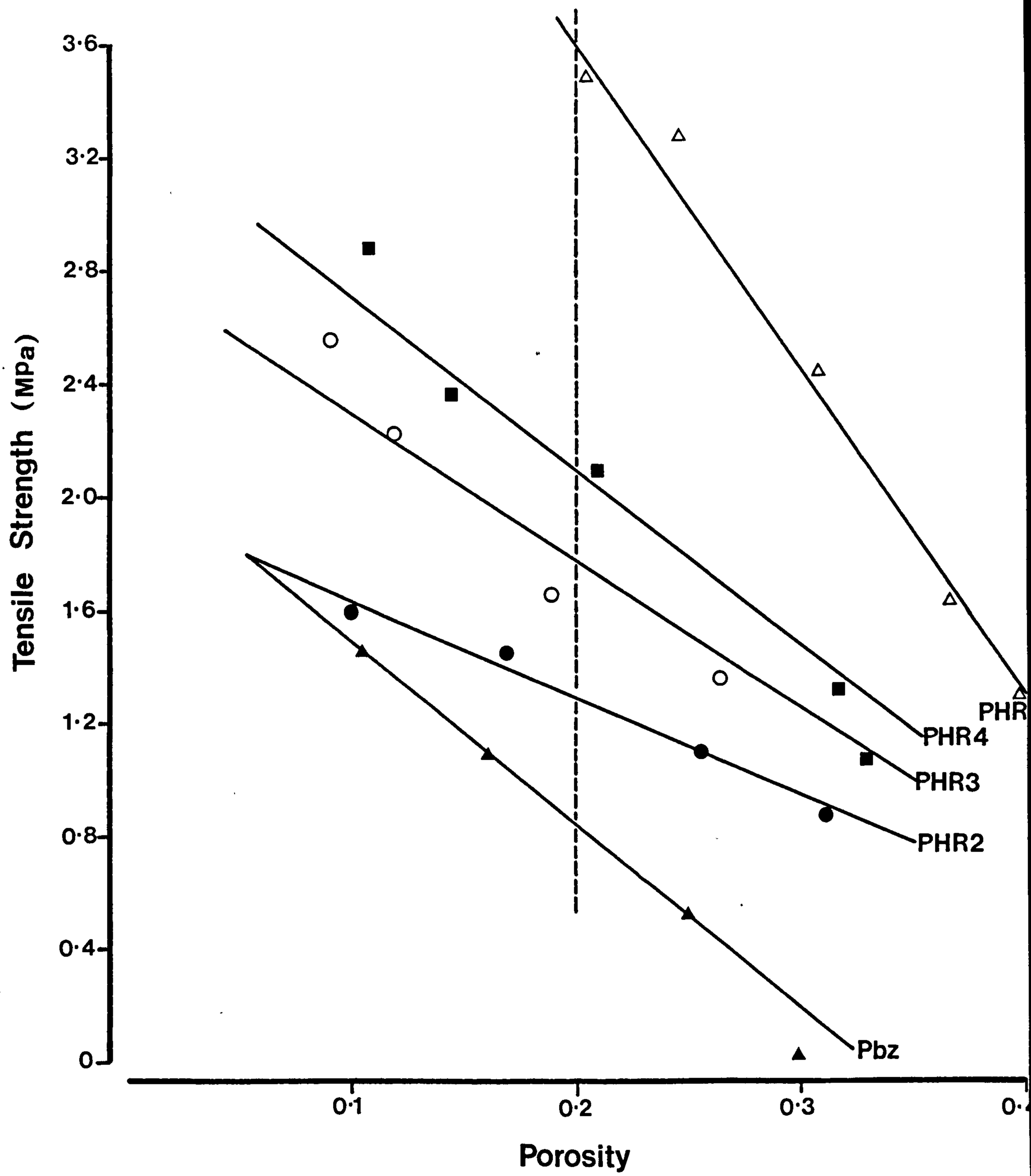

Fig. 7.7

The relation between porosity and tensile strength for samples of phenylbutazone as supplied and samples prepared by crystallising from solutions containing different concentrations of H.P.M.C.

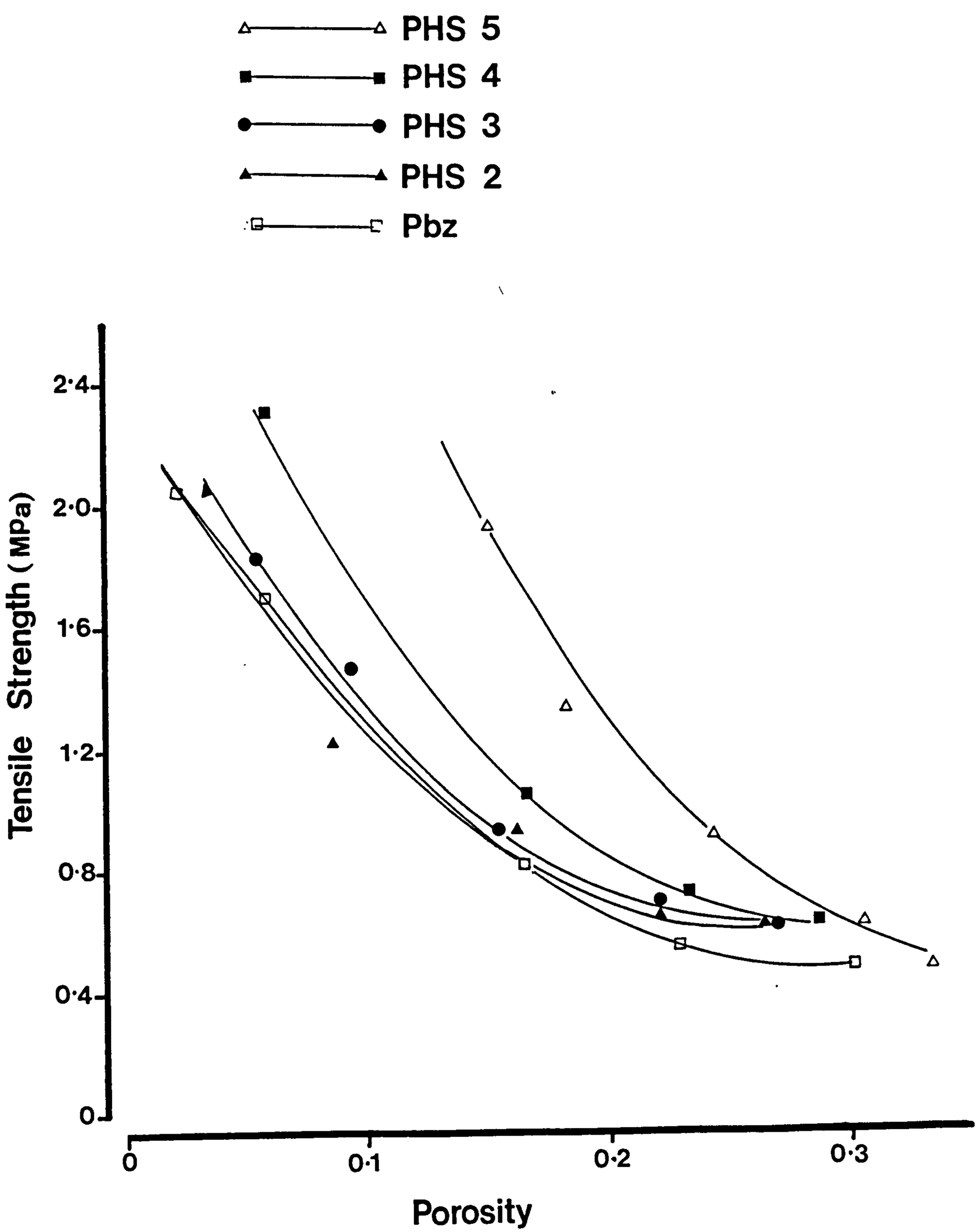

Fig. 7.8 The relationship between tensile strength and porosity for phenylbutazone spray dried alone and for samples spray dried to contain different concentrations of H.P.M.C.

Fig. 7.9

The relationship between tensile strength and percentage of additive for samples of phenylbutazone prepared by crystallisation and spray drying at porosity 0.2.

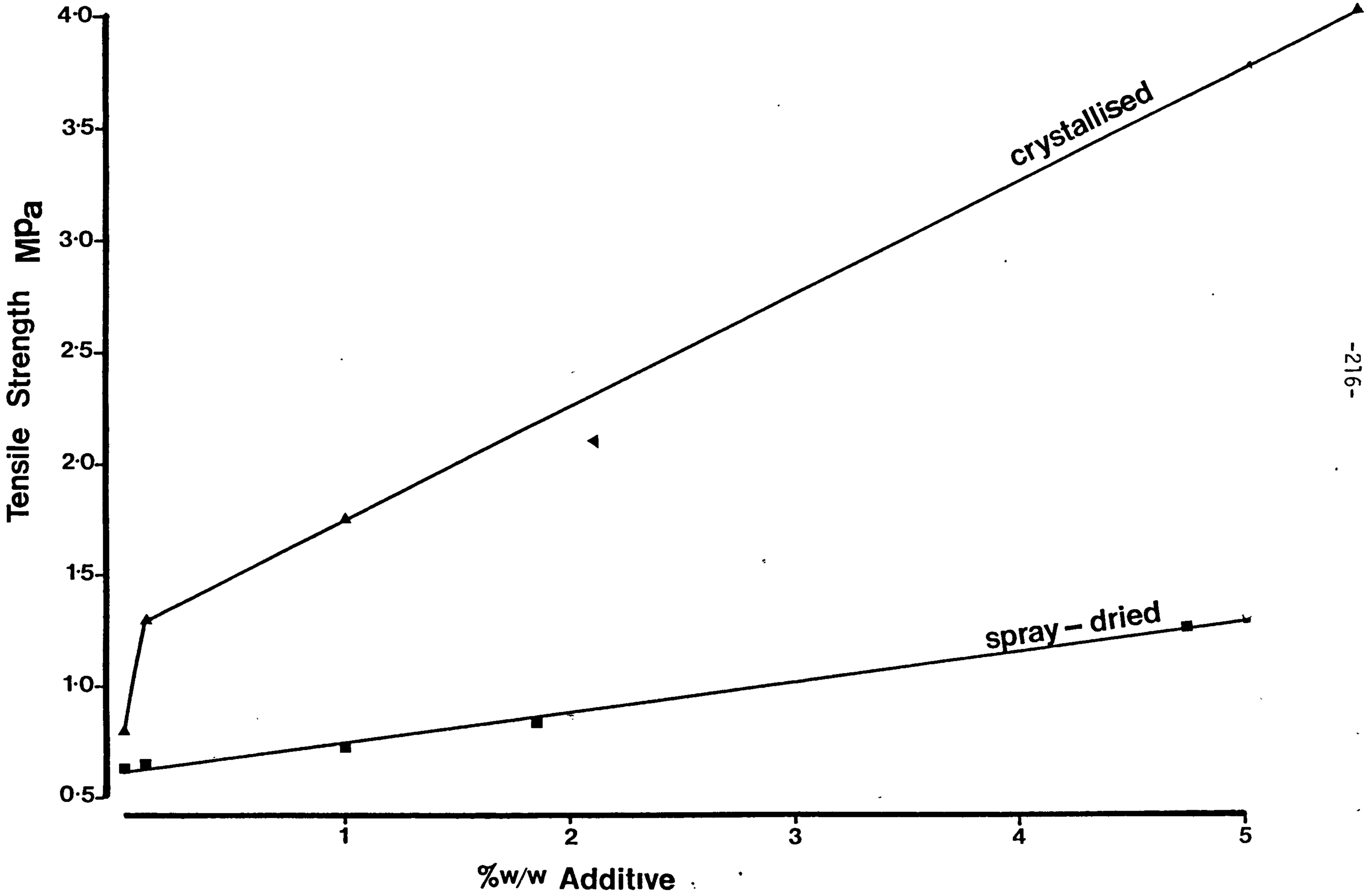

the primary causative feature has not been isolated, but such a study would be worthy of further investigations.

7.4 Conclusion

1. The compressional behaviour of crystallised and spray-dried phenylbutazone alone and phenylbutazone containing known concentration of H.P.M.C. have been studied using Heckel equation analysis, force transmission and tablet tensile strength data.

2. The yield pressure for crystallised samples with different concentrations of H.P.M.C. were similar (mean 147.02 MPa) Spray_dried samples with different levels of H.P.M.C. gave similar yield pressures but exhibited a lower mean value (mean 93.5 MPa) than crystallised samples. The difference in mean values is thought primarily to be due to polymorphic and particulate differences between spray dried and crystallised samples.

3. Force transmission was similar for both spray_dried and crystallised materials. Ratios of $\frac{FL}{Fu}$ rose from 0.65 to 0.81 at a fixed porosity % with increasing H.P.M.C. concentration indicating that the presence of H.P.M.C. reduced die_wall friction.

4. Data for tablet tensile strength at fixed porosity showed that compacts prepared from crystallised samples were generally 3 times higher than for tablets prepared from spray_dried materials. The primary cause of this effect has not been isolated but can be attributed to a number of factors including crystallographic, shape, morphology and polymer distribution differences between the materials.

CHAPTER 8

CHAPTER 8.1 General Discussion

Drug bioavailability is controlled to a greater or lesser extent by the dissolution rate of the drug. For example, for those drugs where the dissolution rate is the rate determining step in absorption, bioavailability can be improved by increasing dissolution rate. Techniques for increasing the dissolution rate include changing the crystal shape, size and structure, or lowering the powder interfacial tension by the incorporation of hydrophilic materials or surface active agents. In this work an attempt to increase the dissolution rate of a model sparingly soluble drug, phenylbutazone by changing the crystalline state as well as incorporating hydrophilic polymer and surfactant by conventional crystallisation and spray drying is reported. The effects of incorporation on the physicochemical properties and stability of the drug as well as the powder behaviour when tableted have been examined.

The study of the polymorphism of phenylbutazone in this work revealed three polymorphic forms. The stable δ form (after Muller (1978) nomination) which is the commercially available phenylbutazone powder, exhibited a single endothermic peak at 107°C on D.S.C. analysis which is in general agreement with the literature figures (Matsuda 1976; Ibrahim 1977; Muller 1978; Tuladhar 1983). The second polymorphic form isolated was the β metastable polymorph which could be obtained by recrystallising from n-heptane. The D.S.C. thermogram showed an endotherm at 95°C, an exothermic peak on recrystallisation at 97°C, followed by a second melting endotherm at 107°C. The third identified polymorph, the α-form which was obtained by recrystallising from 2-propanol, gave an endotherm at 93°C, then recrystallises prior to remelting at 107°C.

The transition energy, obtained using the Kissenger equation (1957), of the β-polymorph to the stable δ form was found to be 796.3 KJ/mol. This is similar to the figure reported by Muller (1978) of 850 KJ/mol. The value is approximately five times higher than that calculated for sulphathiazole form I by Shami et al.(1972). This indicates that the β-polymorph of phenylbutazone was stable enough to perform the physicochemical studies.

The powder X-ray diffraction pattern of the original stable δ form exhibited three strong peaks at the regions of 2θ at 6.95, 8.1 and 20.9° which agrees closely with the figures reported by Muller (1978). For β polymorph movement of these peaks to values of 2θ of 8.6, 20.4 and 7° was associated with increase intensity (see Table 3.6). However, the third polymorph assigned α form was very unstable and could not be isolated for examination by X-ray diffraction.

The powder X-ray diffraction data were found to be useful in differentiating between the polymorphs, supporting the conclusions of Muller (1978). In contrast Ibrahim (1977) and Tuladhar (1983) used differences between I.r. spectra to identify polymorphs rather than X-ray diffraction data. In this work, only minor differences in I.r. traces are evidenced between samples. It is essential to use a combination of techniques, including X-ray diffraction, I.r. analysis and D.S.C., together with information from hot stage microscopy, dissolution and solubility experiments when identifying polymorphs.

Another useful indicator of the presence of polymorphism of a material can be the peaking effect in dynamic solubility studies for metastable forms. The peaking is attributed to the higher solubility levels of the metastable polymorph which, when in solution form can only exist in the stable form. Thus the solution is supersaturated with

respect to the solubility level of the stable polymorph and the solution re-equilibrates to a new lower solubility figure as a portion of the solute crystallises out of solution. Whilst several workers in this field have concentrated solely on equilibrium solubility data (Muller 1978, Ibrahim 1977) this study has shown the peaking solubility effect for the β-phenylbutazone polymorph (see Fig.3.8)

The intrinsic dissolution rate of the β and δ polymorphs was measured using constant surface area compressed discs. It was thought that during compression, a polymorphic transition might take place (Ibrahim 1977, Muller 1978). No transition of δ form to β form during compression was found and examination of a compressed tablet prepared from β polymorph sample (see Table 8.1& Fig.8.1) showed only minimal transition occurred during compression. At the upper surface of the tablet adjacent to the punch the transition to δ form was maximal (53 %) whilst at the surface exposed to the dissolution medium was only 5.3% . This observation is in agreement with that of Chan & Doelker(1984).

The dissolution rate for the β form showed a 2 fold increase compared with the δ form and this finding is consistent with the increases reported by other workers (Muller 1978; Ibrahim 1977; Matsuda 1983; Tuladhar 1983).

Whilst many workers have examined the effect of changing solvent on the polymorphism of phenylbutazone, attention should also be given to the crystallisation rate. This study has shown that the rate of crystallisation achieved by varying the spray drying conditions influences the number of polymorphs present in the samples. It has been found that the slower the crystallisation rate the more favourable the conditions for forming polymorphs, and the higher the number of

Fig. 8.1 D.S.C. endotherms for transition of phenylbutazone β polymorph after compression, at upper, middle and lower sections of the compact (heating rate 10°C/min, sample size 5-9 mg and under nitrogen flow)

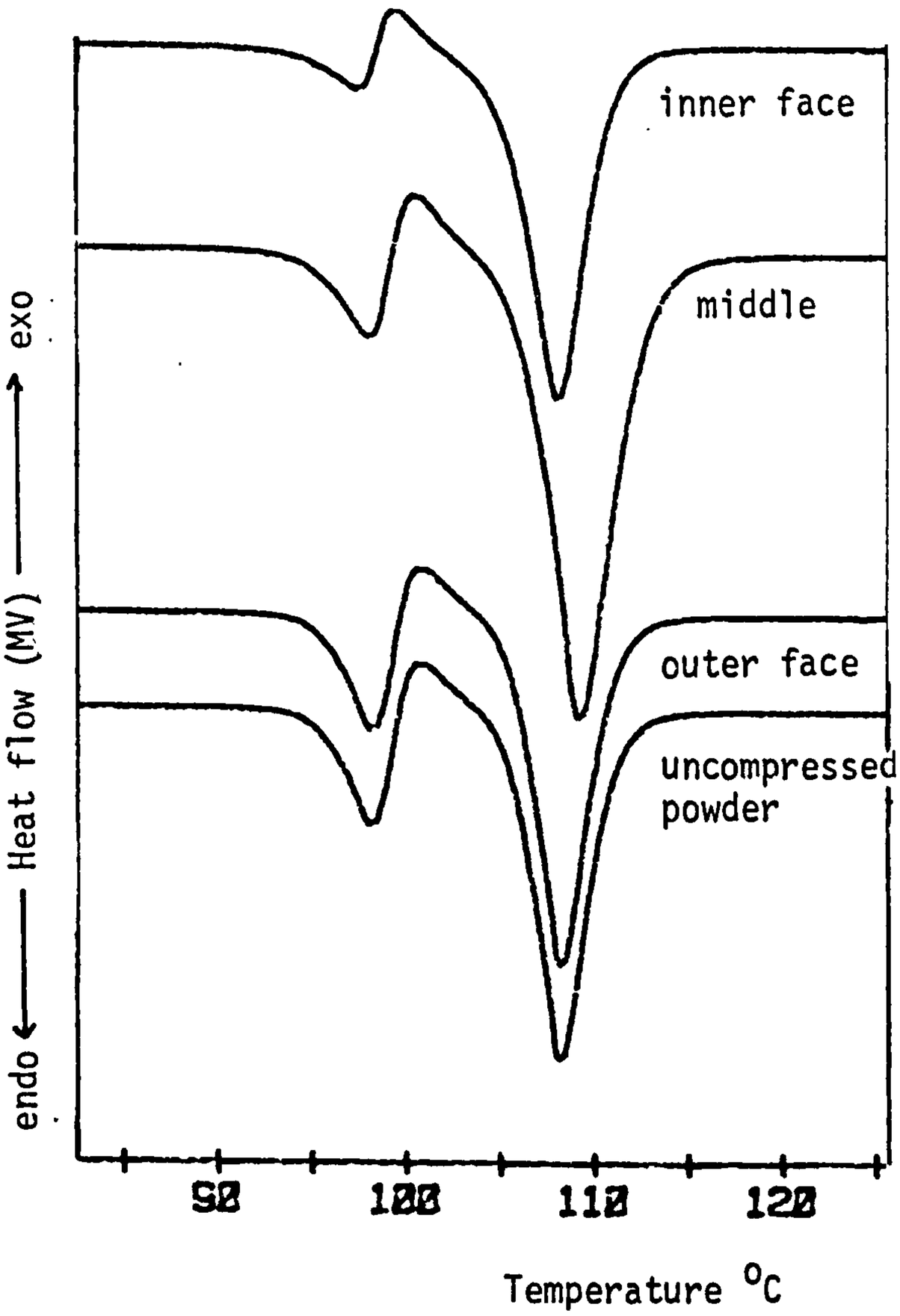

Table 8.1 The % of β polymorph of phenylbutazone transferred to δ form after compression measured by integrating the left β-peak and related to the uncompressed peak

Sample	% transferred	ΔH_f of the remaining β-polymorph endotherm Kj/hr
inner face	52.7%	4.42
middle	36.2%	5.86
outer face	5.3%	7.78
uncompressed powder	-	4.27

polymorphs formed. The D.S.C. thermograms for spray-dried samples of phenylbutazone showed that for the fastest crystallisation rate samples exhibited a single endothermic peak at 107°C which corresponds to the stable δ form thermogram, and showing that no metastable polymorph has been formed. As the crystallisation rate was reduced a small shoulder appeared on the 107°C endotherm, indicating the presence of an additional polymorph. Reducing the crystallisation rate further produced an additional endothermic peak at 95°C, corresponding to the β polymorph. When the rate of crystallisation was reduced further two extra peaks appeared at 95°C and 99°C in addition to the original peak at 107°C. The peak at 99°C may correspond to one of the additional polymorphic forms reported by Tuladhar et al. (1983).

Powder X-ray diffraction traces for these samples showed that for samples exhibiting a single endothermic peak, the trace was similar to that of stable δ form, whilst for samples with two endothermic peaks at 95°C and 107°C, the X-ray diffraction pattern was very similar to that obtained for the β polymorph. The X-ray traces for samples exhibiting three endothermic peaks at 95°C, 99°C and 107°C, were different from those obtained for β and δ polymorphs with extra peaks present.

Solubility testing revealed that the spray-dried samples gave peaking values prior to an equilibrium solubility value, a feature of polymorphic materials. The peaking value of solubility for the different samples increased with increasing number of endothermic peaks in the D.S.C. thermogram and increased with decreasing crystallisation rate. This finding supports the hypothesis that the number of polymorphs increases with decreasing crystallisation rate. The intrinsic

dissolution rate of the spray_dried samples increased in the same sequence, providing further support for the hypothesis. Thus this study has shown that crystallisation rate is a critically important factor in the formation of polymorphic forms.

Another technique which can be used to increase the dissolution rate of aqueous sparingly soluble drugs is to incorporate a hydrophilic polymer into the drug crystals. The way of introducing the polymer and the nature of the polymer is thought likely to produce different effects on both the crystallographic and physicochemical properties of the parent molecule. In this study two types of polymer, H.P.M.C. and poloxamers were introduced by conventional crystallisation and spray drying.

The D.S.C. thermograms of samples prepared by crystallisation to contain H.P.M.C. showed that the presence of H.P.M.C. produced an extra endotherm at 97°C. The area under the curve of this new peak increased with increasing H.P.M.C. concentration. The increase in the endothermic peak at 97°C was accompanied by a decrease in the original peak at 107°C, until at a limiting H.P.M.C. concentration of 2% w/w the original peak was completely absent. This finding raised the possibility that phenylbutazone forms a high energy complex with H.P.M.C. The high energy complex term was first used by Simonelli et al. (1976) to describe drug:polymer complexes which have lower melting point than the parent drug, and were not thought to be polymorphic forms.

Further evidence for complex formation rather than a polymorphic form is provided by the absence of an exothermic peak on the D.S.C. trace between the two endothermic peaks at 97°C and 107°C even when scanned at low heating rate i.e. 2°C/min, and also the absence of endotherm at 107°C at 2% w/w H.P.M.C. concentration and above. If a

polymorphic form had been produced, an exotherm between the two endotherms, particularly at low heating rates might be expected, and the endotherm at 107°C should be present as the metastable polymorph converts to the stable form after melting. In addition no peaking effect was observed on solubility testing, a feature of metastable polymorph solubility.

For samples containing the same concentration of H.P.M.C. prepared by spray drying under conditions which previously produced β polymorph, two endothermic peaks were observed - the first at 95°C, due to β polymorph and the second at 107°C corresponding to the stable form of phenylbutazone. An additional endothermic peak appeared at 99°C which increased in area with increasing H.P.M.C. concentration. This endothermic peak at 99°C is thought to be due to the presence of a complex formed between phenylbutazone and H.P.M.C. The shift in the position of the melting endotherm of the complex compared with the complex formed after conventional crystallisation might be due to differences in the preparation technique, crystallisation rate and time allowed for the complex to form.

The powder X-ray diffraction data showed that for all the samples containing H.P.M.C. and prepared by conventional crystallisation and spray drying were crystalline in character and not amorphous. The appearance of a new peak at 2θ of 18° was thought to be due to the complex formed between phenylbutazone and H.P.M.C. From the X-ray diffraction studies it was also concluded that the presence of H.P.M.C. in the crystallisation medium tend to inhibit the formation of metastable polymorphs. As the concentration of H.P.M.C. in spray-dried samples increased the area of the endotherm at 95°C which is due to the presence of β polymorph, was reduced.

The equilibrium solubility was slightly increased for samples prepared by conventional crystallisation and spray drying with optimal increase obtained for sample containing 2% w/w H.P.M.C. For samples prepared by crystallisation, no peaking solubility effect was noticed which, as mentioned previously, supports the conclusion that polymorphism in these samples is absent and that the peak at 97^{o}C was not due to the presence of a metastable polymorph. Whilst the samples prepared by spray drying showed a peaking effect, a feature which was expected since the samples contained β polymorph, the peaking value decreased with increasing amounts of H.P.M.C. added. This further supports the conclusion drawn from the D.S.C. studies that the presence of H.P.M.C. inhibited the formation of metastable polymorphs.

For both crystallised and spray-dried samples the dissolution rate increased with increasing amounts of H.P.M.C. added until the optimal concentration of 2% w/w H.P.M.C. level was reached. At 5% w/w H.P.M.C. concentration the dissolution decreased. The increase in dissolution rate is attributed to the formation of complexes between phenylbutazone and H.P.M.C. which exist at higher energy levels than the unchanged drug molecules. In addition the presence of hydrophilic polymer eased the wetting of phenylbutazone which may contribute in achieving higher dissolution rates. However at a certain level the effect was reversed. It is thought that above this concentration the H.P.M.C. altered significantly the viscosity in the diffusion layer and decreased the diffusion coefficient of the drug therefore reducing the dissolution rate (Florence et al. 1973, Braun & Parrott 1971).

The second polymer material introduced into the phenylbutazone crystals was the surfactant poloxamer 188. Similar procedures to those used to introduce H.P.M.C. were employed. All the samples prepared by conventional crystallisation exhibited a single endothermic peak at 107°C on the D.S.C. thermogram which is due to the stable δ form of phenylbutazone. A slight decrease in melting point with increasing the amount of poloxamer added, accompanied by a widening of the endothermic peak and decrease in the heat of fusion, was observed. These observations indicate that when added to the crystallisation medium poloxamer 188 did not initiate the formation of other polymorphic forms or any type of complexation with phenylbutazone. It is possible that the poloxamer 188 was either adsorbed physically to the surface of the phenylbutazone crystals and/or acted as impurities (Blain 1982) , forming a solid solution. The incorporated polymeric materials might also lead to additional crystal imperfection and defect.

For samples prepared by spray drying under conditions which previously gave β polymorph, two endothermic peaks at 95°C and 107°C were obtained on D.S.C. thermograms. The size of the endothermic peak at 95°C did not change with increased amounts of poloxamer added. This finding suggests that when poloxamer is added to the crystallisation medium polymorphic formation is neither induced or inhibited.

The powder X-ray diffraction data showed that all the samples prepared by crystallisation exhibited very similar X-ray patterns, similar to the original phenylbutazone pattern, apart from two additional peaks at the region of 2θ at 16.4 and 21.2. These peaks can be attributed to the presence of poloxamer, since the X-ray

diffraction of poloxamer 188 flakes alone gave two peaks at these positions. The samples prepared by spray drying showed similarities in the powder X-ray diffraction patterns, to the pattern exhibited by phenylbutazone spray dried alone (β-polymorphic form), apart from the appearance of one extra peak at the 2θ region at 16.4 due to the poloxamer 188. The second poloxamer peak at the region of 2θ at 21.2^{o} is thought to be masked and overlapped with the β peak in the same region of spectrum. The similarity in the X-ray pattern for samples containing poloxamer and those without poloxamer further supports the hypothesis that when added to the crystallisation medium poloxamer did not initiate or inhibit the formation of polymorphs, or complex with phenylbutazone.

There was no major change in the maximal solubility of the sample containing poloxamer. The solubility increased with increasing amounts of poloxamer added until a limiting effect was observed at 1% w/w level. This suggests that the increase in solubility was not due to micellisation, whilst other factors involved with increasing solubility such as improved solid surface wetting were thought likely to occur. The small increase in solubility, 1.3 folds, was similar for samples prepared by crystallisation and spray drying. The only difference between samples was a peaking solubility effect for spray dried materials. This was expected and attributed to the presence of β polymorph in spray-dried samples. However, it is interesting to note that the peaking value was the same for all the samples containing different amounts of poloxamer, an observation which confirms the suggestion that poloxamers do not inhibit the formation of polymorphs.

A marked increase in intrinsic dissolution rate of more than 3 fold for samples prepared by crystallisation and spray drying was observed

with maximal increase obtained at 1% w/w poloxamer level. The increase in dissolution rate was attributed to lowering of interfacial tension at the solid-liquid interface and facilitated wetting of the powder. The limiting effect at 1% w/w poloxamer can be explained by the adsorption of poloxamer to phenylbutazone surfaces and addition of further poloxamer did not lead to further major effects on wetting and interfacial tension.

An attempt was made in Chapter 6 of this work to examine the chemical stability of selected samples. Phenylbutazone alone and samples containing H.P.M.C. and poloxamer 188 prepared both by crystallisation and spray drying were subjected to HPLC and D.S.C. testing using elevated temperatures. Phenylbutazone was found to be stable at all the testing temperatures during the period of testing.

The stability of phenylbutazone was affected by the type of polymer additive as well as the process of incorporating the polymer. Hydrolysis degradation occurred and degradation product α-carboxy-N-cabroyl-hydrazobenzene was spotted. Samples containing H.P.M.C. were more stable than samples containing poloxamer. This might be due to the nature of the drug and additive combination. For phenylbutazone:H.P.M.C. systems a complex was thought to form, possibly linked through hydrogen bonding and/or Van der Wal forces. On the other hand poloxamer appeared to also physically adsorb to the surface. Possibly the difference in type of associate between drug and polymer, reactivity of the polymer itself as well as the sensitivity of the drug:polymer system to water vapour may all be contributing factors causing observed difference in stability profiles between the products.

The chemical stability testing showed that phenylbutazone alone was stable during the testing period at all the temperatures examined (up to 50°C). In the presence of polymeric additive a chemical breakdown occurred. One degradation product, α-carboxy-N-cabroylhydrazobenzene, was detected and this product resulted from hydrolysing of phenylbutazone (see Fig.6.4). Pawlelzyk & Wachowiak (1969) found a similar hydrolysis of phenylbutazone for stored aqueous injection solutions. The samples were stable at 20°C in closed containers for three months. However, for open-stored samples at RH 40±5% traces of degradation were noticed, which increased in concentration with increasing temperature and time of incubation. No other breakdown products were detected.

The type of additive and way of preparing the samples affected the stability of the product as samples containing H.P.M.C. possessed smaller amounts of breakdown than samples containing poloxamer 188. One possible explanation is that poloxamer may have a higher affinity for water than H.P.M.C. which could lead to increased hydrolysis.

The samples prepared by conventional crystallisation showed less stability than samples prepared by spray drying for both H.P.M.C. and poloxamer containing samples. Differences in preparation conditions thus affect stability and may be attributed either to the β polymorphic form present in the spray-dried samples being inherently more stable to hydrolysis than the δ form in the conventionally crystallised samples, which seems unlikely, or that the conventionally prepared crystals, unlike the spray-dried samples, retain trace amounts of water which initiate a hydrolysis reaction.

The Heckel plot for compressed samples of phenylbutazone containing H.P.M.C. prepared by spray drying and crystallisation showed that the samples

prepared by the same technique and containing up to 5% w/w H.P.M.C. showed similarity in their yield pressure, indicating that adding H.P.M.C. up to this level has not affected the yield pressure material constant. There is however a downward displacement of the curves with increasing H.P.M.C. concentration. This displacement is attributed to increasing cohesiveness of the powder as only minor differences in particle size and shape existed between the samples.

The crystallographic nature and preparation conditions of the powder affected the yield pressure with the conventionally crystallised phenylbutazone exhibiting higher yield pressure than the spray-dried samples. This effect was attributed primarily to the fact that spray-dried samples were β-metastable form of phenylbutazone which because of their higher energy level would be expected to deform plastically at lower pressure than the stable δ form as obtained during conventional crystallisation. In addition the difference in crystal shape and size between samples series as the spherical spray-dried material would require lower pressure to cause particle rearrangement to fill the interparticulate spaces while the crystallised samples were needle-like and thereby likely to exhibit larger frictional forces between particles with higher bed voidage, and so higher pressure would be required to cause rearrangement and subsequent particle deformation.

The force transmission to the lower punch during compression increased with increasing H.P.M.C. concentration in sample due to decreased die-wall and interparticle friction. Crystallographic nature did not seem to affect force transmission as the spray-dried and crystallised samples gave similar results.

The increase in tablet tensile strength with increasing H.P.M.C. concentration for samples prepared by conventional crystallisation and spray drying was attributed to increasing particle cohesiveness and the increasing amounts of a plastically deforming polymeric material. The approximately three-fold increase in tensile strength generally observed for samples prepared by crystallisation compared with tablets prepared from spray-dried samples, was attributed to the difference in crystallographic nature of the samples. The crystallised samples consisted of the stable δ form and/or complex, while the spray-dried samples consisted mainly of the β-metastable polymorphic form. The tensile strength of compact of any material is a function of the area of contact between the particles, and the strength of the bond produced between them (Summers 1977), and as the metastable polymorphic form possess higher potential energy and weaker bonding (Burger 1951), the strength of particle-particle bond will be less for the metastable polymorphic form than the stable form. Also difference in the distribution pattern of H.P.M.C. within the spray-dried and crystallised materials may play a role.

8.2 Conclusions

1. The polymorphism of phenylbutazone was examined and α, β and δ forms (after Muller (1978) nomination) were identified using a combination of analytical techniques.

2. A study on the effect of the operating variables of the Büchi mini-spray dryer showed that all the four variables examined contribute to the efficiency of performance and the particle size of product.

3. Analysis of spray-dried phenylbutazone products revealed that the slower the crystallisation rate, the higher the number of polymorphs formed indicating that slower crystallisation rates favour polymorphic formation.

4. For samples of phenylbutazone containing up to 5% w/w H.P.M.C. incorporated by conventional crystallisation, a higher energy complex was formed which melted 10^{o} lower than the parent drug. The complex containing 2% w/w H.P.M.C. exhibited a 2-fold increase in intrinsic dissolution rates compared with phenylbutazone.

5. When H.P.M.C. was incorporated into phenylbutazone by spray drying a similar level of increase in intrinsic dissolution rate for samples containing 2% w/w H.P.M.C. was observed. The presence of H.P.M.C. appeared to inhibit the formation of β polymorph.

6. Incorporating poloxamer 188 into phenylbutazone increased the intrinsic dissolution rate. This increase was thought to be due to facilitated powder surface wetting due to lowering interfacial tension and not due to micellisation as the increase in solubility was not found to be continuous with increasing poloxamer content. Unlike H.P.M.C. the poloxamer does not form any complex with phenylbutazone.

7. Addition of poloxamer 188 by spray drying using the same conditions gave similar increases in intrinsic dissolution rate compared with crystallised samples. The presence of surfactant did not interfere with polymorphic formation during spray drying.

8. Stability testing of selected products containing polymeric additives showed that phenylbutazone alone was stable during the period of testing at all temperatures up to 50°C. The hydrolysis product No. II (α-carboxy-n-caproyl-hydrazobenzene) was detected in several samples and the degree of decomposition was found to be affected by the type of additive and the technique of incorporation.

9. The yield pressure of materials, determined from Heckel plot analysis, exhibited only minor changes when up to 5% w/w HPMC was incorporated into phenylbutazone, for either conventionally crystallised or spray-dried samples, although the value for spray-dried samples (93.5 MP_a) was lower than that for conventionally crystallised product (147.02 MP_a).

10. The force transmission ratio on compression was similar for both crystallised and spray-dried phenylbutazone samples containing H.P.M.C. The ratio increased with increasing H.P.M.C. concentrations.

11. The tensile strength of tablets obtained from samples prepared by conventional crystallisation was found in general to be three times larger than for tablets prepared from spray-dried products.

8.3. Suggestions for future work

The work in this thesis has dealt with the physicochemical properties of the drug phenylbutazone after changing its crystalline state and also after adding hydrophilic polymers. Increases in *in vitro* dissolution rate were observed. An *in vivo* study to establish whether the *in vitro* increases were observed biologically would give an opportunity of establishing possible *in vitro/in vivo* correlations and developing predictive relationships for the *in vivo* performance of these and similar systems.

Since there is a general interest in retarding dissolution to achieve controlled release preparations, using the same principle developed in this work, a study of the effect of adding hydrophobic polymer to hydrophilic drugs would be worthy of examination.

The degree of disruption occurring in crystals resulting from the incorporation of low level additives has recently been described by a dimensionless parameter - the disruption index (York & Grant 1985) obtained from entropy data. Initial analysis of latent heat of fusion data for phenylbutazone:poloxamer 188 system prepared by conventional crystallisation has revealed that the surfactant acts as a major disrupter of the crystals (Al Meshal *et al.* 1985). Further work examining the disruptive effects of different materials including other polymers together with a study of the sites of location of the additives would provide useful information concerning their thermodynamic and solid-state character and may provide ainsight into potential series of batch variation in these materials.

This study which might involve additional analytical techniques,such as solid-state NMR, would enable the nature of the interaction between host and additive molecules to be explored further.

Whilst interesting differences between the compressional behaviour of prepared samples have been demonstrated in this work, a more vigorous examination of the effect of additive on the elasticity, plasticity and other aspects of tableting of the material and product performance using more elaborate instrumented tableting equipment is required.

REFERENCES

Abdul-Rahman, Y.A.K. & Crosby, E.J.,
Chem.Eng.Sci., 1973, 28, 1273.

Al-Meshal, M., York, P. & Grant, D.J.W.,
British Pharmaceutical Conference, Leeds, 1985.

Aguiar, A.J., Krc, J.R., Kinkel, A.W. & Samyn, J.C.,
J.Pharm.Sci., 1967, 56, 847.

Aguiar, A.J. & Zelmer, J. J.Pharm.Sci., 1969, 58, 983.

Alam, A.S. & Parrott, E.L. J.Pharm.Sci., 1971, 60, 263.

Anastasiadou, C., Henry, S., Legendre, B., Souleau, C. &
Duchene, D. British Pharmaceutical Conference, London,
April, 1982.

Atkinson, R.M., Bedford, C., Child, K.J. & Tomich, E.G.,
Antibiot.Chemother., 1962, 12, 232.

Attwood, D. & Florence, A.T. in "Surfactant System",
Chapman & Hill Ltd. London. 1st Ed., 1983.

Awang, D.V.C. & Vincent, A. J.Pharm.Sci., 1976, 65, 68.

Awang, D.V.C., Vincent, A. & Matsui, F. J.Pharm.Sci., 1973,
62, 1673.

Awe, W. & Kiernert, H.J. Pharm.Act.Helv., 1963, 38, 805.

Banerjee, S., Bandyopadhyay, A., Bhattachrjee, R., Mukherjee, A.
& Halder, A. J.Pharm.Sci., 1971, 60, 153.

Barrett, D. & Fell, J.T. J.Pharm.Sci., 1975, 64, 335.

Bates, J.R. J.Pharm.Pharmacol., 1969, 21, 710.

Bates, T.R., Gibaldi, M. & Kanig, J. Nature, 1966, 210, 1331.

Becher, P.J. Phys.Chem., 1959, 63, 1615.

Beckstead, H.D., Kaistha, K.K. & Smith, S.J. J.Pharm.Sci., 1968, 57, 1952.

Bell, W.E. J.Phys.Chem., 1959, 63, 299.

Bergman, L.A. & Bandelin, F.J. J.Pharm.Sci., 1965, 54, 1796.

Bites, J.A. J.Pharm.Sci., 1963, 52, 1066.

Blaine. DuPont Publications, 1982.

Braun, R.T. & Parrott, E.L. J.Pharm.Sci., 1972, 61, 175.

Bradley, D. J.Phys.D.Appl.Phys., 1973, 6, 1724.

Bradley, D. J.Phys.D.Appl.Phys., 1973, 6, 2267.

British Pharmacopoeia, 1980.

Brockeden, W. British Pat 9973, 1843.

Burger, M.J.in"Phase transformations in solids",Simoluchowiske, R., Mayer, J.E. & Welly, W.A., Ed., Wiley, New York, 1951.

Burlinson, H. & Pickering, C. J.Pharm.Pharmacol., 1950, 2, 630.

Carless, J.E., Moustafa, M.A. & Rapson, H.D.C. J.Pharm.Pharmacol., 1966, 18 suppl., 190S.

Carless, J.E. & Sheak, A. J.Pharm.Pharmacol., 1976, 28, 17.

Carless, J.E. & Leigh,S. J.Pharm.Pharmacol., 1974, 26, 289.

Carstensen, J.T. in "Solid Pharmaceutics mechanical properties and rate phenomena". 1st Ed., Academic Press, New York, 1980.

Carstensen, J.T. & Toure, P. Powder Technol., 1980, 26, 199.

Carstensen, J.T., Marty, J.P., Puisieux, F. & Fessi, H. J.Pharm.Sci., 1981, 70, 222.

Chan, H. & Doelker, E. Proc. 4th Pharm.Tech.Conf., Edinburgh, Scotland, 1984.

Charlesworth, D.M. & Marshal, W.R. Amer.Inst.Chem.Eng.J., 1960, 6, 9.

Chiou, W.L. & Riegelman, S. J.Pharm.Sci., 1971, 60, 1281.

Chiou, W.L., Chen, S.J. & Athanikar, N. J.Pharm.Sci., 1976, 65, 1702.

Chiou, W.L. & Niazi, S.J. J.Pharm.Sci., 1971, 60, 1333.

Chiou, W.L. & Riegelman, S. J.Pharm.Sci., 1969, 58, 1505.

Chopra, K.S. & Dhall, V.K. J.Pharm.Pharmacol., 1981, 25, 39.

Chow, K.Y., Go, J., Mehdizadeh, M. & Grant, D.J.W. Int.J.Pharm., 1984, 20, 3.

Clements, J. & Poli, S. Can.J.Pharm.Sci., 1973, 8, 88.

Cole, E.T., Rees, J.E. & Hersey, J.A. Pharm.Acta.Helv., 1975, 50, 28.

Collet, J.H. & Tobin, E.A. J.Pharm.Pharmacol., 1977, 29, 19p.

Cooper, A.R. & Eaton, L.E. J.Amer.Cerm.Soc., 1962, 45, 97.

Corrigan, O.I., Sabra, K. & Holohan, E.H. British Pharmaceutical Technology Conference, April 20-22, London, 1982.

David, S.J. & Ausburger, L.L. J.Pharm.Sci., 1977, 66, 155.

De Boer, A.H., Bolhuis, G.K. & Lerk, C.F. Powder Technol., 1978, 20, 75.

Dillert, L.W. in "American Pharmacy" J.B. Lippincott Ed .., Philadelphia, (7th Edn), 1974.

Dombrowski, N. & Liod, T.L. Chem.Eng.Sci., 1974, 8, 63.

Dombrowski, N. & Munday in "Biochemical and Biological Engineering Science". Blakebrough, N., Ed, Vol 2, London, Academic Press, 1968.

Dutton, J. U.S. Pat., 163, 488, 1376.

Duvaill, R.N., Koshy, K.T. & Dashiell, R.E. J.Pharm.Sci., 1965, 54, 1196.

Dwiggins, G.W., Bolen, R.J. & Dunning, H.N. J.Phys.Chem., 1960, 64, 1174.

El Banna, H.M., Abd-El Fattah, S. & Daabis, N. Pharmazie, 1974, 29, 396.

Elworthy, P.H. & Lipscomb, F.J. J.Pharm.Sci., 1968, 20, 923.

Esezobo, S. & Pilpel, N. J.Pharm.Pharmacol., 1977, 29, 75.

Ewe, G.E. J.Amer.Pharm.Ass., 1934, 23, 1205.

Fabre, H., Mandrou, B. & Eddine, H. J.Pharm.Sci., 1982, 71, 120.

Fairbrother, J.E. & Grant, D.J.W. J.Pharm.Pharmacol., 1978, 30 Suppl. 19p.

Fairbrother, J.E. & Grant, D.J.W. J.Pharm.Pharmacol., 1979, 31 Suppl. 27p.

Fell, J.T. & Newton, J.M. J.Pharm.Sci., 1970, 59, 688.

Fell, J.T. & Newton, T.M. J.Pharm.Sci., 1971, 60, 1429.

Finholt, P. & Solvang, S. J.Pharm.Sci., 1968, 57, 1322.

Florence, A.T. & Attwood, D. in "Physicochemical principles of pharmacy". Macmillan Press Ltd., London. 1st Edn., 1981.

Florence, A.T., Elworthy, P.H. & Rahman, A. J.Pharm.Pharmacol., 1973, 25, 779.

Ford, J.L. & Rubinstein, M.H. Acta Pharm.Helv., 1979, 54, 353.

Frazer, R.P., Dombrowski, N. & Routley, J. Chem.Eng.Sci., 1963, 18, 315.

Friendman, S.J., Gluckert, F.A. & Marshal, W.R. J.Chem.Eng.Progr., 1952, 48, 181.

Fuher, C. Dtsch.Apoth.Ztg., 1962, 102, 827.

Gibaldi, M., Feldman, S. & Bates, T.R. J.Pharm.Sci., 1968, 57, 708.

Goldberg, A.H., Gibaldi, M. & Kanig, J.L. J.Pharm.Sci., 1966, 55, 482.

Goodhar, F.W., Mayorga, G., Mills, M.N. & Ninger, F.C. J.Pharm.Sci., 1968, 57, 1770.

Gouda, M.W., Ebiah, A.R., Moustafa, M.A. & Khalil, S.A. Drug Dev.Ind.Pharm., 1977, 3, 273.

Guillory, J.K. J.Pharm.Sci., 1967, 56, 72.

Haleblian, J. J.Pharm.Sci., 1975, 64, 1269.

Halbelian, J. & McCek, T. J.Amer.Pharm.Ass.Sci., Ed. 1960, 49, 245.

Hamlin, W.E., Nelson, E., Ballard, B.E. & Wagner, J.G. J.Pharm.Sci., 1962, 51, 432.

Hartshorne, N.H. & Stuart, A. "Crystals and the polarising microscope". Edward Arnold Publishers Ltd., 4th Edn., London, 1960.

Heckel, R.W. Trans.Metal.Soc. A.I.M.E., 1961a, 221, 671.

Heckel, R.W. Trans.Metal.Soc. A.I.M.E., 1961b, 221, 1001.

Hersey, J.A., Cole, E.T. & Rees, J.E. Pro.1st.Int.Conf. on the compaction and consolidation of particulate matter, Brighton, 1972.

Hersey, J.A. & Rees, J.E. Nature Phys.Sci., 1971, 230, 96.

Hersey, J.A., Bayraktar, G. & Shotton, E. J.Pharm.Pharmacol., 1967, 19, Suppl. 245.

Hersey, J.A. & Rees, J.E. Particle size analysis Conf., 1970, I.

Hiestand, E.W., Wells, E., Peot, C.B. & Ochs, J.F. J.Pharm.Sci., 1977, 66, 510.

Higuchi, T., Nelson, E. & Busse, L.W. J.Pharm.Sci., 1954, 43, 344.

Higuchi, T., Shimamoto, T., Eriksen, S.P. & Yashiki, T. J.Pharm.Sci., 1965, 54, 111.

Hine, J. Physical organic chemistry. McGraw-Hill, New York, 1962.

Ho, T. & Hersey, J.A. J.Pharm.Pharmacol., 1980, 32, 160.

Hoelgaard, A. & Møller, N. Arch.Pharm.Chem.Sci. Ed., 1975 3, 65.

Horhota, S.T., Burgio, J., Lonski, L. & Rhodes, C.T. J.Pharm.Sci., 1976, 65, 1746.

Ibrahim, H.G., Pisasso, F. & Bruno, A. J.Pharm.Sci., 1977, 66, 669.

Kata, M.H. Ph.D. Thesis, Bradford University, 1974.

Katta, S. & Gauvin, H.W. Amer.Inst.Chem.Eng.J., 1975, 21, 143.

Kawashima, Y., Lin, S.Y., Ueda, M., Takenaka, H. & Ando, Y. J.Pharm.Sci., 1983, 72, 514.

Kawashima, Y., Lin, S.Y. & Takenaka, H. Drug Dev. & Indust. Pharmacy, 1983, 9, 1445.

Kawashima, Y., Saito, M. & Takenaka, H. J.Pharm.Pharmacol., 1975, 27, 1.

Kawashima, Y., Takenaka, T. J.Pharm.Sci., 1974, 63, 1546.

Kawakita, K. & Ludde, K.H. Powder Technol., 1970/71, 4, 61.

Kellaway, I.W. & Najib, N.M. Int.J.Pharm.Tech. & Prod.Mfr., 1983, 4, 37.

Kissinger, H.F. Analyt.Chem., 1957, 29, 1702.

Knoechel, E.L., Sperry, C.C., Ross, H.E. & Lintner, C.J. J.Pharm.Sci., 1967, 56, 109.

Krycer, L., Pope, I. & Hersey, J.A. Drug Dev. & Ind.Pharm., 1982, 8, 307.

Kuhnert-Brandstatter, M. "Thermomicroscopy in the analysis of pharmaceuticals". Pergamon Press, Oxford, England, 1971.

Kurup, T.R.R. & Pilpel, N. Powder Technol., 1978, 19, 147.

Kurabyasi, T. Japan Soc.Mech.Eng.Bulletin, 1960, 3, 352.

Lachman, L., Lieberman, H.A., Kanig, J.L. in "The theory and practice of industrial pharmacy" 2nd Edn. Lea & Febiger, Philadelphia, 1970.

Lausier, J.M., Chiang, C.W., Zompa, H.A. & Rhodes C.T. J.Pharm.Sci., 1977, 66, 1636.

Leigh, S., Carless, J.E. & Burt, B.W. J.Pharm.Sci., 1967, 56, 888.

Levy, G. Lancet, 1962, 2, 723.

Levy, G. & Gumtow, R.H. J.Pharm.Sci., 1963, 52, 1139.

Lewis, C.J. & Shotton, E. J.Pharm.Pharmacol., 1965, Suppl. 17, 82S.

Long, W.M. Powder metallurgy, 1960, 6, 73.

Malone, M.H., Hochman, H.I. & Nieforth, K.A. J.Pharm.Sci., 1966, 55, 972.

Mankowich, A.M. J.Phys.Chem., 1954, 58, 1028.

Marshal, W.R. Chem.Eng.Prog. Monograph Series, 1954, No. 2, Vol. 50.

Martin, A.N., Swarbrick, J. & Cammarata, A. "Physical pharmacy". Lea & Febiger, Philadelphia, 2nd Edn. 1973.

Master, K. "Spray drying Handbook" 3rd Edn. Gorge Godwin, Great Britain, 1979.

Matsuda, Y., Kawaguchi, S., Usuki, K. & Eguchi, N. Yakugaku Zasshi (Jap), 1982, 102, 76.

Matsuda, Y., Kawaguchi, S., Kobayashi, H. & Nishijo, J. J.Pharm.Sci., 1984, 73, 173.

Matsui, F., Robertson, D.L., Lafontaine, P., Kolasinski, H. & Lovering E.G. J.Pharm.Sci., 1978, 67, 646.

Matsunaga, J., Nambu, N. & Nagai, T. Chem.Pharm.Bull., 1976, 24, 1169.

Mattok, G.L., McGilveray, J.T. & Mainville, C.A., J.Pharm.Sci., 1971, 60, 561.

McFerren, P. U.S.Pat., 152, 666, 1874.

Mesley, R.J. & Clements, R.L. J.Pharm.Pharmacol., 1980, 20, 341.

Mesley, R.J., Clements, R.L., Flaherty, B. & Goodhead, K. J.Pharm.Pharmacol., 1968, 20, 329.

Mesley, R.J. & Houghton, E.E. J.Pharm.Pharmacol., 1967, 19, 295.

Moroney, M.J. in "Facts from figures". Penguin Books, London. 1980.

Moustafa, M.M., Ebian, A.R., Khalil, S.A. & Motawi, M.M. J.Pharm.Pharmacol., 1971, 23, 868.

Muller, B. Pharm.Acta,Helv., 1978, 53, 333.

Mullins, J. & Macek, T. J.Amer.Pharm.Ass.Sci. Ed. 1960, 49, 245.

Mullin, J.W. "Crystallisation", 2nd Edn. Dub. Butterworths, London, 1972.

Myersohn, M. & Gibaldi, M. J.Pharm.Sci., 1966, 55, 1323.

Naggar, V.F.B., El Gamal, S. & Shams El Deen, M. Sci.Pharma AZ, 1980, 48, 335.

Nelson, E. J.Am.Pharm.Ass.Sci. Ed. 1955, 44, 494.

Newton, J.M. "Manufacturing Chemist and Aerosol News", 1966, April.33.

Obiorah, B.A. & Shotton, E. J.Pharm.Pharmacol., 1976, 28, 629.

Okhamafe, O.A. Ph.D. Thesis, Bradford University, 1983.

Ondari, C.O., Prasad, V.K., Shah, V.P. & Rhodes, C.T. Pharm.Acta.Helv., 1984, 59, 149.

Paris, J., Duchene, D. & Puisieux, F. J.Powder & Bulk Solids Tech., 1977, I, 47.

Parrott, E.L. & Sharma, V.K. J.Pharm.Sci., 1967, 56, 1341.

Pawelczyk, E. & Wachowiak, R. Acta.Pol.Pharm., 1969, 26, 425.

Perrin, M. & Michel, P. Acta.Crystallogr., 1973, 1329, 253.

Perrin, M. & Michel, P. Acta.Crystallogr., 1973, 1329, 258.

Paronen, P. & Juslin, M. J.Pharm.Pharmacol., 1983, 35, 627.

Prasad, K., Luong, T.T., Florence, A.T., Paris, J., Vaution, C., Seiller, M. & Pusieux, F. J. of Colloid and Interface Science, 1979, 69, 225.

Rees, J.E. & Rue, P.J. Drug Dev.Ind.Pharm., 1978, 4, 131.

Rees, J.E. & Hersey, J.A. Pharm.Acta.Helv., 1972, 47, 235.

Rees, J.E. & Rue, P.J. J.Pharm.Pharmacol., 1977, 29, 37P.

Rees, J.E. & Collett, J.H. J.Pharm.Pharmacol., 1974, 26, 956.

Robinson, M.J., Raff, A.M. & Svedres, E.V. J.Amer.Pharm.Ass. Sci.Ed., 1961, 50, 57.

Ross, S. & Oliver, J.P. J.Phys.Chem., 1959, 63, 1671.

Rudnick, W.C., Hunter, A.R. & Holden, F.C. Master.Res.Stand., 1963, 3, 283.

Rue, P.J. & Rees, J.E. J.Pharm.Pharmacol., 1981, 30, 642.

Schmolka, I.R., Raymond, A.J. J.Amer.Oil Chem.Soc., 1965, 44, 1088.

Schott, H., Kwan, L.C. & Feldman, S. J.Pharm.Sci., 1982, 71, 1038.

Sekikawa, H., Naganuma, T., Fujiwara, J., Nakano, M. & Arita, T. Chem.Pharm.Bull., 1979, 27, 31.

Sekiguchi, K. & Obi, N. Chem.Pharm.Bull., 1961, 9, 866.

Shotton, E. & Ganderton, D. J.Pharm.Pharmacol., 1960, 12, 87T.

Shotton, E., Deer, J.J. & Ganderton, D. J.Pharm.Pharmacol., 1963, 15 Suppl., 106T.

Shotton, E. & Ganderton, D. J.Pharm.Pharmacol., 1961, 13 Suppl., 144T.

Shotton, E. & Obiorah, B.A. J.Pharm.Pharmacol., 1973, 25 Suppl., 37P.

Shotton, E. & Ganderton, D. J.Pharm.Pharmacol., 1960, 12 Suppl., 87T.

Shinid, R.W. Helv.Chem.Acta., 1970, 53, 2239.

Silver, L. & Rudman, R. J.Phys.Chem., 1970, 74, 3134.

Simonelli, A.P., Metha, S.C. & Higuchi, W.I. J.Pharm.Sci., 1976, 65, 355.

Simonelli, A.P., Metha, S.C. & Higuchi, W.I. J.Pharm.Sci., 1969, 58, 538.

Simonelli, A.P., Metha, S.C. & Higuchi, W.I. J.Pharm.Sci., 1970, 59, 1370.

Speiser, P., Merkle, H.P. & Schibler, L. Gov.Offen., 1973, 2, 428.

Stanley-Wood, N.G. in "Enlargement and compaction of particulate solids". Butterworth & Co. Edn., London, 1983.

Strickland, W.A. Drug Cosmet.Ind., 1959, 85, 318.

Strickland, W.A., Higuchi, T. & Busse, L.W. J.Amer.Pharm.Ass., 1960, 49, 35.

Summers, M.P., Carless, J. & Enever, R. J.Pharm.Pharmacol., 1970, 22, 615.

Summers, M.P., Enever, R. & Carless, J.E. J.Pharm.Sci., 1977, 66, 1172.

Swarbrick, J. J.Pharm.Sci., 1965, 54, 1229.

Tachibana, T. & Nakamura, A. Kolloid-Z Polymer, 1965, 203, 130.

Tate, W.R. Chem.Eng., 1965, 72, 157.

Takenaka, H., Kawashima, Y. & Lin, S.Y. J.Pharm.Sci., 1982, 71, 914.

Takenaka, H., Kawashima, Y. & Lin, S.Y. J.Pharm.Sci., 1981, 70, 1256.

Takenaka, H., Kawashima, Y. & Lin, S.Y. J.Pharm.Sci., 1980, 69, 1388.

Tawashi, R. Science, 1968, 160, 76.

Trivedi, J., Shell, J.W. & Biles, J.A. J.Amer.Pharm.Ass. Sci.Ed., 1959, 48, 583.

Tuladhar, M.D., Carless, J.E. & Summers, M.D. J.Pharm.Pharmacol., 1983, 35, 269.

Tusji, A., Miyamoto, E., Matsuda, M., Nishimura, K. & Yamana, T. J.Pharm.Sci., 1982, 71, 1313.

Tylor, P.W. & Wurster, D.E. J.Pharm.Sci., 1965, 54, 1654.

Varsano, J. & Lachman, L. J.Pharm.Sci., 1966, 55, 1128.

Verma, A.R. & Krishna, P. "Polymorphism and polytypism in crystals". Wiley, New York, 1966.

Voellmy, C., Speiser, P. & Soliva, M. J.Pharm.Sci., 1977, 66, 631.

Watson, J.R., Matsui, F., Lawrence, R.C. & McConnell, J. Chromta., 1973, 76, 141.

Weintraub, H. & Gibaldi, M. J.Pharm.Sci., 1969, 58, 1368.

Windheuser, J.J., Misra, J., Eriksen, S.P. & Higuchi, T. J.Pharm.Sci., 1963, 52, 767.

York, P. J.Pharm.Pharmacol., 1978, 30, 6.

York, P. & Pilpel, N. J.Pharm.Pharmacol., 1973, 25 Suppl., 1.

York, P. & Grant, D.J.W. Int.J.Pharm., 1985, 25, 57.

Symbols and Abbreviations

A	The area of the solvated tablet
A^1	Frequency factor
B.P.	British Pharmacopeia
C_s	Maximal solubility
C_o	The concentration of drug in solution at time t
CMC	Critical micell concentration
D	Tablet diameter
D.S.C	Differential scanning calorimetry
$\frac{dm}{dt}$	Rate of increase in amount of material in solution
E_a	Activation energy
E_a'	Activation energy of degradation
F_D	Die wall reaction as wall friction force
F_L	Force transmitted to the lower punch
F_R	Radical force
F_U	Force applied by upper punch
GLC	Gas liquid chromatography
HPLC	High pressure liquid chromatography
HPMC	Hydroxypropyl methylcellulose
hrs	Hours
ΔH_f	Enthalpy of fusion
ΔH_s	Enthalpy of solution
I.R.	Infra-red
K	Solubility product
$\dot{K}$	The rate constant of intrinsic dissolution
$\dot{K}$	Degradation rate
K_1	Yield pressure

KN	Kilo Newton
Lh^{-1}	Litre/hour
M	Amount of material in solution
m	meter
mins	Minutes
mV	Milli volt
n_1, n_2	Number of moles of the constituents 1 and 2
P	Load applied
PbZ	Phenylbutazone as supplied
PS	Phenylbutazone spray dried alone
PHR1	Phenylbutazone crystallised with 0.01% w/v HPMC
PHR2	Phenylbutazone crystallised with 0.1% w/v HPMC
PHR3	Phenylbutazone crystallised with 1% w/v HPMC
PHR4	Phenylbutazone crystallised with 2% w/v HPMC
PHR5	Phenylbutazone crystallised with 5% w/v HPMC
PHS1	Phenylbutazone spray dried with 0.01% w/w HPMC
PHS2	Phenylbutazone spray dried with 0.1% w/w HPMC
PHS3	Phenylbutazone spray dried with 1% w/w HPMC
PHS4	Phenylbutazone spray dried with 2% w/w HPMC
PHS5	Phenylbutazone spray dried with 5% w/w HPMC
PPR1	Phenylbutazone crystallised with 0.01% w/v poloxamer 188
PPR2	Phenylbutazone crystallised with 0.1% w/v poloxamer 188
PPR3	Phenylbutazone crystallised with 1% w/v poloxamer 188
PPR4	Phenylbutazone crystallised with 2% w/v poloxamer 188
PPR5	Phenylbutazone crystallised with 5% w/v poloxamer 188
PPS1	Phenylbutazone spray dried with 0.01% w/w poloxamer 188
PPS2	Phenylbutazone spray dried with 0.1% w/w poloxamer 188
PPS3	Phenylbutazone spray dried with 1% w/w poloxamer 188
PPS4	Phenylbutazone spray dried with 2% w/w poloxamer 188
PPS5	Phenylbutazone spray dried with 5% w/w poloxamer 188

PM	Mean compaction pressure
R	Universal gas constant
RH	Relative humidity
SEM	Scanning electron microscope
T	Absolute temperature
TLC	Thin layer chromatography
t	Time
t_1	Tablet thickness
Tr	Tablet tensile strength
V	Volume
USP	United States Pharmacopeia
UV	Ultra violet
X_1, X_2	Mole fraction of constituents 1 and 2
Ø	Heating rate
ρ_{F_0}	Initial powder packing fraction
ρ_{F_A}	Total powder packing
ρ_{F_B}	Packing fraction due to particle slippage

APPENDIX 1

Appendix 1 Table 1

Dissolution data for phenylbutazone as supplied without any treatment (pbz) at 37°C.

Experiment A			Experiment B		Average total amount of drug released (mg/600ml)
Time (min)	Absorbence at 264 nm	Concentration (mg/ml)	Absorbence at 264 nm	Concentration (mg/ml)	
30	0.04	0.00006	0.04	0.00007	4.0
60	0.07	0.00011	0.07	0.00011	7.0
90	0.12	0.00017	0.12	0.00017	10.0
120	0.14	0.00022	0.14	0.00022	13.0
150	0.18	0.00027	0.18	0.00027	16.0
180	0.20	0.00030	0.21	0.00032	18.0
210	0.25	0.00036	0.25	0.00036	21.5

Appendix 1 Table 2

Dissolution data for β-polymorph of Phenylbutazone prepared by Crystallisation at 37°C.

Experiment A			Experiment B		Average total amount of drug released (mg/600ml)
Time (min)	Absorbence at 264 nm	Concentration (mg/ml)	Absorbence at 264 nm	Concentration (mg/ml)	
30	0.07	0.00011	0.07	0.00010	6.6
60	0.14	0.00021	0.14	0.00021	12.6
90	0.20	0.00030	0.20	0.00030	18.0
120	0.28	0.00042	0.28	0.00042	25.2
150	0.33	0.00050	0.33	0.00050	30.0
180	0.39	0.00060	0.39	0.00060	36.0
210	0.44	0.00068	0.44	0.00068	40.8

Appendix 1 Table 3

Particle size analysis data of phenylbutazone spray dried under different spray drying conditions

Run No	Particle size in μm							$\leqslant N$	Arithmetic mean (μm)	$\frac{\leqslant nd^3}{\leqslant nd^2}$ (μm)
	1-9.9 μm	10-14	141-19.9	20-28.2	28.3-39.9	40-66.5	66.6-80			
1	24	35	50	90	95	78	10	382	30.59	45.99
2	18	45	65	120	110	40	15	413	31.76	44.06
3	20	42	68	126	102	34	18	410	20.18	44.86
4	54	76	68	58	40	26	28	350	24.38	52.99
5	36	28	36	26	10	6	2	144	17.78	38.44
6	21	40	42	48	58	38	12	259	28.32	47.96
7	36	48	36	24	14	-	-	158	15.33	23.86
8	48	62	42	28	22	6	2	210	17.08	35.68
9	68	78	71	44	30	26	27	344	23.04	53.92
10	69	43	56	35	62	26	15	306	23.84	48.52
11	21	11	20	22	12	15	9	110	27.04	54.04
12	28	25	14	29	26	28	4	154	26.28	47.06
13	37	23	55	28	21	9	8	181	21.28	46.78
14	38	49	23	52	43	25	13	243	25.4	48.94
15	21	19	24	20	45	43	27	199	35.30	56.70
16	40	35	49	50	47	32	43	296	30.8	55.88
17	59	73	58	47	41	19	6	303	20.25	41.80
18	91	105	142	128	42	16	-	524	18.12	29.80
19	21	30	53	85	93	75	-	357	29.63	42.31
20	18	36	51	111	30	7	-	253	21.58	29.49

Appendix 1 Table 3 continued

Run No	Particle size in µm							$\leq N$	Arithmetic mean (µm)	$\frac{\leq nd^3}{\leq nd^2}$ (µm)
	1-9.9	10-14	14.1-19.9	20-28.2	28.3-39.9	40-66.5	66.6-80			
21	37	31	40	52	36	25	29	250	28.69	55.77
22	62	71	88	67	19	10	60	323	18.24	38.59
23	49	73	108	92	25	3	-	350	17.67	25.35
24	63	91	108	92	24	4	-	382	16.99	25.54
25	53	61	42	105	31	-	-	292	18.14	25.30
26	62	121	175	40	3	-	-	401	14.46	18.24
27	145	252	279	20	-	-	-	696	12.88	15.93
28	84	151	152	55	15	2	-	459	14.72	21.86
29	61	100	119	82	58	18	-	438	19.26	32.02
30	227	240	114	6	-	-	-	587	10.37	14.19
31	65	113	93	35	-	-	-	306	13.41	17.74
32	81	98	102	97	27	4	-	409	16.60	25.67
33	67	106	143	91	10	-	-	417	15.75	20.89
34	70	66	105	116	8	-	-	365	16.42	20.9
35	75	100	156	110	10	-	-	451	16.00	21.08
36	26	42	76	41	6	-	-	191	16.32	21.21
37	71	76	74	50	6	2	-	279	14.47	23.01
38	40	51	86	112	15	-	-	304	18.04	23.15
39	48	74	92	68	12	4	-	298	16.60	25.36
40	66	85	166	134	2	-	-	453	16.48	20.60
41	18	21	38	35	21	6	-	139	20.62	32.20
42	25	27	36	52	20	2	-	162	19.15	27.68
43	27	18	38	58	28	8	-	177	21.32	32.48
44	35	55	80	51	19	-	-	240	16.46	23.44
45	49	37	63	85	11	-	-	245	17.06	23.08

Appendix 1 Table 4

Dissolution data for sample PS1 at 37°C.

Experiment A			Experiment B		Average total amount of drug released (mg/600ml)
Time (min)	Absorbence at 264 nm	Concentration (mg/ml)	Absorbence at 264 nm	Concentration (mg/ml)	
30	0.05	0.00007	0.05	0.00007	4.6
60	0.08	0.00011	0.08	0.00011	6.7
90	0.11	0.00016	0.11	0.00016	9.8
120	0.13	0.00019	0.13	0.00019	11.7
150	0.16	0.00024	0.16	0.00024	14.9
180	0.18	0.00027	0.18	0.00027	16.9
210	0.23	0.00034	0.23	0.00034	21.8

Appendix 1 Table 5

Dissolution data for sample PS2 at 37°C.

Experiment A			Experiment B		Average total amount of drug released (mg/600ml)
Time (min)	Absorbence at 264 nm	Concentration (mg/ml)	Absorbence at 264 nm	Concentration (mg/ml)	
30	0.08	0.00012	0.08	0.00012	6.0
60	0.10	0.00014	0.10	0.00014	9.5
90	0.13	0.00014	0.13	0.00019	13.6
120	0.16	0.00025	0.16	0.00025	16.8
150	0.20	0.00030	0.20	0.00030	20.0
180	0.23	0.00035	0.23	0.00035	22.1
210	0.28	0.00043	0.28	0.00043	24.6

Appendix 1 Table 6

Dissolution data for sample PS3 at 37°C.

Experiment A			Experiment B		Average total amount of drug released (mg/600mi)
Time (min)	Absorbence at 264 nm	Concentration (mg/ml)	Absorbence at 264 nm	Concentration (mg/ml)	
30	0.07	0.00010	0.08	0.00011	6.0
60	0.12	0.00018	0.13	0.00019	11.1
90	0.17	0.00025	0.17	0.00025	15.0
120	0.21	0.00031	0.22	0.00032	19.2
150	0.25	0.00038	0.25	0.00038	22.8
180	0.29	0.00045	0.29	0.00045	26.4
210	0.33	0.00050	0.33	0.00050	30.2

Appendix 1 Table 7

Dissolution data for sample PS4 at 37°C.

Experiment A			Experiment B		Average total amount of drug released (mg/600ml)
Time (min)	Absorbence at 264 nm	Concentration (mg/ml)	Absorbence at 264 nm	Concentration (mg/ml)	
30	0.07	0.0001	0.07	0.00010	6.0
60	0.13	0.00020	0.13	0.00020	12.0
90	0.17	0.00025	0.16	0.00024	14.8
120	0.22	0.00033	0.23	0.00035	20.4
150	0.26	0.00040	0.36	0.00040	24.0
180	0.31	0.00047	0.32	0.00048	28.5
210	0.37	0.00056	0.38	0.00058	34.2

Appendix 1 Table 8

Results of solubility experiments for samples of phenylbutazone as supplied (Pbz), and phenylbutazone. β-polymorph at 37°C.

Time (hrs)	(mg/100ml) Pbz			(mg/100ml) PS1			(mg/100ml) PS2			(mg/100ml) PS3			(mg/100ml) PS4			(mg/100ml) β-polymorph		
	Run 1	Run 2	Average	Run 1	Run 2	Average	Run 1	Run 2	Average	Run 1	Run 2	Average	Run 1	Run 2	Average	Run 1	Run 2	Average
1	310	310	310	440	440	440	480	480	480	500	480	490	550	550	550	390	390	390
2	320	320	320	470	450	460	500	500	500	560	540	550	580	560	570	500	500	500
4	345	355	350	500	480	490	535	525	530	610	610	610	625	635	630	570	570	570
8	370	360	365	450	450	450	490	470	480	525	535	530	500	500	500	525	535	530
24	380	380	380	400	400	400	425	435	430	450	450	450	450	450	450	430	410	420
48	380	380	380	390	390	390	395	393	394	404	395	400	410	400	405	380	380	380
72	380	380	380	390	390	390	390	390	390	400	400	400	405	405	405	380	380	380

Appendix 1 Table 9

The relationship between heating rate and peak maximum for heat transition (Kissinger relation) for phenlbutazone β -polymorph.

Heating Rate °/C min	Melting Point		Tm^2 (°K)	$\log \frac{\phi}{Tm^2}$	$\frac{1}{Tm}$
	Tm (°c)	Tm (°K)			
2	94.2	367.2	134835.8	- 4.8288	2.7233
5	95.3	368.3	135644.9	- 4.4330	2.7150
10	96.1	369.1	136234.8	- 4.1343	2.7090
15	96.4	369.4	136456.7	- 3.9600	2.7070
20	98.0	371.0	137641.0	- 3.8400	2.6950

Appendix 1 Table 10

Calibration of dial reading for aspiration rate of the Büchi Spray drier

Rate of Flow	200 L/hr			400 L/hr			600 L/hr		
Dial Reading	Meter reading A	B	Total volume of air (m^3/sec)	Meter reading A	B	Total volume of air (m^3/sec)	Meter reading A	B	Total volume of air (m^3/sec)
0	9.3	9.3	-	9.3	9.3	-	9.3	9.3	-
1	9.7	97	-	9.7	9.7	-	9.7	9.7	
2	10	10	-	10	10	-	10	10	-
3	10.3	10.3	0.008232	10.3	10.3	0.008232	10.3	10.3	0.008232
4	10.5	10.5	-	10.5	10.5	-	10.5	10.5	-
5	11	11	-	11	11	-	11	11	-
6	11.3	11.3	0.00903	11.3	11.3	0.00903	11.3	11.3	0.00903
7	11.6	11.6	-	11.6	11.6	-	11.6	11.6	-
8	12	12	-	12	12	-	12	12	-
9	12.3	12.3	-	12.3	12.3	-	12.3	12.3	-
10	12.6	12.6	-	12.6	12.6	-	12.6	12.6	-
11	13	13	-	13	13	-	13	13	-
12	13.3	13.3	0.0106	13.2	13.3	0.0106	13.3	13.3	0.0106
13	13.7	13.7	-	13.7	13.7	-	13.7	13.7	-
14	14.3	14.3	-	14.3	14.3	-	14.3	14.3	-
15	14.7	14.7	-	14.7	14.7	-	14.7	14.7	-
16	15	15	-	15	15	-	15	15	-
17	Above meter limits								

APPENDIX 2

Appendix 2 Table 1

Dissolution data for sample PHR1 at 37°C.

Experiment A			Experiment B		Average total amount of drug released (mg/600ml)
Time (min)	Absorbence at 264 nm	Concentration (mg/ml)	Absorbence at 264 nm	Concentration (mg/ml)	
30	0.09	0.00007	0.05	0.00006	4.0
60	0.10	0.00011	0.10	0.00011	7.0
90	0.11	0.00016	0.11	0.00016	10.0
120	0.18	0.00028	0.19	0.00029	16.8
150	0.22	0.00030	0.22	0.00030	18.0
180	0.25	0.00040	0.26	0.00041	24.6
210	0.32	0.00048	0.32	0.00048	28.0

Appendix 2 Table 2

Dissolution data for sample PHR2 at 37°C.

Experiment A			Experiment B		Average total amount of drug released (mg/600ml)
Time (min)	Absorbence at 264 nm	Concentration (mg/ml)	Absorbence at 264 nm	Concentration (mg/ml)	
30	0.06	0.00007	0.06	0.00007	4.2
60	0.10	0.00013	0.10	0.00013	7.8
90	0.15	0.00021	0.14	0.00019	11.76
120	0.18	0.00028	0.18	0.00028	16.6
150	0.22	0.00031	0.22	0.00031	18.6
180	0.26	0.00041	0.26	0.00041	24.15
210	0.32	0.00050	0.32	0.00050	30.0

Appenix 2 Table 3

Dissolution data for sample PHR3 at 37°C.

Experiment A			Experiment B		Average total amount of drug released (mg/600ml)
Time (min)	Absorbence at 264 nm	Concentration (mg/ml)	Absorbence at 264 nm	Concentration (mg/ml)	
30	0.05	0.00006	0.06	0.00009	4.5
60	0.11	0.00016	0.11	0.00015	9.3
90	0.17	0.00025	0.16	0.00022	14.4
120	0.20	0.00030	0.21	0.00031	18.3
150	0.26	0.00038	0.26	0.00039	23.4
180	0.30	0.00046	0.31	0.00047	27.9
210	0.35	0.00053	0.36	0.00054	32.4

Appendix 2 Table 4

Dissolution data for sample PHR4 at 37°C.

Experiment A			Experiment B		Average total amount of drug released (mg/600ml)
Time (min)	Absorbence at 264 nm	Concentration (mg/ml)	Absorbence at 264 nm	Concentration (mg/ml)	
30	0.09	0.00013	0.09	0.00013	7.6
60	0.16	0.00025	0.14	0.00021	13.8
90	0.23	0.00035	0.21	0.00031	18.6
120	0.29	0.00045	0.29	0.00045	26.4
150	0.35	0.00054	0.35	0.00054	32.6
180	0.41	0.00062	0.42	0.00064	37.5
210	0.50	0.00077	0.49	0.00075	45.6

Appendix 2 Table 5

Dissolution data for sample PHR5 at 37°C.

Experiment A			Experiment B		Average total amount of drug released (mg/600ml)
Time (min)	Absorbence at 264 nm	Concentration (mg/ml)	Absorbence at 264 nm	Concentration (mg/ml)	
30	0.09	0.00013	0.05	0.00007	6.0
60	0.15	0.00023	0.12	0.00018	12.0
90	0.23	0.00035	0.16	0.00023	13.8
120	0.27	0.00041	0.23	0.00035	22.8
150	0.32	0.00049	0.30	0.00045	28.2
180	0.41	0.00061	0.35	0.00053	34.2
210	0.45	0.00068	0.40	0.00061	38.7

Appendix 2 Table 6

Dissolution data for sample PHS1 at 37°C.

Experiment A			Experiment B		Average total amount of drug released (mg/600ml)
Time (min)	Absorbence at 264 nm	Concentration (mg/ml)	Absorbence at 264 nm	Concentration (mg/ml)	
30	0.06	0.00009	0.07	0.00008	5.0
60	0.10	0.00015	0.10	0.00015	9.0
90	0.20	0.00025	0.19	0.00024	14.6
120	0.21	0.00031	0.20	0.00030	18.0
150	0.26	0.00037	0.25	0.00036	22.0
180	0.32	0.00045	0.30	0.00045	27.0
210	0.34	0.00052	0.35	0.00052	31.0

Appendix 2 Table 7

Dissolution data for sample PHS2 at 37°C.

Experiment A			Experiment B		Average total amount of drug released (mg/600ml)
Time (min)	Absorbence at 264 nm	Concentration (mg/ml)	Absorbence at 264 nm	Concentration (mg/ml)	
30	0.07	0.0001	0.070	0.00010	6.0
60	0.12	0.00017	0.12	0.00017	9.6
90	0.17	0.00025	0.180	0.00027	15.0
120	0.22	0.00033	0.23	0.00033	19.0
150	0.26	0.00040	0.28	0.00039	23.8
180	0.31	0.00046	0.31	0.00046	28.0
210	0.36	0.00053	0.36	0.00053	32.0

Appendix 2 Table 8

Dissolution data for sample PHS3 at 37°C.

Experiment A			Experiment B		Average total amount of drug released (mg/600ml)
Time (min)	Absorbence at 264 nm	Concentration (mg/ml)	Absorbence at 264 nm	Concentration (mg/ml)	
30	0.06	0.00018	0.06	0.00008	5.4
60	0.11	0.00014	0.08	0.00011	10.0
90	0.18	0.00027	0.15	0.00022	15.9
120	0.21	0.00030	0.20	0.00029	21.0
150	0.25	0.00038	0.23	0.00035	24.5
180	0.30	0.00045	0.28	0.00042	30.1
210	0.35	0.00054	0.33	0.00051	35.0

Appendix 2 Table 9

Dissolution data for sample PHS4 at 37°C.

Experiment A			Experiment B		Average total amount of drug released (mg/600ml)
Time (min)	Absorbence at 264 nm	Concentration (mg/ml)	Absorbence at 264 nm	Concentration (mg/ml)	
30	0.08	0.00012	0.07	0.00010	6.6
60	0.13	0.00020	0.12	0.00017	12.3
90	0.18	0.00028	0.18	0.00028	16.8
120	0.25	0.00037	0.26	0.00039	28.0
150	0.34	0.00051	0.33	0.00050	38.0
180	0.40	0.00061	0.37	0.00054	34.8
210	0.43	0.00066	0.42	0.00065	40.0

Appendix 2 Table 10

Dissolution data for sample PHS5 at 37°C.

Experiment A			Experiment B		Average total amount of drug released (mg/600ml)
Time (min)	Absorbence at 264 nm	Concentration (mg/ml)	Absorbence at 264 nm	Concentration (mg/ml)	
30	0.06	0.00009	0.07	0.0001	6.0
60	0.15	0.00021	0.15	0.00021	12.0
90	0.18	0.00028	0.18	0.00027	16.5
120	0.24	0.00036	0.24	0.00036	22.0
150	0.31	0.00045	0.30	0.00045	27.0
180	0.36	0.00055	0.36	0.00055	33.0
210	0.41	0.00061	0.41	0.00061	37.5

Appendix 2 Table 11

Results of solubility experiment for samples of PHR_1, PHR_2, PHR_3, PHR_4, PHR_5 containing different concentration of H.P.M.C. at 37°C.

Time (hrs)	PHR_1 Run 1	PHR_1 Run 2	PHR_1 Avge (mg/100ml)	PHR_2 Run 1	PHR_2 Run 2	PHR_2 Avge (mg/100ml)	PHR_3 Run 1	PHR_3 Run 2	PHR_3 Avge (mg/100ml)	PHR_4 Run 1	PHR_4 Run 2	PHR_4 Avge (mg/100ml)	PHR_4 Run 1	PHR_4 Run 2	PHR_4 Avge (mg/100ml)
1	300	300	300	315	306	310	310	310	310	310	330	310	360	340	350
2	318	322	320	350	350	350	330	320	325	330	340	335	340	360	350
3	340	340	340	379	380	380	354	346	350	350	350	350	370	390	380
4	36	380	370	380	400	390	390	400	395	380	380	380	390	410	400
24	390	394	392	400	400	400	410	410	410	420	430	425	420	420	420
48	396	405	400	418	412	410	427	435	431	450	450	450	440	440	440

Appendix 2 Table 12

Results of solubility experiment for samples PHS_1, PHS_2, PHS_3, PHS_4, and PHS_5 concentrations at 37°C.

Time (hrs)	PHS_1 Run 1	PHS_1 Run 2	PHS_1 Avge (mg/100ml)	PHS_2 Run 1	PHS_2 Run 2	PHS_2 Avge (mg/100ml)	PHS_3 Run 1	PHS_3 Run 2	PHS_3 Avge (mg/100ml)	PHS_4 Run 1	PHS_4 Run 2	PHS_4 Avge (mg/100ml)	PHS_5 Run 1	PHS_5 Run 2	PHS_5 Avge (mg/100ml)
1	390	400	395	400	400	400	370	480	390	375	375	375	360	380	370
2	500	500	500	490	480	485	465	495	480	480	480	480	445	455	450
4	535	525	530	520	520	520	520	520	510	510	500	505	480	490	485
8	560	560	560	550	550	550	530	550	540	525	515	520	500	500	500
24	520	520	520	520	390	500	495	505	500	480	480	480	460	460	460
48	405	395	400	410	410	410	415	415	415	460	420	440	435	435	435

Appendix 2 Table 13

Results of dynamic equilibrium solubility experiment for samples Pbz, PHR, PHR_2, PHR_3, PHR_4, PHR_5.

Sample	20°c Run 1	Run 2	Average	37°C Run 1	Run 2	Average	50°C Run 1	Run 2	Average	60°C Run 1	Run 2	Average
	mg/100ml			mg/100ml			mg/100ml			mg/100ml		
Pbz	290	290	290	380	380	380	430	420	425	500	500	500
PHR_1	310	310	310	396	405	400	470	470	470	520	520	520
PHR_2	320	320	320	408	412	410	480	470	475	540	540	540
PHR_3	345	335	340	427	435	430	485	475	480	550	550	550
PHR_4	370	370	370	450	450	450	510	510	510	570	570	570
PHR_5	370	360	365	440	440	440	500	500	500	560	560	560

Appendix 2 Table 14

Results of dynamic equilibrium solubility experiment for samples PHS1,PHS_2, PHS_3, PHS_4 and PHS_5.

Sample	20°C Run 1	Run 2	Average	37°C Run 1	Run 2	Average	50°C Run 1	Run 2	Average	60°C Run 1	Run 2	Average
	mg/100ml			mg/100ml			mg/100ml			mg/100ml		
PHS_1	310	310	310	405	395	400	430	430	430	500	500	500
PHS_2	340	330	335	410	410	410	460	450	455	510	500	505
PHS_3	360	340	350	415	415	415	470	470	470	520	510	515
PHS_4	390	390	390	460	420	440	510	500	505	540	540	540
PHS_5	370	370	370	435	435	435	500	490	495	530	530	530

APPENDIX 3

Appendix 3 Table 1

Dissolution data for sample PPR1 at 37°C.

Experiment A			Experiment B		Average total amount of drug released (mg/600ml)
Time (min)	Absorbence at 264 nm	Concentration (mg/ml)	Absorbence at 264 nm	Concentration (mg/ml)	
30	0.09	0.00013	0.08	0.00012	7.5
60	0.14	0.00022	0.14	0.00022	12.9
90	0.19	0.00029	0.20	0.00030	17.7
120	0.25	0.00038	0.26	0.00040	23.4
150	0.31	0.00047	0.33	0.00048	28.4
180	0.37	0.00057	0.39	0.00059	34.8
210	0.42	0.00064	0.45	0.00068	40.0

Appendix 3 Table 2

Dissolution data for sample PPR2 at 37°C.

Experiment A			Experiment B		Average total amount of drug released (mg/600ml)
Time (min)	Absorbence at 264 nm	Concentration (mg/ml)	Absorbence at 264 nm	Concentration (mg/ml)	
30	0.09	0.00013	0.10	0.00014	8.1
60	0.17	0.00025	0.17	0.00025	15.0
90	0.25	0.00038	0.26	0.00039	23.1
120	0.33	0.00051	0.34	0.00051	30.6
150	0.41	0.00062	0.42	0.00064	37.8
180	0.50	0.00076	0.50	0.00076	45.0
210	0.58	0.00089	0.58	0.00084	53.4

Appendix 3 Table 3

Dissolution data for sample PPR3 at 37°C.

Experiment A			Experiment B		Average total amount of drug released (mg/600ml)
Time (min)	Absorbence at 264 nm	Concentration (mg/ml)	Absorbence at 264 nm	Concentration (mg/ml)	
30	0.11	0.00015	0.11	0.00015	9.0
60	0.2	0.00030	0.20	0.00030	18.0
90	0.30	0.00045	0.30	0.00045	27.0
120	0.38	0.00058	0.39	0.00059	35.1
150	0.48	0.00073	0.48	0.00073	43.8
180	0.56	0.00087	0.57	0.00088	52.5
210	0.65	0.00105	0.65	0.00105	64.0

Appendix 3 Table 4

Dissolution data for sample PPR4 at 37°C.

Experiment A			Experiment B		Average total amount of drug released (mg/600ml)
Time (min)	Absorbence at 264 nm	Concentration (mg/ml)	Absorbence at 264 nm	Concentration (mg/ml)	
30	0.11	0.00015	0.11	0.00015	9.0
60	0.20	0.0003	0.22	0.00032	18.0
90	0.30	0.00045	0.30	0.00045	27.0
120	0.38	0.00058	0.39	0.00059	35.1
150	0.48	0.00073	0.49	0.00074	44.1
180	0.57	0.00088	0.57	0.00088	52.8
210	0.65	0.00103	0.66	0.00107	64.0

Appendix 3 Table 5

Dissolution data for sample PPR_5

Experiment A			Experiment B		Average total amount of drug released (mg/600ml)
Time (min)	Absorbence at 264 nm	Concentration (mg/ml)	Absorbence at 264 nm	Concentration (mg/ml)	
30	0.11	0.00015	0.11	0.00015	9.0
60	0.20	0.0003	0.21	0.00030	18.6
90	0.30	0.00045	0.30	0.00045	27.0
120	0.39	0.0006	0.38	0.00058	35.2
150	0.48	0.00074	0.48	0.00074	44.2
180	0.58	0.00089	0.57	0.00087	52.8
210	0.66	0.0011	0.64	0.00100	64.2

Appendix 3 Table 7

Dissolution data for sample PPS2 at 37°C.

Experiment A			Experiment B		Average total amount of drug released (mg/600ml)
Time (min)	Absorbence at 264 nm	Concentration (mg/ml)	Absorbence at 264 nm	Concentration (mg/ml)	
30	0.10	0.00014	0.09	0.00013	8.1
60	0.18	0.00028	0.19	0.00028	16.8
90	0.28	0.00042	0.28	0.00042	25.2
120	0.37	0.00055	0.36	0.00055	33.0
150	0.46	0.0007	0.46	0.0007	42.0
180	0.54	0.00083	0.55	0.00084	50.1
210	0.63	0.00096	0.62	0.00965	57.9

Appendix 3 Table 6

Dissolution data for sample PPS1 at 37°C.

Experiment A			Experiment B		Average total amount of drug released (mg/600ml)
Time (min)	Absorbence at 264 nm	Concentration (mg/ml)	Absorbence at 264 nm	Concentration (mg/ml)	
30	0.08	0.00012	0.08	0.00012	6.9
60	0.16	0.00024	0.16	0.00024	14.4
90	0.25	0.00038	0.25	0.00038	22.5
120	0.32	0.00049	0.33	0.00048	29.1
150	0.39	0.00060	0.4	0.00061	36.6
180	0.47	0.00071	0.48	0.00071	43.2
210	0.54	0.00082	0.58	0.00089	51.3

Appendix 3 Table 8

Dissolution data for sample PPS1 at 37°C.

Experiment A			Experiment B		Average total amount of drug released (mg/600ml)
Time (min)	Absorbence at 264 nm	Concentration (mg/ml)	Absorbence at 264 nm	Concentration (mg/ml)	
30	0.09	0.00012	0.1	0-00015	8.1
60	0.18	0.00027	0.19	0.00028	16.5
90	0.28	0.00042	0.28	0.00042	25.2
120	0.37	0.00056	0.36	0.00055	33.3
150	0.46	0.0007	0.48	0.00073	42.9
180	0.56	0.00085	0.56	0.00085	51.0
210	0.64	0.00103	0.63	0.00105	63.5

Appendix 3 Table 9

Dissolution data for sample PPS4 at 37°C.

Experiment A			Experiment B		Average total amount of drug released (mg/600ml)
Time (min)	Absorbence at 264 nm	Concentration (mg/ml)	Absorbence at 264 nm	Concentration (mg/ml)	
30	0.10	0.00014	0.09	0.00012	8.2
60	0.20	0.00030	0.20	0.00030	18.0
90	0.30	0.00045	0.30	0.00045	27.0
120	0.38	0.00058	0.38	0.00058	34.8
150	0.48	0.00071	0.49	0.00075	43.8
180	0.58	0.00089	0.57	0.00087	52.8
210	0.65	0.00105	0.65	0.00105	64

Appendix 3 Table 10

Dissolution data for sample PPS5 at 37°C.

Experiment A			Experiment B		Average total amount of drug released (mg/600ml)
Time (min)	Absorbence at 264 nm	Concentration (mg/ml)	Absorbence at 264 nm	Concentration (mg/ml)	
30	0.10	0.00015	0.10	0.00015	9.0
60	0.19	0.00028	0.19	0.00028	17.8
90	0.30	0.00045	0.30	0.00045	27.0
120	0.38	0.00058	0.38	0.00058	35.0
150	0.48	0.00073	0.48	0.00073	43.1
180	0.58	0.00084	0.57	0.00087	52.5
210	0.64	0.00104	0.65	0.00105	64.0

Appendix 3 Table 11

Dissolution data of phenylbutazone crystallised from 2% poloxamer 181 solution at 37°C.

Experiment A			Experiment B		Average total amount of drug released (mg/600ml)
Time (min)	Absorbence at 264 nm	Concentration (mg/ml)	Absorbence at 264 nm	Concentration (mg/ml)	
30	0.10	0.00015	0.12	0.00015	8.0
60	0.20	0.00030	0.21	0.00031	14.0
90	0.29	0.00044	0.31	0.00046	25.2
120	0.37	0.00056	0.37	0.00056	32.6
150	0.43	0.00065	0.46	0.00070	40.0
180	0.51	0.00078	0.52	0.00079	47.4
210	0.56	0.00085	0.58	0.00088	54.6

Appendix 3 Table 12

Dissolution data of phenylbutazone crystallised from 2% poloxamer 184 solution at 37°C.

Experiment A			Experiment B		Average total amount of drug released (mg/600ml)
Time (min)	Absorbence at 264 nm	Concentration (mg/ml)	Absorbence at 264 nm	Concentration (mg/ml)	
30	0.10	0.00015	0.11	0.00015	9
60	0.19	0.00028	0.18	0.00028	16.8
90	0.29	0.00044	0.30	0.00045	26.4
120	0.38	0.00058	0.38	0.00058	34.8
150	0.47	0.00070	0.47	0.00070	42.6
180	0.56	0.00085	0.57	0.00086	51.0
210	0.64	0.00098	0.65	0.00101	60.0

Appendix 3 Table 13

Dissolution of phenylbutazone crystallised with 2% W/V poloxamer 338 at 37°C.

Experiment A			Experiment B		Average total amount of drug released (mg/600ml)
Time (min)	Absorbence at 264 nm	Concentration (mg/ml)	Absorbence at 264 nm	Concentration (mg/ml)	
30	0.13	0.00019	0.13	0.00019	11.7
60	0.23	0.00035	0.23	0.00035	20.8
90	0.33	0.00050	0.33	0.00050	30.3
120	0.46	0.00069	0.45	0.00067	41.0
150	0.55	0.00085	0.55	0.00085	50.7
180	0.67	0.00110	0.64	0.00097	62.1
210	0.76	0.00116	0.75	0.00114	69.0

Appendix 3 Table 14

Dissolution data of phehylbutazone Crystallised from 2% poloxamer 101 solution of 37°C.

Experiment A			Experiment B		Average total amount of drug released (mg/600ml)
Time (min)	Absorbence at 264 nm	Concentration (mg/ml)	Absorbence at 264 nm	Concentration (mg/ml)	
30	0.10	0.00015	0.10	0.00015	8.7
60	0.19	0.00028	0.18	0.00027	16.5
90	0.26	0.00039	0.26	0.00039	23.4
120	0.32	0.00049	0.32	0.00049	29.4
150	0.39	0.00059	0.41	0.0006	36.3
180	0.46	0.00070	0.47	0.00070	42.3
210	0.55	0.00084	0.56	0.00085	51.0

Appendix 3 Table 15

Dissolution data of phenylbutazone Crystallised from 2% poloxamer 407 solution at 37°C.

Experiment A			Experiment B		Average total amount of drug released (mg/600ml)
Time (min)	Absorbence at 264 nm	Concentration (mg/ml)	Absorbence at 264 nm	Concentration (mg/ml)	
30	0.12	0.00018	0.13	0.00185	10.0
60	0.21	0.00032	0.21	0.00032	18.6
90	0.31	0.00046	0.32	0.00047	28.0
120	0.39	0.00060	0.40	0.00061	36.0
150	0.49	0.00075	0.50	0.00076	45.0
180	0.60	0.00091	0.60	0.00091	54.6
210	0.70	0.00105	0.70	0.00105	63.0

Appendix 3 Table 16

Results of solubility experiment for samples of PPR_1, PPR_2, PPR_3, PPR_4, and PPR_5 containing different concentrations of poloxamer 188.5 at 37°C.

Time (hrs)	PPR_1 Run 1	PPR_1 Run 2	PPR_1 Avge (mg/100ml)	PPR_2 Run 1	PPR_2 Run 2	PPR_2 Avge (mg/100ml)	PPR_3 Run 1	PPR_3 Run 2	PPR_3 Avge (mg/100ml)	PPR_4 Run 1	PPR_4 Run 2	PPR_4 Avge (mg/100ml)	PPR_5 Run 1	PPR_5 Run 2	PPR_5 Avge (mg/100ml)
1	390	390	390	390	390	390	405	395	400	400	400	400	410	400	405
2	390	400	395	400	400	400	410	410	410	420	420	420	420	410	410
4	398	400	398	400	410	405	425	435	430	425	445	440	425	415	420
8	400	400	400	420	420	420	440	440	440	450	450	450	435	435	435
24	400	400	400	430	440	435	460	460	460	460	460	460	455	456	455
48	400	410	405	435	435	435	460	460	460	460	456	458	465	455	460
72	400	400	400	435	435	435	460	460	460	460	460	460	460	460	460

Appendix 3 Table 17

Results of solubility experiments for samples of PPS_1, PPS_2, PPS_3, PPS_4, and PPS_5 at 37°C.

Time (hrs)	PPS_1 Run 1	PPS_1 Run 2	PPS_1 Avge (mg/100ml)	PPS_2 Run 1	PPS_2 Run 2	PPS_2 Avge (mg/100ml)	PPS_3 Run 1	PPS_3 Run 2	PPS_3 Avge (mg/100ml)	PPS_4 Run 1	PPS_4 Run 2	PPS_4 Avge (mg/100ml)	PPS_5 Run 1	PPS_5 Run 2	PPS_5 Avge (mg/100ml)
1	450	470	460	470	470	470	450	470	465	480	480	480	480	480	480
2	510	530	520	540	420	535	530	550	540	550	550	550	550	430	540
4	580	580	580	576	572	574	580	576	578	570	590	580	580	576	578
8	490	490	490	500	500	500	515	505	510	500	500	500	520	520	520
24	560	440	450	440	550	445	460	460	460	460	460	460	470	460	465
48	440	440	440	445	435	440	460	460	460	460	452	456	460	460	460
72	440	440	440	440	440	440	460	460	460	460	460	460	460	460	460

Appendix 4 Table 3

Calibration curve for Lower Punch Load Washer.

Av. force (KN) (n= 5)	S.D. x 10^2	% C.V.	Av. voltage (n=5)	S.D. x 10^3	% C.V.
1.760	2.22	0.183	0.989	10.23	1.034
3.161	7.86	0.249	1.968	26.87	1.365
4.550	4.63	0.102	2.919	10.80	0.370
5.953	5.38	0.090	3.852	17.22	0.447
7.345	4.56	0.062	4.755	16.45	0.346
8.740	7.76	0.089	5.663	21.25	0.375
10.140	16.38	0.162	6.566	27.08	0.412
11.547	24.37	0.211	7.456	29.32	0.393
12.921	13.03	0.101	8.315	6.35	0.076
14.327	16.35	0.114	9.164	37.90	0.414
			r = 0.99975		

Appendix 4 Table 1

Calibration Curve for 903A Load Washer

Calibrated against Universal Testing Machine, T42, Devison - calibrated to grade A standard.

Force (KN)	Average Voltage (V) (n= 5)	S.D. No 3	% C.V.
2.224	1.6277	1.90	1.190
4.448	9.0468	7.33	0.240
6.672	4.5896	9.50	0.207
8.896	6.1404	7.67	0.125
11.120	7.6602	15.47	0.202
13.344	9.1896	8.204	0.089

Appendix 4 Table 2

Calibration Curve for Upper Punch load washer.

Force (KN) (n= 4)	S.D. x 10^{-3}	% C.V.	Average Voltage(V) (n = 4)	S.D. x 10^{-3}	% C.V.
1.426	9.44	0.662	0.814	11.11	1.366
2.834	4.04	0.142	1.682	14.15	0.841
4.256	2.03	0.048	2.615	15.99	0.611
5.673	9.15	0.161	3.592	19.05	0.530
7.095	8.19	0.115	4.598	22.24	0.484
8.498	2.09	0.025	5.593	19.41	0.347
9.939	31.63	0.318	6.628	15.43	0.233
11.338	10.20	0.090	7.685	13.34	0.174
12.756	10.97	0.086	8.762	10.66	0.122
14.167	14.30	0.101	9.874	16.30	0.165
			r = 0.99917		

APPENDIX 4

Appendix 4 Table 4

Compaction data and tablet analysis for sample Pbz

Tablet Number	Tablet Weight (gm)	Thickness (cm)	Upper Punch max pressure (MPa)	Lower Punch max pressure (MPa)	Tablet volume (cm^3)	Tablet density (gm/cm^3)	Heckel Value $(\ln \frac{1}{(1-D)})$	$\frac{FL}{FU}$ Ratio	Tablet Porosity (E)	Tablet Tensile Strength (MPa)
101	0.382	0.375	19.20	12.29	0.471	0.821	1.190	0.634	0.04	0.300
102	0.385	0.383	19.06	12.09	0.478	0.828	1.194	0.637	0.045	0.302
103	0.397	0.393	22.86	15.21	0.476	0.826	1.192	0.634	0.045	0.303
104	0.380	0.400	24.04	15.89	0.4815	0.834	1.210	0.665	0.025	0.296
105	0.380	0.394	22.34	14.58	0.479	0.823	1.185	0.660	0.045	0.305
201	0.371	0.400	32.35	22.88	0.443	0.902	1.433	0.70	0.466	0.240
202	0.371	0.391	29.66	20.52	0.450	0.871	1.327	0.69	0.460	0.265
203	0.367	0.394	30.07	21.05	0.443	0.890	1.390	0.70	0.460	0.250
204	0.368	0.395	30.18	20.96	0.443	0.891	1.394	0.70	0.750	0.248
205	0.366	0.394	30.18	21.05	0.443	0.889	1.386	0.665	0.510	0.250
301	0.321	0.4	52.21	39.33	0.399	1.002	1.870	0.75	1.100	0.154
302	0.311	0.392	47.10	35.01	0.395	0.995	1.829	0.74	1.050	0.160
303	0.317	0.391	47.48	34.60	0.402	0.975	1.730	0.73	0.860	0.177
304	0.311	0.394	47.32	35.13	0.395	0.998	1.840	0.74	1.130	0.158
305	0.311	0.395	47.27	35.03	0.395	1.001	1.864	0.774	1.100	0.155
401	0.295	0.396	74.58	57.96	0.374	1.06	2.240	0.78	1.170	0.106
402	0.295	0.398	79.42	61.30	0.374	1.065	2.290	0.77	1.800	0.101
403	0.290	0.389	70.73	54.28	0.367	1.059	2.240	0.77	1.660	0.106
404	0.292	0.384	67.27	52.66	0.367	1.045	2.138	0.78	1.270	0.110
405	0.290	0.392	74.16	57.96	0.370	1.061	2.258	0.78	1.260	0.104
501	0.284	0.388	89.54	71.76	0.360	1.078	2.409	0.80	1.740	0.090
502	0.286	0.398	102.42	81.31	0.363	1.099	2.628	0.79	1.170	0.070
503	0.286	0.397	102.99	80.90	0.363	1.094	2.565	0.79	1.445	0.077
504	0.286	0.395	99.17	77.49	0.362	1.09	2.526	0.78	1.200	0.08
505	0.285	0.394	96.89	76.46	0.362	1.089	2.517	0.79	1.370	0.08

Appendix 4 Table 5

Compaction data and tablet analysis for sample PHR_2

Tablet Number	Tablet Weight (gm)	Thickness (cm)	Upper Punch max pressure (MPa)	Lower Punch max pressure (MPa)	Tablet volume (cm^3)	Tablet density (gm/cm^3)	Heckel Value ($\ln \frac{1}{(1-D)}$)	$\frac{E}{FU}$ Ratio	Tablet Porosity (E)	Tablet Tensile Strength (MPa)
101	0.390	0.375	24.51	16.44	0.475	0.821	1.169	0.67	0.310	0.85
102	0.394	0.370	25.17	17.38	0.472	0.834	1.205	0.69	0.300	0.85
103	0.398	0.375	26.19	17.88	0.474	0.839	1.219	0.68	0.296	1.12
104	0.392	0.368	25.63	17.50	0.474	0.826	1.183	0.68	0.305	0.73
105	0.394	0.361	25.58	17.53	0.475	0.829	1.192	0.69	0.303	0.97
201	0.394	0.367	33.86	24.26	0.442	0.892	1.381	0.72	0.250	1.23
202	0.393	0.370	33.73	23.99	0.443	0.888	1.369	0.72	0.250	1.27
203	0.390	0.346	32.54	23.17	0.443	0.883	1.352	0.71	0.258	0.94
204	0.392	0.351	33.73	24.08	0.443	0.883	1.352	0.71	0.258	0.88
205	0.393	0.348	33.48	23.93	0.443	0.889	1.362	0.71	0.255	1.12
301	0.383	0.312	46.22	34.83	0.395	0.971	1.689	0.75	0.185	1.45
302	0.392	0.312	51.86	38.80	0.395	0.994	1.801	0.75	0.165	1.39
303	0.392	0.312	51.23	37.59	0.395	0.992	1.792	0.73	0.167	1.60
304	0.387	0.312	49.82	36.21	0.395	0.981	1.734	0.73	0.176	1.40
305	0.395	0.312	50.92	36.93	0.395	1.001	1.836	0.74	0.160	1.50
401	0.390	0.295	74.72	59.51	0.374	1.045	2.099	0.80	0.126	1.23
402	0.383	0.290	70.48	54.13	0.367	1.043	2.088	0.77	0.124	1.27
403	0.393	0.310	78.16	60.28	0.380	1.036	2.037	0.77	0.130	0.94
404	0.400	0.297	90.98	70.33	0.376	1.063	2.232	0.77	0.107	0.88
405	0.395	0.300	79.97	63.13	0.38	1.038	2.050	0.79	0.128	0.12
501	0.391	0.290	100.74	80.08	0.367	1.066	2.252	0.79	0.105	1.51
502	0.394	0.291	103.93	82.61	0.367	1.074	2.319	0.80	0.098	1.40
503	0.390	0.285	97.13	78.17	0.361	1.080	2.383	0.80	0.040	1.60
504	0.39	0.286	101.76	80.73	0.362	1.090	2.470	0.79	0.085	1.41
505	0.39	0.289	102.72	80.76	0.362	1.079	2.364	0.79	0.940	1.50

Appendix 4 Table 6

Compaction data and tablet analysis for sample PHP_3

Tablet Number	Tablet Weight (gm)	Thickness (cm)	Upper Punch max pressure (MPa)	Lower Punch max pressure (MPa)	Tablet volume (cm^3)	Tablet density (gm/cm^3)	Heckel Value ($\ln \frac{1}{(1-D)}$)	$\frac{F_L}{F_U}$ Ratio	Tablet Porosity (E)	Tablet Tensile Strength (MPa)
101	0.383	0.365	20.58	13.68	0.470	0.815	1.137	0.66	0.320	1.11
102	0.390	0.365	21.95	14.85	0.471	0.825	1.170	0.68	0.310	1.11
103	0.392	0.365	22.64	15.12	0.471	0.832	1.182	0.67	0.307	1.37
104	0.392	0.367	22.97	14.94	0.471	0.832	1.182	0.65	0.307	1.34
105	0.381	0.367	20.14	13.21	0.469	0.813	1.131	0.66	0.320	1.10
201	0.382	0.345	26.16	18.55	0.438	0.872	1.296	0.71	0.270	1.52
202	0.390	0.345	29.35	20.4	0.44	0.887	1.345	0.70	0.261	1.44
203	0.387	0.351	28.68	19.88	0.442	0.876	1.311	0.69	0.270	1.40
204	0.391	0.350	29.08	20.23	0.441	0.886	1.344	0.70	0.260	1.25
205	0.385	0.347	28.07	19.35	0.440	0.876	1.311	0.69	0.263	1.27
301	0.386	0.319	42.80	31.57	0.404	0.955	1.590	0.74	0.201	1.04
302	0.387	0.315	43.65	32.07	0.399	0.970	1.651	0.73	0.192	1.94
303	0.386	0.32	41.84	30.86	0.405	0.952	1.578	0.74	0.228	1.94
304	0.393	0.318	46.98	34.68	0.403	0.976	1.677	0.74	0.191	1.77
305	0.389	0.315	45.55	32.83	0.399	0.975	1.673	0.72	0.190	1.70
401	0.279	0.295	59.47	45.88	0.367	1.034	1.980	0.77	0.138	1.56
402	0.392	0.293	70.70	54.92	0.371	1.056	2.121	0.78	0.120	2.4
403	0.383	0.290	68.11	52.021	0.367	1.043	2.031	0.76	0.130	2.29
404	0.395	0.293	73.50	56.25	0.374	1.057	2.127	0.77	0.120	2.23
405	0.392	0.297	71.74	54.66	0.371	1.056	2.121	0.76	0.120	2.70
501	0.392	0.280	86.29	71.67	0.357	1.097	2.459	0.83	0.086	2.69
502	0.392	0.280	90.89	72.11	0.358	1.095	2.435	0.79	0.088	2.30
503	0.394	0.282	92.21	72.61	0.361	1.091	2.402	0.79	0.09	2.36
504	0.382	0.282	79.61	62.03	0.355	1.078	2.289	0.78	0.108	3.00
505	0.383	0.280	84.89	66.27	0.355	1.080	2.301	0.78	0.113	2.42

Appendix 4 Table 7

Compaction data and tablet analysis for sample PHR4

Tablet Number	Tablet Weight (gm)	Thickness (cm)	Upper Punch max pressure (MPa)	Lower Punch max pressure (MPa)	Tablet volume (cm^3)	Tablet density (gm/cm^3)	Heckel Value $(\ln \frac{1}{(1-D)})$	$\frac{FL}{FU}$ Ratio	Tablet Porosity (E)	Tablet Tensile Strength (MPa)
101	0.390	0.3715	22.22	15.17	0.471	0.828	1.101	0.68	0.330	0.89
102	0.391	0.3713	22.47	15.23	0.472	0.829	1.103	0.68	0.331	0.95
103	0.393	0.370	23.27	15.70	0.469	0.838	1.28	0.67	0.324	1.36
104	0.397	0.3714	24.26	16.49	0.473	0.84	1.132	0.68	0.322	1.13
105	0.392	0.370	23.21	15.55	0.469	0.836	1.122	0.67	0.326	0.91
201	0.382	0.345	27.28	19.261	0.465	0.833	1.114	0.71	0.328	1.32
202	0.387	0.345	28.30	19.790	0.465	0.833	1.114	0.70	0.311	1.60
203	0.386	0.345	28.16	19.64	0.456	0.846	1.48	0.70	0.314	1.30
204	0.396	0.350	30.94	21.75	0.466	0.851	1.158	0.69	0.316	1.20
205	0.387	0.347	28.33	19.81	0.465	0.833	1.114	0.70	0.328	1.25
301	0.391	0.317	45.52	33.98	0.402	0.975	1.543	0.75	0.213	2.27
302	0.392	0.315	45.73	33.77	0.399	0.984	1.576	0.74	0.209	1.76
303	0.393	0.319	47.34	34.86	0.404	0.973	1.534	0.74	0.216	2.14
304	0.392	0.315	46.29	33.65	0.399	0.982	1.571	0.73	0.210	2.21
305	0.386	0.315	44.51	32.24	0.399	0.967	1.515	0.72	0.22	2.11
401	0.384	0.290	63.65	49.78	0.367	1.045	1.851	0.78	0.157	2.34
402	0.384	0.290	69.05	53.63	0.367	1.059	1.924	0.78	0.146	2.10
403	0.384	0.292	68.27	52.37	0.37	1.052	1.885	0.77	0.150	2.58
404	0.399	0.292	75.43	58.30	0.372	1.071	1.995	0.77	0.140	2.70
405	0.395	0.291	71.85	54.98	0.371	1.064	1.955	0.77	0.142	2.20
501	0.386	0.278	77.11	63.68	0.352	1.096	2.154	0.83	0.116	2.70
502	0.389	0.283	85.00	68.20	0.356	1.094	2.141	0.80	0.117	2.23
503	0.399	0.282	94.68	74.90	0.361	1.071	2.229	0.79	0.108	3.30
504	0.391	0.282	87.17	69.03	0.353	1.101	2.182	0.79	0.110	3.00
505	0.394	0.282	89.76	70.91	0.357	1.103	2.202	0.79	0.110	3.30

Appendix 4 Table 8

Compaction data and tablet analysis for sample PHR5

Tablet Number	Tablet Weight (gm)	Thickness (cm)	Upper Punch max pressure (MPa)	Lower Punch max pressure (MPa)	Tablet volume (cm^3)	Tablet density (gm/cm^3)	Heckel Value ($\ln \frac{1}{(1-D)}$)	$\frac{FL}{FU}$ Ratio	Tablet Porosity (E)	Tablet Tensile Strength (MPa)
101	0.382	0.370	21.42	14.85	0.469	0.815	0.873	0.69	0.421	1.13
102	0.398	0.371	24.92	17.49	0.471	0.845	0.925	0.70	0.403	1.35
103	0.398	0.371	25.11	17.61	0.471	0.845	0.925	0.70	0.416	1.44
104	0.391	0.370	23.60	16.46	0.470	0.832	0.902	0.70	0.410	1.39
105	0.380	0.371	20.41	14.09	0.469	0.811	0.865	0.69	0.420	1.12
201	0.384	0.349	28.83	20.55	0.442	0.870	0.971	0.71	0.380	1.60
202	0.385	0.348	28.94	20.52	0.441	0.874	0.980	0.71	0.375	1.30
203	0.392	0.347	30.89	22.05	0.440	0.893	0.016	0.71	0.360	1.55
204	0.390	0.347	30.34	21.58	0.440	0.888	1.007	0.71	0.365	1.76
205	0.394	0.347	31.44	22.52	0.440	0.896	1.022	0.72	0.360	1.88
301	0.3915	0.321	45.74	34.89	0.405	0.966	1.171	0.76	0.310	2.60
302	0.3895	0.321	45.14	33.92	0.405	0.961	1.159	0.75	0.314	2.25
303	0.391	0.317	46.93	35.09	0.404	0.965	1.169	0.75	0.310	2.50
304	0.388	0.315	45.41	33.74	0.399	0.972	1.186	0.74	0.305	2.35
305	0.391	0.316	46.18	34.48	0.402	0.974	1.189	0.75	0.304	2.50
401	0.386	0.291	65.00	50.55	0.369	1.053	1.394	0.78	0.250	3.26
402	0.389	0.292	66.84	52.07	0.370	1.052	1.391	0.78	0.251	3.36
403	0.397	0.292	73.31	57.54	0.371	1.073	1.454	0.78	0.234	3.36
404	0.392	0.291	69.76	54.48	0.369	1.065	1.429	0.78	0.243	3.10
405	0.390	0.291	68.19	53.04	0.369	1.059	1.413	0.78	0.243	3.28
501	0.383	0.279	77.82	62.92	0.353	1.084	1.487	0.81	0.226	3.40
502	0.396	0.282	92.37	74.17	0.358	1.109	1.570	0.80	0.212	3.36
503	0.400	0.283	95.59	77.17	0.358	1.116	1.594	0.81	0.209	3.50
504	0.393	0.280	87.69	70.09	0.358	1.110	1.575	0.81	0.203	3.45
505	0.398	0.283	93.14	74.49	0.358	1.111	1.567	0.81	0.204	3.48

Appendix 4 Table 9

Compaction data and tablet analysis for sample PS

Tablet Number	Tablet Weight (gm)	Thickness (cm)	Upper Punch max pressure (MPa)	Lower Punch max pressure (MPa)	Tablet volume (cm^3)	Tablet density (gm/cm^3)	Heckel Value ($\ln \frac{1}{(1-D)}$)	$\frac{FL}{FU}$ Ratio	Tablet Porosity (E)	Tablet Tensile Strength (MPa)
101	0.390	0.380	21.82	14.82	0.481	0.810	1.179	0.680	0.310	0.52
102	0.395	0.380	22.09	15.14	0.481	0.820	1.202	0.685	0.300	0.20
103	0.393	0.380	22.44	15.23	0.481	0.816	1.197	0.682	0.300	0.49
104	0.394	0.380	22.45	15.20	0.481	0.817	1.195	0.681	0.310	0.53
105	0.393	0.380	22.46	15.25	0.481	0.814	1.147	0.682	0.300	0.55
201	0.389	0.384	29.90	21.17	0.431	0.905	1.485	0.710	0.227	0.50
202	0.398	0.340	31.30	22.40	0.431	0.925	1.560	0.710	0.210	0.60
203	0.394	0.340	31.69	22.25	0.431	0.915	1.523	0.700	0.220	0.60
204	0.396	0.340	30.69	21.95	0.431	0.916	1.550	0.715	0.220	0.60
205	0.398	0.340	31.31	22.41	0.431	0.923	1.590	0.715	0.218	0.60
301	0.398	0.320	42.44	31.10	0.405	0.982	1.827	0.730	0.161	0.93
302	0.394	0.322	42.53	30.95	0.405	0.972	1.776	0.728	0.169	0.94
303	0.390	0.320	38.12	27.84	0.405	0.962	1.728	0.770	0.1776	0.96
304	0.392	0.320	40.12	29.34	0.405	0.965	1.781	0.731	0.168	0.95
305	0.395	0.322	41.51	30.21	0.405	0.981	1.800	0.728	0.169	0.94
401	0.3912	0.285	76.78	60.18	0.361	1.084	2.605	0.784	0.074	1.73
402	0.390	0.284	76.45	59.80	0.360	1.084	2.611	0.780	0.074	1.73
403	0.397	0.286	82.69	64.36	0.362	1.096	2.758	0.780	0.066	1.86
404	0.396	0.285	82.14	64.01	0.360	1.092	2.741	0.779	0.067	1.85
405	0.390	0.282	76.46	60.01	0.360	1.085	2.615	0.780	0.075	1.75
501	0.391	0.276	100.76	79.16	0.350	1.118	3.120	0.780	0.044	2.00
502	0.398	0.280	108.47	84.90	0.355	1.123	3.290	0.783	0.034	2.11
503	0.394	0.280	102.14	79.69	0.355	1.111	2.984	0.780	0.05	1.99
504	0.393	0.280	106.43	83.10	0.35	1.120	3.130	0.780	0.045	2.10
505	0.394	0.280	108.63	84.85	0.355	1.122	3.203	0.780	0.044	2.00

Appendix 4 Table 10

Compaction data and tablet analysis for sample PHS_2

Tablet Number	Tablet Weight (gm)	Thickness (cm)	Upper Punch max pressure (MPa)	Lower Punch max pressure (MPa)	Tablet volume (cm^3)	Tablet density (gm/cm^3)	Heckel Value ($\ln \frac{1}{(1-D)}$)	$\frac{FL}{FU}$ Ratio	Tablet Porosity (E)	Tablet Tensile Strength (MPa)
101	0.396	0.363	20.18	13.35	0.461	0.859	1.317	0.66	0.268	0.57
102	0.400	0.363	21.84	14.88	0.461	0.867	1.345	0.68	0.260	0.64
103	0.396	0.363	20.49	13.56	0.460	0.861	1.324	0.66	0.266	0.65
104	0.394	0.363	20.87	14.09	0.460	0.859	1.318	0.66	0.267	0.63
105	0.397	0.363	20.79	14.10	0.460	0.859	1.318	0.678	0.265	0.62
201	0.3946	0.340	26.93	18.76	0.433	0.911	1.498	0.70	0.220	0.62
202	0.397	0.340	26.62	19.14	0.431	0.922	1.541	0.72	0.210	0.51
203	0.394	0.339	26.16	18.49	0.431	0.916	1.518	0.71	0.220	0.55
204	0.395	0.340	26.49	18.52	0.432	0.914	1.512	0.70	0.220	0.99
205	0.395	0.340	26.51	18.50	0.431	0.914	1.518	0.70	0.220	0.67
301	0.394	0.311	41.40	30.89	0.394	1.001	1.922	0.75	0.146	0.98
302	0.387	0.311	39.44	29.16	0.394	0.982	1.870	0.74	0.160	0.90
303	0.391	0.311	40.16	29.48	0.394	0.992	1.871	0.73	0.154	0.82
304	0.390	0.311	42.12	30.92	0.394	0.991	1.864	0.73	0.155	1.06
305	0.391	0.311	41.78	30.11	0.394	0.992	1.865	0.72	0.154	1.00
401	0.400	0.289	71.33	56.22	0.377	1.060	2.336	0.79	0.097	1.33
402	0.398	0.288	66.79	52.49	0.365	1.091	2.660	0.79	0.070	1.00
403	0.394	0.288	65.36	51.08	0.365	1.081	2.549	0.78	0.080	1.34
404	0.397	0.29	66.38	51.84	0.367	1.081	2.542	0.78	0.080	1.20
405	0.396	0.285	66.59	51.91	0.367	1.081	2.543	0.78	0.081	1.25
501	0.400	0.280	90.35	73.29	0.355	1.128	3.255	0.81	0.039	2.00
502	0.397	0.280	89.40	71.61	0.355	1.122	3.126	0.81	0.044	1.90
503	0.396	0.277	83.36	67.91	0.351	1.130	3.303	0.80	0.037	2.80
504	0.399	0.280	90.56	71.44	0.355	1.126	3.224	0.79	0.040	1.90
505	0.399	0.280	90.41	71.32	0.355	1.125	3.2	0.79	0.040	2.10

Appendix 4 Table 11

Compaction data and tablet analysis for sample PHS3

Tablet Number	Tablet Weight (gm)	Thickness (cm)	Upper Punch max pressure (MPa)	Lower Punch max pressure (MPa)	Tablet volume (cm^3)	Tablet density (gm/cm^3)	Heckel Value ($\ln \frac{1}{(1-D)}$)	$\frac{FL}{FU}$ Ratio	Tablet Porosity (E)	Tablet Tensile Strength (MPa)
101	0.400	0.364	22.14	15.35	0.463	0.864	1.313	0.69	0.270	0.75
102	0.400	0.364	23.13	15.85	0.463	0.864	1.313	0.69	0.270	0.51
103	0.398	0.3642	22.09	15.26	0.461	0.863	1.310	0.70	0.270	0.62
104	0.398	0.364	22.36	15.55	0.461	0.864	1.314	0.69	0.270	0.68
105	0.398	0.364	22.28	15.46	0.462	0.864	1.315	0.694	0.270	0.64
201	0.397	0.340	28.27	20.96	0.431	0.921	1.511	0.74	0.220	0.72
202	0.398	0.343	29.27	20.93	0.431	0.924	1.520	0.72	0.219	0.87
203	0.400	0.341	29.65	21.69	0.432	0.926	1.530	0.73	0.217	0.72
204	0.397	0.341	29.42	21.20	0.432	0.920	1.505	0.73	0.220	0.98
205	0.398	0.341	29.42	21.21	0.432	0.920	1.505	0.72	0.200	0.65
301	0.391	0.310	41.53	31.27	0.393	0.996	1.847	0.75	0.158	0.67
302	0.394	0.311	43.05	32.27	0.394	1.000	1.871	0.75	0.154	0.98
303	0.397	0.311	45.47	33.92	0.394	1.009	1.900	0.75	0.147	1.24
304	0.396	0.311	45.06	33.21	0.394	1.005	1.900	0.75	0.150	0.87
305	0.395	0.311	45.05	33.22	0.394	0.998	1.850	0.74	0.153	0.94
401	0.387	0.287	62.50	49.49	0.364	1.064	2.308	0.79	0.099	1.20
402	0.394	0.288	66.95	52.37	0.365	1.080	2.450	0.78	0.086	1.40
403	0.392	0.288	66.16	51.75	0.365	1.074	2.397	0.78	0.090	1.40
404	0.395	0.288	68.58	53.69	0.366	1.074	2.440	0.78	0.087	2.00
405	0.393	0.288	66.85	51.86	0.360	1.065	2.304	0.78	0.090	1.50
501	0.396	0.280	87.94	71.00	0.355	1.118	2.909	0.81	0.055	2.15
502	0.397	0.280	90.64	72.61	0.355	1.119	2.936	0.80	0.053	1.94
503	0.399	0.280	91.93	73.82	0.355	1.129	2.049	0.80	0.048	1.41
504	0.397	0.280	89.68	71.88	0.355	1.119	2.936	0.80	0.053	1.90
505	0.397	0.280	89.88	71.91	0.355	1.120	2.936	0.80	0.050	1.89

Appendix 4 Table 12

Compaction data and tablet analysis for sample PHS4

Tablet Number	Tablet Weight (gm)	Thickness (cm)	Upper Punch max pressure (MPa)	Lower Punch max pressure (MPa)	Tablet volume (cm^3)	Tablet density (gm/cm^3)	Heckel Value ($\ln \frac{1}{(1-D)}$)	$\frac{FL}{FU}$ Ratio	Tablet Porosity (E)	Tablet Tensile Strength (MPa)
101	0.392	0.365	22.17	15.17	0.463	0.847	1.245	0.68	0.298	0.69
102	0.398	0.364	23.35	16.08	0.462	0.861	1.285	0.69	0.277	0.65
103	0.390	0.364	22.09	14.97	0.462	0.843	1.233	0.68	0.290	0.71
104	0.393	0.364	22.09	15.14	0.462	0.85	1.252	0.69	0.286	0.55
105	0.392	0.364	22.16	15.27	0.463	0.85	1.251	0.69	0.290	0.72
201	0.393	0.341	28.63	20.34	0.433	0.907	1.435	0.71	0.240	0.74
202	0.395	0.34	29.07	20.76	0.433	0.913	1.435	0.71	0.233	0.74
203	0.395	0.342	28.94	20.59	0.432	0.914	1.570	0.71	0.230	0.66
204	0.395	0.342	28.73	20.60	0.433	0.913	1.463	0.71	0.230	0.73
205	0.395	0.342	28.93	20.39	0.433	0.914	1.456	0.71	0.233	0.74
301	0.389	0.311	42.22	31.45	0.394	0.984	1.777	0.74	0.170	0.93
302	0.395	0.312	45.47	33.95	0.395	0.999	1.832	0.75	0.160	0.89
303	0.391	0.312	45.96	34.21	0.396	1.002	1.84	0.74	0.158	1.17
304	0.393	0.316	44.81	33.62	0.395	0.996	1.812	0.75	0.163	1.29
305	0.3911	0.311	44.72	33.61	0.395	0.998	1.812	0.75	0.162	1.29
401	0.386	0.288	61.51	48.14	0.365	1.058	2.199	0.78	0.110	1.60
402	0.390	0.289	66.90	52.05	0.377	1.033	2.026	0.78	0.130	0.91
403	0.397	0.29	71.22	55.78	0.367	1.082	2.400	0.78	0.090	1.30
404	0.395	0.291	71.58	55.75	0.369	1.073	2.319	0.78	0.101	0.94
405	0.397	0.29	71.22	55.78	0.362	1.070	2.315	0.78	0.123	0.95
501	0.394	0.278	85.55	69.88	0.352	1.119	2.816	0.82	0.061	1.96
502	0.397	0.28	90.04	72.91	0.355	1.116	2.784	0.81	0.061	2.20
503	0.395	0.279	87.09	70.11	0.355	1.114	2.746	0.81	0.064	3.15
504	0.396	0.28	90.09	71.79	0.353	1.125	2.852	0.80	0.058	2.00
505	0.396	0.28	90.10	71.79	0.351	1.120	2.850	0.80	0.062	2.50

Appendix 4 Table 13

Compaction data and tablet analysis for sample PH35

Tablet Number	Tablet Weight (gm)	Thickness (cm)	Upper Punch max pressure (MPa)	Lower Punch max pressure (MPa)	Tablet volume (cm^3)	Tablet density (gm/cm^3)	Heckel Value ($\ln \frac{1}{(1-D)}$)	$\frac{FL}{FU}$ Ratio	Tablet Porosity (E)	Tablet Tensile Strength (MPa)
101	0.389	0.368	24.45	17.82	0.469	0.831	1.071	0.73	0.343	0.471
102	0.398	0.370	27.01	19.81	0.469	0.840	1.116	0.73	0.336	0.516
103	0.392	0.372	24.59	18.17	0.471	0.832	1.075	0.74	0.340	0.540
104	0.393	0.371	25.39	18.79	0.469	0.838	1.09	0.74	0.336	0.400
105	0.384	0.370	26.27	17.4	0.47	0.804	1.107	0.74	0.341	0.506
201	0.390	0.346	32.84	24.49	0.443	0.883	1.192	0.75	0.304	0.641
202	0.389	0.346	31.71	24.02	0.445	0.875	1.180	0.75	0.307	0.643
203	0.3915	0.350	32.46	24.72	0.443	0.883	1.201	0.76	0.308	0.646
204	0.376	0.344	24.51	18.64	0.443	0.848	1.113	0.76	0.328	0.466
205	0.386	0.350	35.29	24.66	0.443	0.862	1.112	0.76	0.303	0.583
301	0.390	0.321	51.19	39.21	0.405	0.962	1.431	0.77	0.241	1.267
302	0.393	0.322	51.47	39.79	0.405	0.969	1.459	0.77	0.233	0.960
303	0.385	0.314	48.00	37.12	0.405	0.953	1.404	0.77	0.252	0.730
304	0.383	0.320	45.41	35.59	0.402	0.955	1.411	0.77	0.244	0.730
305	0.395	0.317	50.23	37.18	0.401	0.951	1.403	0.78	0.240	0.841
401	0.392	0.311	77.66	61.39	0.374	1.049	1.725	0.79	0.180	1.303
402	0.390	0.2945	96.40	75.32	0.371	1.109	1.821	0.79	0.178	1.370
403	0.387	0.310	80.39	64.09	0.374	1.029	1.630	0.79	0.161	0.913
404	0.394	0.306	77.69	61.40	0.374	1.051	1.161	0.79	0.181	0.421
405	0.391	0.299	92.16	71.34	0.373	1.108	1.590	0.79	0.180	0.208
501	0.392	0.295	115.51	100.26	0.376	1.037	1.719	0.83	0.150	1.822
502	0.389	0.294	115.51	100.58	0.374	1.030	1.721	0.84	0.145	1.972
503	0.390	0.2953	114.91	89.27	0.375	1.042	1.693	0.84	0.151	1.934
504	0.391	0.286	115.62	100.32	0.370	1.048	1.721	0.84	0.153	1.790
505	0.390	0.29	112.98	85.13	0.373	1.047	1.721	0.82	0.140	1.450